Variation in nitrogen cycling activity in soil supporting rice (*Oryza sativa*) cultivars

Mohammad Robel Hossen Patwary

A thesis submitted in partial fulfilment of the requirements for the degree of Doctor of Philosophy

The University of Sheffield
School of Biosciences
Plants, Photosynthesis and Soil

May 2024

Declaration

I, Mohammad Robel Hossen Patwary, declare that this thesis has been composed entirely by myself unless otherwise referenced in the text. I confirm that this thesis has not been submitted for any other degree. All quotations have been distinguished by quotation marks and the sources acknowledged.

Covid Statement

Wet lab work was gridlocked during covid lockdown for six months. I have used paddy soil for my experiment collected from Bangladesh. Soil shipment was delayed one month due to the Brexit issue.

Acknowledgement

First and foremost, I would like to express my heartfelt thanks to my supervisor Tim Daniell who has kept faith in me that I could do this research project. After touring the PhD journey, it seems like learning how to walk like a baby. Thanks for your stretching hands. Without your mentorship, tireless support and constant guidance, I would not be able to reach this page.

I am very much grateful to my co-supervisor Duncan Cameron for assisting me in solving the puzzle while doing isotope modelling. And both my supervisors played an immense role in upholding me with their gracious presence and cheerful spirits.

I would like to give thanks to my collaborator, Ari Sadanadom and Adam Price, for arranging the rice seeds. I would like to acknowledge profoundly to Adrian Brennan, who taught me how to do GWAS. I am very much grateful to him.

I would like to express my heartiest thanks to Heather, who helped me to do mass spec. I was fortunate to have wonderful people of the AWEC lab group. Everyone was so helpful and kind. I am very much thankful to Sara, Sue and Shuwang for your immense help during my experimental harvest days. You people are rock. I am also thankful to Maggi, who help me from the beginning.

Special thanks to Safirun and Luke, previous PhD students, who helped me cop with plant and soil-related experimental work.

I would like to take this opportunity to express my gratitude to my fellow countrymate, Miraj,Tushar and Amit, for giving a social life and helping me on harvesting day.

I want to acknowledge my scholarship awarding body Governance Innovation Unit (GIU) of the Prime minster office of Bangladesh, for funding this research and providing financial support,

without which I could not pursue my dream. I am also grateful to my host organisation Bangladesh Council of Scientific and Industrial Research (BCSIR), for providing the academic leave.

I am especially indebted to my wife, Kishwar, for doing the household work more than me, giving me breathing space to relax more, helping me during my experiment harvesting day, teaching me some plant science, and answering all my silly plant-related questions. Best wishes for your PhD defence next month. Wasit, our boy, I am so sorry I couldn't always take care you. He is such a good boy; when I was busy at the lab, he often accompanied me after touring AWEC lab and learning lots of plant stuff; now, he wants to be vet.

I want to officially acknowledge my mother's effort; she still keeps track of my studies and encourages me to study diligently.

Finally, I would like to remember my late father, who always wanted to see me as a doctor. However, I did not choose the medical profession. But at the end of this journey, I want to dedicate this doctoral fellowship to him. Maybe from heaven, he is observing me.

Not but the least, all my thanks to the Almighty Allah for giving me the knowledge and strength to complete my journey.

Abstract

Nitrogen use efficiency in paddy rice production is estimated to be as low as 40%. The remaining added nitrogen is lost through leaching or gaseous loss, including the potent greenhouse gas nitrous oxide (N_2O). Most Nitrogen transformations in soil are microbial, with four critical processes in paddy systems: nitrification, denitrification, DNRA, and anammox. Rice plays a vital role in manipulating the soil ecology of its rhizosphere through, for example, nitrogen assimilation, respiration, and root exudation that shape the rhizosphere community and affect microbial activity. These effects may be directly linked with rice genetics; I hypothesised that rice-based nitrogen modulation. cycling is genotype-specific and thus linked to rice variety. I screened ~100 rice genotypes using a single optimised microcosm experiment with paddy soil supporting rice growth. In this system, I simultaneously measured actual nitrification, denitrification and anammox process rates and linked these results to the rice line using GWAS. I observed significant variation in activity with all processes. The results suggest that low nitrification-supporting rice genotypes limited nitrification by secreting BNI-like secondary metabolites. Whilst emission of N_2O significantly varied among the tested rice genotypes mainly due to variations in complete denitrification, the degree of partial denitrification was a vital factor droving the variation; this was found to be negatively correlated with the carbon: nitrate ratio. However, speculative at this stage, secondary root development genes were found to be associated with N_2O emission variation. Although links were discovered between rice genotypes and anammox, these were thought to be indirect through the regulation of denitrification. These experimental results suggest that rice breeding could be used to improve agricultural sustainability through microbial manipulation to reduce nitrification and mitigate N_2O emissions from fertilised flooded paddy soil.

List of Abbreviations

AOA	Archaeal ammonia oxidisers
AOB	Bacterial ammonia oxidisers
ATP	Adenosine tri phosphate
AMF	Arbuscular mycorrhizal fungi
AMO	Ammonia monooxygenase
BAAP	Bengal and Assam Aus Panel
BNI	Biological nitrification inhibitors
BNF	Biological nitrogen fixation
DAT	Days after transplantation
DOC	Dissolved organic carbon
GHG	Greenhouse gases
GLM	Generalised linear model
GNR	Gross nitrifiction rate
GWAS	Genome wide association study
GWP	Global warming potential
HDRA	High-density rice array
HAO	Hydroxylamine oxidoreductase

IRMS	Isotope ratio mass spectrometry
NOB	Nitrite oxidising bacteria
NUE	Nitrogen uptake efficiency
ORP	Oxidation reduction potential
PCA	Principal component analysis
QTL	Quantative trait loci
RDP	Rice Diversity Panel
ROL	Radial oxygen loss
SNP	Single nucleotide polymorphism
SOC	Soil organic carbon
SOM	Soil organic matter
WFPS	Water filled pore size

Table of Contents

List of figures

List of tables

Introduction

1.1 Arable agriculture is expanding

Arable agriculture has increased even though agricultural land decreased at the same rate within the last two decades to meet global demand (The coloured numbers in Fig: 1.1). Urbanisation and industrialisation commensurate with the increasing population are the main drivers for agricultural land conversion (Azadi et al., 2011). Advanced agriculture depends on high-yield modern crop varieties, which typically need significant inputs of inorganic nitrogen in cultivated land. The recent use of nitrogen fertilisers is ~110 M tons/ year, which will likely increase threefold by the middle of the century (FAO, 2022)(Tilman et al., 2001). Only 40 to 60 % of applied nitrogen fertiliser is estimated to be recovered by the crop, depending on the species and form of nitrogen used (Sebilo et al., 2013). The nitrogen use efficiency of paddy rice production is estimated to be at the lower end of this spectrum. The remainder is lost through physical, chemical and microbial processes. The remaining applied nitrogen is lost through ammonia volatilisation, leaching and/or gaseous loss, including nitrous oxide (N_2O). Rice is an important crop, feeding over 50% of the world's population (Fukagawa & Ziska, 2019). According to the USAID report from 2019, rice production has increased by 230% since 1960 (Childs & Skorbiansky, 2019). The area for rice production has also increased, and more yield has been produced per unit area since around 2013, but before then, rice production increased with the expansion of the harvested area in the arable lands (FAO, 2022) (Fig:1.1).

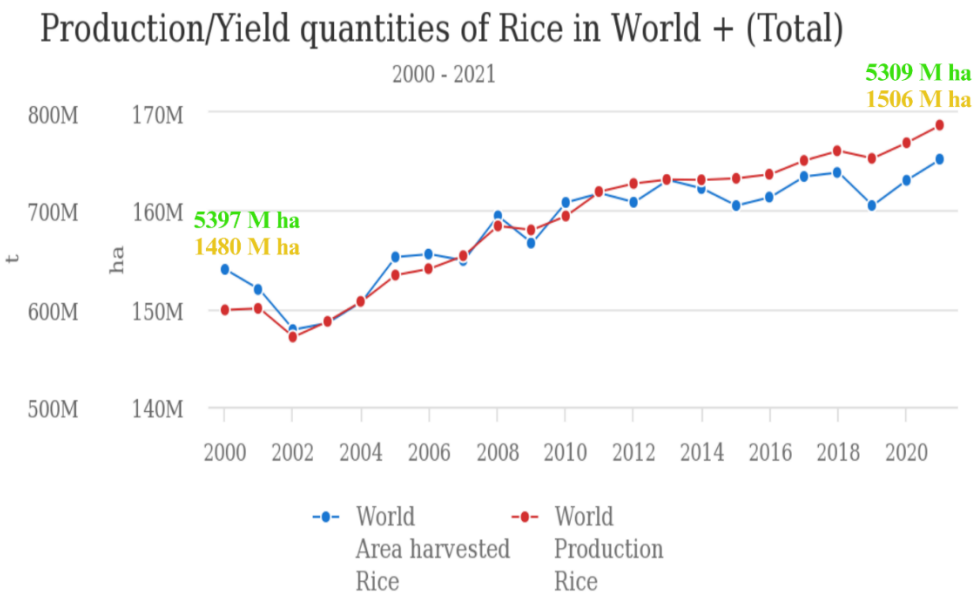

Fig 1.1: Food and Agriculture Organization (FAO) data shows annual rice yield in tons and the harvested area in hectares from 2000 to 2021. The green- and yellow-coloured numbers indicated the hectares used for total agriculture and land used for arable agriculture in 2000 and 2021, respectively.

1.2 Nitrogen cycle

Nitrogen (N) comprises most of the earth's atmosphere and is the fourth most abundant element in cellular biomass after oxygen, carbon, and hydrogen. As with other living organisms, nitrogen (N) is an indispensable element for plant growth. It is an essential component for the building blocks like proteins and nucleotides. It also constitutes the skeleton of chlorophyll, a crucial plant component involved in photosynthesis. However, N is the most common limiting nutrient for plant growth (LeBauer & Treseder, 2008) because most N in the atmosphere is inert from N_2, which is not directly usable by plants. Plants can only uptake specific forms of reactive nitrogens from soil. Inorganic nitrogen takes nine different chemical forms many forms of organic nitrogen in soil corresponding to different oxidative states and is transformed between the states through chemical and microbial processes (Kuypers et al., 2018). However, through the physical processes, atmospheric reactive nitrogens can be deposited through deposition and lost from the soil system

by ammonia volatilisation. The N cycle processes pave the reactive N pools in the soil positively or negatively and might increase and decrease mineral N pools in the soil (Hofman G., 2004).

1.2.1 Physical processes

In the nitrogen cycle, the transportation of reactive nitrogen without changing the oxidative state of reactive nitrogen is termed physical processes. Physical processes, including nitrogen deposition, leaching and runoff and ammonia volatilisation, are natural phenomena; in contrast, N-fertilisation is an artificial physical deposition process.

1.2.1.1 Nitrogen deposition

Nitrogen deposition in the soil is a part of the physical nitrogen cycle process and facilitates atmospheric reactive nitrogen's return to the earth's surface. Atmospheric reactive nitrogen (Nr) (NH_3 and NOx) primarily originates from anthropogenic emissions. They are deposited naturally with or without precipitation (rain or snow) as wet and dry deposition to the earth's surface (Zhang et al., 2021). Deposition is increasing due to anthropogenic emissions and has increased three to five-fold over the past century (Denman et al., 2007). Nitrogen deposition in the soil is also increasing due to artificial nitrogen deposition as fertilisation (Davidson, 2009), with the deposition rate predicted to double by 2050 (Galloway et al., 2004; Phoenix et al., 2011). Excess N deposition, artificially or naturally, can exacerbate environmental problems, including soil acidification (Lu et al., 2014) and freshwater eutrophication (Zhan et al., 2007). Soils release base cations such as magnesium and calcium to neutralise soil acidity; consequently, soils lose fertility (Bowman et al., 2008). Excess N deposition affects the other physical processes, accelerating ammonia volatilisation and the nitrate leaching into groundwater.

1.2.1.2 Leaching and runoff

Leaching and runoff are the physical nitrogen loss processes in the N-cycle processes. Nitrogen is lost vertically to groundwater through leaching and horizontally through runoff to adjacent water bodies (Fig: 1.2). Nitrate is primarily the form of nitrogen prone to loss due to its high mobility in the soil. Unlike ammonium in the soil, nitrate is mobile and easily moved by water. Positively charged ammonium is firmly attached to negatively charged clay particles and resists movement

with water. The prime factors affecting the degree of nitrate leaching are the moisture content of the soil and, simultaneously, how much water is added to the soil (Ramos et al., 1990)(Moreno et al., 1996). For instance, nitrate leaching is more prevalent in sandy soil than clay soil due to the lower water-holding capacity (Beaudoin et al., 2005). When water-holding capacity is exceeded in the soil, most air spaces are filled with water, and gravity causes water to move down through the soil profile.

Deposited nitrogen is also lost from soil through heavy rain runoff, contaminating surrounding water bodies. In recent years, the risk of nitrate contamination in ground and surface water has risen through leaching and runoff due to the excessive use of nitrogen fertilisers with unmanaged irrigation regimes in agricultural land (Abbasi & Sepaskhah, 2023; Wang et al., 2019). Nitrate leaching might be reduced to 30.97% by increasing ammonification and denitrification (Sun et al., 2023).

1.2.1.3 Ammonia volatilisation

Ammonia volatilisation is another nitrogen loss process from the soil. Globally, up to 64% (an average of 18%) of applied nitrogen fertilisers were lost as NH_3 (Pan et al., 2016). Ammonium is deposited in the soil through artificial N deposition and mineralisation from organic N, which undergoes deprotonation and forms ammonia and loss, termed ammonia volatilisation. So, it depends on the soil's equilibrium between ammonium and ammonia, solid and gas equilibrium and mass transfer to the atmosphere. The soil regulates these equilibria by pH, temperature and O_2 (Hofman G., 2004). In alkaline pH, NH_4^+ tends to deprotonate and form NH_3, which might be lost from soil surface ammonia volatilisation. Nitrogen loss through ammonia volatilisation is more in dry arable agricultural land than in paddy soil, as flooding prevents ammonia loss through volatilisation by reducing air exchange (Jayaweera & Mikkelsen, 1991; Liu et al., 2020). The 4R nutrient stewardship concept has been introduced to mitigate ammonia volatilisation in agricultural land after N fertilisation, including the right fertiliser source, rate, place, and time (Bruulsemaa et al., 2009). Ammonia volatilisation also might be reduced by applying slow-release N fertilisers with urease inhibitors that increase the efficiency of applied N fertilisers (Pan et al., 2016). However, applying nitrification inhibitors might exacerbate ammonia volatilisation due to ammonium accumulation.

1.2.2 Chemical processes

Unlike the physical processes described above, reactive nitrogen can also be transformed through oxidation-reduction reactions into another form or oxidative state abiotically by chemical processes. Chemical processes are part of the N-cycle that occurs in the atmosphere, aquatic environment and soil. For example, the transformation of nitrogen dioxide (NO_2) into HNO_3 is a chemical process occurring mainly in the atmosphere that frequently influences atmospheric NO_x ($NO_x = NO + NO_2 + N_2O_5 + HONO + HNO_3 + NO_3^-$) pollution (Liu et al., 2013). In the atmosphere, the chemical reaction of NO_2 with hydroxyl (OH) radical is the key abiotic channel of HNO_3 production (Finlayson-Pitts and Pitts, 1999). The formed HNO_3 is deposited in the soil through acid rain as wet deposition (Calvert et al., 1985). In the soil, the most attributed chemical processes of the N-cycle are chemodenitrification and femammox.

1.2.2.1 Chemodenitrification

The abiotic stepwise reduction of nitrate, nitrite, or nitric oxide by ferrous iron Fe(II) in anoxic environments is termed chemodenitrification. Dhakal et al. (2013) reported that a potent chemical potential exists between Fe(II) and oxidised forms of nitrogen (especially NO_2^-). However, earlier suggestions are that reduced conditions in the natural environment might not be enough to reach significant concentrations or nitrite accumulation that allow oxidation-reduction reactions (Buchwald et al., 2016). Nevertheless, chemodenitrification has been reported, especially nitrite reduction by ferrous ions under various environmental conditions at rates similar to biologically catalysed nitrogen transformations (Grabb et al., 2017; Lim et al., 2018). The interfaces between aerobic and anaerobic zones (naturally occurring fluctuating redox conditions zone) are hotspots for chemodenitrification where high fluxes of Fe(II) released by iron-reducing bacteria and/or by abiotic reduction processes meet with NO_2^- and Fe(III) oxides, which dominate in the oxygenated region (Jones et al., 2015). The redox conditions fluctuate in the periodically flooded soils, hyporheic zones, soil aggregates, sediment porewater, and plant rhizospheres. Indeed, the estuarine and coastal sediments that frequently experience rapid redox cycling of iron and high nitrogen loading are significantly associated with elevated N_2O emissions through chemodenitrification (Jones et al., 2015; Wankel et al., 2017; Yuan et al., 2017). However, biotic N_2O emission processes in the soil override chemodenitrification due to high nitrite reductase

activity (Lim et al., 2018). The gamma radiated and microbiologically active microcosm experiments revealed that chemodenitrfication is responsible for 15-25 % N_2O emission, whereas biotic processes contribute to 75-85 % N_2O emission (Otte et al., 2019).

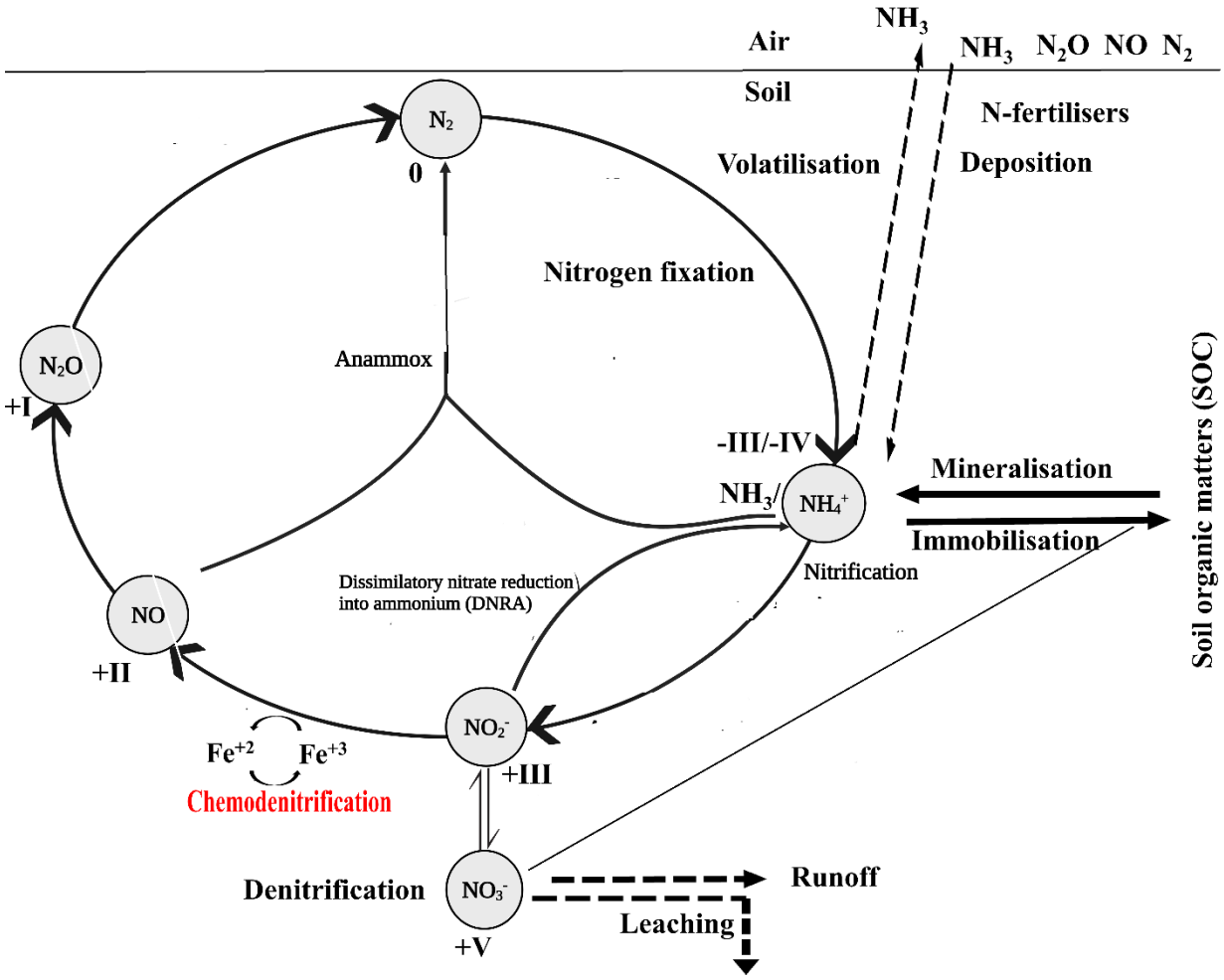

Fig 1.2: A simplified nitrogen cycling process in the soil separating physical, chemical and microbial nitrogen transformations. The dotted-lined processes indicate physical nitrogen cycling processes, and the solid-lined processes with black-cloured are microbial and red-coloured chemical nitrogen transformation processes. Roman letters, either positive or negative, indicate the oxidative status of the respective reactive nitrogen. The top horizontal line shows soil and air interphase.

1.2.3 Microbial processes

Biogeochemical nitrogen cycling between nitrogen species is often attributed to the following six distinct microbial nitrogen-transforming processes: assimilation, ammonification, nitrification, denitrification, anaerobic ammonium oxidation (anammox) and nitrogen fixation. Microbial transformations of nitrogen are depicted as a cycle (Fig: 1.2) consisting of six distinct processes that proceed in an orderly fashion (Kuypers et al., 2018). The redox of the soil is critical to regulating the microbial reactive nitrogen transformations (Pett-Ridge et al., 2006). Ammonification, anammox, biological nitrogen fixation and denitrification processes initiate under anoxic conditions, whereas nitrification occurs in oxic conditions. In agricultural soil, microbial N cycling processes are pivotal as they regulate the N availability to the plant and, simultaneously, the N loss and retention of applied N.

1.2.3.1 Nitrogen fixation

The largest pool of nitrogen in the biosphere, N_2, is not directly available to most organisms but enters the living organisms by diazotrophic prokaryotes naturally via biological N_2 fixation (BNF), though it can deposited geochemically through lightning with input over an order of magnitude smaller than any of the estimates of BNF (Erisman et al., 2008; David Fowler et al., 2013; Godfray et al., 2010). Biological nitrogen fixation (BNF) was discovered by Dutch microbiologist Martinus Beijerinck in 1901. A group of unicellular microorganisms, including bacteria and archaea, and either free-living or in symbiotic relationships (e.g., within plant root nodules) are capable of BNF. Atmospheric N_2 is reduced into NH_4^+ by nitrogenase enzymes through this microbial process, which can then be incorporated into amino acids and into diversified organic compounds (Galloway et al., 2008; Kuypers et al., 2018). All nitrogenases comprise two components: catalytic and metal (iron, vanadium or molybdenum) binding components (Eady, 1996; Zehr et al., 2003). Nitrogen fixation is energetically expensive, with 16 ATP molecules consumed to reduce one molecule of N_2 into two molecules of NH_4^+.

$$N_2 + 8H^+ + 8e^- + 16\,ATP \rightarrow 2NH_3 + H_2 + 16\,ADP + 16Pi$$

This powerful reductant carries electrons to the enzymes and the protection of oxygen-labile nitrogenases (Bothe et al., 2010). Both oxygen exposure and high nitrogen availability in soil, such

as nitrogen fertilisation, limit BNF (DiFonzo & Bordia, 1998). A meta-analysis showed that nutrient enrichment significantly reduced the BNF activity in the soil (Zheng et al., 2019).

1.2.3.2 Mineralisation and immobilisation

Mineralisation and immobilisation are critical in the N cycle since these processes exchange organic and inorganic N. Mineralisation releases soluble inorganic N from organic forms in dead biomass (detritus), that can be incorporated into microbial biomass through immobilisation. The mineralised nutrients are released as a by-products during detritus's microbial consumption. Mineralisation and immobilisation co-occur within the same soil aggregates. The mineral N pools in the soil might be unchanged if the two processes proceed at an equal pace. However, the gross mineralisation and immobilisation rates depend on the C/N ratios of the detritus (Robertson & Groffman, 2006). If plant detritus is rich in N, microbial needs are easily met, and N release, or mineralisation, proceeds. If plant detritus is low in N, microbes must scavenge inorganic N from their surroundings, immobilising N in their biomass. Mineralisation and immobilisation typically do not involve either oxidation or reduction and, as a result, are expected to be unaffected by rapidly fluctuating soil redox potential. However, mineralisation might be reduced under anoxic conditions if organic N is associated with a complex carbonaceous compound such as phenolic lignin, which requires oxidative decomposition (Schmidt-Rohr et al., 2004).

1.2.3.3 Nitrification

Nitrification is a strictly aerobic microbial N-transformation process that converts relatively immobile ammonium N to mobile nitrate N, facilitating leaching and denitrification (Raun & Johnson, 1999; G. Subbarao et al., 2006). It is a two step process where ammonia/ammonium (NH_3/NH_4^+) is first oxidised into nitrite (NO_2^-) via hydroxylamine (NH_2OH). Two enzymes mediate this conversion, ammonia monooxygenase (AMO) and hydroxylamine oxidoreductase (HAO) (Hollocher et al., 1981). In the second step, NO_2^- is converted into NO_3^- by nitrite oxidoreductase (NXR) (Daims et al., 2019). Bacterial (AOB) and archaeal ammonia oxidisers (AOA) oxidise ammonia through the first step of nitrification; in contrast, nitrite-oxidising bacteria (NOB) perform only the second step. Until recently it was thought that no nitrifier accomplished both steps till complete nitrification (Comammox) is reported (Daims et al., 2015; Van Kessel et

al., 2015). Comammox (Equation 3) is bioenergetically more efficient than every single nitrification step (Equations 1 and 2).

$$NH_4^+ + 1.5O_2 \longrightarrow NO_2^- + H_2O + 2H^+ \ (\Delta G^{0,} = -274.7 \text{ kj.mol}^{-1}) \quad (1)$$

$$NO_2^- + 0.5O_2 \longrightarrow NO_3^- \ (\Delta G^{0,} = -74.1 \text{ kj.mol}^{-1}) \quad (2)$$

$$NH_4^+ + 2O_2 \longrightarrow NO_3^- + H_2O + 2H^+ \ (\Delta G^{0,} = -348.9 \text{ kj.mol}^{-1}) \quad (3)$$

1.2.3.4.1 Denitrification

Denitrification is a facultative process that allows the maintenance of respiration in oxygen-limiting environments if sufficient substrate is present (Richardson, 2000). A range of nitrogen oxides are used as an alternate electron acceptor for oxygen and are converted through a series of intermediates to Nitrogen (N_2) (Zumft, 1997). Reduction of these N-oxides is catalysed by a series of reductase enzymes that are nitrate reductase (EC 1.7.99.4*), nitrite reductase (EC 1.7.2.1*), nitric oxide reductase (EC 1.7.99.7*) and nitrous oxide reductases (EC 1.7.99.6*) (L. Philippot, 2006; Zumft, 1997). The *nar* operon is involved in the synthesis of nitrate reductase, and subsequently, the *nir* operon, *nor* and *nos* operons are involved in synthesising nitrite, nitric oxide and nitrous oxide reductase enzymes respectively (Zumft, 1997; Philippot, 2002). Environmentally benign dinitrogen (N_2) is produced when denitrification is complete, but the process is often truncated, resulting in the release of the potent greenhouse gas nitrous oxide (Fig: 1.3).

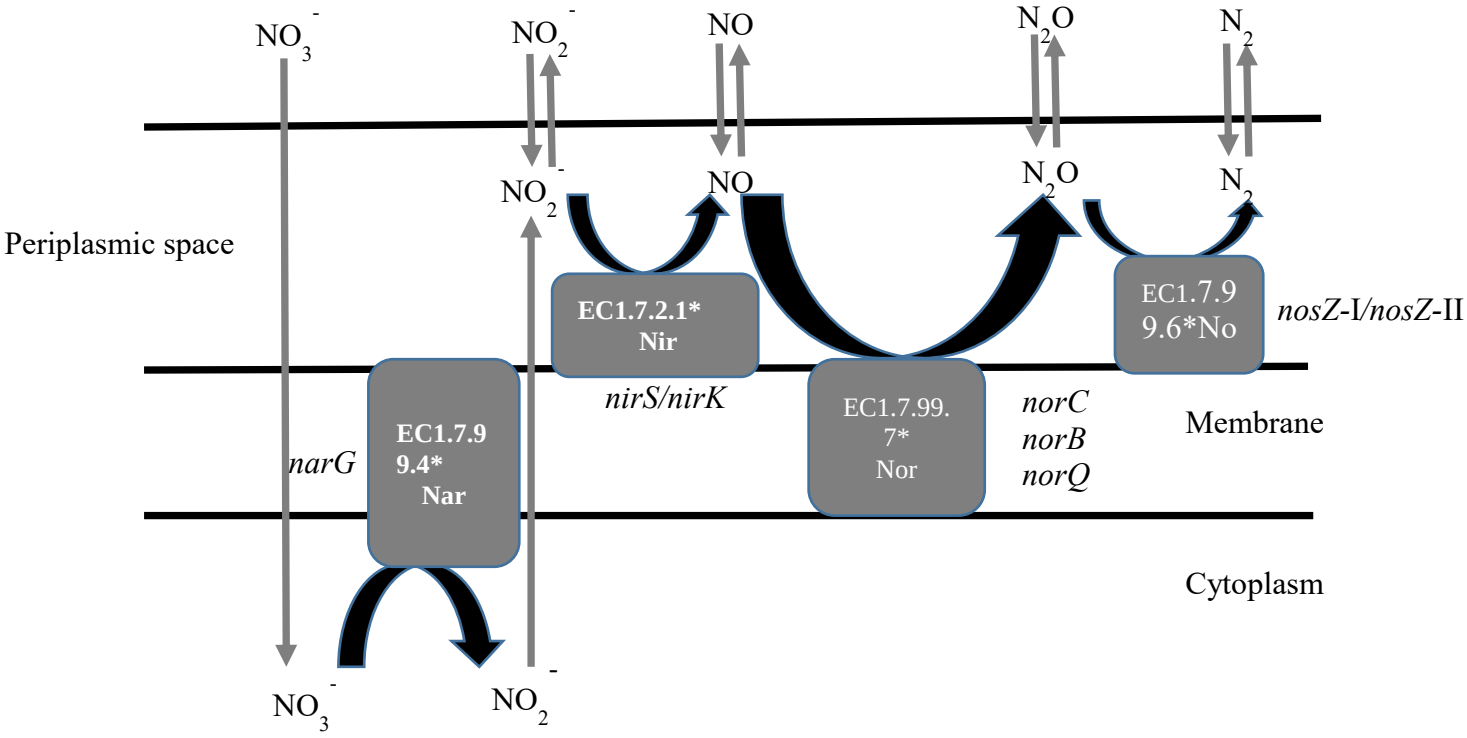

Fig 1.3: Sequential reductive pathway of denitrification showing the location of enzymes with Enzyme Commission number encoding the enzymes: nitrate reductase encoded by Nar is bound to the cytoplasmic membrane whilst the alternative form encoded by the Nap cluster is periplasmic (not shown); nitrite reductase (Nir) is periplasmic, nitric oxide reductase (Nor) is again bound to the cytoplasmic membrane; lastly, nitrous oxide reductase (Nos) is periplasmic (Wallenstein et al., 2006).

1.2.3.4.2 Carbon modelling based on denitrification stoichiometry

Stoichiometry is part of thermodynamics and kinetics, which deals with chemical components' quantitative composition and transformations in chemical reactions. MacCarty developed a stoichiometric equation for bacterial-mediated reactions like respiration and cell synthesis (McCarty, 1972). For instance, bacterial-mediated reactions are oxidation-reduction reactions involving the transfer of electrons, where carbonaceous compounds are used as electron donors (R_d), oxygen is used for aerobic respiration, and N-oxides for denitrification are used as electron acceptors (R_a). For heterotrophic denitrification, carbonaceous substrates such as methanol, ethanol, glucose, aspartic acid, formic acid and/or acetic acid are used as electron donors, and a

range of N-oxides such as NO_3^-, NO_2^-, NO and N_2O are used as electron acceptors. The resulting half-reactions for the electron donors and acceptors with electrons during denitrification are given below according to MacCarty's method and habit.

Reactions for electron donors (e.g. carbohydrates)

$1/q\ C_aH_bO_c + 2a\text{-}c/q\ H_2O = a/q\ CO_2 + H^+ + e^-$ ……...(4)

Where q=4a+b-2c

For example, in case of glucose ($C_6H_{12}O_6$),a=6, b=12, c=6, q= 4x6+12-2x6=24

$1/24\ C_6H_{12}O_6 + ¼\ H_2O = ¼\ CO_2 + H^+ + e^-$ …….(5)

After balancing the equation (4) by multiplying by 24, equation (6) is formed

$C_6H_{12}O_6 + 6\ H_2O = 6\ CO_2 + 24\ H^+ + 24\ e^-$ ……..(6)

For organic acid MacCarty equation is

$1/q'\ C_aH_bO^-_c + 2a\text{-}c+1/q'\ H_2O = a\text{-}1/q'\ CO_2 + 1/q'\ HCO^-_3 + H^+ + e^-$ …….(7)

Where, q'= 4a+b-2c+1

For example for acetic acid ($C_2H_4O_2$), a=2, b=4, c=2, q'=9

$1/9\ C_2H_4O_2 + 1/3\ H_2O = 1/9\ CO_2 + 1/9\ HCO^-_3 + H^+ + e^-$ ……(8)

After balancing the equation (8) by multiplying by 9, equation (9) is formed

Reactions for eletron acceptors (e.g. NO_3^-) during complete denitrifcation

$2\ NO_3^- + 12\ H^+ + 10\ e^- = N_2 + 6\ H_2O$ ……...(10)

Reactions for eletron acceptors (e.g. NO_2^-) during complete denitrifcation

$2\ NO_2^- + 8\ H^+ + 6\ e^- = N_2 + 4\ H_2O$ ……..(11)

Reactions for electron acceptors during partial denitrfication

$NO_3^- + 2\ H^+ + 2\ e^- = NO_2^- + H_2O$……..(12)

$NO_2^- + 2\ H^+ + 2\ e^- = NO + H_2O$……(13)

$2\ NO + 2\ H^+ + e^- = N_2O + H_2O$…….(14)

$N_2O + 2\ H^+ + e^- = N_2 + H_2O$……..(15)

MacCarty's equation also considers carbonaceous compounds used for bacterial cell synthesis. The sum of the fraction of electron donors associated with cell synthesis (f_s) and the fraction associated with energy (f_e) production is always assumed to be one (Zhou, 2001). Bacteria rationale carbon partition between respiration for energy generation and bacterial biomass synthesis and partitioning depends on environmental conditions such as temperature, moisture, and substrate stoichiometry (Manzoni & Porporato, 2009). The quantity and quality of carbon as a substrate are critical for source partitioning between denitrification and cell synthesis, depending on the other conditions. So, the combined stoichiometric equation for denitrification while considering cell synthesis is given below (Zhou, 2001).

$R= R_d-(1-f_s)R_a-f_sR_c$ ……....(16)

Where, R= denitrification, R_d= electron donors, R_a= electron acceptors, f_s= fraction of electrons for cell synthesis, R_c= Other cell synthesis

Electron generation is much higher when glucose is used as an electron donor, comparing organic acids and alcohols according to equations (6) and (9), and NO_3^- is a more efficient electron acceptor than N_2O according to equations (12) and (15). Therefore, carbon sources characterising electron generation, transport, and consumption are crucial to understanding carbon sources' effects on the fate of denitrification (Wei et al., 2022).

1.2.3.5 DNRA

Dissimilatory nitrate reduction into ammonium (DNRA) is also an anaerobic respiration process, but unlike denitrification, NO_3^-/NO_2^- is ammonified into NH_4^+ thus keeping reactive N in the system. The first step is NO_3^- reduction mediated by nitrate reductase encoded by nap/nar genes (Fig: 1.4), while the last step is the conversion of NO_2^- into NH_4^+ either through a respiratory pathway mediated by cytochrome c nitrite reductase (*nrfA*) or a fermentative process mediated by a single subunit nitrite reductase enzyme coded by *nir*B gene (Cole and Brown, 1980; Cole, 1990; Kern and Simon, 2009; Simon and Klotz, 2013; Wang et al., 2018). Denitrification is bioenergetically more efficient than DNRA in the absence of oxygen (comparing equations 17 and 18) (Stouthamer, 1988; Stouthamer et al., 1997). More carbon as electron donors is required for

DNRA than denitrification because only 5 electrons are required for NO_3^- reduction through denitrification (Equation 10), in contrast to DNRA, where eight electrons are required . However, more accessible energy is generated in DNRA per mol of nitrate reduction than denitrification (Equations 20 and 21). So, high organic carbon and low NO_3^- favoured DNRA over denitrification in the absence of oxygen.

$C_6H_{12}O_6 + 6O_2 = 6CO_2 + 6H_2O$ [<Δ>0'= -2870 KJ/mol Glucose] (17) Aerobic respiration

$5C_6H_{12}O_6 + 24NO_3^- + 24H^+ = 30CO_2 + 12N_2 + 42H_2O$ [<Δ>0'= -2670 KJ/mol Glucose] (18) Denitrification

$5C_6H_{12}O_6 + 24NO_3^- + 24H^+ = 6CO_2 + 3NH_4^+ + 3H_2O$ [<Δ>0'= -1870 KJ/mol Glucose] (19) DNRA

$5C_6H_{12}O_6 + 24NO_3^- + 24H^+ = 30CO_2 + 12N_2 + 42H_2O$ [<Δ>0'= -556 KJ/mol Nitrate] (20) Denitrification

$5C_6H_{12}O_6 + 24NO_3^- + 24H^+ = 6CO_2 + 3NH_4^+ + 3H_2O$ [<Δ>0'= -623 KJ/mol Nitrate] (21) DNRA

Δ0'= Gibb's free energy change

1.2.3.6 Anammox

Anammox bacteria carry out the anammox process inside a specilised organelle, the anammoxosome, an intracytoplasmic compartment bounded by a membrane (blue line) (Fig: 1.4) (Kartal et al., 2011). It is challenging to activate NH_4^+ without the presence of molecular O_2. However, in the anammoxosome, NO derived from NO_2^- oxidises NH_4^+ into hydrazine (N_2H_4) by hydrazine synthase, and the pathway is completed into N_2 after the conversion of N_2H_4 to N_2 by hydrazine dehydrogenase (Fig: 1.4). Anammox bacteria gain energy only from the final step (Equation 22) because the first two steps are energy-expending during anaerobic respiration. So, gaseous N_2 loss is inevitable during anammox, especially since accumulation of N_2H_4 in the anammoxosome would be toxic.

$$NH_4^+ + NO_2^- = N_2 + 2H_2O \ (\Delta G^{\circ\prime} = -357 \ KJmol^{-1}) \ (22)$$

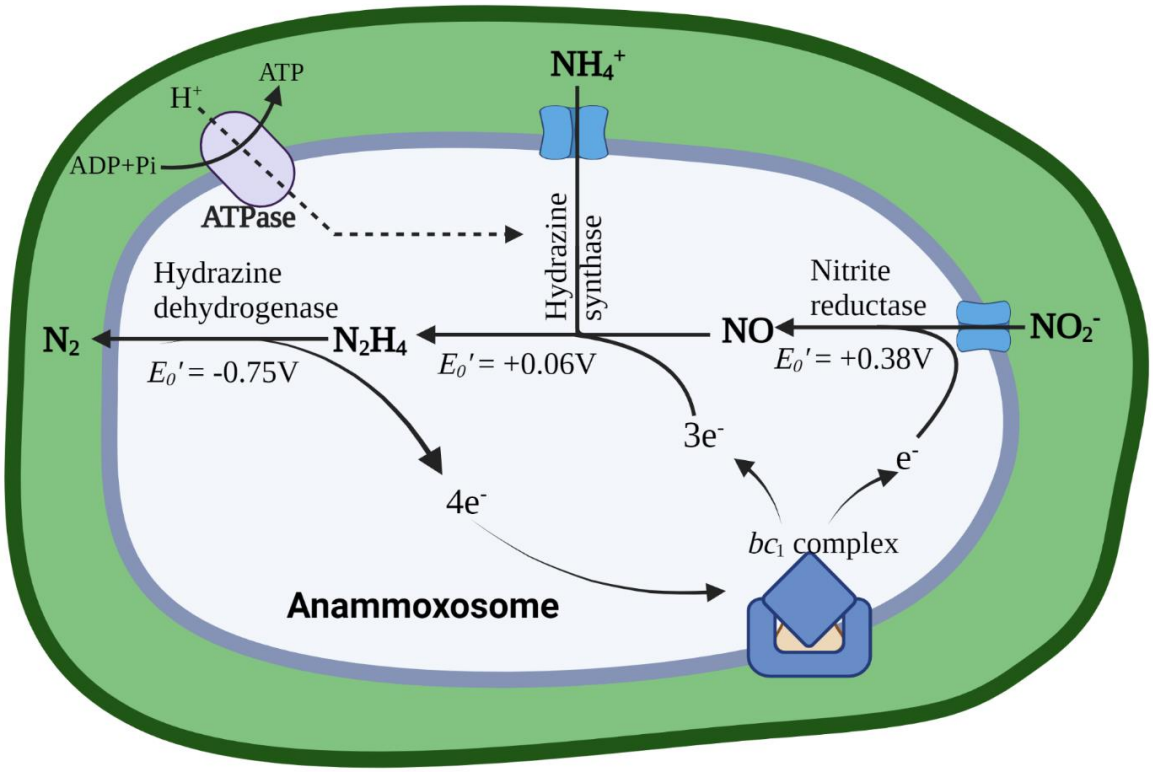

Fig 1.4: The anammoxosome, an intracytoplasmic compartment bounded by a membrane (blue line) of *Kuenenia stuttgartiensis*, where anammox occurs, diagram adjusted from (Kartal et al., 2013).

1.3 Plant's influences on N-cycle processes in the rhizosphere

Since several microbial guilds are important for N availability in soil, it seems reasonable to hypothesise that plants have also evolved multiple mechanisms to acquire N by shaping and recruiting these N-cycling soil microbial communities. Plants can modulate N-cycle-associated microbes in the rhizosphere through 1) Symbiosis, 2) Priming, 3) N uptake efficiency, and 4) secreting secondary metabolites that inhibit processes (Moreau et al., 2019a). Depending on conditions and capability plants use different strategies to modulate the microbial guilds associated with N-cycle based on N availability in the soil.

1.3.1 Plant's influences on N-cycle processes in N-fertilised soil

N-preferences and NUE are keys in modulating the N-cycling-associated microbes by plants in fertilised soil (Artificial N-deposited soil). Plants typically uptake the inorganic form of nitrogens, such as nitrate and ammonium (Courty et al., 2015). Organic forms of nitrogen, such as amino acids, are also absorbed by plants as they are easily incorporated into protein molecules after uptake. Uptaking nitrate is an active and energy-requiring process as it is absorbed against an electrochemical gradient (Haynes & Goh, 1978). In contrast, ammonium, depending on its concentration, could be uptaken either actively or passively, therefore generally more energetically efficient than nitrate uptake (Wang, Siddiqi, Ruth, & Glass, 1993). In addition, nitrate assimilation is also energetically expensive because nitrate needs to be reduced into ammonium to synthesise amino acids and other organic compounds. However, nitrate is more available than ammonium for plant uptake due to its mobility since it does not bind to the cation exchange complexes of soils (Courty et al., 2015). So, the forms of inorganic nitrogen available in the soil and plants' preference for available nitrogen might influence microbial transformations such as nitrification and denitrification.

Soluble inorganic nitrogen in the soil is spatially and temporally variable, and most plants appear to be highly opportunistic in exploiting any transiently available microscale patches of nitrogen (Chapin, Matson, & Mooney,2002). Nitrogen cycle-associated microbes such as denitrifiers and nitrifiers compete for substrates with plants. The outcome of competition for nitrogen between microbes and plants mainly depends on how efficiently the plants and microbes uptake and or use nitrogen. Root traits related to acquisitive strategies, such as high specific root length (Roumet et al., 2016) and/or high root length density, are likely associated with high rates of soil resource acquisition (Abalos et al., 2018; Roumet, Urcelay, & Díaz, 2006; Wright et al., 2004). Inferring that root with the specific traits efficiently uptakes more nitrogen, leaving less deposited nitrogen in the soil for microbial nitrogen transformations. Plants not only limit microbial nitrogen transformations through exploitative competition, restricting the supply of nitrogen to microorganisms, but also in direct interference competition by producing inhibitory secondary metabolites to inhibit the transformations.

1.3.1 Plant's influences on N-cycle processes in N-limited soil

Plants adapt to N-limiting conditions by recruiting fungi and bacteria in the rhizosphere through mutualistic relationships and stabilising the effectiveness of the interactions. Arbuscular mycorrhizal fungi, one of the ancient symbionts, colonise in the specialised root structure and outsource nitrogen for the plant, including nitrate, ammonium, and organic N. Nitrate in the soil is easily accessible for plant uptake due to its mobility. However, integrating fungal hyphae in the roots transfers less mobile ammonium from the distal distance from the roots. In response, plants provide space and photosynthates for the AMFs. In contrast, Ectomycorrhizal and ericoid fungi, other symbiont partners, can produce enzymes that decompose more or less recalcitrant carbon compounds containing nitrogen. Rhizosphere priming is an essential strategy for plants to access organic nitrogen that can influence N-cycling and nitrogen supply to plants through enhanced microbial mineralisation. Extracellular enzymes involved in N mineralisation and increased rhizodeposition intensify the priming effects on N cycling microbes. The priming effects on Ncycle microbes could be positive or negative. The magnitude and direction of priming effects on soil N cycling depend on many factors, including plant species identity and phenology, mycorrhizal status and the type of soil (Bengtson, Barker, & Grayston, 2012; Dijkstra, Bader, Johnson, & Cheng, 2009; Mwafulirwa et al., 2017; Zhu et al., 2014). However, the nutritional status of the soil is one key determinant of plant priming. Plants meet nitrogen demand in nitrogen-limited soil by encouraging the breakdown of soil organic nitrogen pools through positive priming due to root exudations. Extracellular microbial enzymes liberate nitrogen from organic nitrogen pools that meet microbial nitrogen demand and enhance microbial nitrogen mineralisation and nitrogen supply to plants (Meier et al., 2017; Phillips et al., 2011; Zhu et al., 2014).

However, plant and microbial N demand can be high in low N soils, and if plants compete effectively with microbes for N, this can result in negative priming due to a reduction in microbial decomposition (Dijkstra, Morgan, Blumenthal, & Follett, 2010). Negative priming is also thought to occur in N-replete soils, where microbes may use exudates to meet their C and energy needs rather than mining SOM for N, thereby leading to reduced mineralisation of organic N (Cheng, 1999; Dijkstra et al., 2013).

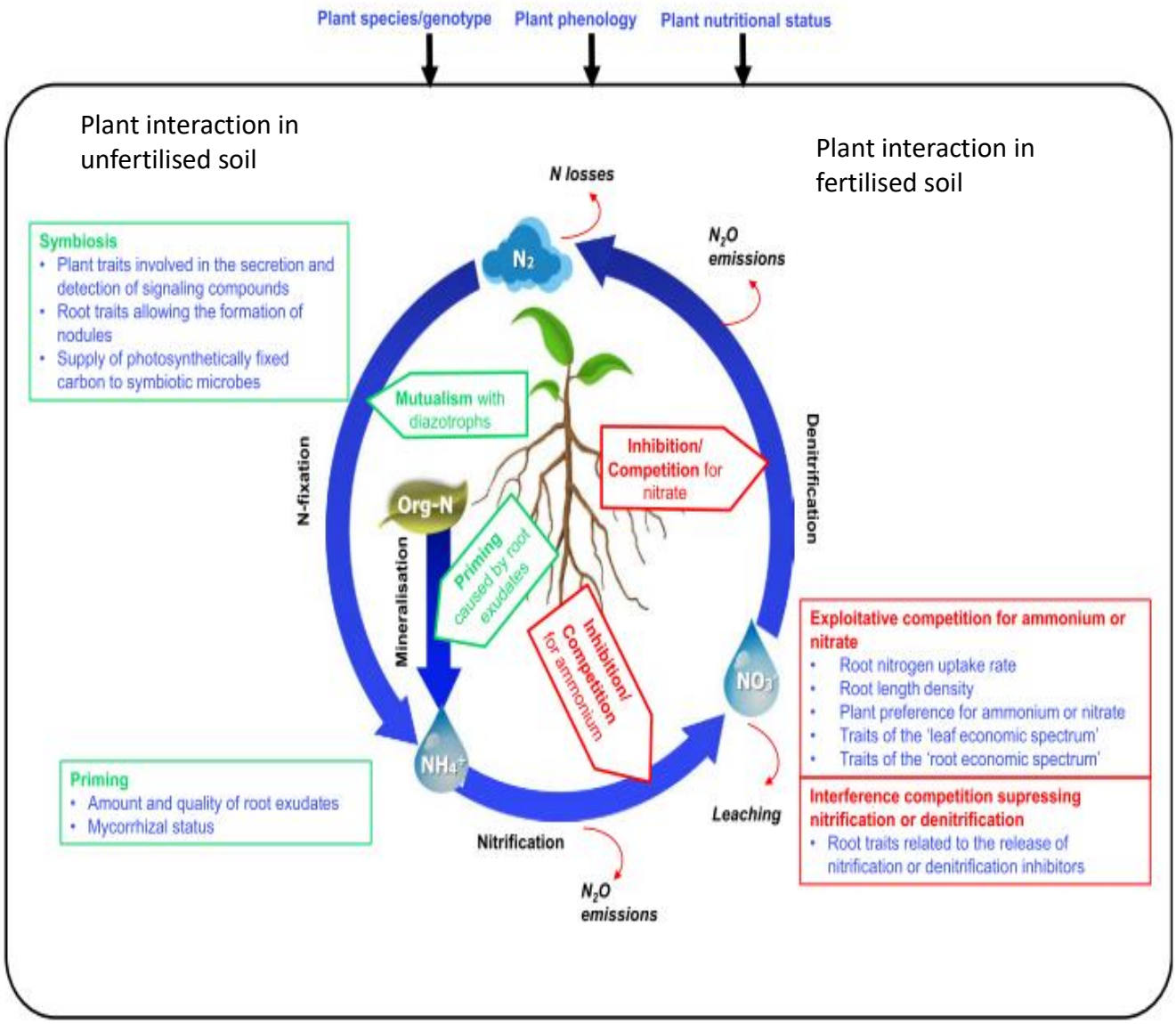

Fig 1.5: This schematic copied from (Moreau et al., 2019a) with a slight modification of how plants can influence N-cycling processes to increase N availability in nitrogen-fertilised and unfertilised soils. The red-marked mechanisms represent typical strategies in nitrogen fertilised soil, and the green in unfertilised soil to modulate N-cycle associated microbial community in the soil. Plant traits affecting the N-cycling processes are shown in blue; some traits are more related to N-cycling processes (in boxes), while others affect all processes (top of the figure).

1.4 Paddy system

Rice is typically grown in lowland paddy soil, maintaining flooded conditions until before harvesting, making rice fields unique agroecosystems and anthropogenic wetlands (Kögel-Knabner et al., 2010). Flooding acts as a barrier between the topsoil and the atmosphere since water replaces the gaseous phase in the soil pores, restricting the oxygen supply. Within 24 hours, oxygen availability is depleted from the bulk topsoil due to reduced oxygen diffusion in water than in air, which is four orders of magnitude lower (Gao *et al.*,2002; Boivin *et al.*, 2002; Tanji *et al.*, 2003). Oxygen limitation in flooded paddy soil inhibits aerobic microbial activities like nitrification (Liu et al., 2019; Verhoeven et al., 2018a). However, rice plants transport oxygen by diffusion through aerenchyma, which is formed when grown in flooded soil. Oxygen leaks from the root surface by radial oxygen loss (ROL), oxygenating the rhizosphere (Armstrong, 1971)

1.5 N-cycle processes are interconnected in the oxic/anoxic interface of flooded paddy

The microbial nitrogen transformation processes are interconnected in the oxic-anoxic interface of the rice rhizosphere and surrounding bulk soil and happen simultaneously (Fig: 1.6) (Nie et al., 2015; Nie et al., 2019). Soil parameters like pH, dissolved oxygen, salinity, oxidation-reduction potential (ORP), dissolved organic carbon (DOC), and substrate concentrations are the crucial soil abiotic factors that determine the dominance of each process (Nie et al., 2019). (Shan et al., 2018). So, dissolved oxygen and [NO_2^-] in the paddy soil control the partition of NH_4^+ oxidation through nitrification or anammox (Ding et al., 2019). However, nitrite is very transiently available in the soil, and the only source of nitrite in the soil is the leakage from nitrification, denitrification and even DNRA processes. Anammox bacterial communities typically lack nitrate reductase genes, so they solely depend on other N-cycling processes for NO_2^- (Zhu et al., 2011). NH_4^+ produced by the DNRA process in anoxic zones is readily oxidised into N_2 through the anammox process (Nie et al., 2019), with the N_2 produced not distinguishable from complete denitrification. NO_3^- is converted into NH_4^+ via NO_2^- through the DNRA process (Tiedje, 1988). As denitrification and DNRA are anaerobic processes using nitrate through a common enzymic step, there is competition between the two processes for that common substrate (Pandey et al., 2018a; Yoon et al., 2015).

Nap/Nrf system is typically associated with DNRA and repressed under high [NO_3^-] in contrast to Nar, associated with denitrification, which is activated predominantly under high [NO_3^-] (Chen & Wang, 2015; Cole, 1996; Stewart et al., 2002; Tyson et al., 1993; Henian Wang et al., 1999; Xiaoguang Wang et al., 2019). As a result, DNRA becomes insignificant in the fertilised paddy soil (Pandey et al., 2018b) compared to denitrification. In addition to this competition for nitrate quality of carbon, C: N-NO_3^-, and [NO_2^-]:[NO_3^-] ratios modulate the source partition of NO_3^- between denitrification and DNRA (Pandey et al., 2020). For example, NO_3^- reduction into NH_4^+ through DNRA is favoured at higher C: N-$NO_3^-$and [NO_2^-]:[NO_3^-] ratios (Pandey et al., 2020; Putz et al., 2018; Senbayram, et al., 2022; Yoon et al., 2015). NO_2^-/NO_3^- derived through nitrification is easily transported to the anaerobic soil microsites from the aerobic soil microsites associated with nitrification due to high mobility in the soil. This can lower the C: N-NO_3^- ratio, imbalance the [NO_2^-]:[NO_3^-] ratio and facilitate denitrification over DNRA. The high NO_3^- concentrations might lower the reduction of the final denitrification step, N_2O, to N_2 mediated by nitrous oxide reductase (Gaskell et al., 1981). Thus, the complex interaction between the different nitrogen cycle-associated bacterial groups and the abiotic conditions in soil determines the N_2O emission potential from rice paddies (Xiao et al., 2023).

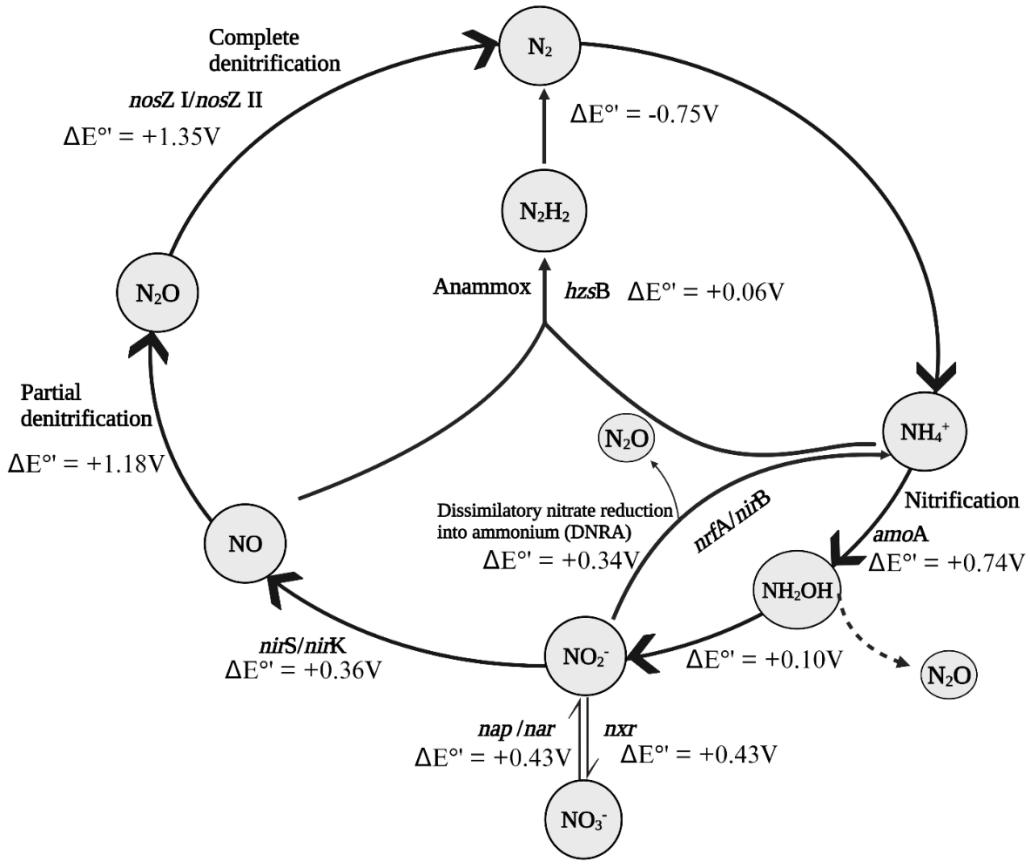

Fig 1 6: Nitrogen cycle processes with functional marker genes of interest in this study marked in italic letters. ΔE°′ is the standard redox potential of each redox pair (oxidised/reduced).

1.6 Microbial pathways responsible for N_2O emission from agricultural land

Microbial pathways (predominantly nitrification and denitrification) are responsible for more than 80% of total global N_2O emissions (Fowler et al., 2015). N_2O is produced as a byproduct during nitrification, and in suboxic conditions, instead of releasing nitrite into the soil, further covert into N2O through nitrifier denitrification (Zhu et al., 2013). N_2O is produced through denitrification when truncated. DNRA bacterial communities that reduce NO_2^- into NH_4^+ via NO also can produce N2O through an additional pathway during DNRA (Einsle et al., 2002; Kern & Simon, 2009) (Fig:1.6). But the amount of N_2O derived through DNRA from agroecosystems is negligible compared with the nitrification and denitrification contribution (Rütting et al., 2011; Stremińska et al., 2012; Yoon et al., 2019). Nitrification and denitrification can happen simultaneously due to

the presence of aerobic and anaerobic microsites within the same soil or even within the same aggregates (Giles *et al.*, 2012). Depending on the soil conditions, denitrification or nitrification dominates N_2O emissions, e.g., over 80% WFPS denitrification dominates in N_2O emission (Bateman and Baggs, 2005; Baggs, 2011).

1.7 Irrigation management systems exacerbate N_2O emission from rice paddies

Agriculture is the primary source of non-CO_2 GHGs such as CH_4 and N_2O producing approximately half of all CH_4 and N_2O emissions (EPA-2020). Carbon present in rice root exudates is easily converted into CH_4 through the methanogenesis process in the flooded conditions of paddy soil (Conrad, 2007; Hou et al., 2022). An intermittent flooding strategy, as an irrigation management system, is frequently applied in rice fields to suppress CH_4 emissions by increasing O_2 availability (Liao et al., 2021; Meijide et al., 2017). Nevertheless, the drainage, while intermittent flooding, stimulates a sharp increase in N_2O emissions (Cai et al., 1997). The gradual decrease of water level during drainage of rice fields increases aeration and might irreversibly inhibit N_2O reductase enzyme activity because the enzyme is more sensitive to oxygen exposure than other denitrifying enzymes. As a result, the last step of denitrification, N_2O reduction into N_2, is inhibited, and N_2O consumption by *nos*Z clade II is also reduced. Complete denitrification and N_2O consumption are even lower in the extended drying period than in the shorter (Smith & Patrick, 1983). Alteration of the water regime mainly controls the redox potential (Eh), influencing the production of two gases as the emission of CH_4 and N_2O are negatively correlated. Emission of N_2O is escalated in higher soil Eh (+0.25V) in contrast to low soil Eh (-0.15 V), favouring CH_4 production more (Fig: 1.6) (Liang et al., 2022; Majumdar, 2003). Alternate wetting and drying (AWD) might increase N_2O emissions through nitrification. So, when managed with intermittent irrigation, there is an apparent trade-off between CH4 and N2O emission in rice paddies (Cai et al., 1997).

1.8 Rice plants can modulate nitrification

Multiple strategies, such as oxygenation, BNI secretion, and/or the association of arbuscular mycorrhizal fungus (AMF), might be involved in the modulation of nitrification in the rice rhizosphere. Oxygenation in the rice rhizosphere facilitates nitrification and increases BNI secretion and AMF association. AMF might increase N supply to the plants, thus reducing nitrification by limiting substrate for nitrification and/or increasing carbonaceous compounds in the root exudates, which might have BNI activity.

1.8.1 Oxygenation

Rice plants grown in paddy systems develop aerenchyma in the roots, gas-filled tissues that counterbalance anaerobic conditions in the flooded paddy soil (Fig: 1.7C). It allows a low-resistance pathway for O_2 diffusion inside the roots to the growing root tip, thus enabling rice root respiration in the flooded paddy soil (Yamauchi et al., 2013). Oxygen diffused from the rice root surface supports nitrification in the narrow space of the rhizosphere (Fig: 1.7B). So, regulating oxygenation is the key strategy for rice plants to modulate nitrifiers since nitrification is strictly aerobic.

1.8.1.1 Formation of aerenchyma

The aerenchyma of rice roots are formed in two ways: constitutively and inducibly. During cortical cell separation while rice root development, aerenchyma is constitutively formed at the middle lamella of the cortex cells and further induced as a response to the soil environment (Colmer & Voesenek, 2009; Drew et al., 2000; Takahashi et al., 2014). Auxin/indole-3-acetic acid protein regulates the constitutive root aerenchyma formation in the rice root through auxin signalling (Yamauchi et al., 2019). In contrast, reactive oxygen species (ROS) produced due to oxidative stress in the root cells and ethylene induce lysigenous aerenchyma formation by the ethylene signalling pathway (Fig: 1.7C) (Yamauchi et al., 2017; Yoo et al., 2015). Lysigenous rice aerenchyma, after induction, is formed by cortical cell death and dissolution in the middle of a rice root cortex (Kawai et al., 1998). The programmed death of cortical cells provides porous space for molecular O_2 transportation and reduces respiratory costs by depleting the consumption of carbohydrates (Drew *et al.,* 2000; Colombi *et al.,* 2021). Atmospheric O_2, transported from shoot

to root via aerenchyma, entrapped in the root aerenchyma, tends to diffuse radially in the rhizosphere rather than longitudinally to the root tip due to the steep concentration gradient between root and rhizosphere paddy soil (Lai et al., 2012; Lin et al., 2022).

Rice plants develop a barrier to radial oxygen loss (ROL) composed of suberin and/or lignin within the epidermis of the root surface to minimise ROL, thus ensuring sufficient O_2 to the root tip (Armstrong W., 1971; Kotula *et al.*, 2009) (Fig:1.7C). (Shiono et al., 2014) reported that genes associated with suberin biosynthesis rather than genes associated with lignin biosynthesis strongly upregulated while forming the barrier to ROL in the rice root. So, suberin is the significant component in the barrier to ROL in rice roots. While suberin biosynthesis, malic acid accumulation in the roots is increased. It is the precursor for long-chain fatty acid biosynthesis and is converted into acetyl CoA by a plastid-bound enzyme in the rice roots. Later, biosynthesised long-chain fatty acids are used in suberin biosynthesis (Kulichikhin et al., 2014). Phytohormones (e.g. abscisic acid (ABA), Brassinosteroids (BRs)) and organic acid accumulation in the rhizosphere trigger deposition of suberin and lignin as a barrier to ROL in the outer part of the rice root (Arch et al., 2001; Colmer et al., 2019; Ogorek et al., 2023; Shiono et al., 2022). Rice plants can manipulate nitrification in the rhizosphere indirectly by controlling the rhizosphere's oxygen status by forming the lysigenous aerenchyma and the barrier to radial oxygen loss (ROL) (Hu et al., 2023; Li et al., 2008; Li & Wang, 2013).

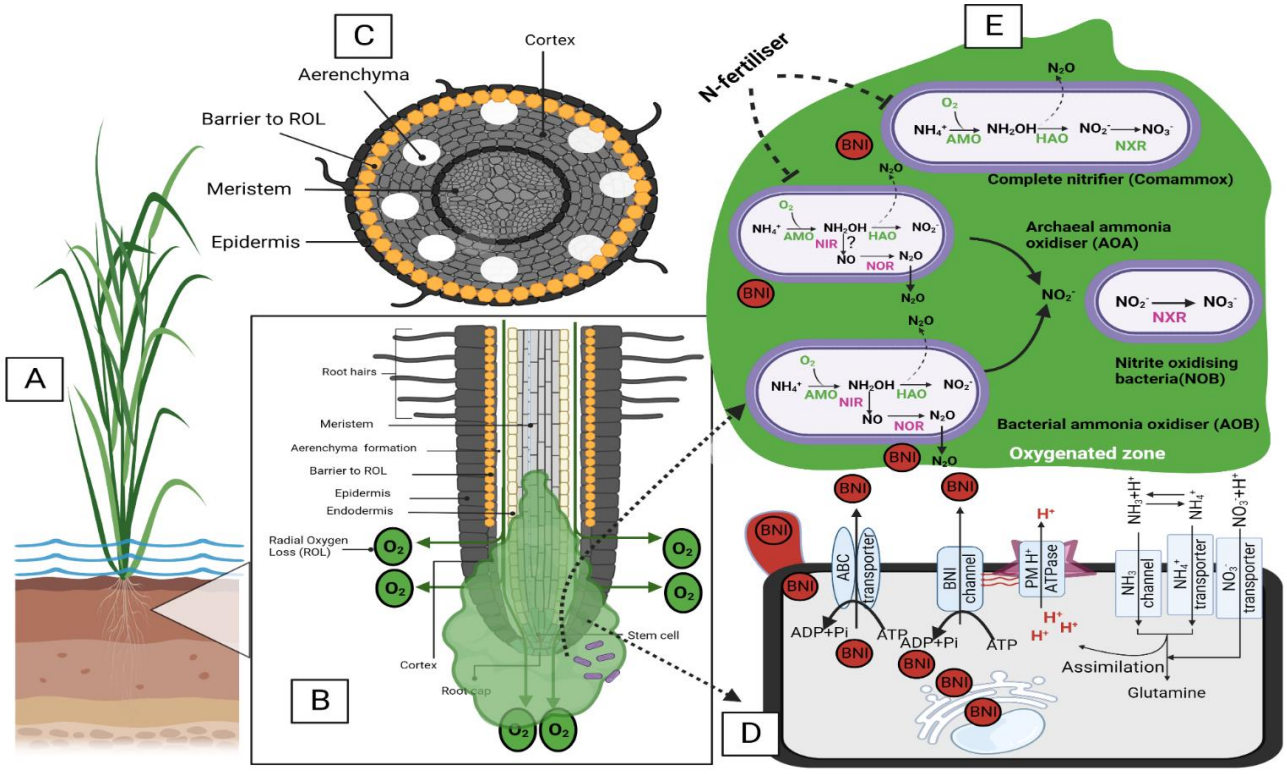

Fig 1.7: Possible mechanisms of rice rhizosphere effects on the nitrifier community. (A) Rice plant at tillering stage (B) Vertical root architecture (C) Horizontal root transsection (D) Root epidermal cell (E) Oxygentated zone in the rhizosphere where nitrification occurs covering near the root tip and associated root surface from where O_2 radially diffused.

1.8.2 Biological nitrification inhibition

Rice plants can inhibit nitrifier activity directly by secreting phenolic compounds and secondary metabolites as root exudates, termed Biological nitrification inhibitors (BNIs), categorised into hydrophilic and hydrophobic BNIs (Subbarao et al., 2015, 2009; Subbarao et al., 2017). Likewise, other secondary metabolites produced by the root system, hydrophilic BNIs, are released utilising proton motive force through H+-ATPase or Voltage-gated anion channels like MATE transporters in the cell membrane. ATP-binding cassette (ABC) transporters as active efflux channels are also used for the secretion of hydrophilic BNIs into the rhizosphere from roots (Fig:1.7D) (Zhang et al., 2022). In contrast, due to their hydrophobicity, the vesicle traffic process mediates hydrophobic BNIs secretions and typically remains close to the root. So, after secretion into the rhizosphere, they are firmly adsorbed by soil particles within the rhizosphere (Subbarao et al., 2012). On the contrary, hydrophilic BNIs travel further from the rhizosphere to bulk soil due to water solubility, which allows nitrification inhibition beyond the rhizosphere. (Yu et al., 2016) reported 1,9-decanediol as hydrophilic BNI, found in the rice root exudates, inhibits ammonia monooxygenase (AMO) activity, initiating enzyme in NH_4^+ oxidation of nitrification pathway. Indeed, applying 1,9-decanediol in the paddy soil reduced nitrifiers, both bacterial and archeal ammonia oxidisers' abundance, and was associated with reduced N_2O emission (Yufang Lu et al., 2019). Secretion of BNIs in the rhizosphere positively correlates with rice plants' nitrogen uptake efficiency (NUE) by inhibiting nitrification, suppressing AMO and/or HAO to increase NH_4^+ retention and reduce N losses in the rhizosphere (Chen et al., 2022; Coskun et al., 2017). NH_4^+ is preferentially taken up by the low-land rice varieties even though they can grow in the presence of both NH_4^+ and NO_3^- (Craswell & Vlek, 1983; Wang et al., 1993; Qian *et al.*, 2004; Chen *et al.*, 2022).

1.8.3 Rice mycorhizal associations

Mycorrhizal fungi, including endomycorrhiza (also known as arbuscular mycorrhizal fungi, AMFs), vesicular-arbuscular mycorrhizas (VAM), and ectomycorrhiza (ECMs), are categorised depending on their colonisation mechanisms in the hosts. AMFs colonise rice roots by penetrating the root cortex and extending their hyphae outside the roots; in contrast, ECMs likely colonise outside the root surface. AMFs only belong to the Glomeromycota phylum, and ECMs belong to

diverse phyla, including Basidiomycota, Ascomycota, and Zygomycota phylum (Brundrett, 2004). Though AMFs belong to a single phylum, the Symbiotic compatibility varies depending on the AMF genotype with rice cultivars (Guigard et al., 2023). *R. irregularis*, the most compatible AMF partner of rice, with high root colonisation intensity, confer beneficial effects on rice growth and increase disease resistance. Establishing a mutualistic relationship between AMF and rice cultivars is not confined to only better rice growth and disease resistance. Rice plants can modulate N-cycling processes through AMFs as they increase plant uptake of soil N in exchange for photosynthates. Thus, nitrification can be reduced by limiting the substrate for nitrification and/or increasing carbonaceous compounds in the root exudates, which might have BNI activity. (Sun et al., 2023) reported that AMFs suppress ammonia oxidisers through substrate competition rather than the production of BNI. Successful establishment of a mutualistic relationship between AMFs and rice cultivars reduces ammonia volatilisation and N_2O emissions by shifting soil bacterial community (He et al., 2023). Nevertheless, the flooding conditions of the paddy system attenuate the AMF colonisation in the rice roots, as oxygen is a prerequisite for AMF growth (Klinnawee et al., 2021).

1.9 Rice plants can modulate denitrification

Denitrification is limited in the distal distance of rice roots due to oxygenation. So, it is critical to understand how rice plants can modulate the denitrifiers present in the bulk soil. In addition, rice rhizospheric effects on the fate of end products during denitrification. Genetic complements of denitrifier communities present in the soil as biotic factors, and carbon, oxygen, moisture content, and nitrogen availability are abiotic factors that regulate denitrification in the soil. Rice plants can modulate denitrification by altering soil biotic and abiotic factors through rhizospheric effects.

1.9.1 Rice plants can control the completion of denitrification by regulating biotic factors

Many factors can determine if denitrification is completed. One of these relates to the gene complement of the soil denitrifier community. Reduction of N_2O into N_2, the last step of denitrification, is the key to mitigating N_2O emission from soil because it is the only known biological N_2O sink process that is catalysed by N_2O reductase enzyme (Nos). Clearly, denitrifiers lacking this enzyme will inevitably produce N_2O during denitrification. However, this N_2O could be consumed and reduced into N_2 by other denitrifiers, including another group lacking denitrifying enzymes other than a distinct form of nitrous oxide reductase, *nos*Z clade II (Jones *et al.*, 2013). The abundance of the *nos*Z clade II denitrifier community thus plays a crucial role in N_2O sink from arable soil (Domeignoz-Horta et al., 2018).

In contrast, complete denitrifiers (containing *nos*Z clade I) can produce a complete set of reductase enzymes with a combination of either (NirK) or (NirS) with these genes mutually exclusive (Jones et al., 2008). Complete denitrifiers do not always conclude the total denitrification pathway despite having all reductase enzymes. When complete denitrification is truncated, N_2O is produced and termed partial denitrification (Fig: 1.7) (Firestone et al., 1980; Graf et al., 2014; Huang et al., 2019; Philippot et al., 2009). NirK-type denitrifiers are more likely to perform partial denitrification due to a lower frequency of co-occurrence of *nosZ* with *nirK* than with *nirS* (Graf et al., 2016). Root-derived carbon directly affects the abundance of NirS and NirK-type denitrifier communities in the rhizosphere (Hou et al., 2018). So, in soil, the relative and absolute abundance of different denitrifier communities is a biotic factor that restricts the emission of N_2O.

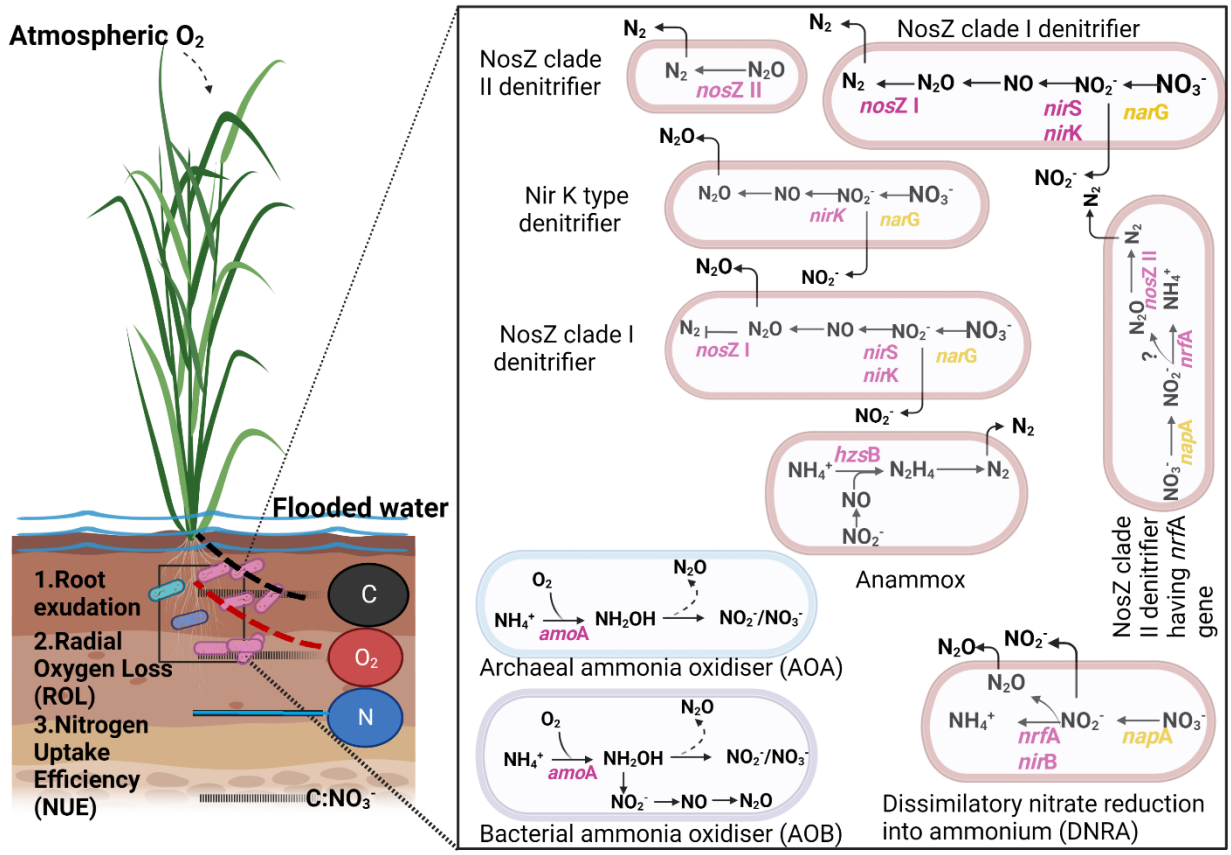

Fig 1.8: Possible mechanism of rice plants modulation effects on denitrifiers community. The denitrifer community and ammonia oxidiser bacteria were indicated by purple and blue, respectively.

1.9.2 Soil abiotic factors regulate N_2O emission

Several abiotic factors modulate denitrifier activity, and thus, the proportion of nitrous oxide is converted to nitrogen (Wallenstein et al., 2006). These include pH, O_2 availability, NO_3^- concentration, soil moisture or Water-filled Pore Space (WFPS) and available respirable carbon, all of these and the ratios between them influence the end product produced during denitrification (Fig: 1.8) (Bateman & Baggs, 2005a; Baumann et al., 1997; Burford & Bremner, 1975; Herold et al., 2018; Klemedtsson et al., 1991; N. Morley & Baggs, 2010; Šimek & Cooper, 2002; Smith & Tiedje, 1979). For instance, O_2 limits reductase enzyme activity by controlling electron transport components' redox state and repressing denitrifying genes' expression (Berks et al., 1995). In addition, oxygen can limit the NO_3^- uptake and nitrate reduction by blocking NO_3^- transportation

from the periplasm to the cytoplasm in the denitrifiers (Hernandez & Rowe, 1987). Frequently, O_2 can shut down the denitrification process partially depending on O_2 concentration and time length of exposure because N_2O reductase is permanently damaged when exposed to oxygen due to oxidative stress (Knowles, 1982; Morley & Baggs, 2010). The remaining three denitrification reductase enzyme activity is reversibly altered after oxygen exposure. So, temporal N_2O emission from arable soil increases notably for partial denitrification after shifting oxic to an anoxic condition or vice versa due to fluctuation of WFPS and also for plant and heterotrophic microbial respiration (Verhoeven et al., 2018b).

Soil pH is another abiotic denitrification influencing factor. At low pH, the NirS-type denitrifier community's abundance is decreased more than the NirK-type denitrifier community (Herold et al., 2018). Also, N-oxide reductase activity is regulated by the pH condition of the soil, and their activity becomes optimum in neutral to alkaline pH. Nevertheless, N_2O reductase activity is inhibited most among other N-oxide reductases at low pH. So, denitrification-associated N_2O emission is increased from soil under low pH due to depletion ratios of NirS: NirK type denitrifier community abundance and inhibition of N_2O reductase activity.

The availability of respirable carbon as a reductant and NO_3^- content as a substrate during denitrification are crucial for regulating the proportion of N2 and N_2O production released as the end product (Blackmer & Bremner, 1978). Not only are respirable carbon concentrations available from root exudates, but different types of organic carbon compounds influence different concentrated emissions of N_2O and N_2 (Giles *et al.*, 2017). So, these abiotic factors control the fate of denitrification by suppressing the last step of the denitrification pathway that facilitates N_2O formation as the terminal product (Hallin *et al.*, 2014; Huang *et al.*, 2019).

1.10 Research question and hypothesis

Nitrogen loss, including N_2O emission and retention in the paddy soil after artificial nitrogen addition, depends on the interaction between rice plants and nitrogen cycle-associated microbes. Multiple rice plant strategies might involve controlling key steps in the microbial nitrogen cycle. Nevertheless, a comprehensive study of how rice plants influence microbial nitrogen transformations to increase nitrogen availability and retention after fertilisation in the plant-soil

system remains unexplored. Rice plants can modulate nitrification through radial oxygen loss (ROL) and biological nitrification inhibition (BNI) activities to maximise nitrogen uptake efficiency (NUE) after nitrogen fertilisation while growing in the flooded paddy soil. (Zhang et al., 2019) reported that the oxygenation in the rhizosphere increased the BNI secretion from rice roots. These two activities embedded in rice plants' genetics modulate nitrification antagonistically in the rhizosphere. In addition, nitrification variations between rice genotypes elicit variations of C: NO_3^- ratios in the bulk soil that might alter denitrification. Rice plants can also directly affect the C quantity and quality through root exudations. (Jiang et al., 2016) reported variation in N_2O emission between two rice genotypes due to photosynthate allocation variations belowground. (Giles et al., 2017) showed that different organic carbon alters the denitrification process; for instance, glucose and glutamine increase N_2O emission; in contrast, citrate reduces N_2O emission. (Langarica-Fuentes et al., 2018a) did an experiment to observe the response of denitrifier communities to artificial root exudates, and they found *Nir*S and *nos*ZI more responsive than the *Nir*K and *nos*ZII. Indeed, significant N_2O emission variation has been measured among barley cultivars due to different root exudations (Not published by Tim J Daniell's research group). Nitrification and denitrification variations might also trigger variations among rice genotypes on anammox and DNRA due to nitrite dependency of anammox from other microbial Ncycle processes and nitrate competition of DNRA with denitrifiers, respectively. So, rice genetics might be identified after comparing the SNPs variations with these process rate among the tested rice genotypes variations through GWAS analysis. Genome-wide association study (GWAS) is frequently used to identify the genetic markers of crops to improve the crop variety. For instance, GWAS was used to identify the genetic markers responsible for aerenchyma-mediated radial oxygen loss, carbon and nitrogen storage in grain and increasing straw biomass of rice (Norton et al., 2018; L. Tang et al., 2019; Van Duyen et al., 2022). However, GWAS analysis has yet to explore rice genetic markers responsible for the modulation of N-cycle-associated microbes in the rhizosphere. (Oyserman et al., 2021) suggested that GWAS might efficiently identify the genetic markers of plants involved in plant-soil microbial interactions after combining microbial population genetics with sufficiently large and genetically diverse plant populations. So, I hypothesised that microbial nitrogen cycle processes associated with nitrogen loss and retention (e.g., nitrification, denitrification, anammox and DNRA) might vary among rice cultivars. If microbial nitrogen transformations varied, rice genetic markers associated with N loss and N_2O

emission might be identified through GWAS for rice selection breeding to mitigate N_2O emissions from rice cultivation. I also hypothesised that denitrification might dominate N_2O emission in fertilised flooded paddy soil as nitrification remains active in the rhizosphere.

1.11 Aims and Objectives

This research project aims to screen selected rice cultivars from south-eastern Asia based on fertiliser-induced microbial nitrogen transformations (e.g., nitrification, denitrification, anammox and DNRA) and, if these processes varied, decipher the mechanism of the variations by genome-wide associations study (GWAS). I planned a single microcosm experiment to screen the selected rice cultivars rather than doing separate microcosm incubations to avoid biases while measuring the microbial nitrogen transformations. To measure the four microbial nitrogen transformation processes simultaneously, I also aimed to apply the ^{15}N stable isotope model. Before the rice screening microcosm experiment, I aimed to run a mini experiment to test the ^{15}N stable isotope ratio modelling in simultaneously measuring the four microbial transformations. Indeed, to understand the dynamics of the nitrogen cycle processes after fertilisation by growing rice with paddy soil to optimise the rice screening conditions.

Chapter 2: Understanding the microbial N-cycle dynamics (Nitrification, denitrification, DNRA and anammox) by growing contrasting nitrification-associated rice in paddy soil after adding N-fertilisers.

2.1 Introduction

2.1.1 Flooded paddy soil is an artificial wetland and a potential source of N_2O emissions following N-fertilisation

Nitrous oxide (N_2O) is a potent greenhouse gas, with a global warming potential 298 times that of carbon dioxide, which can persist in the environment with a half-life of more than 100 years (Forster & Ramaswamy, 2007; Kanter *et al.*, 2013). Agriculture is responsible for approximately two-thirds of the N_2O emissions, driven by intensive N-fertilisation (Janssens-Maenhout et al., 2019; Prokopiou et al., 2018; Wells et al., 2018). Rice cultivation single-handedly contributes around 12.1 % of agricultural N_2O emissions (FAO, 2020)**.** Inherently poor Nitrogen fertiliser use efficiency, over-fertilisation and agronomic practices such as irrigation management drive the high emissions observed from paddy soils (Jiang et al., 2019). Rice is typically grown in lowland paddy soil, maintaining flooded conditions until before harvesting, making rice fields unique agroecosystems and anthropogenic wetlands (Kögel-Knabner et al., 2010). Flooding acts as a barrier between the topsoil and the atmosphere, consequently cutting off the oxygen supply, with water replacing the gaseous phase in the soil pores. Within 24 hours, oxygen availability is depleted from the bulk topsoil due to reduced oxygen diffusion in water than in air, which is four orders of magnitude lower (Gao *et al.*,2002; Boivin *et al.*, 2002; Tanji *et al.*, 2003). Oxygen limitation in flooded paddy soil inhibits aerobic microbial activities like nitrification (H. Liu et al., 2019; Verhoeven et al., 2018a). In addition, it directs the microbial activities in the soil microsites, switching aerobic to facultative or obligate anaerobic respiration (e.g. Denitrification, DNRA and anammox) where alternative electron acceptors to oxygen are utilised. Nitrogenous compounds as alternative electron acceptors become more available after N-fertilisation in the flooded paddy, increasing the N_2O emission through partial denitrification (Fig: 2.2.1) because high NO_3^- concentrations lower the reduction of the final denitrification step, N_2O, to N_2 (Gaskell *et al.*, 1981; Bateman & Baggs, 2005; Giles *et al.*, 2012). Consequently, adding N-fertiliser to the paddy soil lowers the C/NO_3^- ratio exacerbated N_2O emission by increasing denitrification and relatively reducing DNRA activity, a nitrogen retention process that competes with denitrification (A. Pandey et al., 2018a).

2.1.2 Rice rhizosphere oxygenation effects on N_2O emissions from the fertilised flooded paddy soil

Anaerobic conditions prevail in flooded paddy soil, but rice plants transport oxygen by diffusion through aerenchyma formed when grown in flooded soil. Oxygen leaks from the root surface by radial oxygen loss (ROL), oxygenating the rhizosphere (Armstrong, 1971) and diffusing across a gradient into the surrounding bulk soil. Therefore, the rice rhizosphere can support nitrification and limit denitrification in that oxygenated zone. Also, O_2 inhibits the last step of the denitrification process because N_2O reductase is permanently damaged when exposed to oxygen, facilitating temporal N_2O emission (Knowles, 1982; Morley & Baggs, 2010). N_2O is also produced through autotrophic nitrification, nitrifier denitrification and coupled nitrification-denitrification. There remains uncertainty between nitrification and denitrification on which pathway dominates N_2O emission from fertilised paddy soil (Baggs, 2011). The DNRA bacterial community can even produce N_2O by an alternative pathway during DNRA (Einsle et al., 2002; Kern & Simon, 2009).

2.1.3 Rice root exudate's effects on N_2O emissions from the fertilised flooded paddy soil

Denitrification and nitrification are responsible for more than 80% of total agricultural N_2O emissions (D. Fowler et al., 2015). However, denitrification is recognised as the primary pathway for the emission of N_2O from fertilised paddy soil (Kool et al., 2011). N_2 is produced when denitrification is complete, but the process is often truncated, resulting in the release of N_2O (Firestone *et al.*, 1980; Zumft, 1997; Philippot, 2002). The availability of respirable carbon as a reductant and NO_3^- content as a substrate during denitrification are crucial for regulating the proportion of N_2 and N_2O production released as the end product, depending on the soil conditions (Blackmer & Bremner, 1978). N_2O reduction into N_2 decreased at low C: NO_3^- thus increasing N_2O emission (Giles et al., 2012). The quantity of carbon in the root exudates depending on NO_3^- concentration in the soil controls the denitrification rate as carbon fuels denitrification. Not only available respirable carbon concentrations but also types of organic carbon compounds influence different concentrated emissions of N_2O and N_2 (Giles *et al.*, 2017). So, rice plants could regulate N-fertiliser-induced N_2O emissions by providing respirable carbon and influencing denitrifier

communities in the soil through root exudation (Jiang et al., 2016)(Langarica-Fuentes et al., 2018a).

2.1.4 N-cycle processes are interconnected in the oxic/anoxic interface between the rice rhizosphere and surrounding bulk soil

The rhizosphere is the zone around plant roots influenced by the root's activity in contrast to the bulk soil further away from the root (Fig: 2.2.1). The rice rhizosphere is an oxygenated soil zone, whilst paddy bulk soil is mainly anoxic. However, diffused oxygen may oxygenate the bulk soil across a gradient. N-cycle processes (Nitrification, denitrification, DNRA and anammox) are interconnected and likely to coincide around the oxic-anoxic interface of the rice rhizosphere and surrounding bulk soil (Nie et al., 2019; Nie et al., 2015)

Variations in nitrification rate in soil supporting different rice genotypes have been reported due to variations in a range of factors, including oxygenation, nitrogen uptake efficiency (NUE), pH and biological nitrification inhibitions (BNI) (Hu et al., 2023; Li et al., 2008; Li & Wang, 2013; Sun et al., 2016; Yu et al., 2016). Denitrification is regulated by nitrification in the rice rhizosphere and depends on the NUE of rice depending on the types of applied N (Yang et al., 2017). Nitrification fuels denitrification in the surrounding bulk soil of rice rhizosphere by providing NO_3^- as substrate through coupled nitrification-denitrification (Arth et al., 1998). N_2O is also produced through nitrification as a byproduct during NH_4^+ oxidation and nitrifier denitrification under low oxygen availability, which is also likely to contribute to N_2O emission (Lipschultz et al., 1981; Firestone and Davidson, 1989; Zhu et al., 2013). Nitrification might be responsible in N_2O emission variations in the rice rhizosphere. Nitrification and denitrification need to be measured simultaneously to measure the potential of nitrification in N_2O emission variations between the contrasting nitrification rice cultivars. So, the following hypotheses have been made:

- There would be a difference in the emission of N_2O after adding N-fertiliser between rice cultivars with varied nitrification rates.
- DNRA might not be involved in the N_2O emission variations between the contrasting nitrification-associated rice cultivars.
- It would be possible to partition the emitted N_2O between denitrification and nitrification using stable isotope methods, as these processes utilise different nitrogen sources.

- It would also be possible to measure the N_2O reduction into N_2 by dissecting the emitted N_2 source between complete denitrification and anammox using a single stable isotope.

2.2 Aim and Objectives

To test the hypothesis, I analysed the previously collected gas samples from the rice screening based on nitrification variations. A previous PhD student from our lab group screened 56 rice lines with four randomised blocks using the ^{15N}nitrate pool dilution method. She collected gas samples before harvesting the microcosm pots to measure the gross nitrification rate (GNR). After analysing the gas samples through an isotope ratio mass spectrometer (IRMS), I found no significant variations among the 56 rice lines, even though these lines were significantly varied based on GNR. The source of emitted N_2O measured from gas samples might be DNRA, but it is impossible to dissect the source partition between DNRA and denitrification because both processes utilise the same nitrate pool. Though it is impossible to source partition of emitted N_2O between DNRA and denitrification, it is possible to source partition of N_2 between complete denitrification and anammox after discussions with my supervisors. So, I decided to understand the nitrogen cycling dynamics up to five days after N-fertilisation using two rice lines with contrasting nitrification rates from the previous study (High and low nitrification-associated rice cultivars). I used a similar microcosm supporting rice growth differentiated rhizosphere (oxic) and bulk (anoxic) compartments from the previous rice screening study. The study had three main objectives.

1. To measure the four nitrogen cycle process rates simultaneously, rather than the potential rates up to five days after N-fertilisation, by applying the ^{15}N nitrate as a tracer.
2. Dissecting the mechanisms involved in the N-cycle processes variations between the tested rice cultivars.
3. To design a robust screen to assess differences in N cycling rates in soil-supporting rice cultivars by using the results from this experiment.

2.3 Methodology

2.3.1 Microcosm soil packing

Paddy soil for this study was imported from the International Rice Research Institute (IRRI) farm in Los Baños, Philippines (14° 10′ 12″ N, 121° 15′ 25.2″ E), a field under standard agronomic practice with urea fertilization and a typical rice-rice crop rotation. The site has a tropical monsoon climate with a yearly precipitation of 1860.8 mm and an average yearly temperature of 26°C. The paddy soil's basic properties were clay 21.5 %, $N\text{-}NH_4^+$ 35 mg kg^{-1}, NO_3^- 1.5 mg kg^{-1} and pH 6.5. The microcosm pot, with a 5 cm diameter and 7 cm height (Fisher Scientific, UK), was used to grow rice plants and compartmentalised into rhizosphere and bulk compartments, with each representing 50% of the total soil (Fig: 2.3.1). This was achieved by first packing the rhizobag with a bulk density 1.2 g/cm^3 dry weight soil outside of the microcosm pot in a plastic pipe (4cm diameter and 5 cm height) lined with 35µm nylon mesh barrier (Plastok, UK). The packed rhizobag was placed at the centre of the microcosm pot, followed by packing the bulk soil using a similar bulk density with the rhizosphere compartment in situ (Fig: 2.3.2). Prepared soil microcosms were flooded and incubated for seven days before seedlings transfer with a 12 h 30°C: 12 h, 26°C light: dark cycle, at 65% humidity at the Arthur Willis Environment Centre, University of Sheffield, UK.

2.3.2 Seed germination

The study was designed to grow each line with four replications for a single day. So, considering germination rates, seventy rice seeds of each rice cultivar were germinated by submerging them with 15ml of deionised water in a plastic petri dish (8 seeds per plate). The plastic petri dishes were incubated for 7 days in a growth cabinet with a 12 h 30°C: 12 h, 26°C light: dark cycle, at 65% humidity at the Arthur Willis Environment Centre, University of Sheffield, UK.

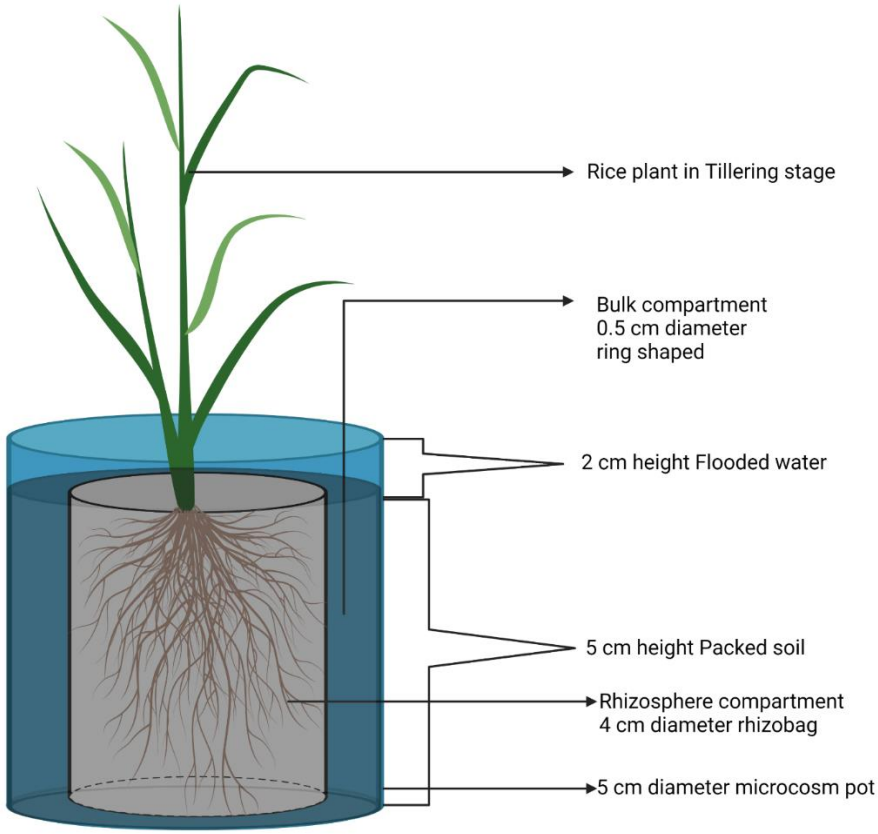

Fig 2.3.1 Rice microcosm pot with two distinct compartments: a rhizosphere compartment, established with a rhizobag with rice roots indicated by the grey colour at the centre of the pot and 0.5 cm ring-shaped bulk compartment indicated by the dark blue colour.

2.3.3 Rice seedling transfer and plant growth

Two germinated seedlings were planted near the centre of the rhizosphere compartment. NH_4NO_3 was applied into the microcosm pot as N-fertiliser at the recommended agronomic rate of 130 kg N/ha (IRRI recommended rate, http://irri.org/, 2017), equivalent to 200 μg N/g dry weight of soil. N-fertilisation was segmented into two periods. The first half was added to the pot on the 7^{th} day after the transfer of the seedlings when the weakest seedling was also removed from the microcosm. The second half was added at the tillering stage, on the 30^{th} day after seedlings transfer. During the second fertilisation, 5% ^{15}N labelled $NH_4{}^{15}NO_3$ was used as enrichment fertilisation. The microcosm experiment was done in a growth cabinet at the Arthur Willis Environment Centre, University of Sheffield, UK, and maintained the same growth condition of seed germination

(Section 2.2.3). The flooded condition was maintained in the microcosm pot throughout the rice growing period by watering every two days until microcosm harvesting. The growth and sampling of the experiment were summarised in (Fig: 2.3.2).

2.3.4 Harvesting the microcosm pots

Microcosm pots were destructively harvested at three points. The first (D0) was harvested on the point of enrichment fertilisation, the second (T0) immediately after the enrichment fertilisation and the final set was harvested daily after gas collection (T1, T2, T3, T4, and T5) (Fig:2.3.2). The rhizobag was removed during harvesting, and the roots were separated from the soil. Then the roots were washed, blotted dry and placed in a bag for biomass estimation. Rhizosphere and bulk soil were sieved separately and aliquoted with 20g used for KCl extraction, 10g for moisture content estimation, 3g for pH estimation and 0.5g for molecular analysis. The aliquots for molecular analysis were snap-frozen in liquid nitrogen and stored at -80^{o}C. The other assessments were performed on the day of harvest (Fig: 2.3.2).

2.3.5 Gas collection from Microcosm pots

After the enrichment fertilisation, gas samples were collected daily for 5 days (T1, T2, T3, T4, and T5) using a separate replicate for each sampling point. The shoot was removed by cutting and placed in a bag for drying. The microcosm pots were then placed immediately into 500 mL Kilner jars fitted with a suba seal, sealed and incubated for five hours. The syringe was repeatedly flushed into the jar before gas collection to ensure good mixing of gas across the jar, and then two reps of 15mL gas samples were collected hourly from each jar and stored in separate evacuated vacutainers (Labco Exetainer, UK). After taking gas samples, volume was maintained by injecting air into the jar. N_2O emitted, and $^{14/15}N$ balance of both N_2O and N_2 were measured from the collected gas samples by a continuous-flow ANCA GSL 20-20 Ion Ratio Mass Spectrometer (Sercon PDZ Europa, Cheshire, UK) at the Stable Isotope Facility, University of Sheffield.

2.3.6 Soil physical properties measurement

Soil physical properties measurement methods are described in the book "Methods of soil analysis, part 1, physical and mineralogical methods (2nd Edition)" by (Holliday, 1990). Briefly, a 3g soil aliquot for pH estimation was mixed at a 1: 5 w/v ratio with 0.05M $CaCl_2$ and continuously mixed with a magnetic stirrer. pH measurement was taken using a pH meter (JENWAY, Cole-Parmer Ltd, UK). Soil water content was assessed by mass loss after heating at 105^{o}C for 48 hours.

2.3.7 KCl extraction of soil

The soil was extracted with 2M KCl at a ratio of 1:4 (w/v) in 120 ml plastic bottles (VWR International, UK). The method is described in the book mentioned above (Holliday, 1990). Bottles were shaken for one hour before filtering through the Whatman no. 42 filter paper. Extracts were stored in 50mL falcon tubes at -20℃ for short-term use.

2.3.8 Soil nitrate analysis

Soil nitrate concentrations from KCl soil extracts were assessed using the reduction of vanadium(III) complex solution modified from (Miranda, 2001) adjusted by volume for a microtitre plate format. The principle behind the titration method is the reduction of nitrate by vanadium (III) complex solution and acidic Griess reaction (Miranda et al., 2001). Briefly, 0.5M VCl_3 dissolved in 1M HCl (Sigma-Aldrich, USA),2% sulphanilamide solution (SULF) (Sigma-Aldrich, USA) and 0.1% N-(1-Naphthyl) ethylene diamine di-hydrochloride (NEDD) (Sigma-Aldrich, USA) were mixed to prepare a vanadium(III) cocktail. 100 µl of soil KCl extracts and standards were transferred to a 96-well, flat-bottomed, polystyrene microtiter plate (Corning, USA). Immediately, 100 µl of vanadium cocktail was added and mixed with the samples. The plate was incubated in the dark for 10 hours at room temperature before absorbance measurement at 540 nm using the Tecan Spark 10M plate reader (Tecan, Switzerland).

2.3.9 Soil ammonium analysis

Ammonium NH4-N concentration was determined by the colourimetric analysis method relying on the ammonium ion reaction with a weakly alkaline mixture of sodium salicylate and hypochlorite in the presence of sodium nitroprusside (Baethgen & Alley, 1989). The assay was amended to microplate format, with volumes adjusted proportionally. Briefly, a salicylate cocktail solution was made with sodium salicylate (Sigma-Aldrich, USA), (tri)sodium citrate (Sigma-Aldrich, USA), sodium tartrate (Sigma-Aldrich, USA), sodium nitroprusside (Sigma-Aldrich, USA) and hypochlorite/NaOH solution (Sigma-Aldrich, USA). Soil extracts and standards (40µl) along with the salicylate cocktail solution (80µl) and hypochlorite (80µl) were mixed in a 96-well, flat-bottomed, polystyrene microtiter plate (Corning, USA) and incubated at room temperature for 45 minutes. The absorbance was measured at 650 nm in the Tecan Spark 10M plate reader (Tecan, Switzerland).

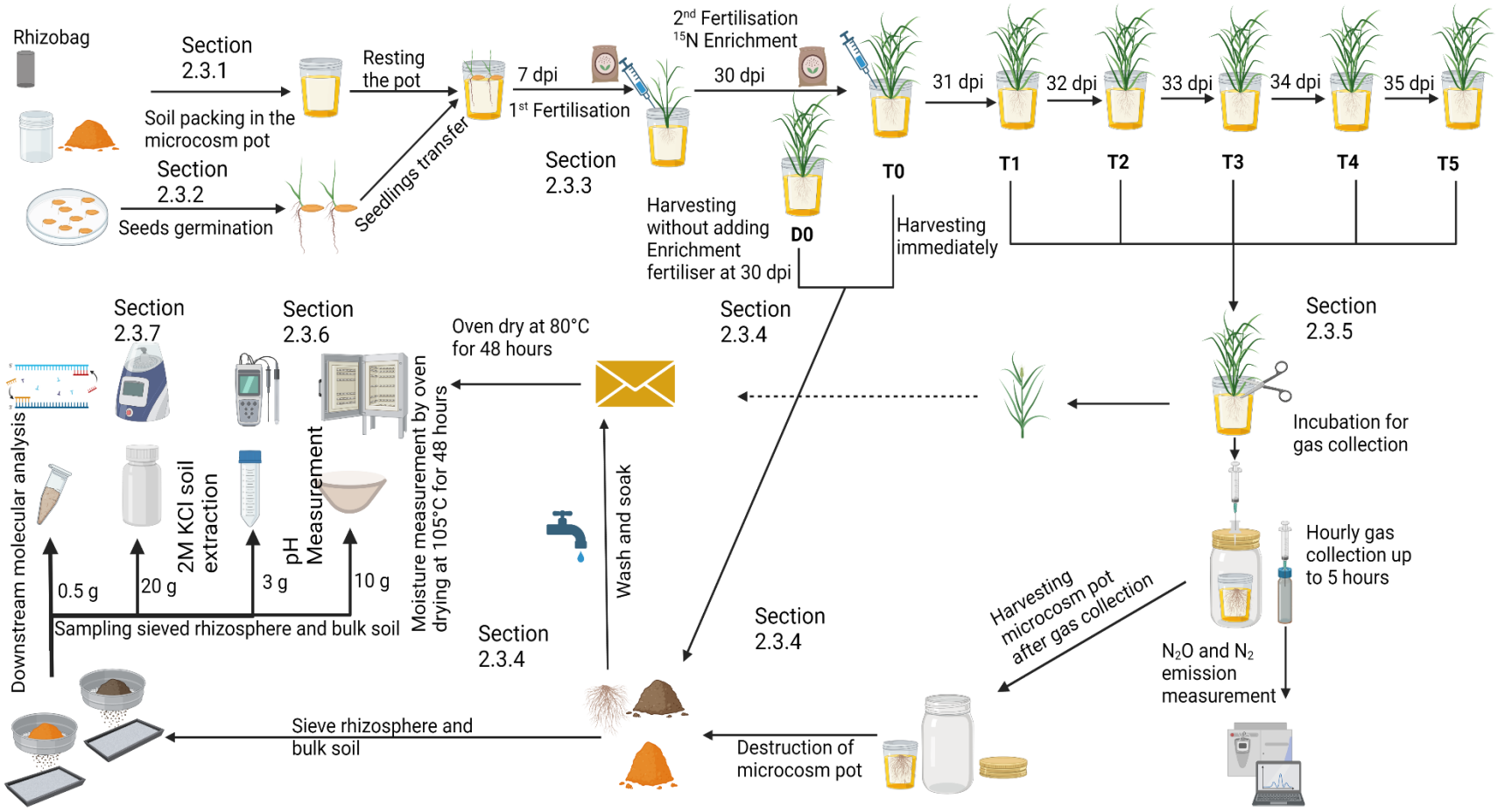

Fig 2.3.2: Schematic workflow of N-cycle dynamics measuring experiment showing microcosm soil packing to downstream collected samples analysis.

2.3.10 Assessment of ^{15}N enrichment from the KCl soil extracts

25 mL of the KCl extract was transferred into a gas leak-proof 60 ml plastic bottle (VWR International, UK), and a bent syringe needle with two 6 mm glass fibred filter disks (Whatman, GF/A, 6mm, UK) spiked with $KHSO_4$ (2.5 M) (Sigma-Aldrich, USA) attached to the lid using blue tack. The lid was immediately closed after adding 0.3 g anhydrous MgO (Sigma-Aldrich, USA) into the bottle to prevent loss of volatilised ammonium. Bottles were incubated for 7 days with gentle mixing three times over the diffusion period. After 7 days, the ammonia-diffused filter disks were removed and placed in tin capsules (Sercon, UK), and the bottle was left open for several hours to ensure all residual ammonia was volatilised. Two new $KHSO_4$-treated filter discs were then added with a new needle and blue tack for nitrate diffusion. Anhydrous MgO (0.05g) (Sigma-Aldrich, USA) and Devarda's alloy (0.25g) (Sigma-Aldrich, USA) were then added into the sample bottles along with a few drops of Brij 35 solution (to prevent bubble formation) (Thermo Scientific, USA) and the bottles again sealed. After 7 days, the nitrate filter disks were removed, placed in tin cups (Sercon, UK), dried at 40°C for 2 hours and stored in a desiccator before analysis. The collected $N\text{-}NH_4^+$ and $N\text{-}NO_3^-$ filter disks were analysed by a continuous-flow ANCA GSL 20-20 Ion Ratio Mass Spectrometer (Sercon PDZ Europa, Cheshire, UK) at the Stable Isotope Facility at the University of Sheffield for measuring ^{15}N atom % in $N\text{-}NH_4^+$ and NO_3^- from KCl soil extracts.

2.3.11 Measurement of N-cycling Processes rates

The four microbial reactive nitrogen transformations of nitrogen cycle processes were measured simultaneously by applying a ^{15}N stable isotope. The heavier ^{15}N stable isotope is known to be discriminated against compared to the more common ^{14}N during biochemical, biogeochemical and physiological processes due to a greater atomic mass (He et al., 2009). For instance, nitrate reductase, an enzyme that mediates the first step of denitrification, is reported to discriminate ^{15}N isotopes up to 5-30 % (Granger et al., 2004; Schmidt & Medina, 1991). (Carlisle et al., 2014) suggested that the ^{15}N enrichments in NO_3^- should be limited to less than 10 atom % to avoid the significant result drifting due to ^{15}N discrimination by the enzymes involved in the nitrogen biogeocycle. So, the application of a diluted ^{15}N stable isotope in the soil might effectively

minimise the ^{15}N isotope discrimination effects while measuring microbial nitrogen transformations. However, there must be a sufficient difference of $\delta^{15}N$ between the soil and atmosphere to measure dilution effects, and usually, the difference is approximately 3 to 4 ‰ (Boddey et al., 2000; Evans, 2001; Robinson, 2001; Shearer & Kohl, 1986). In this study, ~5 atom % of ^{15}N enrichments in NO_3^- was applied. Nitrification was measured by the degree of dilution of ^{15}N in the NO_3^- pool; in contrast, the DNRA rate was measured by the degree of enrichment of ^{15}N in the NH_4^+ pool. Partial and complete denitrification and anammox were separated by ^{14}N and ^{15}N balance in N_2 and N_2O (Fig: 2.2.3).

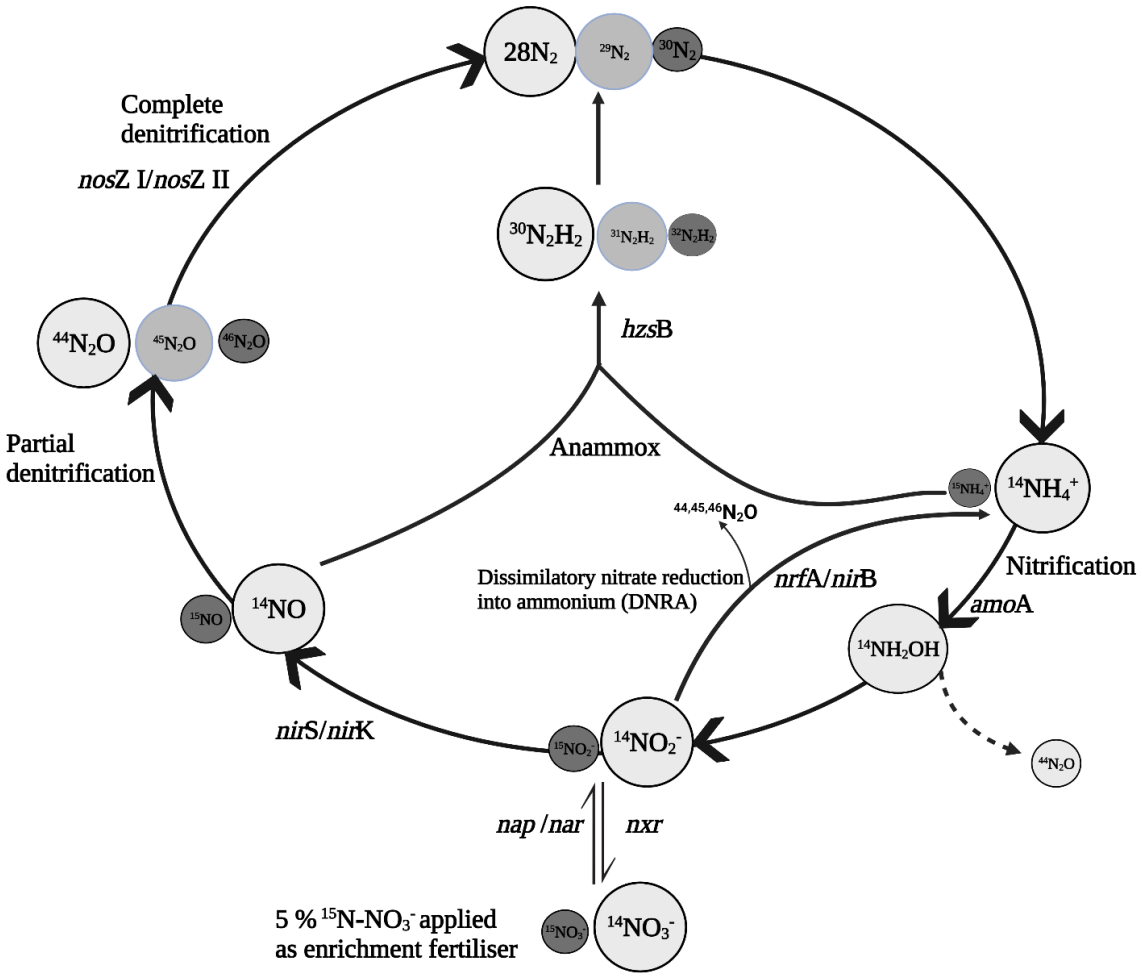

Fig 2.3.3: The nitrogen cycle processes showing nitrification, denitrification, DNRA and anammox pathways. The shade and size of the isotope correspond to the isotope and likely pool size (product ratio), respectively, after applying 5 % ^{15}N-NO_3^-. Marker genes for respective processes were marked with italic letters. N_2O derived through DNRA, mentioned without being bounded in the circle, is not included in isotope ratio modelling.

2.3.11.1 Measurement of Nitrification Rate

Soil gross nitrification rate (GNR) was measured by a modified ^{15}N nitrate pool dilution method (Brooks et al. 1989, Yang et al. 2007) (Fig: 2.3.1). This method allows estimation of nitrification rates discounting for losses of the product nitrate through other processes such as plant uptake, denitrification and leaching. The following equation calculated the nitrification rate.

$GNR = (\{[NO_3^-]_0 - [NO_3^-]_t\}/t) \times (\log \{APE_0/ APE_t)\}/\log \{[NO_3^-]_0 / [NO_3^-]_t\})$

Where GNR = gross nitrification rate (µg of N g^{-1} dry weight soil h^{-1})

APE = the atom% excess (^{15}N enrichment of an N pool enriched with ^{15}N subtracted by the atom% ^{15}N enrichment of background or "natural" ^{15}N abundance, 0.3663).

APE_0 = the atom% ^{15}N excess of NO_3^- pool at T0.

APE_t = the atom% ^{15}N excess of NO_3^- pool at the time of microcosm destruction

$[NO_3^-]_0$ = the NO_3^- concentration (µg N g-1 dry weight soil) at T0; (Immediately after the addition of enrichment fertilizers)

$[NO_3^-]_t$ = the NO_3^- concentration (µg N g-1 dry weight soil) at the microcosm destruction time

t = Duration of incubation hour after enrichment fertilization.

2.3.11.2 Measurement of dissimilatory nitrate reduction into ammonium (DNRA) Rate

The rate of DNRA was determined through the ^{15}N tracer enrichment in N-NH_4^+ modified from (Song et al., 2014) discounting ^{15}N nitrate pool dilution by nitrification, plant uptake and anaerobic ammonium oxidation (Anammox), but not the aerobic oxidation (Nitrification). NO_3^- immobilisation into NH_4^+ by microbes would be negligible because both inorganic N (NH4NO3) forms of N were used for fertilisation. Biological nitrogen fixation (BNF) was not measured because the process is likely insignificant under the N-fertilised condition (Pandey et al., 2018a). The following equation was used to calculate the DNRA rate.

$$\text{DNRA rate} = \frac{\int_{t}^{0} (APNH_4^+)_t - (APNH_4^+)_0}{\int_{t}^{0} (APNO_3^-)_0 - (APNO_3^-)_t} \times \frac{\int_{t}^{0} [NH_4^+]_0 - [NH_4^+]_t}{t}$$

Where,

$(APNH_4^+)_0$ = ^{15}N atom% in $N\text{-}NH_4^+$ pool at T0.

$(APNH_4^+)_t$ = ^{15}N atom% in $N\text{-}NH_4^+$ pool at the time of microcosm destruction

$[NH_4^+]_0$ = $N\text{-}NH_4^+$ concentration (µg N g-1 dry weight soil) at T0

$[NH_4^+]_t$ = $N\text{-}NH_4^+$ concentration (µg N g-1 dry weight soil) at microcosm destruction time.

2.3.11.3 Measurement of partial denitrification associated $N\text{-}N_2O$ emission rate

Collected gas samples were run through Isotope Ratio Mass Spectrometer (IRMS) to measure N_2O gas emission and enrichment. The detected beam area of N_2O by IRMS was converted into ppm value compared with a regression line constructed from the standards. The measured N_2O ppm value is converted into the mass of $N\text{-}N_2O$ in µg by the following equation.

$N\text{-}N_2O$ (g) = (Cppm X n X mwN_2O)/1000000

Where,

Cppm is the calculated ppm value of measured N_2O. n is the moles number of gas in the headspace and is calculated by standard gas equation (PV=nRT). Here P=atmospheric pressure in Pascal, V=is the volume of headspace in the Kilner jar, R= Gas constant and T= Temperature in the Kelvin scale. mwN_2O is the molecular weight of N_2O= 44.018 g. The partial denitrification rate was calculated by dividing the measured $N\text{-}N_2O$ (g) with incubation time in the Kilner jar and the equivalent dry weight of soil in the microcosm.

2.3.11.4 Source partition of emitted N_2O between nitrification and denitrfication

The source of N-N_2O was confirmed after comparing the atom % excess of ^{15}N in measured N-N_2O and N-NO_3^- (Bergsma et al., 2001). If denitrification solely contributes to N_2O emission from rice microcosm, the ratio of atom % excess of ^{15}N in N-N_2O and N-NO_3^- would be one. However, the ratio would be decreased due to dilution of atom % excess of ^{15}N in N-N_2O by gas produced by nitrification and thus from the unlabelled NH_4^+ pool. So, the percentage contribution of denitrification and nitrification in N_2O emission from rice microcosm was measured using the following equations.

$$\% \ N_2O \text{ gas derived through denitrification} = \frac{^{15}N \text{ Atom \% excess of } N_2O \text{ in headspace}}{^{15}N \text{ Atom \% excess of } NO_3^- \text{ in soil}} \times 100$$

2.3.11.5 Indirect measurement of total N-N_2 (complete denitrification and anammox) emission rate

Total N_2 (derived through complete denitrification and anammox) emitted from the microcosm was measured indirectly due to the high background N_2 in the atmospheric air. The following equation calculated the percentage of N_2 derived from the microcosm by considering the isotopic enrichment of the N-N_2 and N-NO_3^- (Bergsma et al., 2001).

$$\% \ N_2 \text{ gas soil derived } (N\%)_S = \frac{^{15}N \text{ Atom \% excess of } N_2 \text{ in headspace}}{^{15}N \text{ Atom \% excess of } NO_3^- \text{ in soil}} \times 100$$

The mass of total soil-derived N-N_2 from the microcosm was measured by the following equation using the percentage of N2 derived from the soil.

Mass of N-N_2 derived from microcosm (g) = $(N\%)_S \times mwN_2 \times n \times (N\%)_A$

Where,

$(N\%)_S$ = % N_2 gas soil derived

mwN_2 = molecular weight of N_2 (28.02 g)

n = moles number of gas in the headspace

$(N\%)_A$ = % N_2 gas in air (78.09 %)

The total N-N_2 emission rate was calculated by dividing the calculated soil-derived mass of N-N_2 (TN) from the microcosm with incubation time in the Kilner jar and the equivalent dry weight of soil in the microcosm. The contribution of complete denitrification and anammox in the total emission of N-N_2 from the microcosm was source partitioned by comparing the ratios of $^{29}N_2/^{30}N_2$: $^{45}N_2O/^{46}N_2O$.

% contribution of complete denitrification was separated from the total N-N_2 emission from the soil core and was calculated by the following equation.

$$\%\ N_2 \text{ gas derived through complete denitrification (CD)} = \frac{^{29}N_2/^{30}N_2}{^{45}N_2O/^{46}N_2O} \times 100$$

So, soil-derived mass of N-N_2 (including ^{14}N-N_2+^{15}N-N_2) through complete denitrification was measured by multiplying the % N_2 gas derived through complete denitrification (CD) with soil-derived total mass of N-N_2 (TN). Anammox contribution in N-N_2 emission was calculated by deduction of complete denitrification contribution from total N-N_2 emission.

2.3.11.6 Source partition of complete denitrification total N-N_2 Emission

The source of emitted N-N_2 through complete denitrification was N-N_2O (Fig: 2.2.1). So, the ratio of $^{45}N_2O/^{46}N_2O$ should be equivalent to $^{29}N_2/^{30}N_2$. However, equivalent ratios would be imbalanced by anammox contributing $\mathbf{^{29}N_2/^{30}N_2}$ (Table: 2.2.1). If complete denitrification were the sole contributor to total N_2 emission hypothetically after applying 5% ^{15N}nitrate , then the ratio of $^{28}N2/^{29}N2/^{30}N2$ would be 0.9025/0.0475/0.0025 ($^{28}N2:^{29}N2:^{30}N2$ = 361:19:1), and if anammox were the sole contributor, then the ratio would be 0.9462/0.0536/0.0002 ($^{28}N2:^{29}N2:^{30}N2$ =

4731:268:1). If complete denitrification and anammox contributed equally then the ratio $^{28}N2:^{29}N2:^{30}N2$ would be 686:36:1 (Table: 2.2.1).

Table 2.2.1: Hypothetical product ratio of $^{28}N2:^{29}N2:^{30}N2$ in emitted N-N_2 through complete denitrification and anammox when 5% ^{15}N-NO_3^- is used and ^{15}N atom % ^{15}N-NH_4^+ remained at natural abundances.

N Source for N_2	**%**	**N Source for N_2**	**%**	**N_2 Product**	**N-cycling process**	**Probability**
$^{14}NO_3^-$	95	$^{14}NO_3^-$	95	$^{28}N_2$	Complete denitrification	0.95X0.95=0.9025
$^{14}NO_3^-$	95	$^{15}NO_3^-$	5	$^{29}N_2$	Complete denitrification	0.95X0.05=0.0475
$^{15}NO_3^-$	5	$^{15}NO_3^-$	5	$^{30}N_2$	Complete denitrification	0.05X0.05=0.0025
$^{14}NO_3^-$	95	$^{14}NH_4^+$	99.6	$^{28}N_2$	Anammox	0.95X0.996=0.9462
$^{14}NO_3^-$	95	$^{15}NH_4^+$	0.4	$^{29}N_2$	Anammox	0.95X0.004=0.0038
$^{15}NO_3^-$	5	$^{14}NH_4^+$	99.6	$^{29}N_2$	Anammox	0.05X0.996=0.0498
$^{15}NO_3^-$	5	$^{15}NH_4^+$	0.4	$^{30}N_2$	Anammox	0.05X0.004=0.0002

2.3.12 Statistiscal analysis

Analysis of variance (ANOVA), including one-way, two-way and three-way, was performed after checking the data conformed to analyse the effects of the rice cultivars, compartment and incubation time effects on different parameters ([NO3-], [NH4+], pH and microbial nitrogen transformation processes) measured in this study and their interaction on different parameters by using R Studio version 4.0.2 (R Core Team, 2022). Generalised linear modelling (GLM) and polynomial modelling were also performed to understand the N_2O emission trend and the enrichment trend of ^{15}N atom % excess in the emitted N_2O using the same R version. The other figures were prepared using the Biorender app.

2.4 Results

2.4.1 Effects of rice cultivars and compartments at different days on residual $N\text{-}NO_3^-$ and $N\text{-}NH_4^+$ concentration after enrichment fertilisation

Variation between tested two rice cultivars and compartments on residual $N\text{-}NO_3^-$ and $N\text{-}NH_4^+$ concentration at different days after enrichment fertilisation (5 % $^{15}NO_3^-$ enriched NH_4NO_3 as N-fertiliser at the rate of 100 N μg /g dry weight) were analysed by three-way ANOVA analysis. Residual $N\text{-}NO_3^-$ μg/g dry weight soil (p<0.001) and $N\text{-}NH_4^+$ μg/g dry weight (p<0.01) soil varied between the high and low nitrification-associated rice cultivars, but no variation was observed between the bulk soil and rhizosphere compartments. The measured residual N, both $N\text{-}NO_3^-$ (p<0.001) and NH4+ (p<0.001) after the incubation, was significantly varied over incubation time. These main effects were complicated by significant interactions between the tested rice cultivars and days on residual $N\text{-}NO_3^-$ (p<0.01) and $N\text{-}NH_4^+$ (p<0.001) concentration. Furthermore, there was a significant interaction between days and compartments (p<0.001) on residual N-NO3- concentration (Table 2.4.1).

The interaction between time and cultivar was driven by a higher residual $N\text{-}NO_3^-$ in soil supporting the high nitrification rice cultivar on day 1 (10.2±1.75 μg/g dry weight), more than double that of the low nitrification rice cultivar (4.75±0.735 μg/g dry weight); there was no significant variation after day 1 (Fig 2.4.1). The residual $N\text{-}NH_4^+$ concentration on day 2 in high nitrification rice cultivar (9.79±0.835) μg N/g dry weight was observed to lower significantly than that of low nitrification rice cultivar (16.7±0.341 μg/g dry weight) (Fig 2.4.2). The interaction between time and cultivar for ammonium was also due to differences in depletion over time. Here, the high nitrification line showed a more rapid depletion in the first 24 hours, which was then stable for the next period before a second drop in concentration to background levels. The low nitrification line showed a more uniform depletion (Fig 2.4.2).

The pH varied interactively between the rice cultivars and days after enrichment fertilisation (Table: 2.4.2). pH dropped uniformly in the high-nitrification rice cultivar within the time of

enrichment fertilisation. However, in the low nitrification-associated rice cultivar, pH fluctuated within the days after enrichment fertilisation (Fig: 2.4.3)

Table 1 2.4.1: Three-way ANOVA results for the effect of rice cultivar, compartments and days on residual N-NO_3^- µg/g dry weight, N-NH_4^+ µg/g dry weight and pH at the significance levels' ***' 0.001 '**' 0.01 '*' 0.05 '.' 0.1

Response: Residual [NO_3^-]	**Sum Sq**	**Df**	**F value**	**Pr(>F)**	**Significance code**
Rice	95.41	1	27.6356	1.60e-06	***
Days	362.58	4	26.2554	3.51e-13	***
Compartment	3.84	1	1.1118	0.30	
Rice X Days	66.55	4	4.8193	0.002	**
Rice X Compartment	2.76	1	0.7989	0.37	
Days X Compartment	102.17	4	7.3986	5.23e-05	***
Rice X Days X Compartment	5.20	4	0.3768	0.82	
Residuals	234.767	80	NA	NA	
Response: Residual [NH_4^+]	Sum Sq	Df	F value	Pr(>F)	Significance code
Rice	23.49	1	10.1043	0.00215	**
Compartment	0.26	1	0.11	0.74106	
Days	2241.17	4	241.0595	<2.2e-16	***
Rice X Compartment	0.23	1	0.0990	0.7539	
Rice X Days	307.47	4	33.0712	6.923e-16	***
Compartment X Days	1.15	4	0.1236	0.9736	
Rice X Compartment X Days	1.06	4	0.1143	0.9771	
Residuals	174.32	80	NA	NA	
Response: pH	Sum Sq	Df	F value	Pr(>F)	Significance code
Rice	0.21753	1	9.7390	0.00251	**
Compartment	0.14319	1	6.4106	0.06330	
Days	0.79993	4	8.9535	5.003e-06	***
Rice X Compartment	0.01309	1	0.5859	0.44625	
Rice X Days	0.75867	4	8.4916	9.201e-06	***
Compartment X Days	0.01158	4	0.1296	0.97122	
Rice X Compartment X Days	0.03957	4	0.4429	0.77726	
Residuals	1.78686	80	NA	NA	

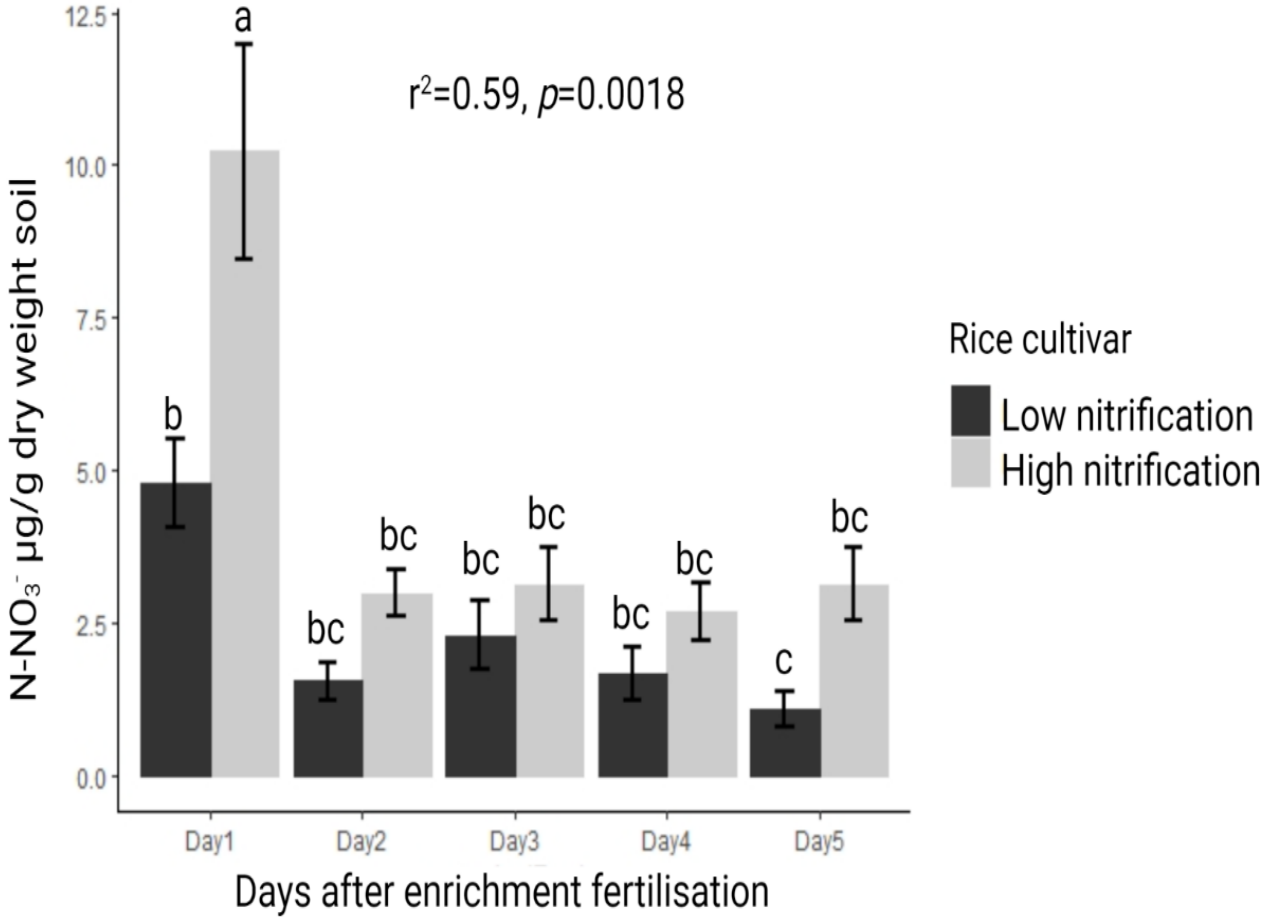

Fig 2.2.1: Mean ± SE (n=8) from the two-way ANOVA of residual $N\text{-}NO_3^-$ µg/g dry weight between the tested two rice cultivars on different days after enrichment fertilisation. The different letter indicates a significantly different group (r^2= adjusted residual errors, P <0.05, ANOVA, Tukey HSD).

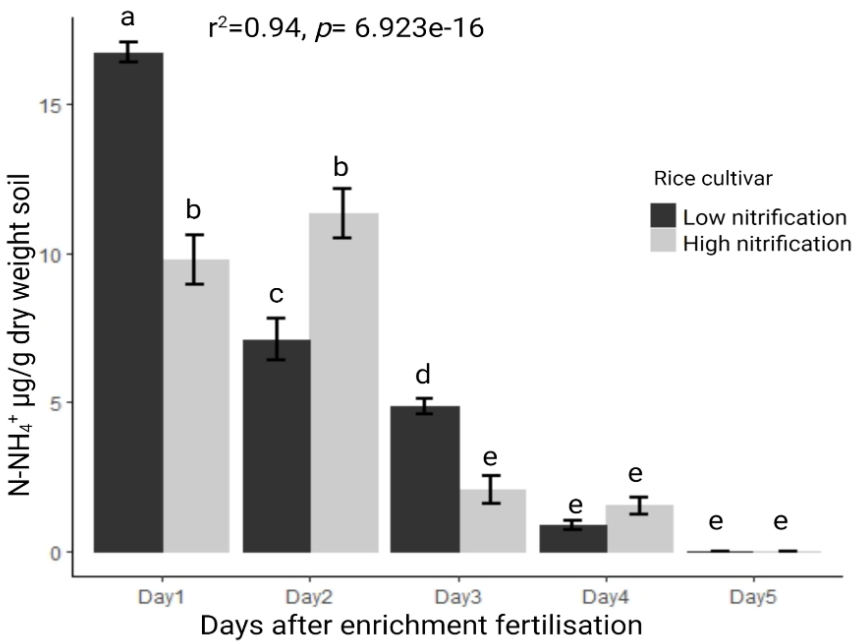

Fig 2.4.2: Mean ± SE (n=8) from the two-way ANOVA of residual $N\text{-}NH_4^+$ µg/g dry weight between the tested two rice cultivars on different days after enrichment fertilisation. The different letter indicates a significantly different group (r^2= adjusted residual error, P <0.001, ANOVA, Tukey HSD).

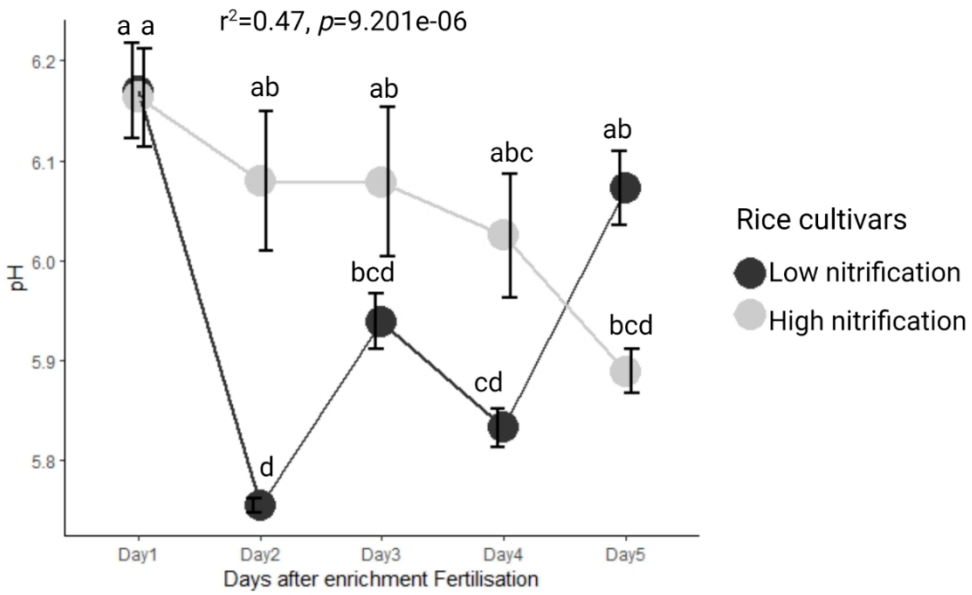

Fig 2.3.3: Mean ± SE (n=8) from the two-way ANOVA of pH between the tested two rice cultivars on different days after enrichment fertilisation. The different letter indicates a sig*nificantly different group (r^2=* adjusted residual error, *P <0.001, ANOVA, Tukey HSD).*

2.4.2 Nitrification dynamics over the incubation period after enrichment fertilisation

The nitrification rate was significantly varied between the rice cultivars (p<0.01), compartments (p<0.001), and days (p<0.05) after enrichment fertilisation with no interactive effects (Table: 2.4.2). The nitrification rate was significantly higher in the rhizosphere than in the bulk compartment (p=2.845e-05) (Fig: 2.4.4A). The box whisker plot indicated that the median nitrification rates were 300 ng N/g dry-weight soil/hour and 175 ng N/g dry-weight soil/hour, respectively, in the rhizosphere and bulk compartments. The measured pH did not vary significantly between the compartments (Table: 2.4.2) (Fig: 2.4.4B). The nitrification rate in the high nitrification-associated rice cultivar remained unchanged until day 2 after enrichment fertilisation, declined significantly on day 3, and remained static until the experiment's end. Whereas on day 2 and day 5, the nitrification rate was measured significantly lower from the other days in the low nitrification-associated rice cultivar (Fig: 2.4.4C)

Table 2.4.2: Three-way ANOVA results for the effect of rice cultivar, compartments and days on nitrification (ng N/g dry weight soil/hour) at the significance levels' ***' 0.001 '**' 0.01 '*' 0.05 '.' 0.1.

Response: Nitrification rate	**Sum Sq**	**Df**	**F value**	**Pr(>F)**	**Significance code**
Rice	155967	1	7.9978	0.006636	**
Compartment	410729	1	21.0618	2.845e-05	***
Days	228039	4	2.9234	0.029581	*
Rice X Compartment	315	1	0.0162	0.899292	
Rice X Days	84311	4	1.0809	0.375563	
Compartment X Days	42112	4	0.5399	0.707090	
Rice X Compartment X Days	38483	4	0.4933	0.740610	

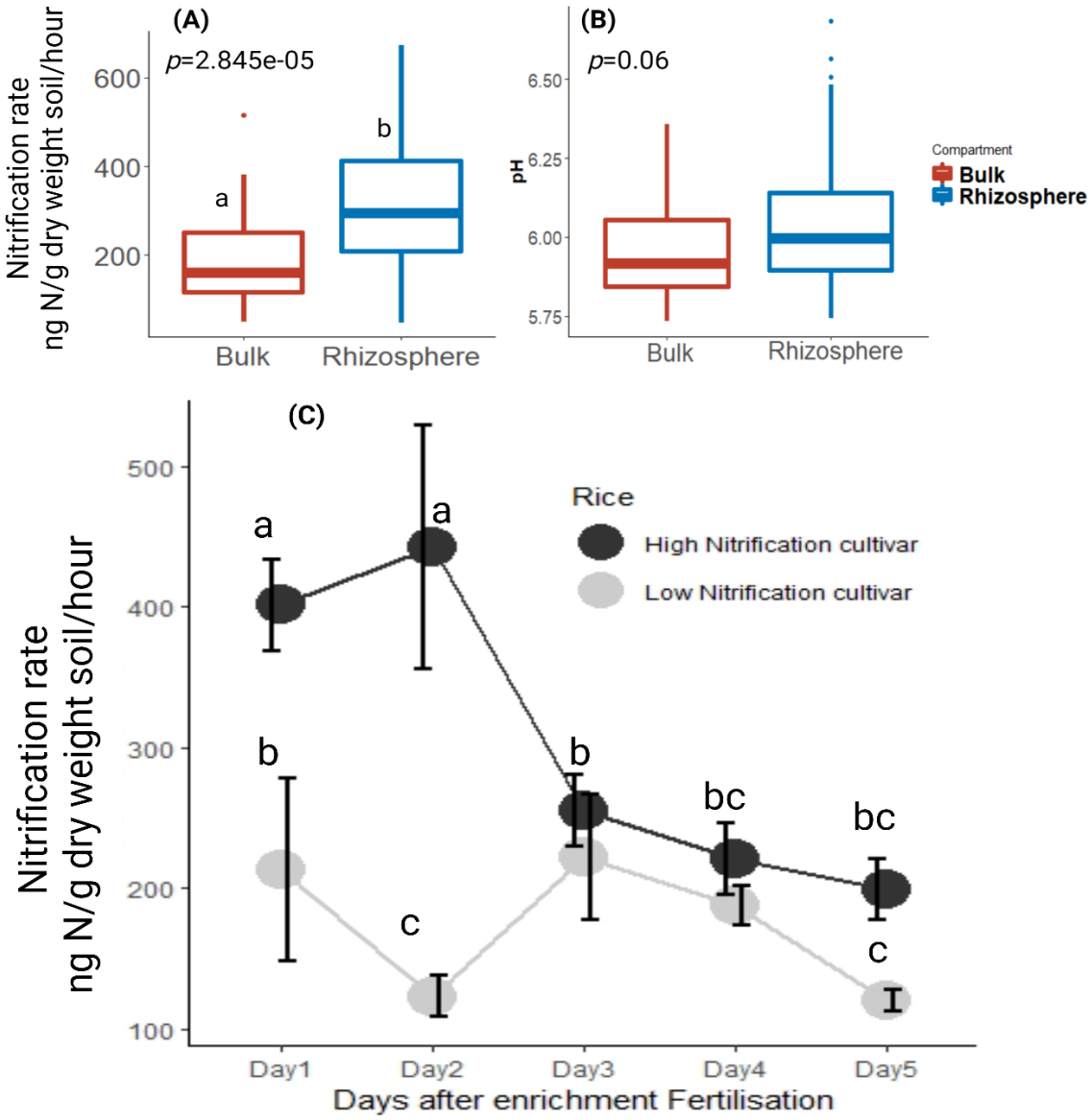

Fig 2.4.4: **(A)** Box whisker plot of Gross nitrification rate between the compartments. The box shows a 95 % quartile nitrification rate observation with the median (n=20) as the thick internal line. Lowercase letters denote significantly different groups (P <0.001, ANOVA, Tukey HSD). **(B)** Box whisker plot of pH between the compartments. The box with the vertical line shows 95 % quartile pH observation with a median (n=20), indicated by a horizontal line inside the box. **(C)** Mean ± SE (n=8) from the two-way ANOVA of nitrification rate ng N/g dry weight of soil/hour between the tested two rice cultivars after enrichment fertilisation. Lowercase letters denote significantly different groups (P <0.001, ANOVA, Tukey HSD).

2.4.3 Denitrification dynamics over the incubation period after enrichment fertilisation

Total denitrification varied significantly between the rice cultivars (p<0.01) and days (p<0.001) after the enrichment fertilisation with no interactive interaction. On day 1, total denitrification was significantly higher, and from day 2, it became flat till the end of the experiment period in both rice cultivars(Fig: 2.4.5A). In contrast, partial denitrification varied significantly between the rice cultivars (p<0.01) and days (p<0.001) interactively between rice and day (Table: 2.4.3). The partial denitrification was only significantly higher in high nitrification associated rice cultivar than in the low nitrification associated rice cultivar only on day 1 after enrichment fertilisation (Fig: 2.4.5B) The ratio of partial and total denitrification (Fig: 2.4.5C) were also significantly higher in high nitrification associated rice cultivar than the low nitrification associated rice cultivar on day 1 after enrichment fertilisation. On day 1 after enrichment fertilisation as T1, the average ^{15}N atom % in NO_3^- of bulk and rhizosphere compartments was measured at 3.6 %, indicated by the dotted line after applying 5% ^{15}N atom % NO_3^- as enrichment fertiliser (Fig: 2.4.5D). Different emission trends in N_2O emission were observed between the rice cultivars while incubating in the Kilner jar. N_2O emission increased linearly during incubation in the high nitrification rice cultivar (r^2= 0.48, p= 0.0016). In contrast, N_2O emission was observed flat till five hours of incubation in the low nitrification rice cultivar (r^2= 0.11, p= 0.1045) (Fig: 2.4.5D). However, the trend of increasing ^{15}N atom % in N_2O was similar between the rice cultivars (Polynomial fitted curve line equation, $y=x+ax^2$, where, y= ^{15}N atom % in N_2O, x= incubation time and a=constant). The ratios of ^{15}N atom % in emitted N_2O and residual NO_3^- were (equation given in Section: 2.3.12.4) one or above from two hours of incubation.

Table 2.4.3: Two-way ANOVA results for the effects of rice cultivar and days after enrichment fertilisation on partial and denitrification rate (ng N/g dry weight soil/hour) at the significance levels' ***' 0.001 '**' 0.01 '*' 0.05 '.' 0.1.

Response: Partial denitrification rate	**Sum Sq**	**Df**	**F value**	**Pr(>F)**	**Significance code**
Rice	60.20	1	8.6896	0.007956	**
Days	345.63	4	12.4716	2.999e-05	***
Rice X Days	117.90	4	4.2542	0.011865	*
Response: Total denitrification rate	**Sum Sq**	**Df**	**F value**	**Pr(>F)**	**Significance code**
Rice	91221	1	11.7490	0.002299	**
Days	432361	4	13.9218	6.574e-06	***
Rice X Days	10648	4	0.3428	0.846195	

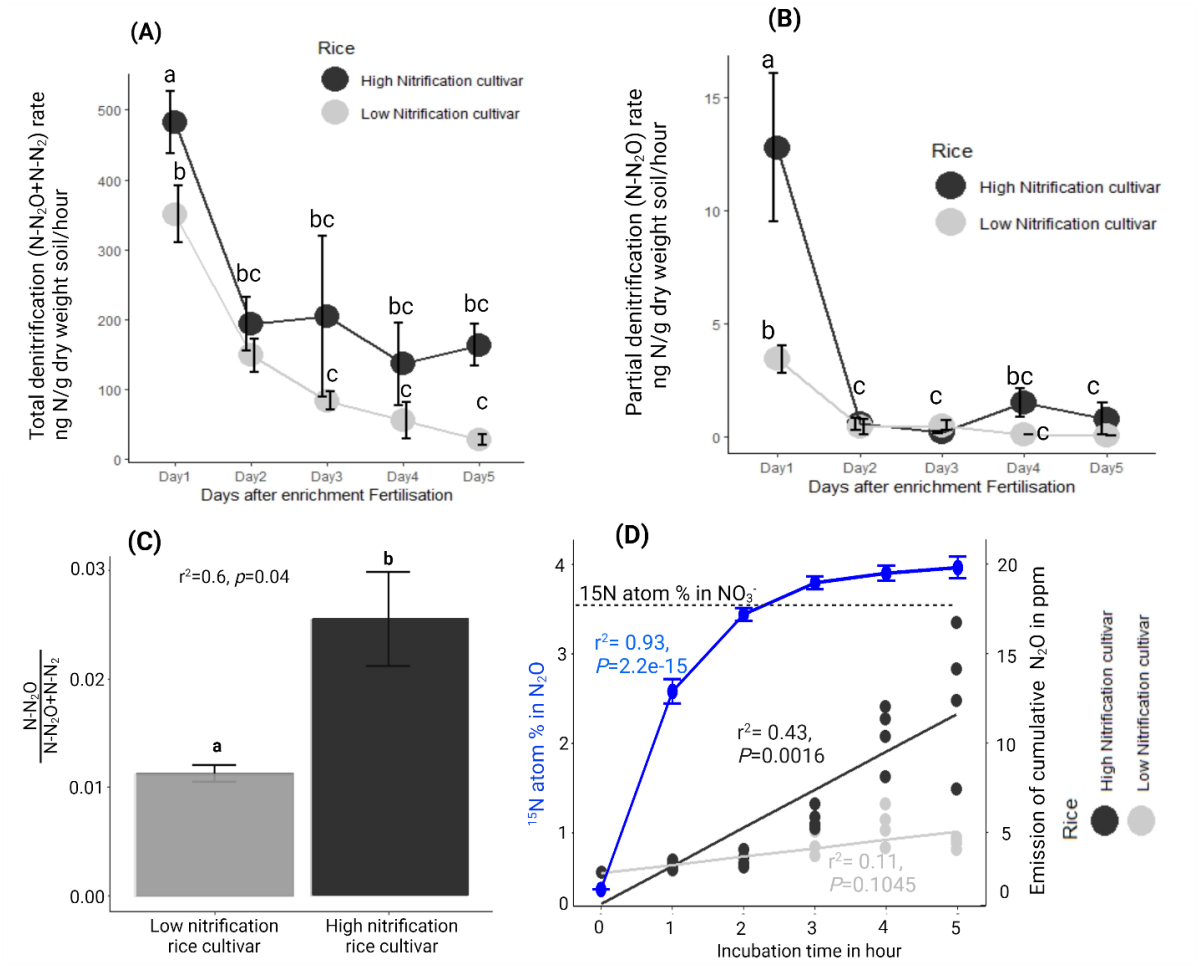

Fig 2.4.5: Mean ± SE (n=4) from the two-way ANOVA of **(A)** Total denitrification rate in ng N/g dry weight soil/ hour **(B)** partial denitrification rate ng N/g dry weight soil/ hour between the tested two rice cultivars after enrichment fertilisation. Lowercase letters denote significantly different groups (P <0.001, ANOVA, Tukey HSD). **(C)** Mean ± SE (n=4) from the one-way ANOVA of the ratio of $N\text{-}N_2O/N\text{-}N_2O+N\text{-}N_2$ between the tested two rice cultivars on day 1 after enrichment fertilisation. The different letter indicates a significantly different group (r^2= adjusted residual error P <0.05, ANOVA, Tukey HSD). **(D)** Generalised linear model (r^2= adjusted residual error) of N_2O (ppm) emission of (n=4) replications of high nitrification rice cultivar (Black) and low nitrification rice cultivar (Gray) during incubation enclosed incubation 1 day 1 after enrichment fertilisation. Blue indicates a polynomial fitted curve ($y=x+ax^2$) of mean ± SE (n=8) of ^{15}N atom % enrichment in emitted N_2O and r^2= adjusted residual error for the model. The horizontal black dotted line indicated an average (n=16) ^{15}N atom % in residual $N\text{-}NO_3^-$ on day 1 after enrichment fertilisation.

2.4.4 DNRA dynamics over the incubation period after enrichment fertilisation

There were no significant variations in DNRA rate between the rice cultivars after enrichment fertilisation; however, DNRA significantly varied between the compartments interactively with rice cultivars (Table: 2.4.4). DNRA rate was significantly higher in the rhizosphere compartments than the bulk compartments in both the rice cultivars. In addition, DNRA was highest and lowest in the rhizosphere and bulk compartments of the high nitrification-associated rice cultivar, respectively (Fig: 2.4.6B).

Table 2.4.4: Three-way ANOVA results for the effect of rice cultivar, compartments and days on DNRA rate (ng N/g dry weight soil/hour) at the significance levels' ***' 0.001 '**' 0.01 '*' 0.05 '.' 0.1

Response: DNRA rate	**Sum Sq**	**Df**	**F value**	**Pr(>F)**	**Significance code**
Rice	0.373	1	0.8078	0.371456	
Compartment	57.97	1	125.5994	<2.2e-16	***
Days	2.157	4	1.1684	0.331040	
Rice X Compartment	13.005	1	28.1763	9.673e-07	***
Rice X Days	6.908	4	1.4210	0.2334	
Compartment X Days	0.505	4	0.2733	0.894406	
Rice X Compartment X Days	0.980	4	.5311	0.713239	

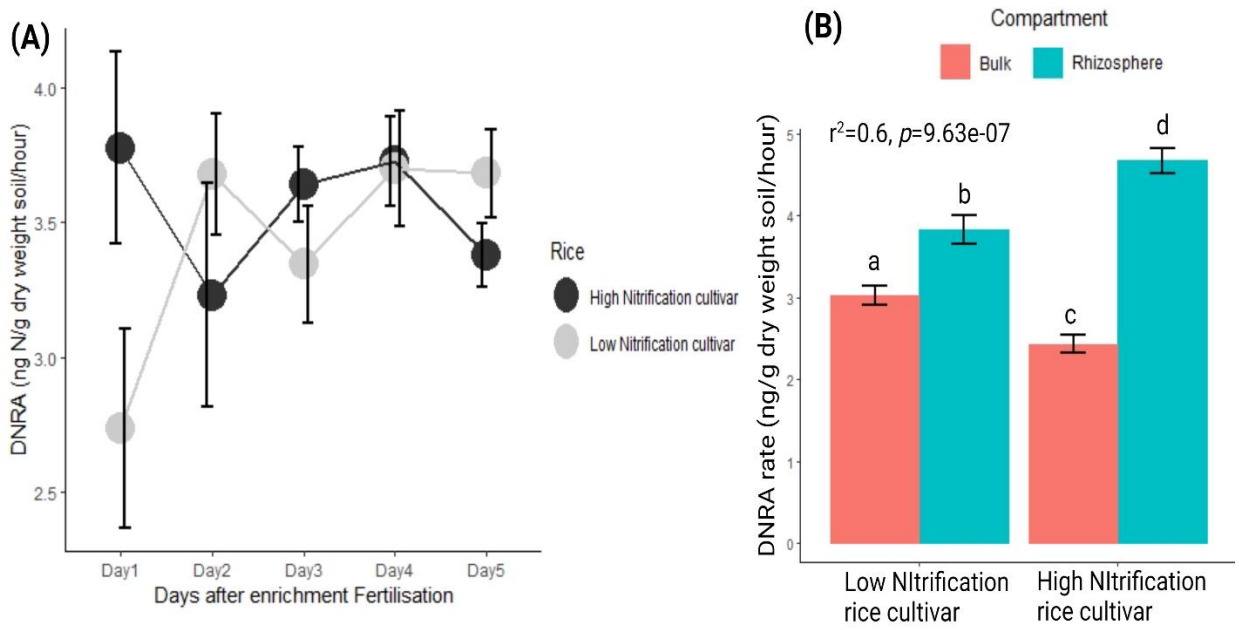

Fig 2.4.6: **(A)** *Mean ± SE (n=8) from the three-way ANOVA of DNRA rate in ng N/g dry weight soil/ hour* ***(B)*** *Mean ± SE (n=20) from the two-way ANOVA of cumulative DNRA rate ng N/g dry weight of soil/hour between the compartments of tested two rice cultivars after enrichment fertilisation. The different lowercase letter indicates a significantly different group (r^2 = adjusted residual error, P <0.001, ANOVA, Tukey HSD).*

2.4.5 Anammox dynamics over the incubation period after enrichment fertilisation

Anammox rate significantly varied between the tested rice cultivars and noninteractively with days (Table: 2.4.6). Anammox rate was higher in the high nitrification-associated rice cultivars (Fig: 2.4.7A). The percentage contribution to gaseous N_2 loss through anammox and complete denitrification varied between the rice cultivars interactively with days after enrichment fertilisation (Table: 2.4.6). Anammox contributed approximately one-fourth of the total N_2 emission on day 1 after enrichment fertilisation in both rice microcosms. Nevertheless, after day 1, both processes (anammox and complete denitrification) contributed equally to the total N_2 emission from the high nitrification-associated rice cultivar's microcosms. In contrast, N_2 emission through anammox gradually increased from the low nitrification-associated rice cultivar's microcosms with days (Fig: 2.4.7B).

Table 2.4.5: Two-way ANOVA results for the effects of rice cultivar and days after enrichment fertilisation on anammox rate (ng N/g dry weight soil/hour) at the significance levels' ***' 0.001 '**' 0.01 '*' 0.05 '.' 0.1

Response: Anammox	**Sum Sq**	**Df**	**F value**	**Pr(>F)**	**Significance code**
Rice	114354	1	17.9278	0.0003406	***
Days	10866	4	0.4259	0.7883026	
Rice X Days	35562	4	1.3938	0.2687446	

Table 2.4.6: Three-way ANOVA results for the effects of rice cultivar, N-cycle processes (Complete denitrification and anammox) and days after enrichment fertilisation on the percentage contribution to gaseous N_2 loss at the significance levels' ***' 0.001 '**' 0.01 '*' 0.05 '.' 0.1

Response: % to gaseous N_2 loss contribution	**Sum Sq**	**Df**	**F value**	**Pr(>F)**	**Significance code**
Rice	0.0	1	0.0000	1	
Days	0.0	1	0.0000	1	
N-cycle processes	257.9	1	1.6648	0.2040	
Rice X Days	0.0	4	0.0000	1	
Rice X N-cycle processes	257.0	1	1.6590	0.2048	
Days X N-cycle processes	11986.4	4	19.3464	4.335e-09	***
Rice X Days X N-cycle processes	5660.5	4	9.1362	2.104e-05	***

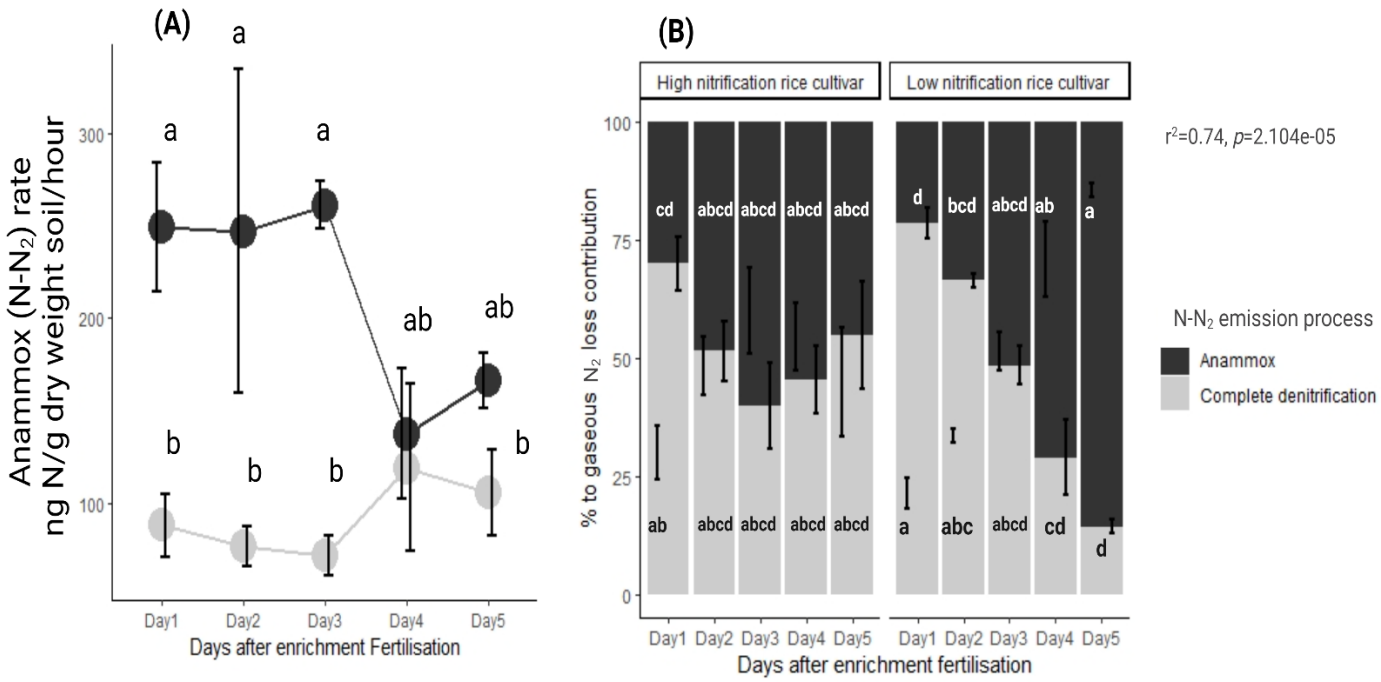

Fig 2.4.7: **(A)** Mean ± SE (n=4) from the two-way ANOVA of anammox rate in ng N/g dry weight soil/ hour between the tested two rice cultivars after enrichment fertilisation. Lowercase letters denoted significantly different groups (*P* <0.001, ANOVA, Tukey HSD). **(B)** Mean ± SE (n=4) from the three-way ANOVA of the % contribution to total gaseous $N\text{-}N_2$ loss through complete denitrification and anammox of the tested two rice cultivars in different days after enrichment fertilisation. The different letter indicates a significantly different group (*P* <0.001, ANOVA, Tukey HSD).

2.5 Discussion

2.5.1 Rice genotype effects on dynamics of N-cycle processes up to five days after N-fertilisation

2.5.1.1 Nitrification

As expected from the previous study, variations in nitrification rate were observed between the tested rice cultivars, and the difference in rate persisted until day 3 of the incubation due to NH_4^+ depletion, which is the first substrate in the nitrification pathway (Fig: 2.4.2). The basis for nitrification variations between the tested rice cultivars before the NH_4^+ limitation could be of oxygenation, pH and BNI or the combination of these three effects. The nitrification rate was measured significantly higher in the rhizosphere than in the bulk compartment (Fig:2.3.5A). It was indicated that radial oxygen loss (ROL) from the rice root surface oxygenated the rhizosphere compartment and supported nitrification (Li et al., 2008); furthermore, diffusing oxygen typically formed a gradient into the surrounding bulk soil allowed some nitrification in the bulk compartment (Li & Wang, 2013). However, no interaction was observed between the rice cultivar and the compartments on nitrification rate (Table: 2.4.2). So, it could be speculated that both the rice cultivars oxygenate the respective microcosms evenly, and oxygenation might not be involved in the nitrification variation between the rice cultivars. In addition, on day 1, after enrichment fertilisation, the pH between the rice cultivar was similar (Fig: 2.4.3). The results suggested that the low nitrification-associated rice cultivar might have secret BNI-like compounds through root exudation that might trigger the nitrification variation between the tested rice cultivars on day 1 after enrichment fertilisation.

2.5.1.1.1 Source of N_2O emissions

Nitrification remained active in both compartments of rice microcosms. So, I have source-partitioned the measured N-N_2O between nitrification and denitrification from collected gas samples. I have found that the source of emitted N_2O was overwhelmingly NO_3^- through partial denitrification in this microcosm experiment. Denitrification is reported to be the dominating pathway in the emission of N_2O at over 80% WFPS (Bateman & Baggs, 2005; Wang et al., 2023), but this could have been complicated by oxygenation of the rhizosphere in the paddy system. If nitrification contributes to N_2O emission from an unenriched source (N-NH_4^+), then ^{15}N atom %

excess would be further diluted from ^{15}N atom % excess in $N\text{-}NO_3^-$ (Fig: 2.4.5D). Nitrification did not directly influence the observed N_2O emission between the tested rice cultivars since there was no significant dilution of ^{15}N atom % in $N\text{-}N_2O$ from that of $N\text{-}NO_3^-$. However, NO_3^- produced from nitrification might lower the C/NO_3^- ratios, facilitating partial denitrification as the $N\text{-}N_2O/(N\text{-}N_2O+N\text{-}N_2)$ ratio was significantly higher in the high nitrification-associated rice cultivar (Fig: 2.4.5C).

The low contribution could also have been complicated by the methodology in which the shoot was cut prior to incubating the microcosm pot in the Kilner jar for collecting gas samples. The rice rhizosphere in microcosms will have rapidly became predominantly anaerobic during the incubation because atmospheric oxygen transportation to the rhizosphere via shoot was blocked after cutting the shoot. Artificial defoliation (Cutting shoot) might also influence the ratio of $N\text{-}N_2O/(N\text{-}N_2O+N\text{-}N_2)$ through changing carbon influx in the rhizosphere **(Discussed in Chapter 6, Section: 6.5.1)**.

2.5.1.2 Denitrification

The total denitrification became limited after day 1 of enrichment fertilisation due to NO_3^- limitation in both rice cultivars (Fig: 2.4.5A). The mean residual $N\text{-}NO_3^-$ concentration from bulk and rhizosphere compartments in the low nitrification-associated rice cultivar was measured <5 μg/g dry weight soil even after day 1 of N-fertilisation (Fig: 2.4.1). Denitrification was reported to be limited when $N\text{-}NO_3^-$ concentration dropped to <5 μg/g dry-weight soil (Ryden et al., 1979). Nevertheless, in $N\text{-}NO_3^-$ nonlimiting condition on day 1, N_2O emission through partial denitrification was significantly higher in the high nitrification-associated rice cultivar. The result indicated that the last step of denitrification is mediated by nitrous oxide reductase, which might be limited more in the high nitrification-associated rice cultivar than the low nitrification-associated rice cultivar. Nitrous oxide reductase is more sensitive to oxygen than other elementary enzymes involved in denitrification (Knowles, 1982; N. Morley & Baggs, 2010). So, the high nitrification-associated rice cultivar might oxygenate more than the low nitrification-associated rice cultivar in the microcosm pot, which might inhibit the enzyme irreversibly and could be associated with temporal N_2O emission.

Nevertheless, based on nitrification results, it seemed that oxygenation variation might not be enough to trigger temporal N_2O emission variations between the rice cultivars. The variations in low molecular weight organic carbon in the root exudates between the rice cultivars might trigger the N_2O emission variation by altering the source partition between denitrifiers' growth and respiration or might inhibit nitrous oxide reductase activity (Giles et al., 2017). Indeed, the partial and total denitrification ratio ($N\text{-}N_2O$: $N\text{-}N_2O+N\text{-}N_2$) was significantly higher in the high nitrification-associated rice cultivar on day 1 after enrichment fertilisation (Fig: 2.4.5C). It has already been reported that the quantity and quality of carbon in root exudates as reductants and $N\text{-}NO_3^-$ availability as substrate regulate the fate of the end product during denitrification (Blackmer & Bremner, 1978; Langarica-Fuentes et al., 2018; Morley et al., 2014; Weier et al., 2010). The *nos*Z clade II potentially consumes N_2O before emitting from soil because it only use N_2O as an electron acceptor (C. M. Jones et al., 2013). After N-fertilisation, the interaction with nosZ clade II between the rice cultivars might also influence the N_2O emission variations.

2.5.1.3 Dissimilatory nitrate reduction into ammonium (DNRA)

The average DNRA rate was <5 ng/g dry weight soil/hour, more than 100 fold lower than the total denitrification rate on day 1 after enrichment fertilisation. In addition, the DNRA rate remained static throughout the incubation period after fertilisation in both tested cultivars (Fig: 2.4.6A). Nitrification, in combination with oxygenation in the rhizosphere, might affect the DNRA. DNRA rate was found to be significantly higher in the rhizosphere of high nitrification-associated rice cultivar than that of low nitrification-associated rice cultivar (Fig: 2.4.6B). NO_3^- from nitrification might trigger the variations as the DNRA rate was positively correlated with nitrification (Zhang et al., 2015). A contrasting result was observed in the bulk compartments: ammonified NH_4^+ by DNRA might be anaerobically oxidised through anammox into N_2 more in the bulk compartment of the high nitrification-associated rice cultivar that might induce the variations between the bulk compartments (Qiao et al., 2022)(Valiente et al., 2022).

2.5.1.4 Anammox

The anammox rate remained static till the end of the experiment after N-fertilisation in both rice cultivars. Unlike other N-cycle processes, anammox depends on the presence of both oxidised and

reduced N compounds (NH_4^+ and NO_2^-). The coexistence of NH_4^+ and NO_2^- in the oxic/anoxic soil microsites of the rice rhizosphere and surrounding bulk soil where N-compounds are easily exchanged in their reduced and oxidised state by nitrification, denitrification and DNRA might maintain the anammox rate in similar pace throughout the incubation period (Zhu et al., 2010). The results suggested that fertilisation may indirectly affect the anammox, i.e. induced by other N-cycle processes (nitrification, denitrification and/or DNRA). Anammox-associated gaseous N_2 loss was significantly higher after N-fertilisation in the rice cultivar, favouring high nitrification and denitrification (Fig: 2.4.7A). NO_2^- from nitrification and denitrification would be more available in the high nitrification-associated rice cultivar, thus favouring a higher anammox rate. The contribution in total N_2 emission between anammox and complete denitrification was dissected by using the isotope ratio modelling discussed in the method (Section 2.3.11.6) within the days after enrichment fertilisation. N_2 contribution through complete denitrification was decreased in both rice cultivars, which might be due to NO_3^- limitation. NosZ clade I denitrifiers may sustain their anaerobic respiration by completing the denitrification pathway rather than truncating in the N-NO_3^-limiting condition (Simon & Klotz, 2013). However, NosZ clade II activity might be reduced due to the reduction of NirS and NirK denitrifiers activity as they only use N_2O as the electron acceptor during anaerobic respiration.

2.6 Concluding remarks

This experiment was done to understand N-cycle dynamics over five days after enrichment fertilisation to optimise the conditions of the rice screening experiment described in the following chapters. Nitrification, denitrification, and anammox significantly varied, but DNRA did not show any difference between the tested rice cultivars. Therefore, a screen was designed to assess selected rice cultivars (100 rice cultivars) simultaneously based on nitrification, denitrification and anammox processes using the single microcosm experiment using stable isotope-based techniques validated in this chapter. The results of the rice screening are discussed in the following three chapters (Chapters 3,4 and 5) utilising the same microcosm experiment. Denitrification was limited after day 1 of enrichment fertilisation, whereas nitrification was limited after day 2, and anammox variations were sustained throughout the five days. Thus, harvesting was performed one day after enrichment fertilisation to screen the rice cultivars based on nitrification, denitrification, and anammox. Indeed, I changed the microcosm design for the rice screening experiment after

observing nitrification in the bulk compartment, indicating that the microcosm pot was largely aerobic, which might limit denitrification.

Chapter 3: Exploring the rice genetics relatedness with nitrification in paddy soil

3.1 Introduction

3.1.1 Nitrification is the major N-sink from arable agricultural land

Nitrogen is an essential nutrient for plant growth, so applying nitrogen fertiliser is a common agricultural practice to maintain or increase yields. Advanced agriculture depends on high-yield modern crop varieties, which typically need significant inputs of inorganic nitrogen in cultivated land. The recent use of nitrogen fertilisers is ~110 M tons/ year, which will likely increase three fold by the middle of the century (FAO, 2022)(Tilman et al., 2001). 40 to 60 % of applied nitrogen fertiliser applied to agricultural land is recovered to plant biomass depending on the crop type and types of added nitrogen (Sebilo et al., 2013). The remainder is lost through chemical and microbial processes. Nitrification is arable agricultural land's major nitrogen sink process (Raun & Johnson, 1999; G. Subbarao et al., 2006). Nitrification is a strictly aerobic microbial process (Warington, 1878). The first step of nitrification, which is rate limiting, is the conversion of ammonia/ammonium into nitrite via hydroxylamine (Kowalchuk & Stephen, 2001). In the second step, nitrite further oxidised into nitrate. Commamox nitrifiers complete both processes because completion of the process is energetically efficient in inorganic limited conditions (Daims et al., 2019) (Hollocher et al., 1981). The nitrification labour is divided into two groups of nitrifiers. Ammonia oxidisers, including archaea (AOA) and bacteria (AOB), perform the first of nitrification, and nitrite oxidising bacteria (NOB) accomplish the second step of the process. Comammox is a suitable option in N-limited soil, but incomplete nitrifiers dominate in fertilised soil (e.g., AOB, AOA and NOB) (Costa et al., 2006). Ammonia oxidisers crossfeed the NOB by providing the substrate because NO_2^- is transiently available in the fertilised soil.

Ammonia oxidisers are the primary concern for arable agriculture because this process converts immobile inorganic N into mobile form, which is readily lost through leaching applied N unexploitable for plant uptake (Raun & Johnson, 1999; G. Subbarao et al., 2006). Aerobic and anaerobic soil microsites could be present in the same soil aggregates. So, when it reaches anaerobic soil microsites, nitrite/nitrate is lost gaseously, including N_2O (potent greenhouse gas) from the arable agricultural soil through anaerobic respiration processes. Subsequently, ammonia oxidisers also produce N_2O as a byproduct, and in suboxic conditions, instead of releasing nitrite

into the soil, they further covert into N_2O through autotrophic denitrification/nitrifier denitrification (X. Zhu et al., 2013).

3.1.2 Nitrification in rice rhizosphere

Flooded paddy soil inhibits nitrification due to predominant anaerobic conditions (Liu et al., 2019; Verhoeven et al., 2018). However, rice plant physiology provides a lifeline to nitrifiers. Rice plant genetics evolve to grow under artificial wetlands like paddy systems (Discussed in Chapter 1, section 1.5). Rice plants transport oxygen through aerenchyma to maintain root respiration in the flooded paddy soil (Armstrong, 1971). Oxygen is leaked from the root surface by radial oxygen loss (ROL) due to anoxic conditions in the flooded paddy soil, thus oxygenating the rice rhizosphere (Fig: 3.1.1). Rice genetics evolved to protect this oxygen loss while growing in flooded paddy soil. Rice plants deposit suberin and/or lignin in between cortex and root epidermal cells to curtail ROL that indirectly affects nitrification (Li et al., 2008; Kotula *et al.*, 2009; Li & Wang, 2013). Nevertheless, rice plants can inhibit nitrifier activity directly in soil by secreting phenolic compounds and secondary metabolites as root exudates, termed Biological nitrification inhibitors (BNIs)(Subbarao *et al.*, 2015, 2009; Subbarao *et al.*, 2017). (F. Yu et al., 2016) reported 1,9-decane diol as hydrophilic BNI, found in the rice root exudates, inhibits ammonia monooxygenase (AMO), and initiates the first of nitrification. Indeed, BNI secretion varied between their tested rice genotypes. (Yufang Lu et al., 2019) observed the reduction of both bacterial and archeal ammonia oxidisers' abundance after applying 1,9-decanediol in the paddy soil (Yufang Lu et al., 2019). Secretion of BNIs in the rhizosphere positively correlates with rice plants' nitrogen uptake efficiency (NUE) by inhibiting nitrification, suppressing AMO and/or HAO to increase NH_4^+ retention and reduce N losses in the rhizosphere (Chen et al., 2022; Coskun et al., 2017). (X. Zhang et al., 2019) reported that the oxygenation in the rhizosphere increased the BNI secretion from rice roots. Rice plants' genetics regulate oxygenation and BNI, which might modulate nitrification antagonistically in the rhizosphere. So, I hypothesised that the genetic variations of rice plants might elicit the rhizosphere's nitrification variations in the paddy soil after nitrogen fertilisation.

To test the hypothesis, Rice cultivars (n=100) originated from South-East Asia, including 3KG, Rice Diversity Panel 1 (RDP1), Rice Diversity Panel 2 (RDP2), and Bengal and Assam Aus Panel (BAAP) panels were randomly selected by using R software (R Core Team, 2020) for this

screening study. These four panels were chosen due to genomic data accessibility. Among the 100 rice cultivars, 2 rice cultivars failed to grow. The details of the 98 rice cultivars are given in the table (Table: 3.3.2).

3.2 Aims and Objectives

Before this rice screening experiment, I optimized growth conditions and labelling of the nitrate pool to simultaneously measure active N-cycle processes in fertilised paddy soil supporting rice growth and assess variation in the activity of soil between rice lines growing in that soil after adding N-fertiliser (Discussed in Chapter 2). The ^{15N} Nitrate pool dilution method efficiently measured the four nitrogen cycle processes from a single microcosm pot experiment. In addition, I observed that fertiliser-induced nitrification and denitrification became limited after day 1 of enrichment fertilisation. However, nitrification variation between the tested rice cultivars persisted to day 2 after fertilisation. So, I decided to harvest the microcosms on day 1 after enrichment fertilisation to screen the tested rice cultivars. The microcosm pot used in the initial experiment was largely aerobic (Fig: 3.3.1)). So, I altered the design of the microcosm pot to allow better assessment of both aerobic and anaerobic N-cycle processes in a single microcosm pot experiment. There were two primary objectives in this study.

1. Screen the selected rice cultivars based on nitrification variations using rice growth paddy soil.
2. Assuming significant variation is found, a genome-wide association studies (GWAS) approach is used to identify quantitative trait loci (QTLs)/probable candidate genes in the rice genome relating to reduced nitrification rate.

3.3 Methodology

3.3.1 Microcosm pot optimisation

A new microcosm pot was designed for this rice screening study to further improve the simultaneous analysis of nitrification, denitrification and anammox and their interaction with rice growth. The previous design of the microcosm pot used in Chapter 2 (designed by the previous PhD student for screening of nitrification variation only) from the N-cycle dynamics study may impose stringent conditions for denitrification as the pot has remained predominantly aerobic due to radial oxygen loss from the root surface. The rhizosphere compartment with a 4 cm diameter rhizobag of nylon mesh was positioned in the 5 cm pot (Fig: 3.3.1A), giving 50% of the pot volume as rhizosphere and bulk soil. However the bulk compartment, the hot zone for denitrification, had only a 0.5 cm diameter ring-shaped area surrounding the rhizosphere compartment in the pot. Oxygen by radial oxygen loss from roots may transport towards the bulk compartment with a gradient up to 0.4 cm from the mesh surface of the rhizobag (Y. Li & Wang, 2013)**.** Thus, the hypothetically anaerobic zone in the microcosm pot was reduced into only a 0.1cm ringed-shaped area. So, a new microcosm pot was designed by placing a window-shaped separator with glued mesh instead of rhizobag to increase the anaerobic zone in the same sized (5cm diameter pot) pot in such a way that makes a balance between the rhizosphere and bulk compartments (Fig: 3.3.1B).

3.3.2 Microcosm packing

Paddy soil (imported from Nimtoli farm, Munshiganj, Bangladesh (23° 37′ 00″ N 90° 19′ 16″ E)) was collected from a paddy field under the standard agronomic practice with urea fertilization and rice-mustard rotation. The soil was packed at 1.2 g dry weight soil/cm^3 maintained the same bulk density that (Langarica-Fuentes et al., 2018b) used for their model root exudates effect study. The physicochemical parameters of the soil are given in Table: 3.3.1. Before packing, the soil was sieved through a 4mm sieve to remove plant debris and stone. 117 g dry weight equivalent total soil was packed in each microcosm pot. The diameter and height of the microcosm pots are 5.0 cm and 7.0 cm, respectively (Gosselin™ Straight Polypropylene Container, Fisher Scientific). Each microcosm pot was subdivided into rhizosphere and bulk compartment (Fig: 3.3.1B)). A window-shaped separator with 35 µm glued nylon mesh was placed to make the rhizosphere

compartment half the volume of the bulk compartment. The rhizosphere and bulk compartment packed 39 g and 78 g of dry-weight soil, respectively. Soil packing was done in two stages. First, 50% of the soil for each compartment was packed and compressed to the desired bulk density, with a wooden object having a similar shape to the compartments. Afterwards, the rest half of the soil was added and packed to maintain an equivalent height within the pot. Prepared soil microcosms were rested and flooded for ten days before seedling transfer at the Arthur Willis Environment Centre, University of Sheffield, UK.

Table 3.3.1: The physicochemical parameters of the paddy soil used in this rice screening study.

Parameter	**Results**
Moisture	19.4 %
pH	6.18
Organic Carbon	1.4012 %
Nitrogen (N)	0.196 %
C:N Ratio	7:1
Phosphorus (P)	0.103 %
Sulphur (S)	0.25 %
Sand (%)	18.16
Silt (%)	43.38
Clay (%)	38.46
Textural class	Silty clay loam

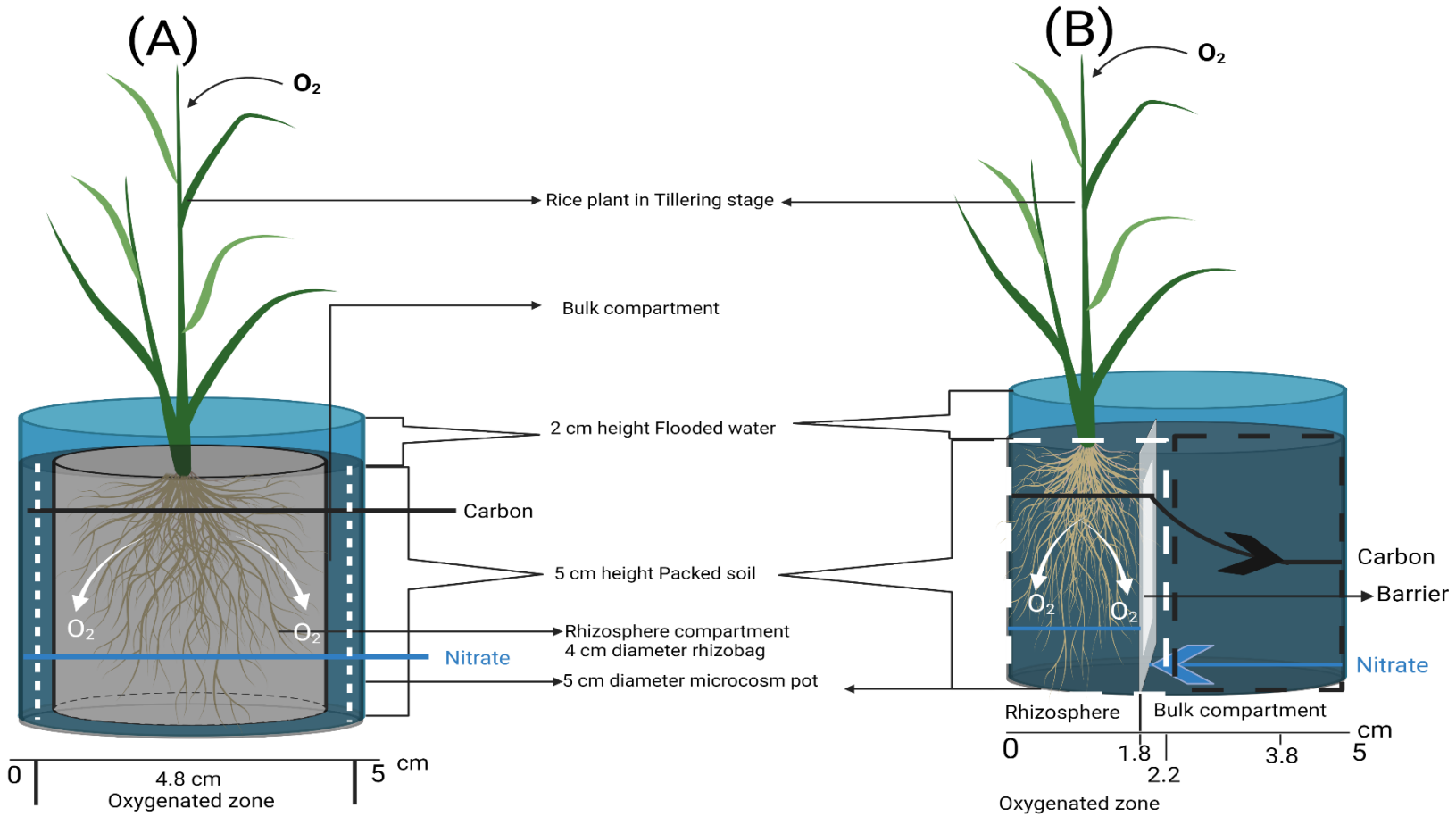

Fig 3.3.1: Schematic diagram of designed microcosm pots. (A) The previously designed microcosm pot used by the previous PhD student for the rice screening to analyse nitrification variations was used in the N-cycle dynamics experiment. (B) The newly designed microcosm pot for the rice screening simultaneously analysed variations in nitrification, denitrification, and anammox.

3.3.3 Plant growth, harvesting and nitrification rate measurement

The selected rice cultivars were grown with (four replicates) in a randomized block design with additional unplanted microcosm pots as control. Each block was planted and harvested with a week gap to allow sufficient time for all manipulations and preparation. Plant growth conditions, N-fertilisation rate and harvesting were maintained to measure the nitrification rate as described in (Chapter 2, Section 2.3.3). But we amended the enrichment fertilisation procedure for T0 samples. The enrichment fertiliser was added after the destruction of the T0 microcosm pots instead of injecting immediately before dismantling the pots. The SOP for harvesting T0 (Fig: 3.3.2) and T1 (Fig: 3.3.3) microcosm pots were outlined below. The gross nitrification rate was measured by previously described methods (Chapter 2, Section 2.3.11.1).

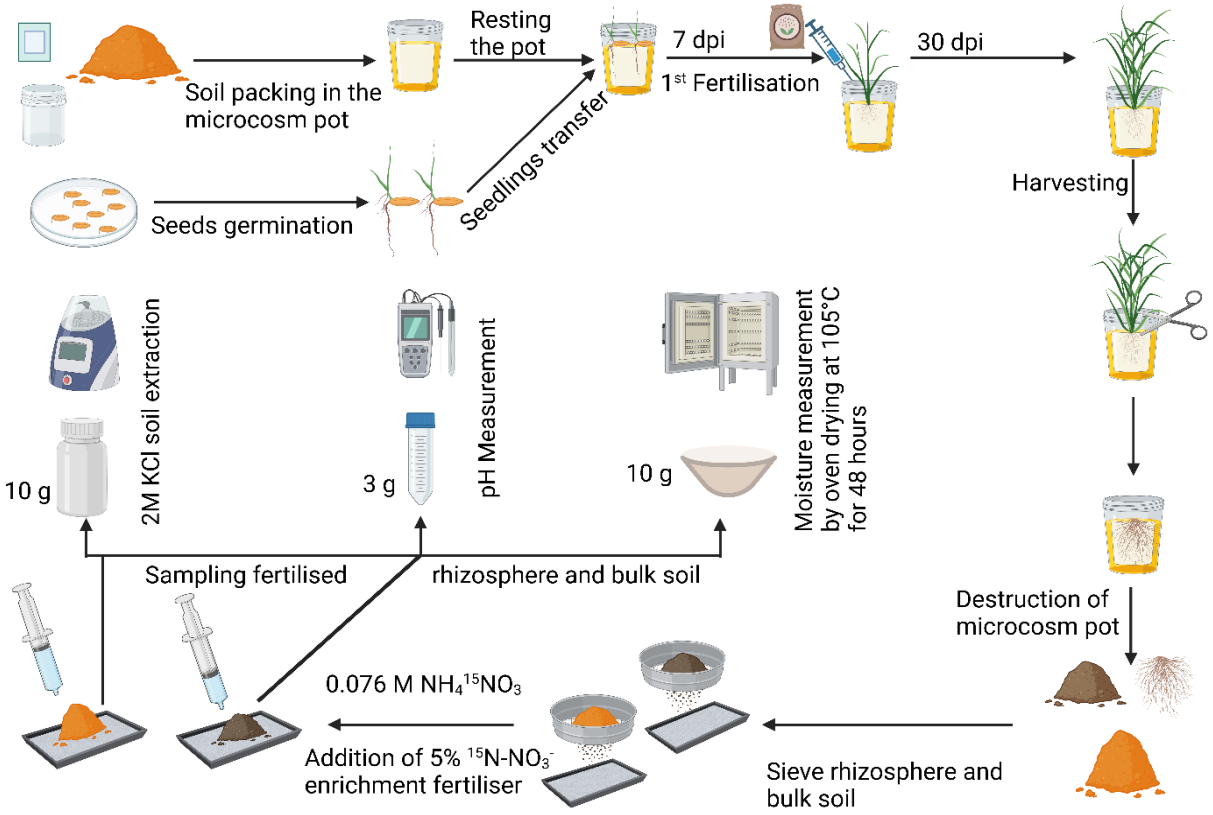

Fig 3.3.2: Schematic outline for T0 harvesting performed on day 30 after seedling transfer into the microcosm pots. After cutting the shoot, the rhizosphere and bulk compartment soil were collected and sieved into two trays. Soil samples were aliquoted for KCl soil extraction, pH and moisture measurement.

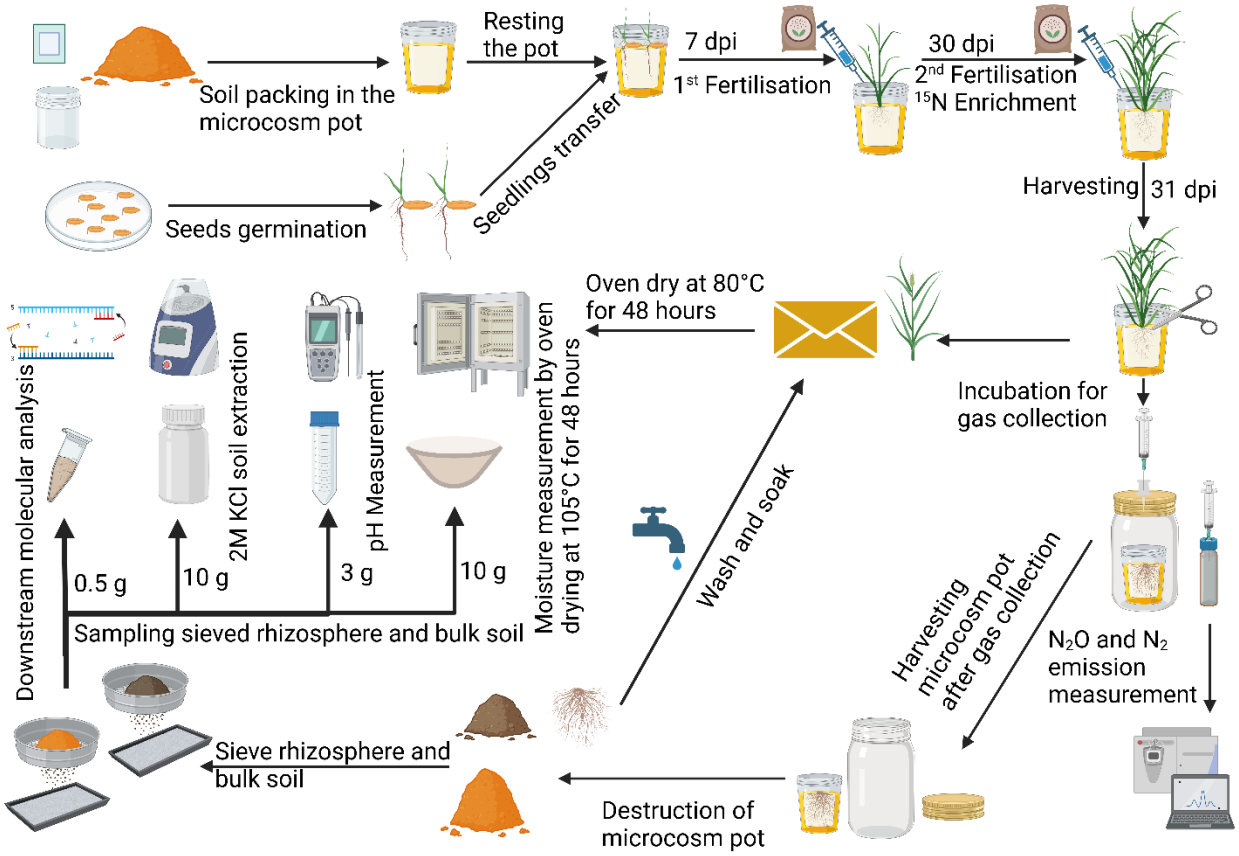

Fig 3.3.3: T1 microcosms pots were harvested 24 hours after enrichment fertilisation on the 31st day of plant growth after seedling transfer. Gas samples were collected before T1 harvesting for downstream denitrification and anammox analysis. 0.5 g soil samples were aliquoted and snap-frozen for downstream molecular analysis. Root and shoot were collected in paper bags for dry-weight biomass measurement.

Table 3..3.2: Description included germplasm accession name, genotype ID, country of origin, panel and sub-population of selected 98 rice cultivars. All selected rice lines belonged to *Oryza sativa* species but in different sub-population, where ADM-IND and ADM-JAP are hybrid rice varieties. ADM-IND and ADM-JAP are admixed indica and admixed japonica varieties, respectively. TRJ and IND are the tropical japonica and indica rice varieties.

Rice ID	GS_accession_name	Genotype_assay_ID	Country	Sample Set	Subpop
R3	RAYADA::IRGC 27594-1	IRIS_313-9108	Bangladesh	RDP2	ADM-IND
R4	P. TINGAGEW DAYKET QAY DAYON::IRGC 8046-1	fc730730.0	Philippines	RDP2	TRJ
R5	Padi Ladang Ase Polo Komek	B026	Indonesia	3KG	ADM-IND
R6	IR 65600-27-1-2-2	CX117	Philippines	3KG	IND1
R7	IR 47686-6-2-1-1	CX243	Philippines	3KG	TRJ
R8	IR 42	CX161	Philippines	3KG	IND2
R9	RANTAT::IRGC 43563-3	IRIS_313-11316	Indonesia	3KG	IND2
R10	LEMUNGSIR::IRGC 18116-3	IRIS_313-10788	Indonesia	3KG	TRJ
R11	PADI MIAT (KECIL)::IRGC 97366-1	IRIS_313-12285	Malaysia	3KG	TRJ
R12	KAUKHNYIN ANI::IRGC 33176-1	498a66b3.0	Myanmar	RDP2	IND3
R13	PAYO TINGGI::IRGC 73778-1	IRIS_313-11905	Indonesia	3KG	IND2
R14	TI NGI::IRGC 73620-1	IRIS_313-11901	Thailand	3KG	IND2
R15	NEANG LAU::IRGC 81328-1	IRIS_313-12040	Cambodia	3KG	IND2
R16	CHAN LEUY::IRGC 81223-1	IRIS_313-12036	Cambodia	3KG	IND2
R17	KHAO HAE::IRGC 29773-3	IRIS_313-11085	Laos	3KG	IND3
R18	EA TIA::IRGC 29713-2	IRIS_313-11083	Laos	3KG	ADM-IND
R19	PADI HANGIR::IRGC 79507-1	IRIS_313-12006	Malaysia	3KG	TRJ
R20	MOK::IRGC 107804-1	IRIS_313-12353	Laos	3KG	ADM-JAP
Rice ID	**GS_accession_name**	**Genotype_assay_ID**	**Country**	**Sample Set**	**Subpop**

R21	KHAO' DAENG HAWM::IRGC 71001-1	IRIS_313-11831	Thailand	3KG	ADM-JAP
R22	MAE YEU::IRGC 64509-1	IRIS_313-9575	Thailand	3KG	IND2
R23	KUATEK::IRGC 14285-1	IRIS_313-9210	Malaysia	3KG	IND2
R24	LAI HANG HMA::IRGC 29608-2	IRIS_313-11077	Laos	3KG	ADM-JAP
R25	KAUK PAHLING::IRGC 95823-2	IRIS_313-12266	Myanmar	3KG	ADM-JAP
R33	KOMPIT::IRGC 73716-1	IRIS_313-11903	Indonesia	3KG	TRJ
R34	KHAW KAR 13::IRGC 36711-1	IRIS_313-11195	Myanmar	3KG	ADM-JAP
R35	DAMNOEUB KHSE SAUT::IRGC 22819-2	IRIS_313-10899	Cambodia	3KG	IND2
R36	STRAW 23-438::IRGC 38426-2	IRIS_313-11230	Bangladesh	3KG	IND3
R37	PENDEK LAYUNG::IRGC 43542-2	IRIS_313-11315	Indonesia	3KG	IND2
R38	MAUNG NYO::IRGC 33351-2	IRIS_313-11135	Myanmar	3KG	IND3
R39	LAI NOK KHA::IRGC 29604-2	IRIS_313-11076	Laos	3KG	ADM-IND
R42	BAZAIL 980::IRGC 32817-2	IRIS_313-11124	Bangladesh	3KG	ADM-IND
R43	PAE MEETO::IRGC 27254-1	IRIS_313-11003	Indonesia	3KG	TRJ
R44	TJ PERAK::IRGC 19141-1	IRIS_313-10821	Indonesia	3KG	IND2
R45	SRAU THMOR::IRGC 29904-1	IRIS_313-11089	Cambodia	3KG	ADM-IND
R46	SINTHA::IRGC 24687-1	IRIS_313-10941	Indonesia	3KG	IND2
R48	SAITA::IRGC 31618-1	IRIS_313-11111	Bangladesh	3KG	AUS
R49	SADUMONI::IRGC 25919-1	IRIS_313-10964	Bangladesh	3KG	AUS
R50	PULUT PUTIH::IRGC 27426-1	IRIS_313-11010	Indonesia	3KG	IND2
R51	PULU RENNI::IRGC 27386-1	IRIS_313-11006	Indonesia	3KG	IND2
R52	PUEY TAW::IRGC 71405-1	IRIS_313-11844	Thailand	3KG	ADM-IND
Rice ID	**GS_accession_name**	**Genotype_assay_ID**	**Country**	**Sample Set**	**Subpop**

R53	PLAWNG SAENG::IRGC 64595-1	IRIS_313-11685	Thailand	3KG	IND3
R54	PA KHENG::IRGC 12996-1	IRIS_313-10682	Laos	3KG	ADM-IND
R55	NIAW KHAMIN::IRGC 40222-1	IRIS_313-11248	Thailand	3KG	TRJ
R63	KALABOKRI::IRGC 43872-1	IRIS_313-11324	Bangladesh	3KG	AUS
R64	J 6 IR 520 (WC 693)::IRGC 57600-1	IRIS_313-11538	Philippines	3KG	IND2
R66	HEGAR MANAH::IRGC 17733-1	IRIS_313-10774	Indonesia	3KG	IND2
R67	GI TAH::IRGC 74883-1	IRIS_313-11920	Thailand	3KG	IND3
R68	GASET BOW::IRGC 64316-1	IRIS_313-11679	Thailand	3KG	ADM-IND
R69	EA POUAK::IRGC 89748-1	IRIS_313-12194	Laos	3KG	IND3
R70	DV 110::IRGC 8855-1	IRIS_313-10606	Bangladesh	3KG	AUS
R72	DB 3::IRGC 8361-1	IRIS_313-10587	Bangladesh	3KG	AUS
R73	CHON::IRGC 78776-1	IRIS_313-11991	Laos	3KG	ADM-IND
R74	CHAO LAO SOUNG::IRGC 78799-1	IRIS_313-11992	Laos	3KG	ADM-IND
R75	CHAN THANH HOA::IRGC 60647-1	IRIS_313-11594	Vietnam	3KG	ADM-IND
R76	BKN BR 1031-78-5-4::IRGC 55927-1	IRIS_313-11515	Thailand	3KG	IND2
R77	BATIBATIKAN::IRGC 96098-1	IRIS_313-12271	Philippines	3KG	TRJ
R78	BALIBUD::IRGC 26871-1	IRIS_313-10990	Philippines	3KG	ADM-IND
R79	BABELIONG::IRGC 82688-1	IRIS_313-12070	Malaysia	3KG	TRJ
R80	AUS 242::IRGC 29040-1	IRIS_313-11051	Bangladesh	3KG	AUS
R81	KINANDANG BUSIKSIK::IRGC 74607-1	IRIS_313-9389	Philippines	3KG	TRJ
R82	SAHULO FACHE SOYO::IRGC 66630-1	IRIS_313-9470	Indonesia	3KG	TRJ
R83	KHAO THI RATE::IRGC 58041-1	IRIS_313-8793	Myanmar	3KG	ADM-IND
Rice ID	**GS_accession_name**	**Genotype_assay_ID**	**Country**	**Sample Set**	**Subpop**

R84	IRRIBINI::IRGC 49094-1	IRIS_313-8437	Bangladesh	3KG	IND3
R85	DAM::IRGC 23710-1	IRIS_313-8580	Thailand	3KG	ADM-JAP
R86	E WAWNG::IRGC 71140-1	IRIS_313-8884	Thailand	3KG	TRJ
R100	YEBAWYIN::IRGC 33885-1	IRIS_313-8697	Myanmar	3KG	IND3
R101	KINYO::IRGC 47248-1	f3b98222.0	Philippines	RDP2	TRJ
R104	IR 57924-24::IRTP 16675-C1	IRIS_313-7699	Philippines	RDP2	IND2
R106	GOGO::IRGC 43390-C1	2257c553.0	Indonesia	RDP2	TRJ
R107	GANIGI::IRGC 48698-C1	7504add9.0	Indonesia	RDP2	TRJ
R108	CHA LOY OE::C1	IRIS_313-7856	Thailand	RDP2	ADM-JAP
R109	YN 2484-507-21::IRGC 117364-1	c52e90d8.0	Myanmar	RDP2	IND2
R110	IR 2006-P12-12-2::IRGC 32675-C1	04a06fb8.0	Philippines	RDP2	IND2
R111	TOANG::IRGC 19144-1	1e443ba8.0	Indonesia	RDP2	TRJ
R112	PSBRC 18::IRGC 117375-1	a79461d6.0	Philippines	RDP2	IND2
R113	MOSHUR::IRGC 64789-1	2bfcbe44.0	Bangladesh	RDP2	AUS
R114	EMATA A 16-34	d0392fe8.0	Myanmar	RDP1	ADM-IND
R115	DHALA SHAITTA	7d4c6c4e.0	Bangladesh	RDP1	AUS
R116	BR24	872ec0b4.0	Bangladesh	RDP1	IND2
R117	ARANG::IRGC 43322-1	IRIS_313-8791	Indonesia	3KG	IND2
R118	IR 64-21	f66e275e.0	Philippines	RDP1	IND2
R119	AWD036-AUS-22-FT80	19_19	Bangladesh	BAAP	AUS22
R120	AWD034-AUS-12-FT74	17_17	Bangladesh	BAAP	AUS12
R121	AWD038-AUS-28-FT80	20_20	Bangladesh	BAAP	AUS28
R122	AWD035-AUS-16-FT80	18_18	Bangladesh	BAAP	AUS16
R123	AWD031-BOWALIA-2-FT80	16_16	Bangladesh	BAAP	BOWALIA 2
R124	AWD030-BOWALIA-FT80	15_15	Bangladesh	BAAP	BOWALIA
R126	AWD026-ARC-11600-FT74	13_13	India	BAAP	AUS MURALI
R127	AWD025-ARC-11340-FT80	12_12	India	BAAP	ARC 11600
R128	AWD023-ARC-11205-FT80	11_11	India	BAAP	ARC 11340
R129	AWD015---FT80	9_9	India	BAAP	ARC 11205
R130	AWD022-ARC-10392-FT74	10_10	India	BAAP	AS 2
R131	AWD012-ARC-6240-FT84	6_6	India	BAAP	ARC 10392
Rice ID	**GS_accession_name**	**Genotype_assay_ID**	**Country**	**Sample Set**	**Subpop**

R133	AWD009-ARC-5977-FT80	4_4	India	BAAP	ARC 6240
R134	AWD006-ASSAM-4BORO-FT80	1_1	India	BAAP	ARC 6000
R135	AWD051-AUS-68-FT84	29_29	Bangladesh	BAAP	ARC 5977
R136	AWD048-AUS-63-FT84	27_27	Bangladesh	BAAP	ASSAM 4(BORO)
R137	AWD040-AUS-31-FT74	22_22	Bangladesh	BAAP	AUS 68

3.3.4 Dissolved organic carbon (DOC) measurement

The DOC measurement method was adapted from Bartlett and Ross's (1988) method with a 96-well microplate reader. It relies on the loss of colour from an Mn(III)-pyrophosphate complex as Mn(III) becomes reduced by organic C in the presence of concentrated H_2SO_4. Carbon compounds such as sugar, organic acids and amino acids were used as standards with concentrations ranging from 0- to 4-mM C (Soil extracts were diluted five-fold with dH_2O). This method could not detect efficiently above 4mM C concentration solution. 100 µl of Soil extracts and standards were sampled into a 96-well, flat-bottomed, polystyrene microtiter plate (Corning, USA). Immediately, 50 µl of 10 mM Mn(III)- pyrophosphate solution and 50 µl of concentrated sulfuric acid were mixed with soil extracts and standards—the microtitre plate was incubated in the dark for 18 hours at room temperature. Absorbance was measured at 495 nm using the Tecan Spark 10M plate reader (Tecan, Switzerland). Soil extract absorbance was converted to C concentration using a linear calibration curve based on standards.

3.3.5 Genome-wide association studies (GWAS)

Genome-wide association studies (GWAS) analysed the major and minor quantitative trait locus (QTLs) in rice cultivars' genetics associated with the variations in nitrification rates as the phenotypic trait, were analysed by Genome-wide association studies (GWAS). Public genotype datasets include a high-density rice array (HDRA) consisting of 700,000 single nucleotide polymorphisms (SNPs) generated from 1568 diverse rice varieties (McCouch et al., 2016) and the imputed two SNPs database. Imputed Rice Reference Panel (RICE-RP) consists of 5231433 SNPs from 4591 rice varieties, and the other imputed BAAP consists of 2053863 informative SNPs from 299 aus accessions (Norton et al., 2018)(Mansueto et al., 2017). I used the merged RICE-RP and

BAAP dataset because it contained all the rice varieties used in our study, and this dataset includes a phenotype file, genotype data and a pipeline for performing GWAS with a kinship matrix and principal coordinates. The merged dataset had 5.2M SNPs dropping to 2.5M after minor alleles (frequency less than 0.1) were removed. The merged genomic RICE-RP and BAAP data was filtered at MAF >0.01 using the PLINK toolkit (https://zzz.bwh.harvard.edu/plink/) (Purcell et al., 2007) for the varieties with nitrification rate. This genetic data analysis was performed in the high-performance computer system of the University of Durham using a Linux environment. The statistical principal generated the principal coordinates (PCs) coordinates analysis (PCoA) tool using R software (R Core Team, 2015). PCs were screened based on Eigenvalues to include as covariates in the final analysis. Then, the python-coded pipeline (Supplementary 1) was used to run GWAS with a linear mixed model with kinship matrix and PC covariates by using the R package GENABLE (Aulchenko et al., 2007), and output was plotted as Manhattan and QQ plots, where the p values were transformed as -log10(p) so that larger values corresponded to stronger associations. The final Manhattan plot was used to highlight and visualise the distribution of associated p-values for significant single nucleotide polymorphisms (SNPs), where the top hit p-value of the SNPs indicates their significant association with nitrifcation phenotypic trait. Moreover, the quantile-quantile (QQ) plot was used to present the variation of detected p-values from the null hypothesis of non-associated SNPs and the rank the p-values of each SNP to plot against a hypothetical $\chi 2$-distribution in the QQ-plot.

3.3.6 Candidate gene identification

The top SNPs (p-value beyond the threshold limit of QQ plot) and the associated chromosome number were input in the online rice genome browser (http://ricediversity.org/tools/) to identify nearby genes potentially linked with the trait of interest. Gene loci present in the 10 Kb upstream or downstream (moderate search window for the website) of the particular SNP were considered associated with genes for the trait of interest. The potential candidate genes were short-listed based on the general gene ontology, and then genes were categorised for their respective function.

3.3.7 Statistical analysis

R studio version 4.0.2 (R Core Team, 2022) software was used for ANOVA to analyse the nitrification rate variations between the selected rice cultivars. The principal component analysis and Spearman correlation matrix analysis from the same R package were used to observe the correlation between tested parameters and nitrification rates. All the results figures were made using R and the rest were prepared using the Biorender app.

3.4 Results

3.4.1 Rice plant effects on residual inorganic N

Rice plants significantly affected the applied inorganic N in the rhizosphere and bulk soil of planted microcosms (Table: 3.4.1). Still, there was no significant rice genotype effect in planted microcosms (Table: 3.4.2). The residual N-NH_4^+ concentration (μgN/g dry-weight soil) was approximately two-fold higher than the residual N-NO_3^- concentrations (μgN/g dry-weight soil) in the unplanted soil (Fig: 3.4.1A). In contrast, there was no significant difference between the residual inorganic N in the rhizosphere soil of planted microcosms. Still, in the bulk soil of planted microcosms, residual N-NH_4^+ concentration (μgN/g dry-weight soil) was significantly higher than the residual N-NO_3^- concentrations (μgN/g dry-weight soil)(Table: 3.4.2), which was a similar concentration of unplanted soil (Fig: 3.4.1A).

Table 3.4.1: Two-way (Type II) Anova results for the rice plant effects on residual inorganic N in the rhizosphere (with plant) (n=343) and bulk (plant adjacent) compartments (n=349) of planted microcosms and in unplanted (without plant) microcosms (n=4) at the significance levels' ***' 0.001 '**' 0.01 '*' 0.05 '.' 0.1.

Response	Sum Sq	Df	F value	Pr(>F)	Significance
Plant (P)	9923	1	66.4302	<2.2e-16	***
Residual N (N)	9	1	0.0573	0.81095	
P x N	1692	1	11.3277	0.000802	***

Table 3.4.2: Three-way (Type II) Anova results for the rice genotypes (n=98) effects on residual inorganic N in rhizosphere (n=343) and bulk compartments (n=349) of planted microcosms at the significance levels' ***' 0.001 '**' 0.01 '*' 0.05 '.' 0.1.

Response	Sum Sq	Df	F value	Pr(>F)	Significance
Rice genotypes (R)	17906	97	1.1638	0.1414	
Compartment (C)	12988	1	81.8801	<2e-16	***
Inorganic N (N)	1692	1	953.1936	<2e-16	***
R X C	151198	97	0.8714	0.8046	
R X N	13408	97	1.0353	0.3920	
C X N	15930	1	756.6426	<2e-16	***
R X C X N	120021	97	1.0231	0.4228	

3.4.2 Rice plant effects on Nitrification

Nitrification was inhibited in the unplanted microcosm, and the gross nitrification rate was negative. The residual N-NO_3^- from first fertilisation (unenriched NH_4NO_3) diluted the ^{15}N signature in N-NO_3^- of applied 4.67% enriched $NH_4{}^{15}NO_3$ in T0 samples of unplanted soil. The ^{15}N signature in N-NO_3^- of T0 was measured lower than that of T1 samples of unplanted soil, measuring calculated GNR as a negative value. The mean gross nitrification rate in rhizosphere soil of planted microcosms was 929.9±68.9 in ng N/g dry-weight soil/hour (n=343) (Fig: 3.4.1B).

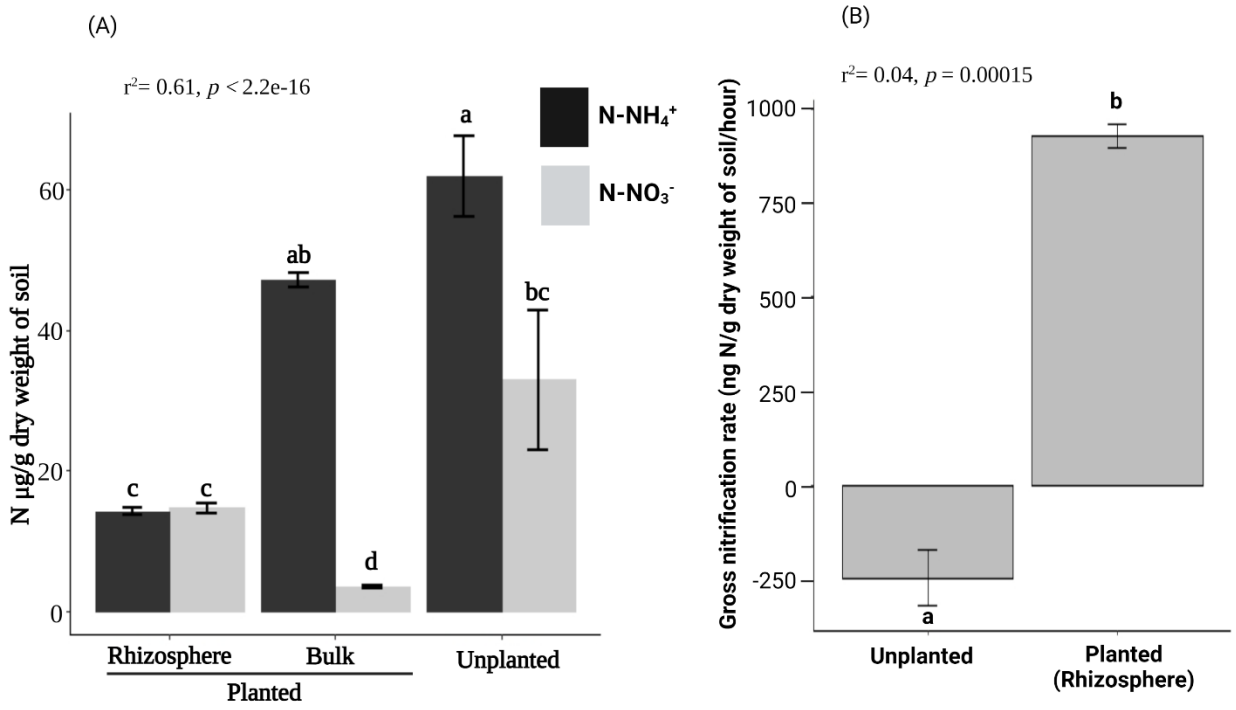

Fig 3.4.1: **(A)** Mean ± SE from two-way (Type II) ANOVA of residual $N\text{-}NH_4^+$ and $N\text{-}NO_3^-$ µg N/g dry weight of soil in unplanted soil (n=4), rhizosphere (n=343), and bulk soil (n=349) of planted microcosms. The letters indicated a significantly different group (P<0.001, ANOVA, Tukey HSD). **(B)** Mean ± SE from one-way (Type II) ANOVA of gross nitrification rate in ng N/g dry weight soil/hour of unplanted soil (n=4) and rhizosphere (n=343) soil of planted microcosms. The letters indicated a significantly different group ($r^{2=}$ = adjusted residual error, P<0.001, ANOVA, Tukey HSD).

3.4.3 Rice genotypes effects on nitrification

The gross nitrification rate (GNR) in ng N/g dry weight of soil/hour in the rhizosphere after 1 day of enrichment fertilisation significantly varied ($p<0.05$) between rice cultivars (Fig: 3.4.2). The rice cultivar R77, high GNR rice cultivar, supported significantly higher GNR in the rhizosphere coloured as red than twenty-two rice cultivars that I have labelled as low GNR rice cultivars, coloured green. The remaining seventy-five cultivars were intermediate and uncoloured.

3.4.4 Relationship between nitrification and measured soil biotic and abiotic factors

Spearman correlation matrix analysis was performed to understand the relationship between rhizosphere GNR with other measured nitrogen cycle processes and measured soil biotic and abiotic parameters in planted rice microcosms. Rhizosphere GNR was positively correlated with dry-weight biomass of root (r^2= 0.28, P<0.01) and shoot (r^2= 0.2, P<0.001), residual N-NH_4^+ (r^2=0.21, P<0.01) and N-NO_3^- (r^2=0.46, P<0.001) and DOC: N-NO_3^- ratios (r^2=0.15, P<0.05) in the bulk soil. In contrast, rhizosphere GNR reciprocally related to ^{15}N atom % in NO_3^- of the rhizosphere (r^2= -0.78, P<0.001), dry weight shoot: root ratios (r^2= -0.15, P<0.05) and DOC: N-NO_3^- ratios (r^2= -0.27, P<0.001) in the bulk soil. No correlation existed with other analysed N-cycle processes (Table: 3.4.3).

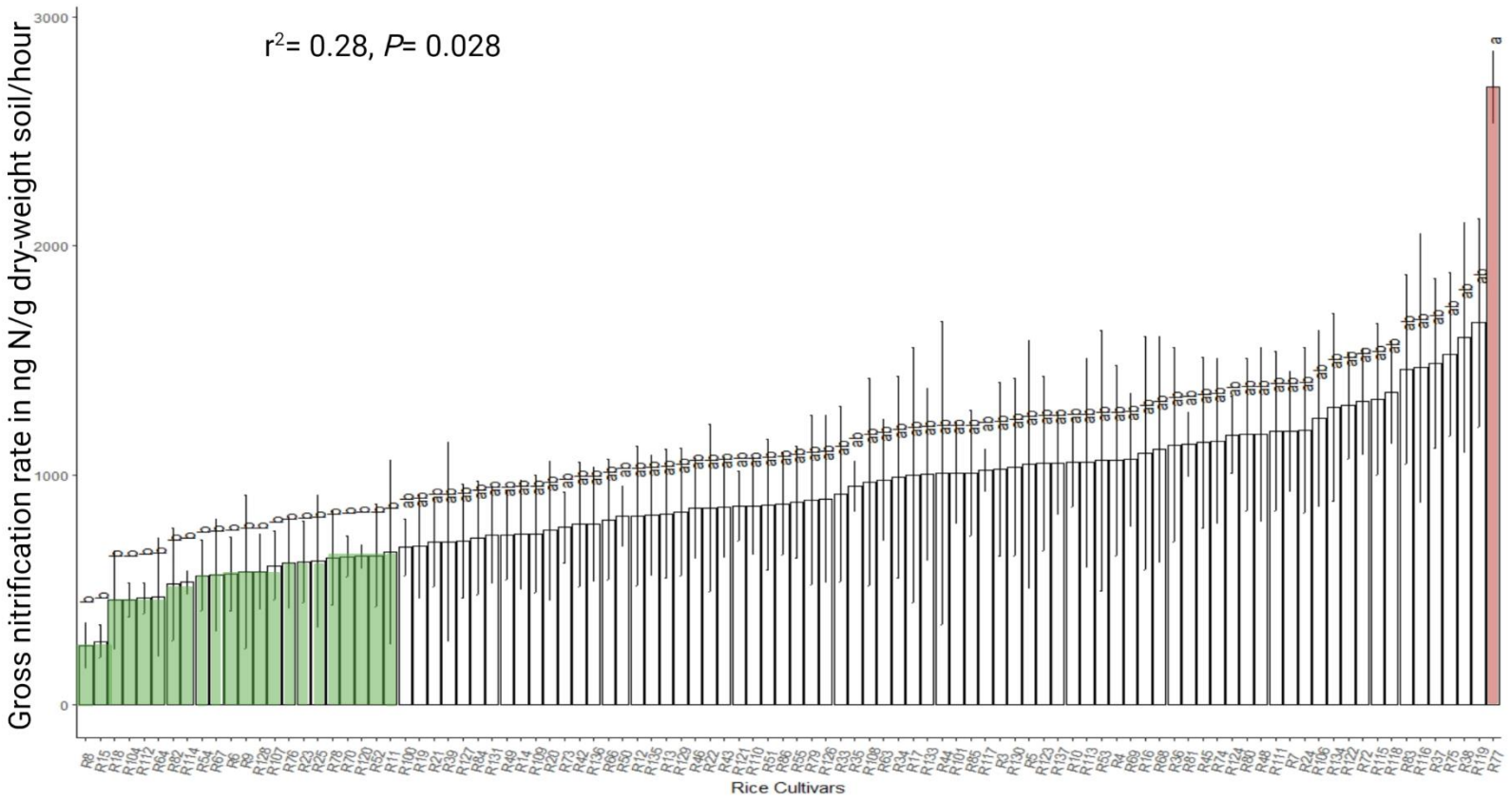

Fig 3.4.2: Mean±SE (n=4) from one-way (Type II) ANOVA of gross denitrification rate (GNR) in ng N/g dry-weight soil/hour in the rhizosphere compartment of microcosms growing tested rice cultivars (n=98). Rice cultivars associated with low rhizosphere GNR were indicated by green-coloured bars, and the single rice cultivar associated with high activity is indicated in red. The letters indicated a significantly different group (r^2 = adjusted residual error $P<0.05$, ANOVA, Tukey HSD).

Table 3.4.3: Relationship of rhizosphere GNR with N-cycle processes and tested soil parameters (Biotic and abiotic factors) in the rice microcosms by Spearman correlation matrix analysis. Rhizosphere and bulk compartments were denoted by R and B, respectively.

Responses	**$^{15}NO_3^-$**	**CD**	**TD**	**Ratio**	**PD**	**ANX**	**R [N-NH_4^+]**	**B [N-NH_4^+]**	**R [N-NO_3^-]**	**B [N-NO_3^-]**	**R DOC**	**B DOC**	**R C/N**	**B C/N**	**Root**	**Shoot**	**SR**	**R pH**
r^2	-0.78	0.10	0.02	0.02	0.02	0.06	0.21	0.09	0.46	-0.02	0.02	0.11	-0.27	0.15	0.23	0.20	-0.15	0.04
P	<0.001	ns	ns	ns	ns	ns	<0.001	ns	<0.001	ns	ns	ns	<0.001	<0.05	<0.001	<0.001	<0.05	ns

$^{15}NO_3^-$= ^{15}N atom % in NO_3^-, PD=Partial denitrification rate, CD=Complete denitrification rate, TD=Total denitrification rate, Ratio= N-N_2O: N-N_2O+N-N_2, ANX=Anammox, C/N= DOC: NO_3^-, SR= Dry weight shoot and root biomass ratio and ns= no significance

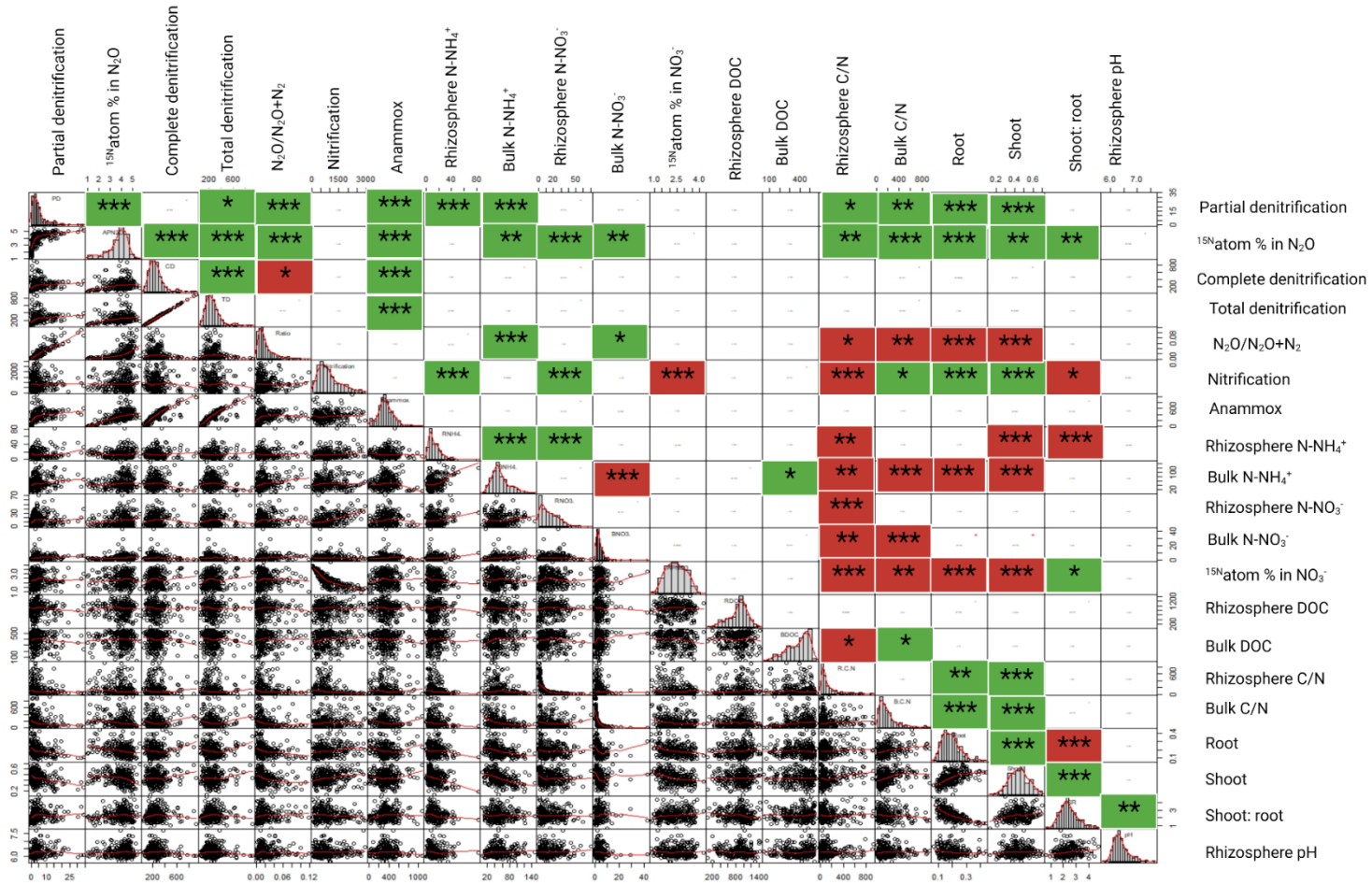

Fig 3.4.3: Spearman correlation matrix analysis between all tested parameters from this study. Uncoloured boxes indicate no significant correlation; green boxes indicated positive and red indicated negative correlations at the significance levels of '***'0.001, '**'0.05, '*' 0.01

3.5 GWAS results for nitrification variations as the phenotypic trait of tested rice cultivars

The GWAS analysis yielded a summary output file containing the most significant SNPs with the calculated major and minor allele effects. A Manhattan plot was produced displaying significant single nucleotide polymorphisms (SNPs) associated with variation in rhizosphere GNR activity from the genome-wide analysis. Genome order per chromosome was plotted on the X-axis against the −log10 of the p-values of SNPs on the Y-axis (Fig: 3.4.4) (Norton et al., 2018). The Significant threshold limit for the SNPs was set at –log10 (4.8) for a false discovery rate (FDR) limit of 0.05, where SNPs significantly deviated from the null hypothesis in the (QQ) plot (Fig: 3.4.5) (Kaler & Purcell, 2019). SNPs significantly deviated from the null hypothesis (Grey straight line), suggesting less chance of being falsely positive. (The genomic inflation factor (known as λgc) value was 0.824 in the QQ plots, indicating that fewer biases were anticipated while modelling, but phenotype data and the p-values of most SNPs were sparsely distributed in the chromosomes. The low λgc value also indicated a low number of SNPs as variants within a gene. Ten significant SNPs were observed above the FDR limit of 0.05 (Fig and details of the significant SNPs with identified loci as quantitative trait loci (QTLs) and annotated genes and protein and function from Uniport Blast website (www.uniprot.org) summarised in the table (Table: 3.4.4).

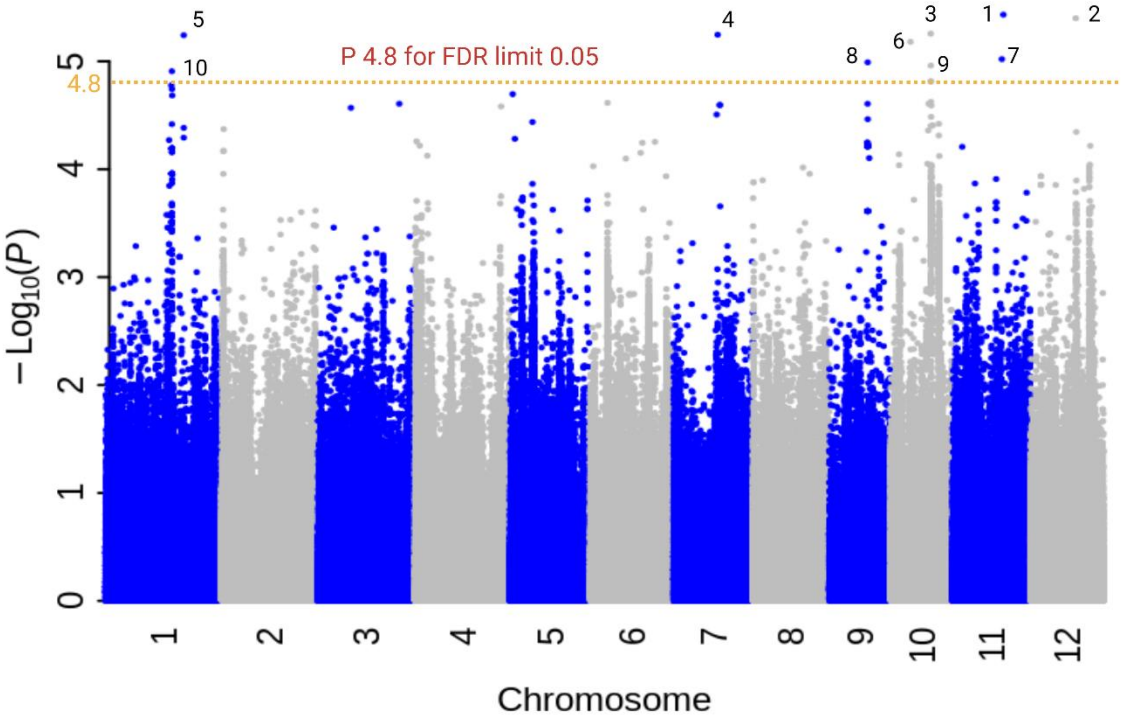

Fig 3.4.4: Manhattan plot from the GWAS analysis of SNPs in the chromosomes associated with rhizosphere GNR variations. Significant SNPs were above the yellow dotted line, having $-Log_{10}(P) > 4.8$ for the FDR limit ($P<0.05$) marked with their rank number.

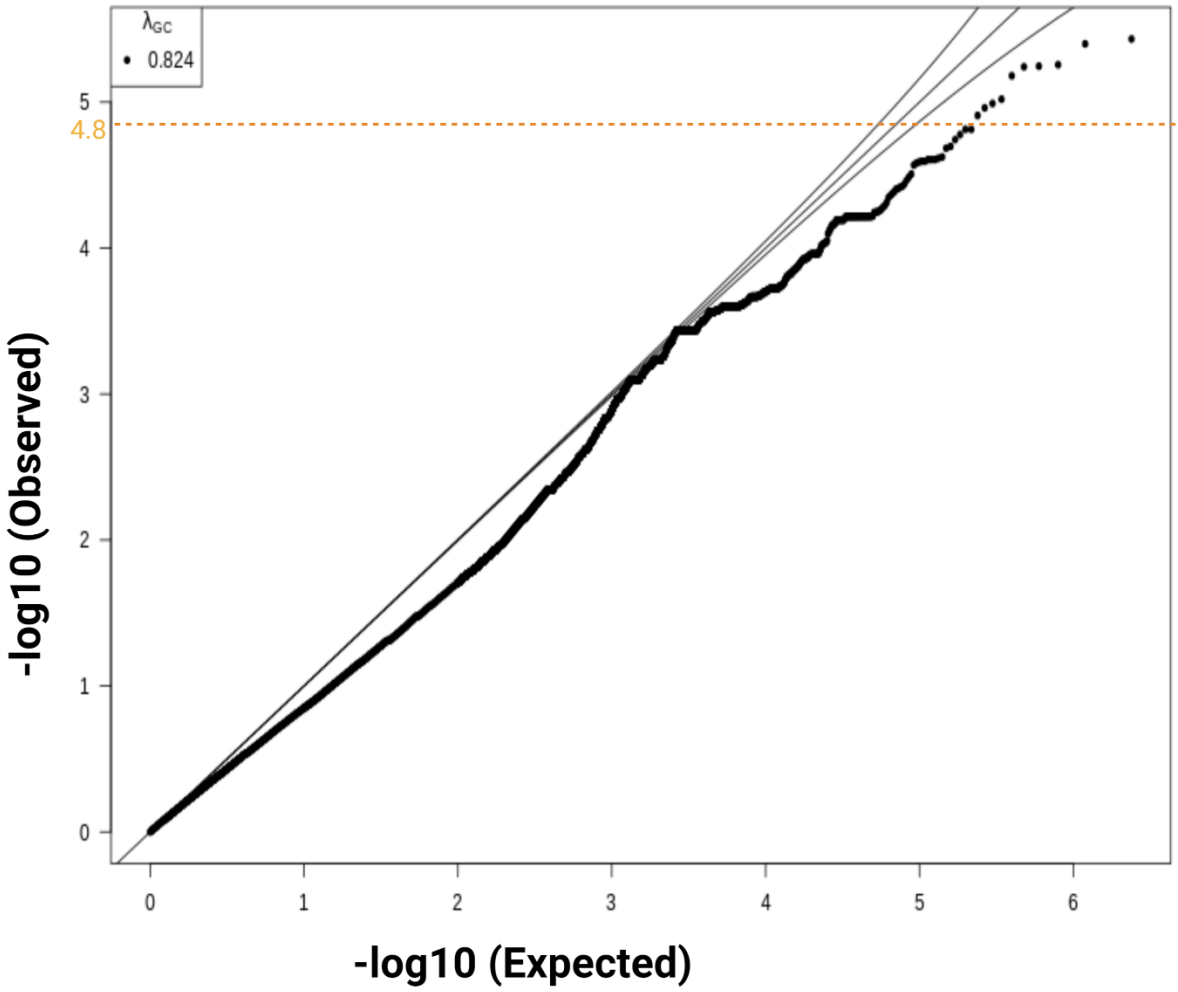

Fig 3.4.5: QQ-plot showing the distribution of the observed against the expected –log10 (P) for the SNPs of the rice genome associated with rhizosphere GNR variations, where the expected –log10 (P) under the null hypothesis were indicated by the straight grey line and observed values were indicated as the cluster of dots in black. The λ_{GC} at the left top corner, bounded by a box, indicated the genomic inflation of the model. The yellow dotted line indicated the SNPs threshold limit -log10(p)= 4.8 where observed and expected values were separated.

Table 3.4.4: Significant SNPs above the FDR limit (P<0.05) identified by the GWAS associated with the rhizosphere GNR variations among the tested rice cultivars, their location and position in the chromosome, -log10(P-value), and loci found within 10 kb upstream and downstream from the particular significant each SNP in the rice genome, annotated gene and annotated protein and their associated function together with % similarity % from the http://rice.uga.edu website are mentioned in the table.

SNP rank	SNPs name	Chr No.	Position	-log10(P)	Locus name	Annotated gene	Similarity %	Annotated protein	Function
1	mlid0076571321	11	18980242	5.43	LOC_Os11g32140.1		NA	Transposon protein	Transposon activity
					LOC_Os11g32150.1		NA	Transposon protein	Transposon activity
					LOC_Os11g32160.1	OsJ_34073	100	Expressed protein	Uncharacterized
2	mlid0083673869	12	17037216	5.40	LOC_Os12g28800.1		NA	Transposon protein	Transposon activity
					LOC_Os12g28810.1		NA	Transposon protein	Transposon activity
					LOC_Os12g28830.1		NA	Retrotransposon protein	Retrotransposon activity
					LOC_Os12g28820.1	LOC_Os12g28820	62.36	Expressed protein	Uncharacterized
3	mlid0070193580	10	15051371	5.26	LOC_Os10g28860.1	LOC_Os10g28860	93.58	MBTB39	Ubiquitination process
					LOC_Os10g28870.1	LOC_Os10g28870	83.63	MBTB40	Ubiquitination process
					LOC_Os10g28890.1		NA	Retrotransposon protein	Retrotransposon activity
4	7:16451660	7	16451660	5.25	LOC_Os07g28160.1	OsI_25919	90.28	Cytochrome P450 51	Sterol biosynthesis
					LOC_Os07g28170.1	OsJ_24167	90.35	Expressed protein	Uncharacterized

					LOC_Os07g28180.1	P0473C09.124	61.6	Expressed protein	Uncharacterized
					LOC_Os07g28190.1		NA	Retrotransposon protein	Retrotransposon activity
5	mlid0006648298	1	29148317	5.24	LOC_Os01g50730.1	OsI_03421	97.22	Polynucleotide adenylyltransferase	mRNA processing
					LOC_Os01g50740.1	P0421H07.22	62	Expressed protein	Uncharacterized
					LOC_Os01g50750.1	Os01g0703300	89.14	zinc finger, C3HC4 type domain containing protein	Transporter channel
					LOC_Os01g50760.1	OsJ_03166	100	Farnesyl pyrophosphate synthase	Isoprenoid biosynthetic process
6	10:7468731	10	7468731	5.18	LOC_Os10g13730.1		NA	Retrotransposon protein	Retrotransposon activity
					LOC_Os10g13740.1		NA	Retrotransposon protein	Retrotransposon activity
					LOC_Os10g13760.1		NA	Transposon protein	Transposon activity
7	mlid0076437007	11	18443230	5.02	LOC_Os11g31550.1	OsI_36256	85.32	BAK1	Phytohormone biosynthesis rmPoneresponse
					LOC_Os11g31560.1	OsJ_34034	80.63	BAK1	Phytohormone biosynthesis
					LOC_Os11g31570.1	OsI_36259	95.05	Expressed protein	Uncharacterised
8	mlid0064475382	9	14417317	4.99	LOC_Os09g24260.1		NA	Expressed protein	Uncharacterized
					LOC_Os09g24270.1		NA	Retrotransposon protein	Retrotransposon activity
					LOC_Os09g24280.1	P0465E03.12	100	Hypothetical protein	Uncharacterized
9	mlid0070206066	10	15098298	4.96	LOC_Os10g28950.1		NA	Retrotransposon protein	Retrotransposon activity

					LOC_Os10g28970.2	OsI_33656	82.83	BTB6	Ubiquitination process
					LOC_Os10g28960.1		NA	Expressed protein	Uncharacterized
					LOC_Os10g28975.1	Os10g0425500	93.27	Os10g0425500 protein	Ubiquitination
10	mlid0005739355	1	24736313	4.91	LOC_Os01g43280.1	OSNPB_010620800	82.05	Hydroquinone glucosyltransferase	Arbutin biosynthesis
					LOC_Os01g43290.1	OsI_02901	85.86	Expressed protein	Uncharacterized
					LOC_Os01g43310.1		NA	Retrotransposon protein	Retrotransposon activity
					LOC_Os01g43300.1		NA	Retrotransposon protein	Retrotransposon activity

3.5 Discussion

3.5.1 Rice rhizospheric effects on nitrification by radial oxygen loss (ROL)

Anaerobic conditions due to flooding likely prevented nitrification in the unplanted and bulk soil. Bulk soil GNR was not measured, but it was assumed that nitrification was also inhibited in the largely anaerobic bulk soil of planted microcosms because there was no variation in residual N-NH_4^+ concentration between bulk soil and unplanted soil (Fig: 3.4.1). So, nitrification was restricted to the rhizosphere compartment of planted microcosms (Fig: 3.4.1B). Oxygen from the rice root, due to radial oxygen loss (ROL), oxygenated the rhizosphere and adjacent bulk with a gradient up to 4 mm soil from root surfaces, allowing the nitrification process in that oxygenated zone of planted microcosms (Fig: 3.3.1) (Armstrong, 1971; Li & Wang, 2013; Morley & Baggs, 2010). So, the interaction between rice plants and the nitrifier community is limited only in the rhizosphere of flooded paddy soil.

3.5.2 Rice genotype effects on nitrification

Nitrification significantly varied between the tested rice cultivars (Fig: 3.4.2). The rhizosphere gross nitrification rate (GNR) in ng N/g dry weight of soil/hour after 1 day of enrichment fertilisation in the rhizosphere significantly varied ($p<0.05$) between rice cultivars. The identified known mechanisms for the modulation of nitrification by rice plants are oxygenation, pH alteration and biological nitrification inhibition (BNI), which are directly linked with rice plant genetics (Li & Wang, 2013) (F. Yu et al., 2016)(Yufang Lu et al., 2022)(Skiba et al., 2011). Rhizosphere GNR was found to be positively correlated with residual N-NH_4^+ concentration ($r^2=0.21$, $P<0.001$) only in the rhizosphere (Table: 3.4.3) (Fig: 3.4.3). So, N-NH_4^+ concentration was unlikely to be limiting for the nitrifier community on day 1 after enrichment fertilisation discounting the possibility that competition for ammonium drove the variation. No correlation was observed between rhizosphere GNR and rhizosphere pH. However, nitrification was positively correlated with root ($r^2=0.23$, $P<0.001$) and shoot dry-weight biomass ($r^2=0.20$, $P<0.001$). A similar result was found by (Li et al., 2008), suggesting higher root biomass associated with developed porous root may enhance radial oxygen loss from the root surface, facilitating higher nitrification in the rhizosphere (Fig:

3.1.1). Rice plants with a high shoot and root biomass might also have more actively growing branched root tips. Oxygen is readily diffused from actively growing root tips (Fig: 3.1.1). So actively growing root tips may provide a suitable niche for the nitrifier community.

Simultaneously low shoot: root biomass is likely to secret more carbon, including BNI, to the rhizosphere through root exudates (McCarthy & Enquist, 2007). In addition, oxygenation simultaneously enhances BNI secretion from rice roots (X. Zhang et al., 2019). So, low rhizosphere GNR cultivars might apply genetic regulations to counterbalance oxygenation by increasing carbon allocation to the roots to specifically enhance BNI secretion in the root exudates and/or synthesizing barrier to ROL to protect oxygen leakage from the root surface. So, GWAS analysis was performed to locate the genetic region associated with the rhizosphere nitrification variations among the tested rice cultivars.

3.5.3 Probable Candidates' genes associated with the rhizosphere nitrification variations

In total, 35 loci associated with annotated proteins were identified in the ± 10 kb of those significant SNPs of the rice genome from the Rice Genome Annotation Project (RGAP) - Rice Genome Annotation (Osa1) Release 7 (http://rice.uga.edu/cgi-bin/gbrowse/rice/) (Table: 3.4.4). 9 expressed and retrotransposon proteins, respectively, 5 transposon proteins, 4 BTB proteins (Bric-a-Brac, Tramtrack), 2 Brassinosteroid insensitive 1 associated receptor kinase-1 and 1 zinc finger (C3HC4 type domain) containing protein, cytochrome P450 51 protein, hydroquinone glucosyltransferase protein, WD (G-beta repeat domain) containing protein, and polyprenyl synthetase were detected respectively among these 35 annotated proteins. Transposon, retrotransposon, and expressed proteins with anonymous functions were excluded from further discussion, while the rice gene's involvement in nitrification variations in the rhizosphere was corroborated.

LOC_Os11g31550.1 and LOC_Os11g31560.1 annotated with Brassinosteroid insensitive 1 associated receptor kinase-1 (BAK1) precursor protein. BAK1 is involved in Arabidopsis's abscisic acid (ABA) biosynthesis pathway (Deng *et al.*, 2022). ABA and Brassinosteroid are required for exodermal suberisation in the rice root as phytohormones (Shiono et al., 2014, 2022). So, those two loci might be involved in the suberin deposition process in the rice root that acts as

a barrier to ROL (Fig: 3.1.1). LOC_Os07g28160.1 annotated with Cytochrome P450 51 (Obtusifoliol 14-alpha demethylase) involved in sterol biosynthesis and expression of the protein found upregulated while suberin biosynthesis in rice (Shiono et al., 2014). The protein, WD domain, G-beta repeat domain-containing protein annotated from LOC_Os09g24260.1, acts as protein interaction scaffolds in multiprotein complexes; in rice, it is involved in abiotic responses tolerance (e.g., salt and drought response) (Eryong & Bo, 2022). In maize root, ethylene signalled cortical cell death to form aerenchyma through a G-protein (Drew et al., 2000). Brassinosteroids are de-repressed in rice by E3 ubiquitin ligase with G-protein (Xingming Hu et al., 2013; D. Liu et al., 2022).

LOC_Os01g50760.1 annotated polyprenyl synthetase, terpenoid synthase superfamily group, synthesises isoprenoid quinones, carries electrons and proton to photosynthetic and respiratory electron transport chains, and acts as antioxidants nullify reactive oxygen species (ROS) produced from oxidative stress in the roots (You et al., 2020). However, ROS accumulation in the rice root cells activates lysigenous aerenchyma formation (Yamauchi et al., 2017). Zinc finger, C3HC4 type domain-containing protein annotated from LOC_Os01g50750.1 associated with drought and salt tolerance in rice by altering the Na^+/K^+ transporter genes (J. H. Kim et al., 2023; Ma et al., 2009).

LOC_Os10g28860.1, LOC_Os10g28870.1, LOC_Os10g28970.2 and LOC_Os10g28975.1 annotated with MBTB39, MBTB40, BTB6 and BTB/POZ domain-containing protein respectively that are in the superfamily of Bric-a-Brac/ Tramtrack/ Broad Complex BTB proteins. MBTB39 and MBTB40 have a domain with Meprin and TRAF Homology MATH domain, and BTB6 is also a BTB/POZ domain-containing protein. (Gingerich et al., 2007) described 149 BTB-domain-containing genes with 43 putative pseudogenes in the rice. These proteins are known to act as substrate-specific adaptors for ubiquitin-protein ligase (ES3) during protein degradation through ubiquitination, and ubiquitination is essential to process programmed cell death. So, it could be speculated that BTB proteins also play a critical role in the cytoskeleton protein degradation of the rice root cortex through ubiquitination to form lysigenous aerenchyma. Defective root growth and an altered pavement of epidermal cells were observed in *Arabidopsis* due to overexpression of TaMAB2, an MTH-BTB protein (Bauer et al., 2019). (Nini Ma *et al.*,2023) reported a ubiquitination pathway involved in rice root meristem modulation.

Hydroquinone glucosyltransferase is annotated from LOC_Os01g43280.1, a UDP-glycosyltransferase superfamily protein that glucosylates hydroquinone, a urease inhibitor (Mazzei et al., 2022). Glucosylation increases the water solubility of hydroquinone, thus facilitating compartmentalization from the root surface into the rhizosphere (Joachim *et al.*, 2001). Syringic acid, a urease inhibitor secreted from rice roots, showed higher BNI activity due to synergetic effects with 1,9-decanediol (Yufang Lu et al., 2022). Syringic acid also showed BNI activity as well. However, glucoside hydroquinone is arbutin, which is commonly used as a cosmetic on the skin to inhibit melanin formation. Arbutin inhibits tyrosinase, a copper-containing oxidase enzyme involved in melanin formation. So, it could be speculated that arbutin might also be a potential BNI, as with syringic acid. (Casali et al., 2022; Yufang Lu et al., 2022).

3.6 Concluding remarks

Nitrification did not contribute to N_2O emission in the microcosm system as no correlation was observed between rhizosphere GNR and N-N_2O emission and also with ^{15}N signature of emitted N_2O (Fig: 3.4.3). Nevertheless, the shoot was cut before putting the microcosm into the Kilner jar in order to collect gas samples for gas analysis (Fig: 3.3.3). Oxygen supply from the atmosphere through the shoot to root channel was shut down immediately that might disrupt the aerobic microbial community belowground. However, nitrification might still be active till residual O_2 consumption (Fig: 2.3.7, Chapter 2). Indeed, N_2O emission was not differentiated between the two compartments in the microcosm setup. So, collecting pore water to assess gas source partitioning with intact plants may have been more accurate in fully understanding the role of nitrification and denitrification in emission. Rhizobox experiments to assess this with selected lines would be a logical next step to dissect this (Discussed in Chapter 6, Section 6.7.2).

GWAS identifies with relatively low-resolution areas of the genome linked to the trait assessed rather than identifying specific genes. Multiple biological factors might be involved in the nitrification variations as phenotypic traits. Further studies are required to confirm rice genetic relatedness with rhizosphere GNR variations among the tested rice cultivars. The expressed and hypothetical proteins associated with the significant SNPs also need to be considered to identify their role in rice plants and their association with nitrification. The transposon and retrotransposon elements, jumping DNA, mobilise and amplify within the genome and regulate other functional

genes' activation or downregulation (Piegu et al., 2011). Activations of those transposon elements in the rice are triggered by environmental stimuli rather than transposon element silencing pathways (Carpentier et al., 2019). Other expressed proteins with uncharacterised functions

A whole genome sequence or segment of chromosomes based on our GWAS results of high and low-nitrification-associated rice cultivars might help identify the genes that triggered the variations. Further confirmation is also needed by transcriptomics analysis to understand the expression of those associated genes from the GWAS output, with the combination of root exudation analysis of the high and low nitrification associated rice cultivar will generate comprehensive results to understand rice plant and nitrifier community interaction. The soil samples from the rhizosphere and bulk compartments were stored for community analysis (Discussed in Chapter 6, Section 6.7.1).

Chapter 4: Screening the rice germplasms based on denitrification variations and exploring the genetics relatedness of the variations

4.1 Introduction

4.1.1 Need immediate actions to control anthropogenic/agricultural N_2O emission

N_2O is the third most emitted greenhouse gas in volume after CO_2 and CH_4 due to anthropogenic activities but the most potent greenhouse gas per unit volume among these three gases because it has 298 and 14 times the Global Warming Potential of CO_2 and CH_4, respectively (Linquist *et al.*, 2012; Davidson & Kanter, 2014). It is more damaging overall than CO_2 or methane, or a disproportionate benefit can be achieved by controlling anthropogenic N_2O emissions. Agriculture is responsible for approximately two-thirds of these emissions, driven predominantly by intensive fertilisation (Janssens-Maenhout et al., 2019; Prokopiou et al., 2018; Wells et al., 2018). Control of agricultural emissions of N2O is, therefore, a priority, but a US environmental protection agency report suggested that only circa 10% of agricultural N_2O emissions may be controllable through existing methods with varying costs (Bracmort, 2010). These control measures include restricting the applications of nitrogen fertiliser or the addition of synthetic nitrification inhibitors. The remaining 90% of emissions are recalcitrant, with a clear need for novel control measures.

4.1.2 Modulating the denitrifier community is key to curbing N_2O emission from rice paddies

In 2019, the FAO reported that rice cultivation emitted an average of 7.5 Tg CO_2 eq/hectare as N_2O, representing 10.1 % of total agricultural N_2O emissions (FAO, 2019). Rice is an important agricultural crop, feeding over 50% of the world's population (Fukagawa & Ziska, 2019). According to the USAID report from 2019, rice production has increased by 230% since 1960 (Childs & Skorbiansky, 2019). To meet global demand in 2021, 165M ha of land, approximately 12% of total agricultural land, was used for rice cultivation (FAO, 2022). Rice is typically grown in lowland paddy systems, maintaining flooded conditions until just before harvest, making rice fields unique agroecosystems and anthropogenic wetlands (Kögel-Knabner et al., 2010). Paddy soil is enriched with soil organic carbon (SOC) due to frequent flooding and puddling and readily fuels denitrification after the addition of inorganic N-fertilisers, depending on the flooding

conditions (Liu et al., 2021). Denitrification is the dominant pathway for the emission of N_2O from rice cultivation because nitrification is relatively limited in paddy soil (Yang et al., 2017) as the largely flooded conditions in paddy soil prevent nitrification in bulk soil (Liu et al., 2019; Verhoeven et al., 2018). Denitrification is a facultative anaerobic microbial respiration process using nitrogen oxides as alternate electron acceptors with nitrate converted through a series of intermediates to Nitrogen (N_2) (Zumft, 1997). Complete denitrifiers (NosZ clade I) typically have the full set of reductase enzymes with a combination of either (*nir*K) or (*nir*S) with these genes mutually exclusive in denitrifier genome (C. M. Jones et al., 2008). Not all denitrifiers have the complete set of denitrifying genes (Discussed in Chapter 1, section 1.9.1). NirK-type denitrifiers are more likely to perform partial denitrification due to a lower frequency of co-occurrence of *nosZ* with *nirK* than with *nirS* (Graf et al., 2016). Atypical NosZ clade II denitrifiers likely carry only the nitrous oxide reductase gene (Jones et al., 2008; Graf et al., 2016). So, in oxygen-limiting conditions, during denitrification, NirK and NirS denitrifier communities lacking nitrous oxide reductase genes produce N_2O inebitably as the end product; in contrast, NosZ clade II denitrifiers consume N_2O to sustain respiration. So, the abundance of the NosZ clade II denitrifier community thus plays a crucial role as an N_2O sink from arable soil (Domeignoz-Horta et al., 2018). Nevertheless, the relative abundance of NosZ clade I and NosZ clade II denitrifiers is lower in rice paddy than in dryland arable soils (Jones et al., 2013). Furthermore, complete denitrifiers do not always complete the denitrification pathway despite having all reductase enzymes. Soil biotic factors (e.g. types of C, NO_3^- availability, C: NO_3^- ratio, O_2 availability and pH) regulate the expression of genes in complete denitrifiers affecting completion of the denitrification pathway (Discussed in Chapter 1, Section 1.9.2). When denitrification is truncated, N_2O is produced as the end product (Mary K. Firestone et al., 1980; Graf et al., 2014; Huang et al., 2019; Laurent Philippot et al., 2009). So, the ratio of NirS and NirK to NosZ clade I and NosZ clade II genes and their relative activities interact in a complex fashion to control N_2O emission from fertilised paddy soil.

4.1.3 Rice plants modulate the denitrifier community

Rice plants, like other crops cultivated in arable land, can modulate denitrifiers community by regulating the soil biotic factors such as pH, O_2 availability, NO_3^- concentration, and the quality of available respirable carbon, all of these and the ratios between C: NO_3^- influence the end product produced during denitrification (Moreau et al., 2019b)(Burford and Bremner, 1975; Smith and

Tiedje, 1979; Klemedtsson *et al.*, 1991; Baumann *et al.*, 1997; Šimek and Cooper, 2002; Bateman and Baggs, 2005a; Morley and Baggs, 2010; Giles et al., 2012; Giles, Daniell and Baggs, 2017; Herold *et al.*, 2018). Exceptionally, rice plants introduce oxygen to the surrounding rhizosphere, both supporting nitrification in that oxygenated zone of flooded paddy soil and potentially regulating N_2O emissions by limiting the total denitrification pathway by negatively influencing the N_2O reduction step (Discussed in Chapter 3, Section 3.1.2**).** The distribution of organic compounds present in the root exudates regulates the abundance of and balance between NirS, NirK and NosZ clade I and II denitrifier communities by and can thus determine the fate of the end product during denitrification (S. Hou et al., 2018; Langarica-Fuentes et al., 2018b). Nitrogen uptake efficiency also varies within rice germplasm, facilitating nitrogen cycling variation through competition for substrate (L. Sun et al., 2016; Y. Yang et al., 2017). For example, one single nucleotide polymorphism (SNP) variation in the *NRT1.1B* gene (encoding the nitrate transporter and sensor) between indica and japonica rice varieties elicits variation in DNRA bacterial abundances in the rhizosphere (Jingying Zhang et al., 2019). So, rice plants may modulate N_2O emission by several mechanisms, including alteration of denitrification gene expression, community structuring, or recruitment of competitors of denitrifiers retaining nitrogen in the rhizosphere. Still, understanding how rice plants modulate denitrifier communities in the bulk soil (beyond the rhizosphere's oxygenated zone) remains elusive. The quality of respirable carbon in the root exudates and the ratio of respirable carbon and NO_3^- are crucial for regulating the proportion of N_2 and N_2O during denitrification (Bateman & Baggs, 2005a; Baumann et al., 1997; Burford & Bremner, 1975; Herold et al., 2018; S. Hou et al., 2018; Klemedtsson et al., 1991; Langarica-Fuentes et al., 2018b; N. Morley & Baggs, 2010; Šimek & Cooper, 2002; M. S. Smith & Tiedje, 1979). Rice root-derived carbon has been shown to travel 2cm across a gradient from root surface to bulk soil partially due to the flooded conditions in paddies (Fig: 4.5.1) (Xiaoting Wang et al., 2018) and exudation varies between the rice lines, which may elicit denitrification-associated N_2O emission variation (Aulukh *et al.*, 2001; Gogoi and Baruah, 2012; Jiang *et al.*, 2016; Bhattacharyya *et al.*, 2019; Rummel *et al.*, 2021; Ding *et al.*, 2022).

4.2 Aims and Objectives

I have demonstrated that it is possible to simultaneously assess the major N cycling processes in paddy soil supporting rice growth (Chapter 2) and generated a microcosm system that allows separation of largely aerobic and anaerobic rhizosphere and bulk soil compartments and applied this to show significant variation in nitrification between rice genotypes (Chapter 3). In this chapter, I aim, using the same screen, to assess the impact of rice lines on denitrification activity, assessing both complete and incomplete denitrification and the balance between them. Thus, I pose the following hypotheses:

1. There is significant variation in denitrification-related nitrous oxide emissions and total denitrification from paddy soil supporting different rice lines.
2. Variation in emission is driven by changes in the efficiency of complete denitrification.
3. Variation is linked to plant genetics.

To test these hypotheses, I collected gas samples following incubation in Kilner jars following fertilisation. The emission of nitrous oxide and nitrogen linked to denitrification was assessed by IRMS in relation to background parameters. Where variation was observed, a GWAS analysis was performed to link emissions to plant genetics.

4.3 Methodology

4.3.1 Plant growth and sampling

A common microcosm experiment was used for screening nitrification variation, as described in Chapter 3 (Section 3.3.3). Briefly, a microcosm was established with a bulk soil and rhizosphere compartment (66:33%) using a divider with 32um mesh. The microcosm was packed with paddy soil and rice lines grown under standard agronomic fertilisation rates with an unplanted control. Samples were taken after the second fertilisation in which the nitrate was supplemented (~5%) with ^{15}N nitrate. During sampling, gas samples were taken for direct measurement of N_2O emission, and enrichment of N_2 emissions was assessed by isotope ratio modelling to partition gas between complete denitrification and anammox; the method is discussed in detail in Chapter 2 (Section 2.3.11.5). Briefly, N_2 from complete denitrification will have a signature matching that of N_2O. After collecting gas samples, microcosm pots were destructed, and physicochemical

parameters (Fig: 3.3.3) (e.g. DOC) were measured and discussed in Chapter 3 (Section 3.3.4). Statistical analysis was performed as described in Chapter 3 (Section 3.37) using R (Rstudio 4.0.2). GWAS analysis was performed as described in Chapter 3 (Section 3.3.5).

4.4 Results

4.4.1 Rice plant effects on organic carbon (DOC), residual inorganic N and DOC: N-NO_3^- between planted (Rhizosphere and Bulk) and unplanted microcosms

Rice plants significantly affected the applied inorganic N in the rhizosphere and bulk soil of planted microcosms (Table: 3.4.1). Still, there was no significant rice genotype effect in planted microcosms (Table: 3.4.2). The residual N-NH_4^+ concentration (μgN/g dry-weight soil) was approximately two-fold higher than the residual N-NO_3^- concentrations (μgN/g dry-weight soil) in the unplanted soil (Fig: 3.4.1A). In contrast, there was no significant difference between the residual inorganic N in the rhizosphere soil of planted microcosms. Still, in the bulk soil of planted microcosms, residual N-NH_4^+ concentration (μgN/g dry-weight soil) was significantly higher than the residual N-NO_3^- concentrations (μgN/g dry-weight soil)(Table: 3.4.2), which was a similar concentration of unplanted soil (Fig: 3.4.1A). (Chapter 3, Section 3.4.1)

The DOC (r^2=0.52, p< 0.001) and DOC: N-NO_3^- ratio (r^2=0.48, p< 0.001) were significantly varied between rhizosphere, bulk and unplanted soil (Table: 4.4.1). The highest and lowest DOC, 845.1±7.3 ng C/g dry weight of soil and 103±18.9 ng C/g dry weight of soil were measured respectively in the rhizosphere and unplanted soil (Fig: 4.4.1A). DOC: N-NO_3^- ratio was measured to be lowest in unplanted soil (Fig: 4.4.1B).

Table 4.4.1: One-way Anova results (Type II tests) between planted and unplanted microcosms of DOC (ng C/g dry-weight soil) and the ratio of DOC: NO_3^- among rhizosphere (n=343) and bulk compartments (n=349) of planted microcosms and unplanted microcosms (n=4) at the significance levels' ***' 0.001 '**' 0.01 '*' 0.05 '.' 0.1.

Response	Sum Sq	Df	F value	Pr(>F)	Significance
DOC: NO_3^-	501432	2	9.3229	0.0001102	***
DOC	39831669	2	459.71	< 2.2e-16	***

4.4.2 Rice plant effects on denitrification between planted and unplanted microcosms

The partial (N-N_2O), complete (N-N_2) and total denitrification (N-N_2O+N-N_2) rates in ng N/g dry-weight soil/ hour and N-N_2O: N-N_2O+N-N_2 ratio significantly varied between planted and unplanted microcosms (Table: 4.4.2). Total denitrification was increased approximately two folds but partial denitrification increased six folds in the unplanted microcosms than in the planted microcosms (Fig: 4.4.1C, 4.4.1E). The ratio of partial and total denitrification (N_2O: N_2O+N_2) was incresaed three folds in the unplanted microcosms (Fig:4.4.1F).

Table 4.4.2: One-way (Type II) ANOVA results for the rice plant effects on total denitrification, including partial and complete denitrification and the ratio of N-N_2O: N-N_2O+N-N_2 planted microcosms (n=332) and unplanted microcosms (n=4) at the significance levels' ***' 0.001 '**' 0.01 '*' 0.05 '.' 0.1.

Response	Sum Sq	Df	F value	Pr(>F)	Significance
Partial denitrification (N-N_2O)	26520.4	1	951.15	< 2.2e-16	***
Complete denitrification (N-N_2)	196514	1	9.1269	0.002715	**
Total denitrification (N-N_2O+N-N_2)	367418	1	16.888	5.003e-05	***
N-N_2O: N-N_2O+N-N_2	0.073402	1	220.13	< 2.2e-16	***

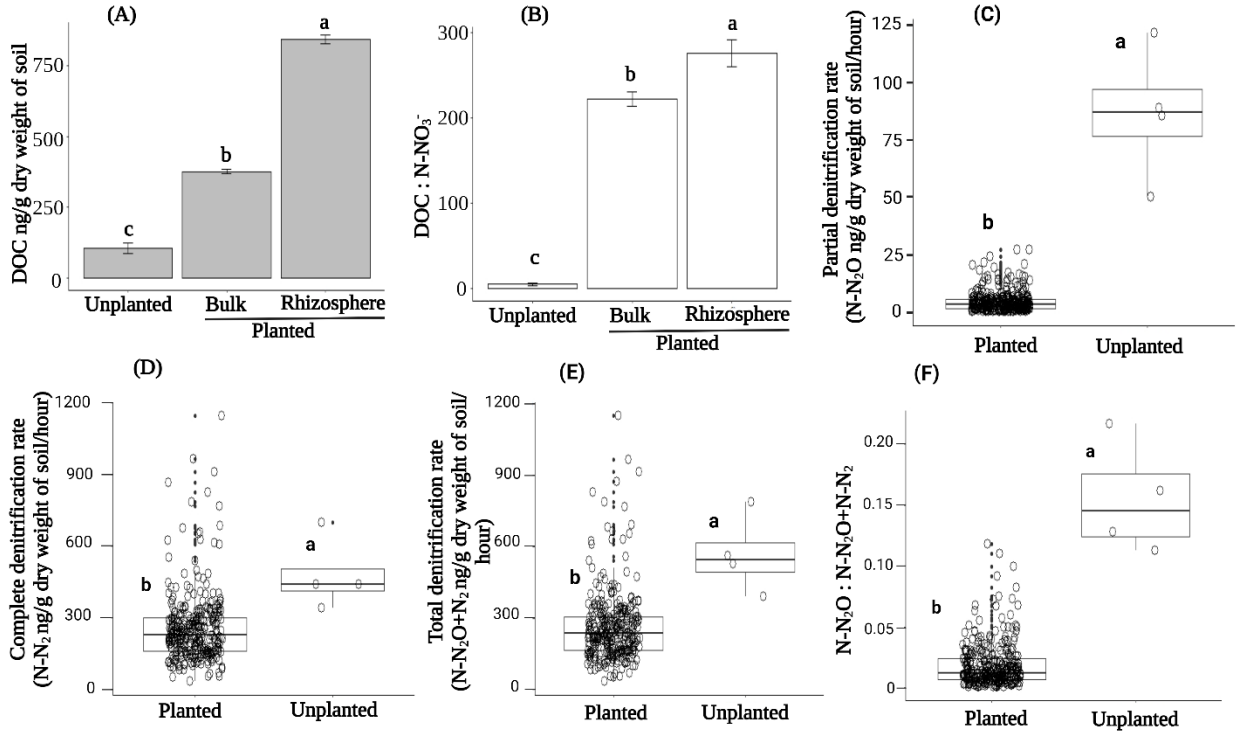

Fig 4.4.1: **(A)** Mean±SE from two-way (Type II) ANOVA of DOC ng C/g dry weight of soil in unplanted soil (n=4), rhizosphere (n=343), and bulk soil (n=349) of planted microcosms. **(B)** Mean±SE from one-way (Type II) ANOVA of DOC/N-NO_3^- ratio in unplanted soil (n=4), rhizosphere (n=343), and bulk soil (n=349) of planted microcosms. The letters indicated a significantly different group. Box whisker plot of **(C)** partial denitrification rate ng N/g dry weight of soil/hour, **(D)** complete denitrification rate ng N/g dry weight of soil/hour, (E) total denitrification rate ng N/g dry weight of soil/hour, and (F) N-N_2O/N-N_2O+N-N_2 ratio between planted (n=332) and unplanted (n=4) microcosms. Box pot showing 95 percentile observation with a median, indicated by a thick horizontal line inside the box. The lowercase letters indicated a significantly different group ($P<0.001$, Type II ANOVA, Tukey HSD).

4.4.3 Rice genotype effects on denitrification in the planted microcosms

Total denitrification rates (N-N_2O+N-N_2), complete denitrification rates, partial denitrification rates (N-N_2O) in ng N/g dry-weight soil/hour and ratio of partial and total denitrification (N-N_2O: N-N_2O+N-N_2) were significantly varied between the tested rice cultivars (n=98) after 24 hours of enrichment fertilisation (Table: 4.4.3). Lower and higher N_2O-emitting rice cultivars formed distinct groups based on N-N_2O emission rates. High and low complete denitrification-associated

rice cultivars were also shown to have high and low total denitrification, respectively (Fig:4.4.2) . The ratio of partial and total denitrification ($N\text{-}N_2O$: $N\text{-}N_2O+N\text{-}N_2$) was also low in the low complete denitrification associated rice cultivar (R83); nevertheless the ratio was high in other two low complete denitrifications associated rice cultivar (R79 and R74) (Fig: 4.4.5). The low complete denitrification associated rice cultivar (R83) also observed as low N_2O-emitting rice cultivars. In contrast, high complete denitrification associated rice cultivars R6, R3 and R9 were observed as lower N_2O-emitting rice cultivars (Fig: 4.4.4). Indeed, the ratio of partial and total denitrification was low and similar among the three rice cultivars (Fig: 4.4.5). On the other hand, the ratio was observed high in higher N_2O-emitting rice cultivars (Fig: 4.4.5). However, there was no variation between lower and higher N_2O-emitting rice cultivars in total denitrification (Fig: 4.4.2).

Table 4.4.3: One-way (Type II) ANOVA results for the rice genotype effects on total denitrification (n=4), including partial (n=4) and complete denitrification (n=4) and the ratio of $N\text{-}N_2O$: $N\text{-}N_2O+N\text{-}N_2$ (n=4) among the tested rice cultivars (n=98) in the planted microcosms at the significance levels' ***' 0.001 '**' 0.01 '*' 0.05 '.' 0.1.

Response	Sum Sq	Df	F value	Pr(>F)	Significance
Partial denitrification ($N\text{-}N_2O$)	4256.3	97	4.1834	< 2.2e-16	***
Complete denitrification ($N\text{-}N_2$)	4619206	97	4.5136	< 2.2e-16	***
Total denitrification ($N\text{-}N_2O+N\text{-}N_2$)	4656243	97	4.5012	< 2.2e-16	***
$N\text{-}N_2O$: $N\text{-}N_2O+N\text{-}N_2$	0.064081	97	3.8212	2.24e-06	***

4.4.4 Relationship between denitrification with soil biotic and abiotic factors in planted microcosms

Spearman correlation matrix analysis was performed to understand the inter-correlation between denitrification processes and other measured soil biotic and abiotic factors in planted rice microcosms. Total denitrification was positively correlated with partial denitrification (r^2=0.15, P<0.05) and complete denitrification (r^2=0.99, P<0.001). Complete denitrification was only positively correlated with total denitrification and reciprocally correlated with the ratio of partial and total denitrification ($N\text{-}N_2O/N\text{-}N_2O+N\text{-}N_2$) ($r^2$= -0.15, P<0.05). Total denitrification and

complete denitrification were not related to any other measured soil parameters (Chapter 3, Fig: 3.4.2)

Partial denitrification ($N\text{-}N_2O$) rate was positively correlated with the ratio of $N\text{-}N_2O/N\text{-}N_2O+N\text{-}N_2$ (r^2=0.9, P<0.001), total denitrification (r^2=0.15, P<0.05), anammox (r^2=0.33, P<0.001), residual $N\text{-}NH_4^+$ in the rhizosphere (r^2=0.17, P<0.01) and bulk compartment (r^2=0.2, P<0.01) and residual $N\text{-}NO_3^-$ in the rhizosphere (r^2=0.11, P<0.05) and bulk compartment (r^2=0.11, P<0.05). In contrast, the $N\text{-}N_2O$ emission rate from rice cultivar's microcosms reciprocally related to dry-weight biomass of root (r^2= -0.26, P<0.001) and shoot (r^2= -0.25, P<0.001), the ratio of DOC: $N\text{-}NO_3^-$ in the rhizosphere (r^2= -0.14, P<0.05) and bulk compartments (r^2= -0.18, P<0.01) (Table: 4.4.4). In our microcosm system, denitrification was the sole source of N_2O emission (Chapter 2, section 2.4.1.1b). So, ^{15}N atom % in N_2O was representative of ^{15}N atom % in NO_3^- and was found to be positively correlated with N_2O emission.

Table 4.4.4: Relationship of partial and complete denitrification and the ratio of partial and total denitrification from planted microcosms with measured other N-cycle processes and tested soil parameters (Biotic and abiotic factors) in the rice microcosms by Spearman correlation matrix analysis. Rhizosphere and bulk compartments were denoted by R and B, respectively.

Responses (PD)	$^{15}N_2O$	CD	TD	Ratio	NIT	ANX	R $[N\text{-}NH_4^+]$	B $[N\text{-}NH_4^+]$	R $[N\text{-}NO_3^-]$	B $[N\text{-}NO_3^-]$	R DOC	B DOC	R C/N	B C/N	Root	Shoot	SR	R pH
r^2	0.54	0.10	0.15	0.9	0.02	0.33	0.17	0.2	0.11	0.11	-0.06	-0.06	-0.14	-0.18	-0.26	-0.26	0.05	0.03
P	<0.001	ns	<0.05	<0.001	ns	<0.001	<0.01	<0.01	<0.05	<0.05	ns	ns	<0.05	<0.01	<0.001	<0.001	ns	ns

Responses (CD)	$^{15}N_2O$	PD	TD	Ratio	NIT	ANX	R $[N\text{-}NH_4^+]$	B $[N\text{-}NH_4^+]$	R $[N\text{-}NO_3^-]$	B $[N\text{-}NO_3^-]$	R DOC	B DOC	R C/N	B C/N	Root	Shoot	SR	R pH
r^2	0.218	0.10	0.99	-0.15	0.02	0.83	0.08	-0.11	0.11	-0.08	-0.05	-0.09	-0.01	0.11	0.1	0.11	0.005	-0.03
P	<0.001	ns	<0.001	<0.05	ns	<0.001	ns	ns	ns	ns	ns	ns	ns	ns	ns	ns	ns	ns

Responses (Ratio)	$^{15}N_2O$	PD	CD	TD	NIT	ANX	R $[N\text{-}NH_4^+]$	B $[N\text{-}NH_4^+]$	R $[N\text{-}NO_3^-]$	B $[N\text{-}NO_3^-]$	R DOC	B DOC	R C/N	B C/N	Root	Shoot	SR	R pH
r^2	0.5	0.9	-0.15	-0.11	0.02	0.07	0.11	0.22	0.09	0.13	-0.03	0.002	-0.12	-0.17	-0.26	-0.25	0.06	0.02
P	<0.001	<0.001	<0.05	<0.001	ns	ns	ns	<0.001	ns	<0.05	ns	ns	<0.05	<0.01	<0.001	<0.001	ns	ns

$^{15}N2O$= 15N atom % in N2O, CD=Complete denitrification rate, TD=Total denitrification rate, Ratio= $N\text{-}N_2O$: $N\text{-}N_2O+N\text{-}N_2$, NIT=Nitrification, ANX=Anammox, C/N= DOC: NO_3^- and SR= Dry weight shoot and root biomass ratio

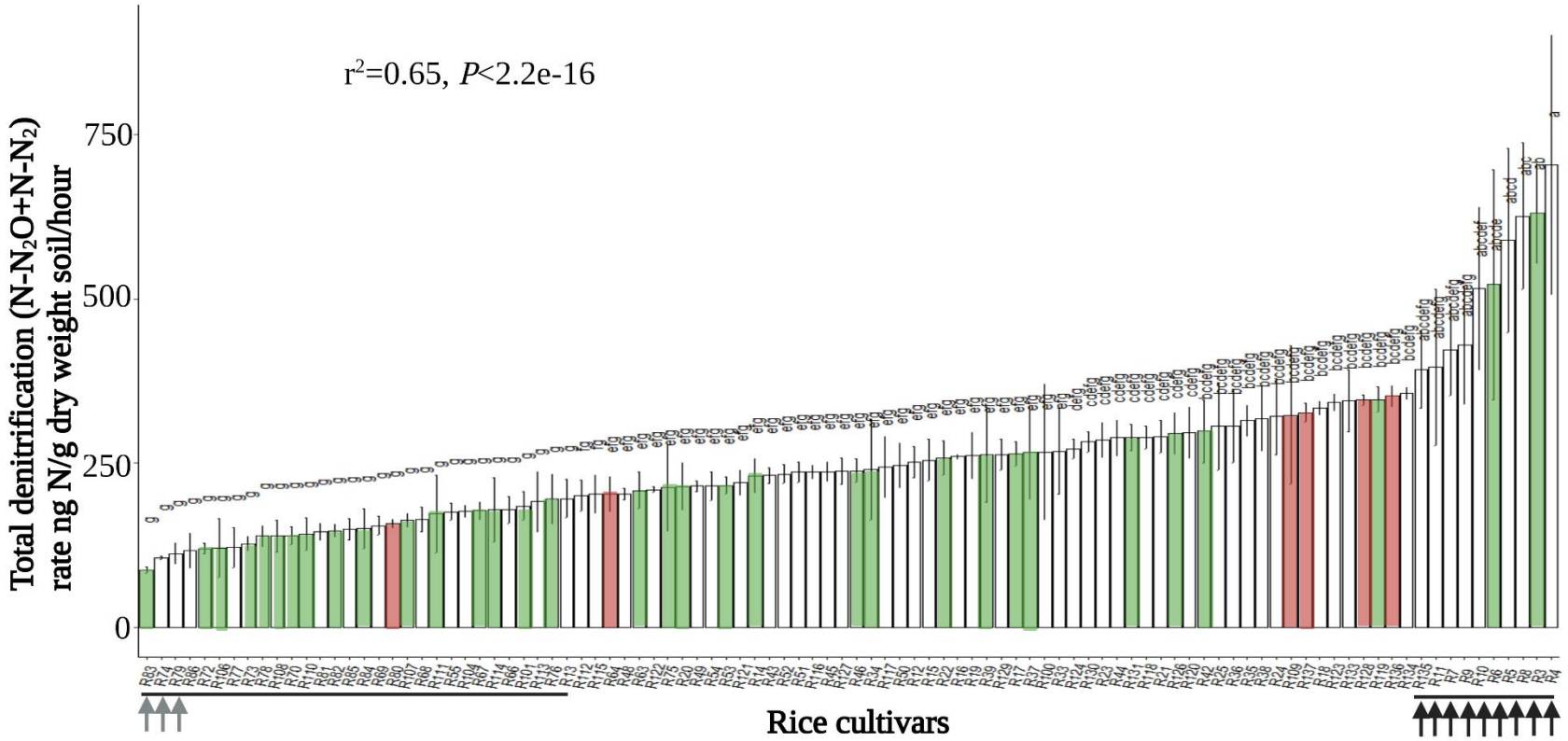

Fig 4.4.2: Mean±SE (n=4) from one-way (Type II) ANOVA of total denitrification rate in ng N/g dry-weight soil/hour of tested rice cultivars (n=98). The underlined rice lines indicated the low and high total denitrification associated with rice cultivar groups. Rice cultivars associated with low N_2O emissions were indicated by green-coloured bars, and rice cultivars associated with high N_2O emissions were indicated by red-coloured bars. The black and shaded arrows indicated rice cultivars with high and low complete denitrification, respectively. The letters indicated a significantly different group (r^2 = adjusted residual error, P<0.001, ANOVA, Tukey HSD).

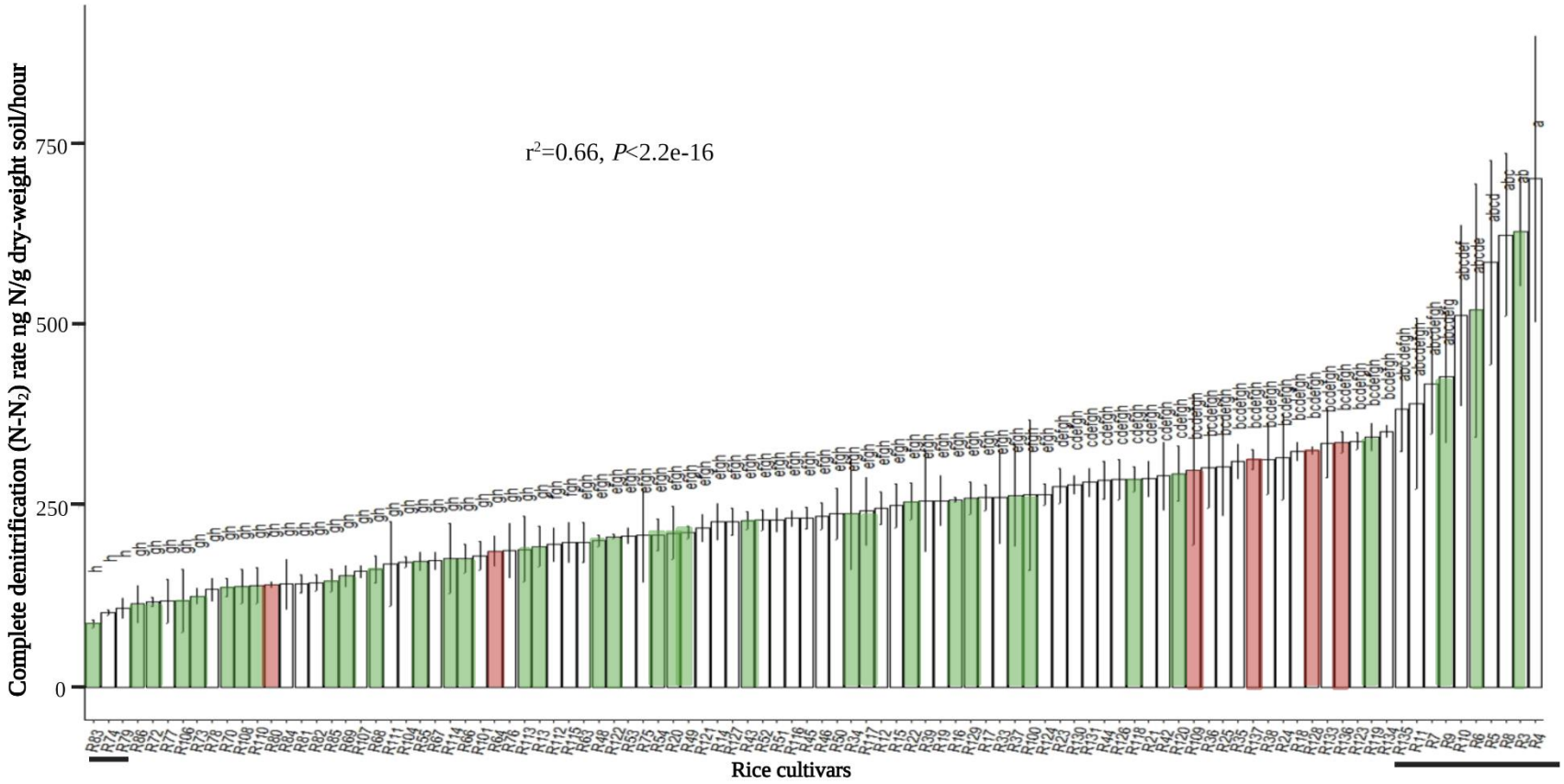

Fig 4.4.3: Mean±SE (n=4) from one-way (Type II) ANOVA of complete denitrification ($N\text{-}N_2$) rate in ng N/g dry-weight soil/hour of tested rice cultivars (n=98). The underlined rice lines indicated low and high complete denitrification associated with the rice cultivars group. Rice cultivars associated with low N_2O emissions were indicated by green-coloured bars. The letters indicated a significantly different group (r^2 = adjusted residual error, P<0.001, ANOVA, Tukey HSD).

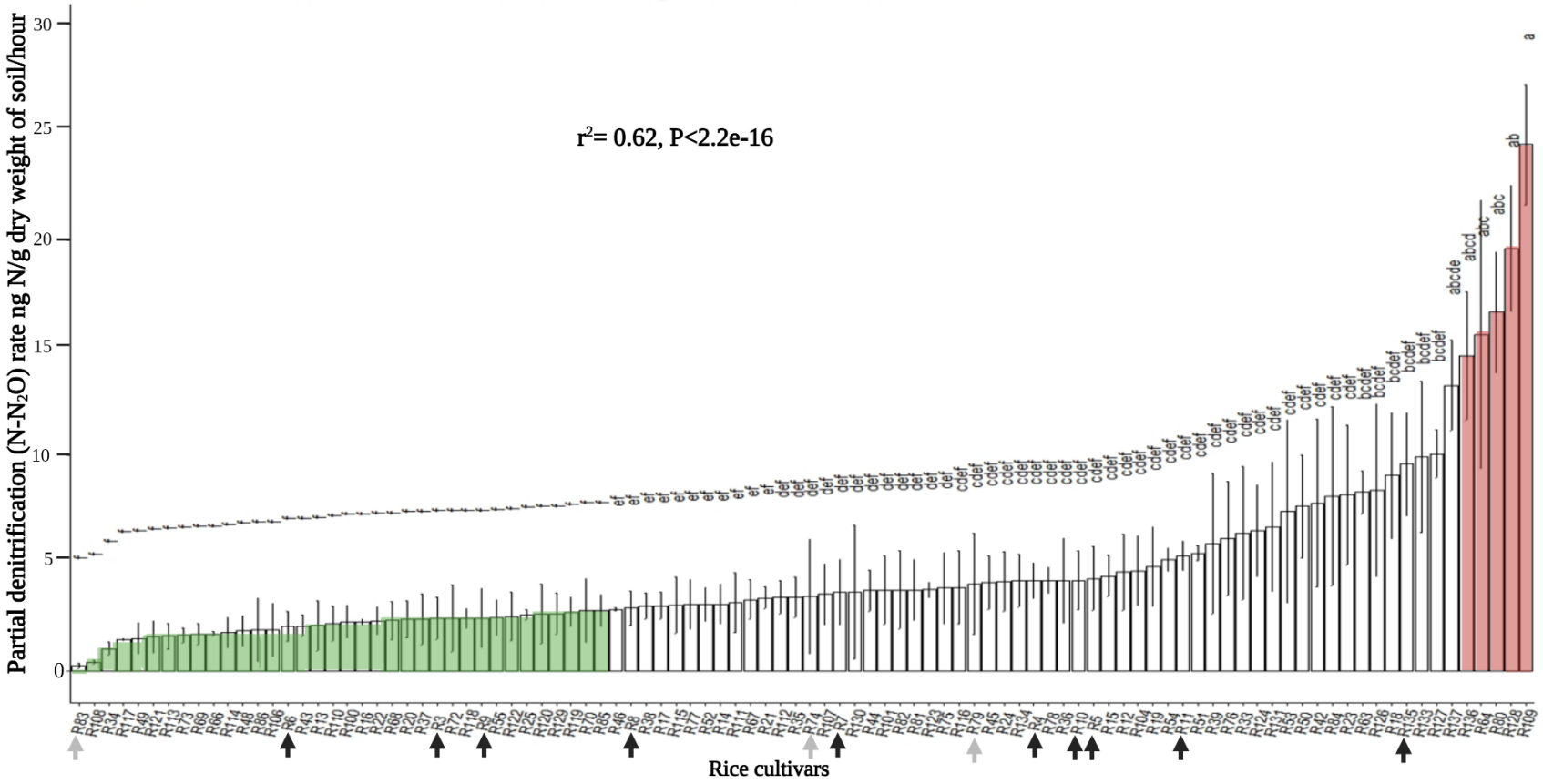

Fig 4.4.4: Mean±SE (n=4) from one-way (Type II) ANOVA of partial denitrification (N-N_2O) rate in ng N/g dry-weight soil/hour of tested rice cultivars (n=98). Rice cultivars associated with low N_2O emissions were indicated by green-coloured bars, and rice cultivars associated with high N_2O emissions were indicated by red-coloured bars. The black and shaded arrows indicated high and low complete denitrification rice cultivars. The letters indicated a significantly different group (r^2 = adjusted residual error, P<0.001, ANOVA, Tukey HSD).

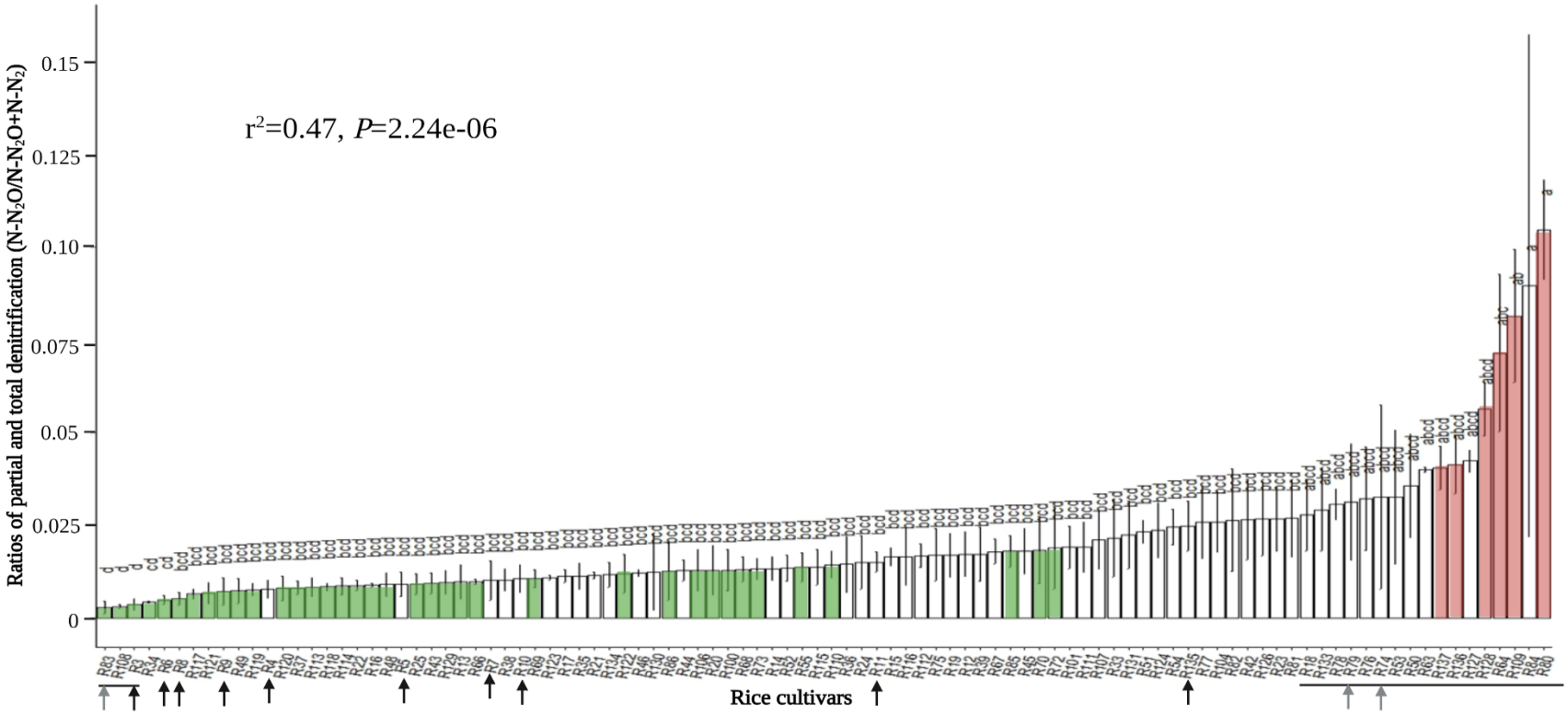

Fig 4.4.5: Mean±SE (n=4) from one-way (Type II) ANOVA of the ratio of N-N_2O: N-N_2O+N-N_2 of tested rice cultivars (n=98). Underlined rice lines indicated low and high partial and total denitrification ratios associated with the rice cultivars group. Rice cultivars associated with low N_2O emissions were indicated by green-coloured bars, and rice cultivars associated with high N_2O emissions were indicated by red-coloured bars. The black and shaded arrows indicated high and low complete denitrification rice cultivars. The letters indicated a significantly different group (r^2 = adjusted residual error, P<0.001, ANOVA, Tukey HSD).

4.4.5 GWAS results for partial denitrification, complete denitrification and the ratio of N-N_2O: N-N_2O+N-N_2 traits of tested rice cultivars

The GWAS analysis for each trait yielded a summary output file containing the most significant SNPs with the calculated major and minor allele effects (Supplementary table:). Manhattan plots were produced displaying significant single nucleotide polymorphisms (SNPs) associated with variation in partial (Fig: 4.4.6) and complete denitrification activity (Fig: 4.4.8) and the ratio of N-N_2O: N-N_2O+N-N_2 (Fig: 4.4.10) from the genome-wide analysis. Genome order per chromosome was plotted on the X-axis against the −log10 of the p-values of SNPs on the Y-axis (Norton et al., 2018). The significant threshold limit indicated by grey line for the SNPs associated with partial denitrification (Fig: 4.4.6), complete denitrification (Fig: 4.4.8) and the ratio of N-N_2O: N-N_2O+N-N_2 (Fig: 4.4.10) were measured at –log10 (4.3), –log10 (6.4) and –log10 (4.5) respectively for a false discovery rate (FDR) limit of 0.05 after generating a quantile-quantile (QQ) plots (Figs: 4.4.7, 4.4.9 and 4.4.11) by plotting –log10 (expected p-value) and –log10 (observed p-value) on the X-axis and Y-axis respectively (Kaler & Purcell, 2019). SNPs associated with complete denitrification rate significantly deviated from the null hypothesis (Grey straight line), suggesting less chance of being falsely positive (Fig: 4.4.9). The genomic inflation factor (known as λgc) value was 1.0 in the QQ plot, indicating that the model was well fitted with the complete denitrification rate phenotyping trait and –log10 of the p-values of most SNPs were uniformly distributed among the chromosomes means any bias occurred while modelling. Fourteen significant SNPs (indicated by their rank number) associated with complete denitrification variation trait were observed above the FDR limit of 0.05 (Fig: 4.4.8).

The λgc values were 1.2 and 1.136 for the QQ plots of partial denitrification (Fig: 4.4.7), and the ratio of N-N_2O: N-N_2O+N-N_2 (Fig: 4.4.11) above 1 indicated more bias occurred while modelling as SNPs were not uniformly distributed among the chromosomes and the λgc value would vary among the chromosomes (van den Berg et al., 2019). Most of the significant SNPs with higher –log10 (P) resided in chromosomes 4 and 10 for partial denitrification phenotypic trait and only in chromosome 4 for the ratio of N-N_2O: N-N_2O+N-N_2 and these two phenotypic traits were

connected. To be conservative, I, therefore, increased the significance threshold limit to –log10 (8.8) (Fig: 4.4.6) and –log10 (10.1) (Fig: 4.4.10) indicated by the red dotted line for partial denitrification and the ratio of $N\text{-}N_2O$: $N\text{-}N_2O+N\text{-}N_2$ GWAS output based on –log10 (expected p-value) and –log10 (observed p-value) separation of respective QQ plots. The details of the SNPs associated with partial denitrification (Table: 4.4.5), complete denitrification (Table: 4.4.6) and the ratio of $N\text{-}N_2O$: $N\text{-}N_2O+N\text{-}N_2$ (Table: 4.4.7) were summarised with loci associated within 10 kb upstream and downstream from the particular significant SNP in the rice genome, annotated gene and annotated protein and their function.

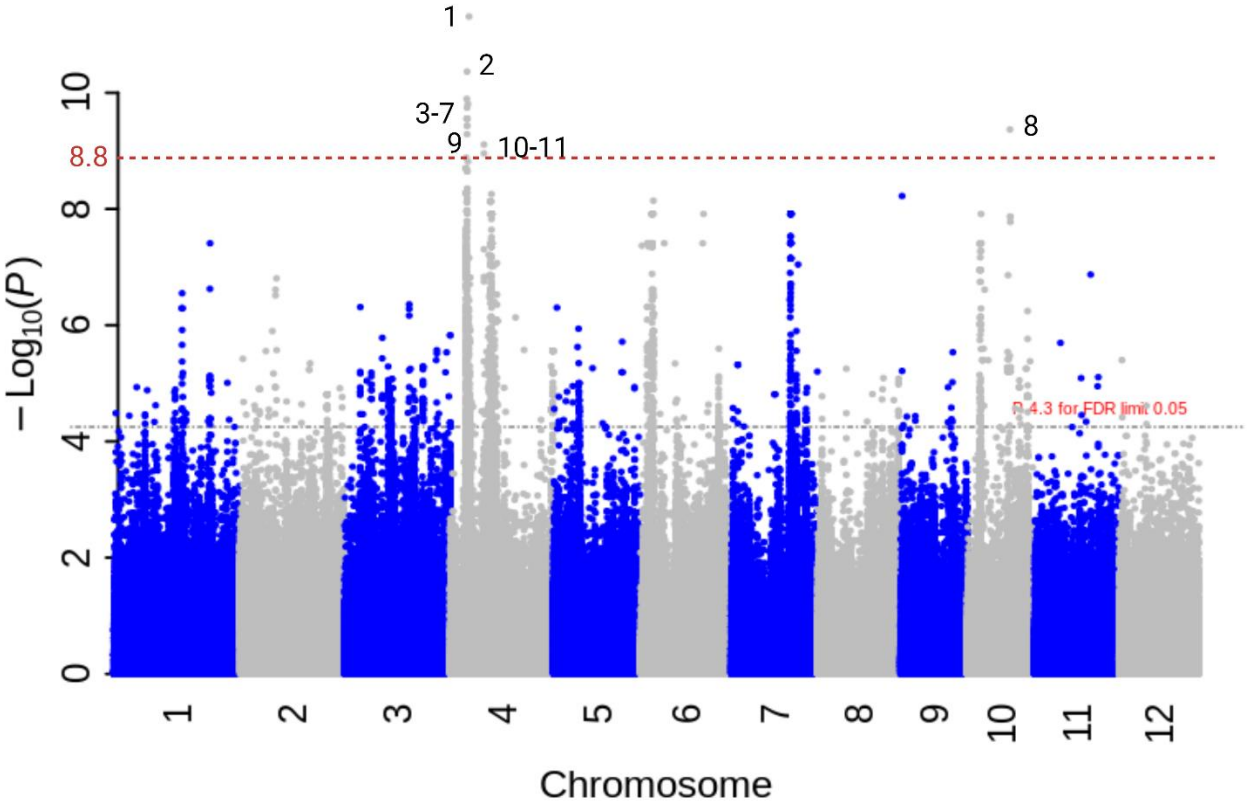

Fig 4.4.6: Manhattan plot from the GWAS analysis of SNPs in the chromosomes associated with partial denitrification ($N\text{-}N_2O$ emission) rate variations. Significant SNPs were above the grey dotted line, having $-Log_{10}$ (P) > 4.3 for the FDR limit (P<0.05). Top-ranked SNPs marked with their rank indicated above the red dotted line having $-Log_{10}$ (P) > 8.8 after increasing the limit from FDR limit (P<0.05).

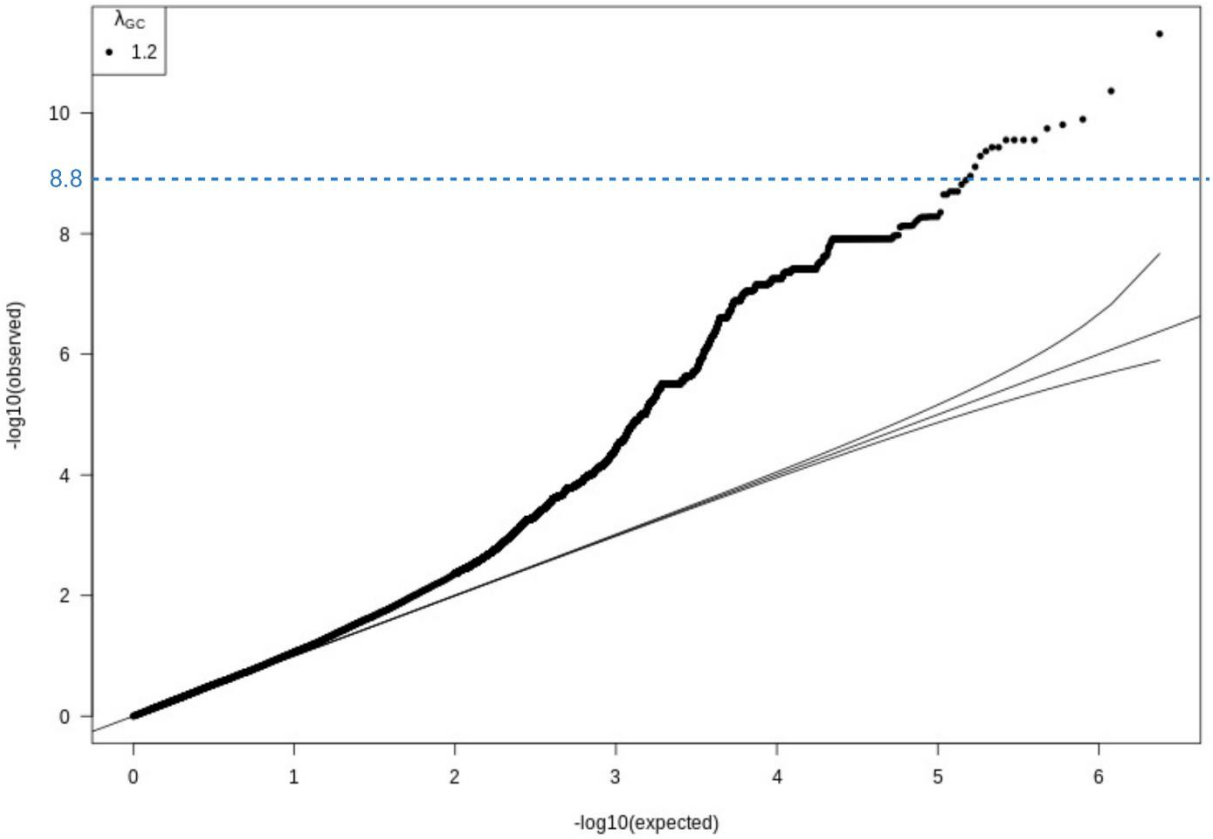

Fig 4.4.7: QQ-plot showing the distribution of the observed against the expected –log10 (*P*) for the SNPs of the rice genome associated partial denitrification (N-N_2O emission) rate variations, where the expected –log10 (*P*) under the null hypothesis were indicated by the straight grey line and observed values were indicated as the cluster of dots in black. The λ_{GC} at the left top corner, bounded by a box, indicated the genomic inflation of the model. The blue dotted line indicated the top-ranked SNPs threshold limit -log10(p)= 8.8 where observed and expected values were separated.

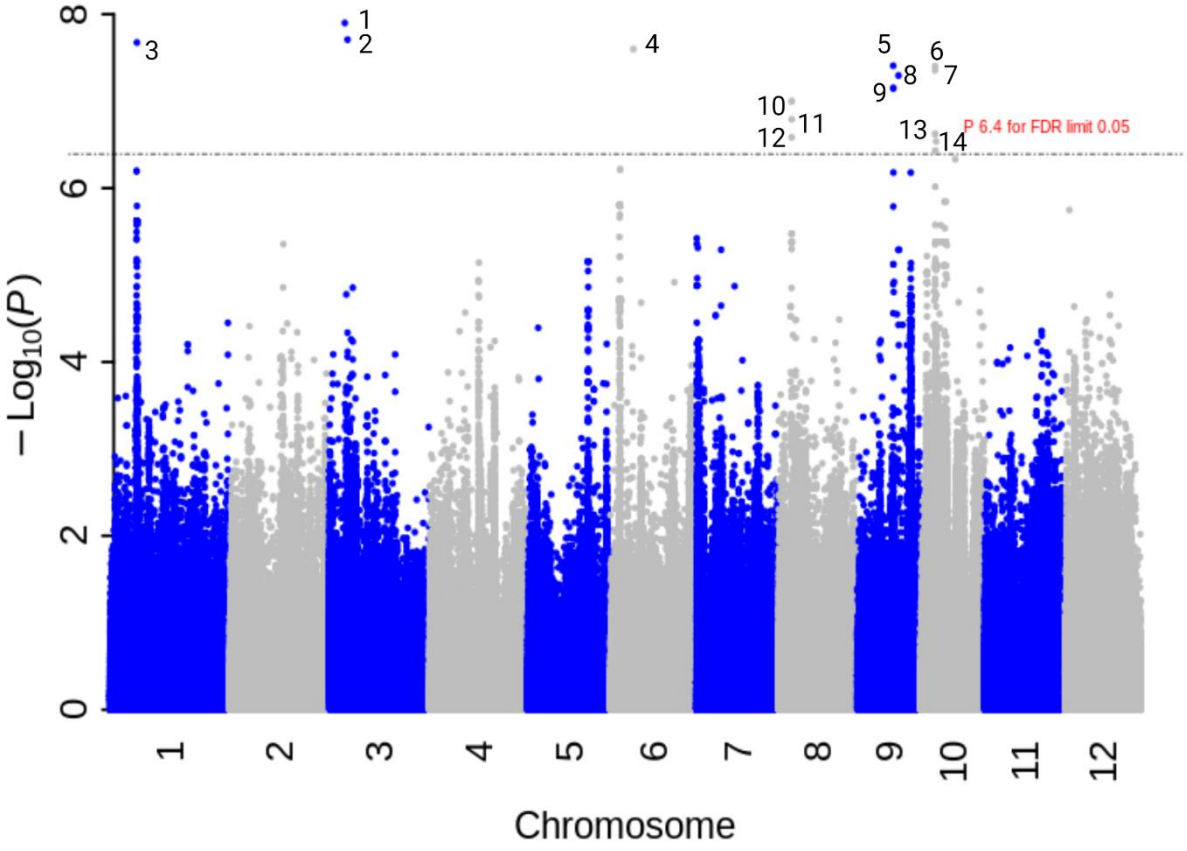

Fig 4.4.8: Manhattan plot from the GWAS analysis of SNPs in the chromosomes associated with complete denitrification (N-N_2 emission) rate variations. Significant SNPs were above the grey dotted line, having $-Log_{10}(P) > 6.3$ for the FDR limit ($P<0.05$) marked with their rank number.

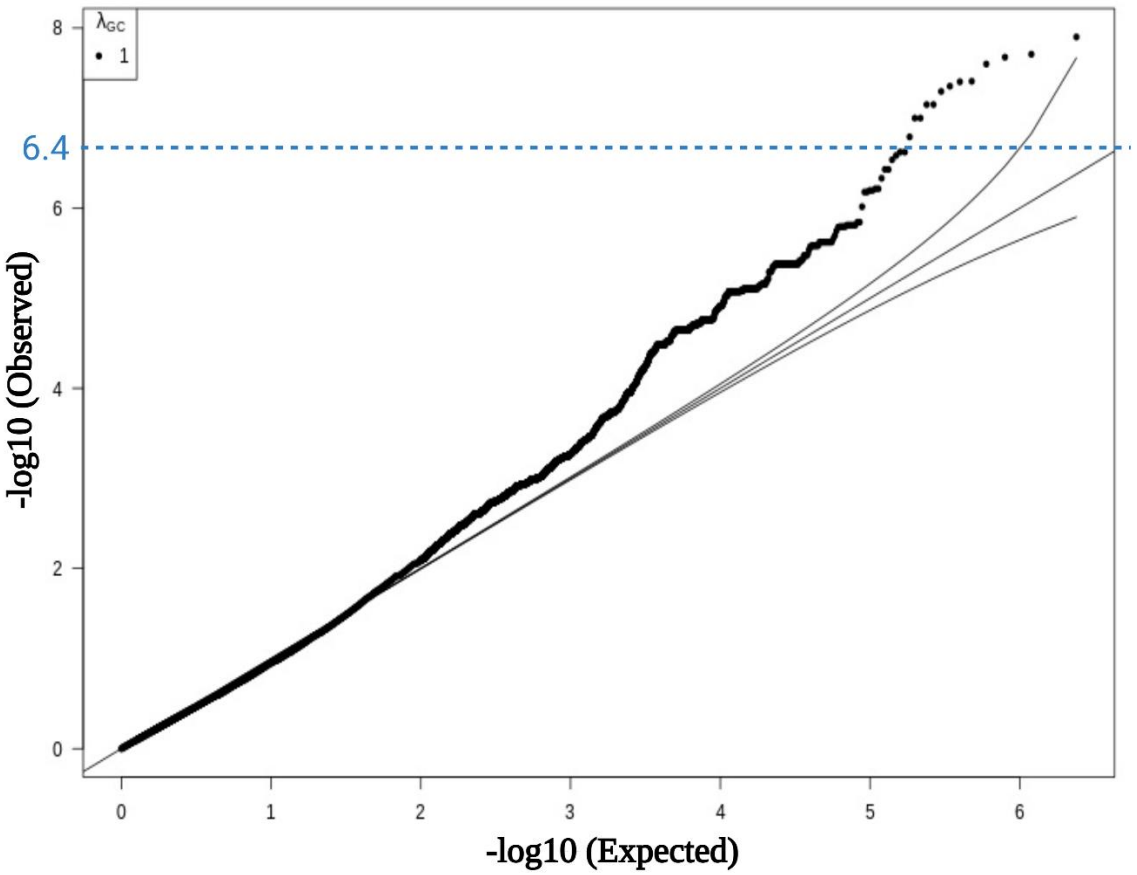

Fig 4.4.9: QQ-plot showing the distribution of the observed against the expected –log10 (P) for the SNPs of the rice genome associated with complete denitrification (N-N_2 emission) rate variations, where the expected –log10 (P) under the null hypothesis were indicated by the straight grey line and observed values were indicated as the cluster of dots in black. The λ_{GC} at the left top corner, bounded by a box, indicated the genomic inflation of the model. The blue dotted line indicated the SNPs threshold limit -log10(p)= 6.4 where observed and expected values were separated.

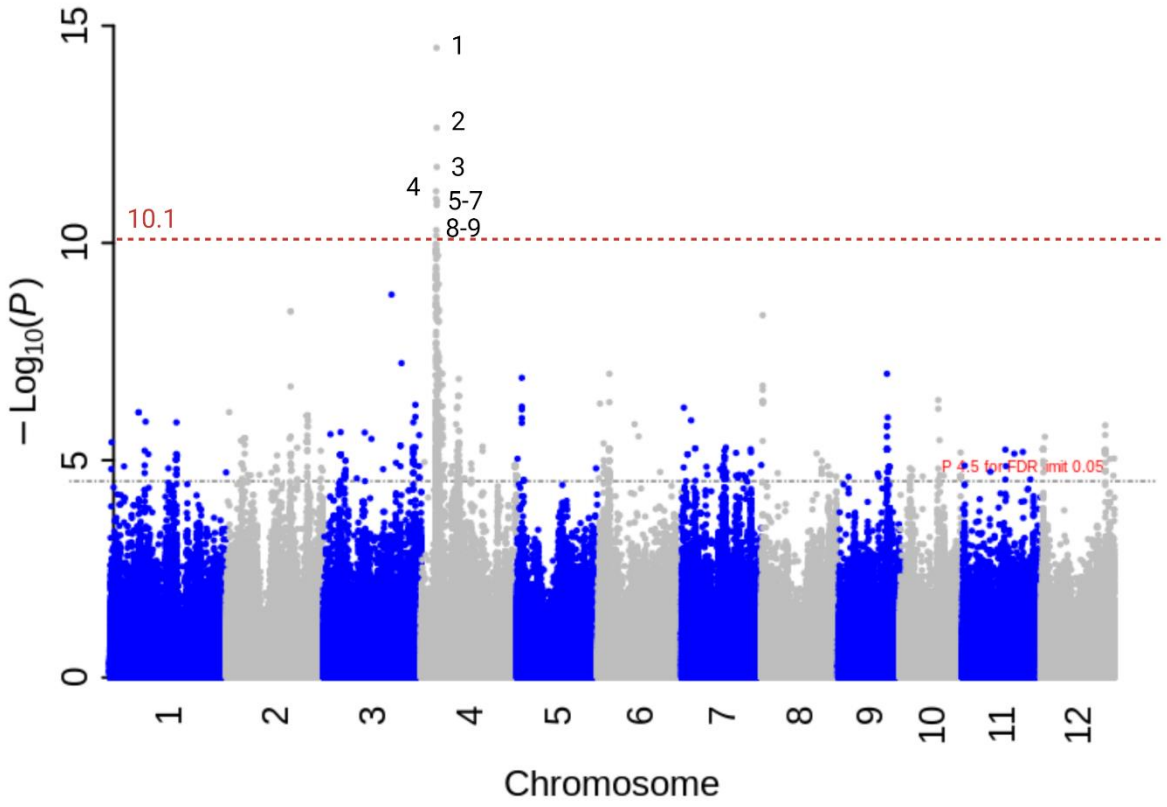

Fig 4.4.10: Manhattan plot from the GWAS analysis of SNPs in the chromosomes associated with partial and complete denitrification ratio ($N\text{-}N_2O/N\text{-}N_2O+N\text{-}N_2$) variations. Significant SNPs were above the grey dotted line, having $-Log_{10}(P) > 4.5$ for the FDR limit ($P<0.05$). Top-ranked SNPs marked with their rank belonged above the red dotted line having $-Log_{10}(P) > 10.1$ for the FDR limit ($P<0.05$).

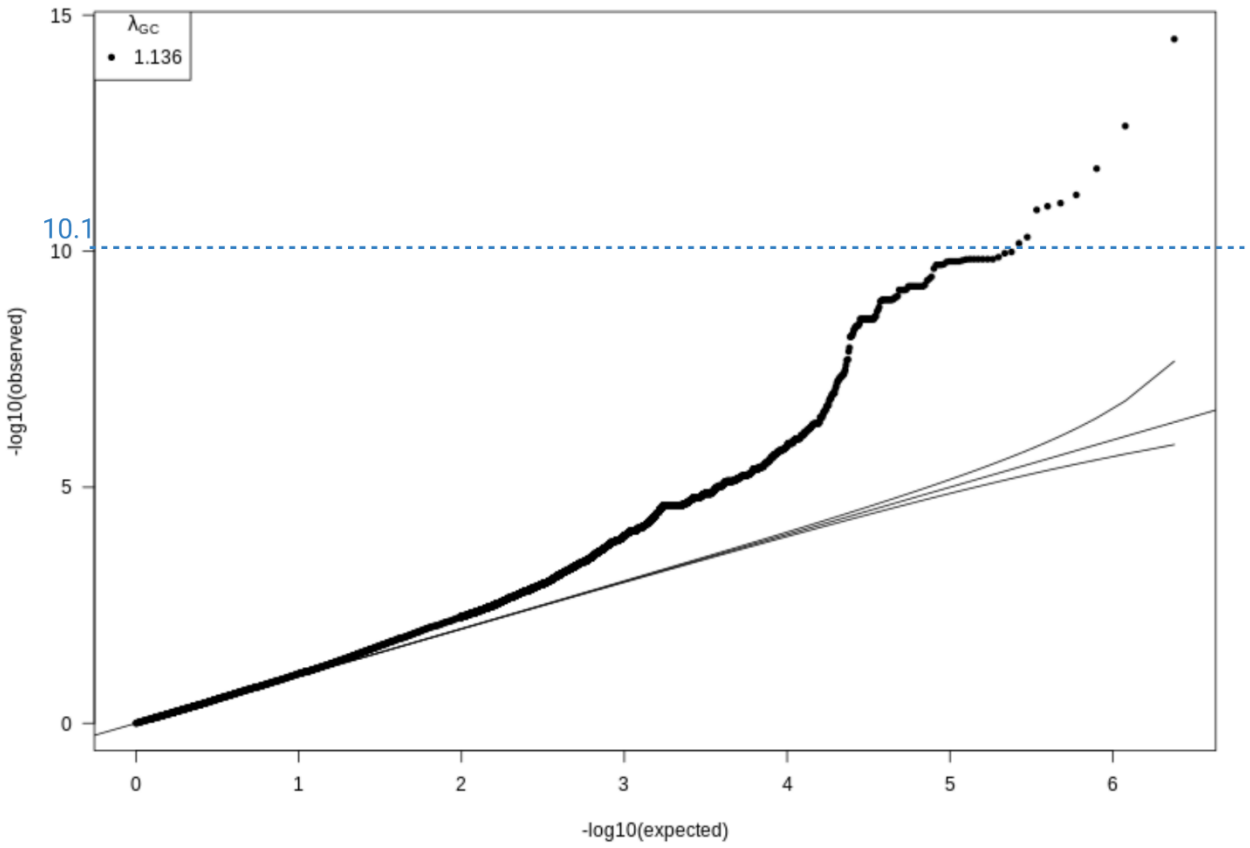

Fig 4.4.11: QQ-plot showing the distribution of the observed against the expected –log10 (*P*) for the SNPs of the rice genome associated partial and complete denitrification ratio (N-N_2O/N-N_2O+N-N_2) variations, where the expected –log10 (*P*) under the null hypothesis were indicated by the straight grey line and observed values were indicated as the cluster of dots in black. The λ_{GC} at the left top corner, bounded by a box, indicated the genomic inflation of the model. The blue dotted line indicated the top-ranked SNPs threshold limit -log10(p)= 10.1 where observed and expected values were separated.

Table 4.4.4: Significant SNPs above the FDR limit (P<0.05) identified by the GWAS associated with the partial denitrification (N-N_2O emission) variations among the tested rice cultivars, their location and position in the chromosome, -log10(P-value), and loci found within 10 kb upstream and downstream from the particular significant SNP in the rice genome, annotated gene and annotated protein and their function with similarity % from the http://rice.uga.edu website are mentioned in the table.

SNP rank	SNP Name	Chr No.	Position	-log$_{10}$(P)	Locous name (± 10 kb)	Annotated gene	Similarity %	Annotated protein	Function
1	mlid0026561114	4	6449119	11.31	LOC_Os04g11760.1	OsI_14983	99.05	Uncharacterised	disease resistance protein
					LOC_Os04g11770.1	OSJNBa0017B10.1	96.97	retrotransposon protein	retrotransposon activity
					LOC_Os04g11780.1	OSJNBa0040D17.10	100	resistance protein LR10	Leaf rust resistance protein
					LOC_Os04g11790.1	OsJ_13920	95.14	OsFBX120 - F-box domain-containing protein	Ubiquitination
2	mlid0026353227	4	5737153	10.36	LOC_Os04g10530.1	OSIGBa0148J22.2	91.5	OSIGBa0140C02.7	Amidase activity
					LOC_Os04g10550.1		NA	Expressed protein	Uncharacterised
					LOC_Os04g10569.1	Os04g0184500	76.37	Os04g0184500 protein	glutamyl-tRNA amidotransferase
					LOC_Os04g10590.1	OSJNBa0079I01.24	95.32	Putative gag-pol polyprotein	retrotransposon activity

3	mlid00263 26409	4	5631827	9.90	LOC_Os04g1 0380.1	OSJNBa0027 O01.13	88.5	Glycine rich protein	ABA activated signaling pathway
					LOC_Os04g1 0390.1	OSJNBb0006 L01.4	100	transposon protein	transcription activator
					LOC_Os04g1 0400.1	OSJNBb0006 L01.5	96.05	electron transfer flavoprotein subunit beta	Alternative electron acceptor for dehydrogenase
4	mlid00264 30543	4	6026555	9.81	LOC_Os04g1 1070.1	OSJNBa0045 O17.12	82.58	retrotransposon protein	Retrotransposon activity
					LOC_Os04g1 1080.1	OSJNBb0013J 13.3	85.14	retrotransposon protein	retrotransposon activity
					LOC_Os04g1 1090.1	OSJNBb0033 G08.12	94.12	retrotransposon protein	DNA directed DNA polymerase
5-7,9 and 10	mlid00263 53363	4	5737585	9.74	LOC_Os04g1 0530.1	OsJ_13958	100	Amidase protein	Hydrolase activity
	mlid00263 53460		5737895	9.55	LOC_Os04g1 0550.1		NA	Expressed protein	Uncharacterised
	mlid00263 53467		5737915	9.55	LOC_Os04g1 0569.1	Os04g0184100	80.14	Os04g0184100 protein	glutamyl-tRNA amidotransferase
	mlid00263 53469		5737920	9.55	LOC_Os04g1 0530.1	OSJNBa0079I 01.24	95.32	Putative gag-pol polyprotein	retrotransposon activity
8	mlid00701 32094	10	14764919	9.55	LOC_Os10g2 8360.1	ARD4	100	Acireductone dioxygenase 4	Catalyzes 1,2-dihydroxy-3-keto-5-methylthiopentene

					LOC_Os10g28370.1	AT5G43860	63.4	chlorophyllase-2, chloroplast precursor	Chlorophyll degradation
					LOC_Os10g28380.1	MTN26L3	100	MtN26 family protein precursor	Provide immunity from microbial infection
					LOC_Os10g28390.1		NA	Expressed protein	Uncharacterised
					LOC_Os10g28400.1	MTN26L4	100	MtN26 family protein precursor	Provide immunity from microbial infection
11	4:5796956	4	5796956	9.43	LOC_Os04g10650.1	OSIGBa0132G14.1	88.27	OSIGBa0132G14.1 protein	DNA replication factor Cdt1
					LOC_Os04g10660.1		NA	Expressed protein	Uncharacterised
					LOC_Os04g10680.1	Os04g0185500	95.63	Os04g0185500 protein	zinc finger, C3HC4 type domain containing protein

Table 2 Table 4.4.5: Significant SNPs above the FDR limit (P<0.05) identified by the GWAS associated with the complete denitrification (N-N_2 emission) variations among the tested rice cultivars, their location and position in the chromosome, -log10(P-value), and loci found within 10 kb upstream and downstream from the particular significant SNP in the rice genome, annotated gene and annotated protein and their function with similarity % from the http://rice.uga.edu website are mentioned in the table.

SNP rank	SNP Name	Chr No.	Position	-log10 (p)	Locus	Annotated gene	Annotated protein	Similarity %	Function
1	mlid00180498 36	3	5750 805	7.90	LOC_Os03g11140.1	OSNPB_030 209800	pleckstrin homology domain-containing protein-related taxo	91.2	nucleobase, nucleoside, nucleotide and nucleic acid metabolic process
					LOC_Os03g11150.1		Expressed protein	NA	uncharacterised
					LOC_Os03g11160.1	OsJ_09870	Oryzacystatin-9	100	cysteine proteinase inhibitor precursor
					LOC_Os03g11170.1	OsJ_09871	Oryzacystatin-7	84.62	cysteine proteinase inhibitor precursor
					LOC_Os03g11180.1	Os03g021020 0	Oryzacystatin-6	89.38	cysteine proteinase inhibitor 6 precursor
					LOC_Os03g11190.1		Expressed protein	NA	uncharacterised
2	mlid00182110 01	3	6730 958	7.71	LOC_Os03g12650.1		Retrotransposon protein	NA	retrotransposon activity
					LOC_Os03g12660.1	CYP90B2	Steroid (22S)-hydroxylase	94.47	brassinosteroid biosynthesis
3	1:9717 828	1	9717 828	7.68	LOC_Os01g16970.1	OsI_01383	Glucosidase 2 subunit beta	77.04	Glycan metabolism; N-glycan metabolism

					LOC_Os01g16980.1	OSNPB_010276900	Os01g0276900 protein	82.79	uncharacterised
4	mlid00415146 12	6	8387927	7.60	LOC_Os06g14790.1	OSJNBa0092H22.7	Ulp1 protease-like protein	100	peptidase activity
					LOC_Os6g147800.1	Not found	Expressed protein	Not found	
5	mlid00641486 32	9	13089525	7.41	LOC_Os09g21600.1	OSJNBb0015G09.8	OSJNBb0015G09.8 protein	93.15	retrotransposon activity
					LOC_Os09g21610.1	OSJNBb0086I08.6	Gag-pol	93.9	retrotransposon activity
6	mlid00676759 27	10	5313635	7.40	LOC_Os10g09810.1	OSIGBa0157N01.6	RNA-directed DNA polymerase	93.55	retrotransposon activity
					LOC_Os10g09820.1	OsI_37448	NAC domain-containing protein	84.67	root meristem activity
					LOC_Os10g09830.1		Expressed protein	NA	uncharacterised
7	mlid00676732 69	10	5304063	7.35	LOC_Os10g09790.1		Retrotransposon protein	NA	retrotransposon activity
					LOC_Os10g09800.1		Retrotransposon protein	NA	retrotransposon activity
					LOC_Os10g09810.1		Retrotransposon protein	NA	retrotransposon activity
8	mlid00645982 30	9	15000927	7.30	LOC_Os09g25070.1	OsWRKY62	WRKY transcription factor	75.25	DNA binding transcription factor activity
					LOC_Os09g25080.1	P0014G10.45	Expressed protein	92.05	uncharacterised
					LOC_Os09g25090.1	CIPK16	CBL-interacting protein kinase 16	93.42	calcium/calmodulin depedent protein kinases
9	mlid00641553 86	9	13115748	7.15	LOC_Os09g21640.1		Retrotransposon protein	NA	retrotransposon activity
	mlid00641553 85		13115747		LOC_Os09g21650.1		Retrotransposon protein	NA	retrotransposon activity
					LOC_Os09g21660.1		Expressed protein	NA	uncharacterised
10 to 13	mlid00548108 18	8	4732469	7.00	LOC_Os08g08260.1		Expressed protein	NA	uncharacterised
	mlid00548108 29		4732519						

	mlid00548105 74		4731 791	6.79					
	mlid00676749 24	10	5311 383	6.62	LOC_Os10g09800.1		Retrotransposon protein	NA	retrotransposon activity
14	mlid00676749 27		5311 389		LOC_Os10g09810.1		Retrotransposon protein	NA	retrotransposon activity
					LOC_Os10g09820.1	OsI_37448	NAC domain-containing protein	85.48	root meristem activity
					LOC_Os10g09830.1		Expressed protein	Not found	uncharacterised

Table 4.4.6: Significant SNPs above the FDR limit (P<0.05) identified by the GWAS associated with the ratio of partial and complete denitrification ($N\text{-}N_2O$/ $N\text{-}N_2O+N\text{-}N_2$ +) variations among the tested rice cultivars, their location and position in the chromosome, -log10(P-value), and loci found within 10 kb upstream and downstream from the particular significant SNP in the rice genome, annotated gene and annotated protein and their function with similarity % from the http://rice.uga.edu website are mentioned in the table.

SNP rank	SNP Name	Position	-log10(P)	Locous name (within 20 kb)	Annotated gene	Similarity %	Annotated protein	Function
1	mlid00263264 09	563182 7	14.49	LOC_Os04g10590.1	OSJNBa0079I01.24	95.32	Putative gag-pol polyprotein	retrotransposon activity
				LOC_Os04g10380.1	OSJNBa0027O01.13	88.5	Glycine rich protein	ABA activated signaling pathway
				LOC_Os04g10390.1	OSJNBb0006L01.4	100	transposon protein	transcription activator
				LOC_Os04g10400.1	OSJNBb0006L01.5	96.05	electron transfer flavoprotein subunit beta	Alternative electron acceptor for dehydrogenase
2	mlid00263375 16	567735 4	12.65	LOC_Os04g10434.1	OSIGBa0140C02.5	100	OSIGBa0140C02.5 protein	Amidase activity
				LOC_Os04g10450.1		NA	Hypothetical protein	Uncharacterised
				LOC_Os04g10460.1	OSJNBb0006L01.9	88.64	OSJNBb0006L01.9 protein	Amidase activity
3	mlid00263511 38	573173 5	11.75	LOC_Os04g10530.1	Os04g0184100	93.8	Os04g0184100 protein	Amidase activity
				LOC_Os04g10550.1	NA	NA	Expressed protein	Uncharacterised
				LOC_Os04g10569.1	Os04g0184100	80.14	Os04g0184100 protein	Amidase activity
4 and 5	mlid00262897 55	547778 0	11.19	LOC_Os04g10130.1	OSJNBa0052P16.21	87.77	OSJNBa0052P16.21 protein	retrotransposon activity
				LOC_Os04g10140.1	OSJNBa0052P16.22	100	OSJNBa0052P16.22 protein	hypothetical protein
				LOC_Os04g10150.1	NA	NA	Expressed protein	Uncharacterised
				LOC_Os04g10160.1	CYP99A2	92.86	Cytochrome P450 99A2	momilactone phytoalexins biosynthesis

6	4:5843004	5843004	10.95	LOC_Os04g10740.1	OSJNBb0003A12.9	97.62	OSJNBb0003A12.9 protein	retrotransposon activity
				LOC_Os04g10750.1	PHT1-4	94.98	(OsPT4) Probable inorganic phosphate transporter 1-4	High-affinity transporter for external inorganic phosphate
				LOC_Os04g10760.1	NA	NA	Expressed protein	Uncharacterised
7	mlid00263395 17	5686118	10.87	LOC_Os04g10450.1	NA	NA	Hypothetical protein	Uncharacterised
				LOC_Os04g10460.1	OSJNBb0006L01.9	88.64	OSJNBb0006L01.9 protein	Amidase activity
				LOC_Os04g10470.1	NA		Expressed protein	Uncharacterised
8	mlid00263112 66	5563388	10.30	LOC_Os04g10280.1	OSJNBa0027O01.10	90.54	RNA-directed DNA polymerase	retrotransposon activity
				LOC_Os04g10290.1	NA	NA	Expressed protein	Uncharacterised
				LOC_Os04g10300.1	NA	NA	Hypothetical protein	Uncharacterised
				LOC_Os04g10310.1	NA	NA	Hypothetical protein	Uncharacterised
				LOC_Os04g10320.1	OsJ_13973	99.25	Expressed protein	Uncharacterised
9	4:5542841	5542841	10.17	LOC_Os04g10250.1	OSJNBa0027O01.7	95.67	OSJNBa0027O01.7 protein	Uncharacterised
				LOC_Os04g10260.1	OSIGBa0101K10.2	92.46	OSIGBa0101K10.2 protein	nucleobase, nucleoside, nucleotide and nucleic acid metabolic process
				LOC_Os04g10270.1	NA	NA	retrotransposon protein	retrotransposon activity
				LOC_Os04g10280.1	OSJNBa0027O01.10	NA	RNA-directed DNA polymerase	retrotransposon activity

4.5 Discussion

4.5.1 Rice plant effects on N_2O emission

Rice plants reduced denitrification by approximately half in planted microcosms compared to unplanted microcosms (Fig: 4.4.1E). There are many reasons for this, including the level of oxygenation, competition for N and carbon exudation from the roots. Oxygen from the rice root from radial oxygen loss (ROL) will oxygenate the rhizosphere and adjacent bulk soil, thus limiting the denitrification process in that oxygenated zone of planted microcosms where carbon is at its highest concentration (Fig: 4.5.1) (Armstrong, 1971; Morley & Baggs, 2010). In contrast, barley plants, while growing in wet (above 80% WFPS) arable soil, induced denitrification by consuming oxygen near the root and, in addition, fueled the process by providing respirable C (Klemedtsson et al., 1987). Paddy soil is relatively more enriched with soil organic carbon (SOC) than dry arable soil and is likely to provide sufficient C as the reductant for denitrification after the addition of N-fertiliser (Z. Qin et al., 2013). DOC was measured as lowest in the unplanted soil but may be enough to fuel the denitrification in the unplanted microcosm (Fig: 4.4.1A).

Heterotrophic denitrifiers metabolise carbon sources to produce nicotinamide adenine dinucleotide (NADH), a direct electron donor, circulating in the electron transport system at the end transferred to the corresponding denitrification reductases (Berks et al., 1995). According to carbon stoichiometry, electron generation varies between carbon sources (Zhou, 2001). For example, twenty-four electrons are generated if one molecule of glucose (4 electrons/Carbon) enters into respiration, whereas nine electrons are generated if one molecule of acetic acid (4.5 electrons/Carbon) is respired (Equation 6 and 9, Chapter 1, Section 1.2.3.5.2). So, two carbons, either from acetic acid or glucose, are insufficient to fuel complete denitrification of NO_3^- ($2\ NO_3^- + 12\ H^+ + 10\ e^- = N_2 + 6\ H_2O$). In contrast, only one carbon is enough from carbohydrates or organic acids to reduce N_2O into N_2 since only one electron is required for the reduction ($N_2O + 2\ H^+ + e^- = N_2 + H_2O$). However, NO_3^- is a more efficient electron acceptor, two times higher than N_2O (Equation 12 and 15, Chapter 1, Section 1.2.3.5.2). So, NO_3^- served as a better substrate option than the other N-oxides in the denitrification pathway. Ten electrons in total are required to denitrify NO_3^- ultimately into N_2 (Equation 10, Chapter 1, Section 1.2.3.5.2). In unplanted pots, the DOC: NO_3^- ratio (8:1) was significantly lower than in the bulk and rhizosphere compartments (Fig: 4.4.1B). All the carbons in the soil do not participate in respiration for energy production; a

fraction of carbons are used for microbial biomass synthesis (Equation 16, Chapter 1, Section 1.2.3.5.2). The source partitions of carbons between microbial biomass synthesis and respiration depend on soil abiotic conditions (Manzoni & Porporato, 2009). For instance, microbial biomass content was approximately twice higher than in the upland soil due to reduced microbial activity and slower microbial turnover under oxygen-limited flooding conditions (Wei et al., 2022). N_2O reduction into N_2 is decreased at low C: NO_3^- thus increasing N_2O emission from the unplanted microcosms (Fig: 4.4.1C) (Giles et al., 2012; Lycus et al., 2017). Indeed, the lack of carbon (Precisely organic acids and alcohols) input through root exudation decreased the N_2O reduction into N_2 in the unplanted soil since the types of carbon dictate the fate of denitrification end products depending on the O_2 concentration (Morley & Baggs, 2010). Adding DOC-rich liquid at 20 mg DOC/cm^2 decreased one-third of the ratio of N_2O/N_2O+N_2 in the irrigated experimental field (Qin et al., 2017). In contrast, adding active carbon as the root exudation of mustard plants at the rate of 630 ng DOC/ml in the groundwater decreased the ratio to a thousandfold (Jahangir et al., 2014). In this study, the difference in average DOC between planted and unplanted microcosm pots due to rice plant input was 1000 ng/g dry weight of soil equivalent to 6 mg/cm^2 that triggered fifteen times reduction of the ratio of N_2O/N_2O+N_2 in the planted microcosms compared with unplanted microcosms (Fig: 4.4.1A and 4.4.1F). Denitrifers responded merely to similar bioenergetics gained by complete or incomplete denitrification (Simon & Klotz, 2013). So, complete denitrifiers (NosZ clade I) are likely to truncate the denitrification pathway in carbon limiting and NO_3^- non-limiting unplanted flooded paddy soil (Fig: 4.4.1F). However, the ratio of DOC: N-NO_3- was 8:1 in the unplanted soil, which might be enough to fuel the complete denitrification since the ratio 5:1 efficiently reduced the NO_3^- into N_2 (Dahab & Woon Lee, 1988; Qin et al., 2017). Nevertheless, NO_3^- accumulation in the bioavailable organic carbon-limited unplanted microcosms due to lack of plant uptake might inhibit N_2O reductase activity associated with high N_2O emission compared to the planted microcosms (Ge et al., 2015; Kakuda et al., 2000; Morley et al., 2014; M Senbayram et al., 2012).

After applying 200µg N/g dry-weight soil (100 µg N-NH_4^++ 100 µg N-NO_3^-), approximately 60% N-NH_4^+ and 35% N-NO_3^- of it were recovered after the incubation in the unplanted microcosms (assumption taken after excluding leaching, mineralisation and DNRA) (Fig: 3.4.1A). The source of emitted N_2O from the unplanted microcosm was NO_3^- since NH_4^+ contribution in the emission through nitrification was inhibited due to prevailing anaerobic conditions. Approximately 15 %

N_2O was emitted without further reduction in the denitrification pathway (Fig: 4.4.1F). This percentage is approximately 1% in the rice microcosms. The presence of rice plants reduced N_2O emissions in microcosms by both taking up $N\text{-}NO_3^-$ and releasing organic carbon through root exudation, altering this ratio and encouraging higher levels of complete denitrification (Rummel et al., 2021). In a flooded paddy system, carbon from root exudates could travel with a gradient of up to 2 cm from the root surface, increasing the C: NO_3^- ratio in the bulk compartment of planted microcosms (Fig: 4.5.1) (Xiaoting Wang et al., 2018). The higher C: NO_3^- possibly induced NO_3^- source partitioning into the DNRA pathway rather than denitrification in the planted microcosms (Nojiri et al., 2020; Pandey et al., 2019; Putz et al., 2018; Tiedje, 1988; Tiedje et al., 1983; Z. Wei, Jin, et al., 2022; Z. Wei, Senbayram, et al., 2022).

Furthermore, in high NO_3^- concentrations, the final step of denitrification, N_2O to N_2 reduction, is reduced (Gaskell et al., 1981; Bateman and Baggs, 2005; Giles et al., 2012). Residual $N\text{-}NO_3^-$ concentration was 33±10 µg/g dry weight of soil in unplanted microcosm (n=4) significantly (P<0.001) higher than in the rhizosphere and bulk compartments (n=331) of planted microcosms, and at levels likely to decrease the activity of the last step of denitrification, thus increasing $N\text{-}N_2O$ emission (Fig: 4.5.1). (Mehmet Senbayram et al., 2019) reported that the reduction of N_2O to N_2 becomes minimised at a concentration of 44.9 µg $N\text{-}NO_3^-$ / g dry-weight soil. Apart from residual $N\text{-}NO_3^-$ concentration and C: NO_3^- ratios, the abundance of complete denitrifiers might be another factor behind the N_2O emission variations. Complete denitrifiers (particularly NirS type with NosZ clade I) are responsive to artificial root exudates, indicating that the presence of rice root exudates may influence the completion of the denitrification pathway by increasing complete denitrifiers abundance in planted microcosms (Langarica-Fuentes et al., 2018b). It, therefore, seems likely that rice plants reduced N_2O emission from planted microcosms overall by limiting the denitrification rate and/or encouraging N_2O reduction by NosZ clade I and II through oxygenation, root exudation, and/or competitive uptake of NO_3^-.

4.5.2 Rice genotype effects on complete denitrification (N_2 emission)

N_2 through complete denitrification was the dominating product in denitrification, which drove the total denitrification variations among the tested rice cultivars in this microcosm experiment (Fig: 4.4.2). The observed results concerted with (Giles et al., 2017), where it was observed that N_2 was

dominating product of denitrification during soil incubation at 90 % WPFS with the fortification of C and N. So, complete denitrification-associated variations among the tested rice cultivars may arise due to inhibition/limitation of flux through the pathway denitrification and/or truncation of the denitrification. Complete denitrification tended to decrease with increased truncation of the process as complete denitrification was negatively correlated with the ratio of partial and total denitrification ($N\text{-}N_2O$: $N\text{-}N_2O+N_2$) (Chapter 3, Fig: 3.4.2). Furthermore, there was no correlation found between complete denitrification ($N\text{-}N_2$) and partial denitrification ($N\text{-}N_2O$) suggesting that N_2O production by incomplete denitrifiers which lack nitrous oxide reductase and N_2O consumption by NosZ clade II along with NosZ clade I co-occurred depending on the C and N availability in each anaerobic soil microsites in the microcosm pots (Fig: 4.5.1). There was also no correlation between complete denitrification and C: NO_3^- ratios either in any compartments of microcosm pot **(**Table: 4.4.4**)** suggesting nitrate was non-limiting in the experiment and it could be caused by gene complements of denitrifier community present in the soil or by other physicochemical parameters such as C or O distribution. So, in NO_3^- non-limiting conditions, the NO_3^- source partitioning effect between denitrifiers and DNRA community might not affect the complete denitrification variations among the tested rice cultivars in this microcosm experiment (Pandey et al., 2019).

Low complete denitrification was observed in rice cultivars R83, R74 and 79 (Fig: 4.4.3), and these cultivars also had low (Fig: 4.4.2). However, two of these had relatively high partial denitrification rates, suggesting that there any be a number of mechanisms at play. The mechanism is unlikely to relate to low C and N levels as these are non-limiting in this microcosm system. Other mechanisms seem more likely. For example, rice cultivars might limit the activity of the NirS/Nirk community by secreting biological denitrification inhibitors (BDI) like the compound found in *Fallopia* spp (Bardon et al., 2014) but this would most likely be apparent in R83 or similar where flux appears limited. Total denitrification was two-fold higher in the unplanted than planted microcosms (Fig: 4.4.1E). Indeed, on day 1, after enrichment fertilisation, N was found in non-limiting conditions for the denitrifier community. Complete denitrification was observed to be low in the other two rice cultivars (R74 and R79) due to the reduction of N_2O consumption by NosZ clade I and II (Fig: 4.4.5). The high complete denitrification-associated rice cultivars might accelerate N_2O consumption by increasing low molecular weight organic carbon (LMW-C) in the secreted root exudates or secreting compounds that more effectively drive complete denitrification

(Giles et al., 2017). (Hu Li et al., 2016) found that higher and diversified LMW-C at seedling and tillering stages compared to other phenological stages in the rhizosphere and bulk soil could be due to high root meristem activity in those stages. So, it could be speculated that the high root meristem activity in the high complete denitrification-associated rice cultivars drove the complete denitrification variations. Further studies are required to confirm these findings.

4.5.3 Rice genotype effects on partial denitrification (N_2O emission)

In this rice screening study, rice genotypes with high root and shoot biomass reduced N_2O emission by increasing C: NO_3^- ratios in the fertilised paddy soil (Table: 4.4.4). The higher rice plant biomass reflects better nitrogen uptake efficiency (NUE) and limits nitrification and denitrification in flooded soil (Yang et al., 2017). Indeed, these rice genotypes push more carbon into the soil as root exudates due to high root biomass(Yahai Lu et al., 2002). However, the interaction between the denitrifier communities varied with specific rice genotypes, thus facilitating varied N_2O emissions among tested rice genotypes (Fig: 4.5.1). The low N_2O emission group marked in green (Fig: 3.4.2) reduced N_2O emission by limiting the total denitrification process except for rice cultivars R3, R6 and R9 (Fig: 3.4.4). There may be a number of mechanisms that drive this observation with further experimentation needed to dissect which one or which combination drive lower emissions. These include inhibition of the denitrification, oxygenation status, and change in the C profile, thus affecting the ratio of N_2O and N_2 emission. Suggesting those rice cultivars may inhibit denitrification through the secretion of secondary metabolites like biological nitrification inhibition (BNI) (Bardon et al., 2014) as discussed above. In the rhizosphere compartment of the lower N_2O emitter, the denitrification process was limited due to oxygenation from the rice root (Fig: 4.5.1). A different pattern was observed in lowering the N_2O emission in rice cultivars R3,R6 and R9 discussed earlier. Instead of limiting the denitrification process, these two rice cultivars increased N_2O reduction to N_2 might be enhancing NosZ clade I and/or NosZ clade II denitrifiers community through root exudation (Fig: 3.4.3) (Langarica-Fuentes et al., 2018b) perhaps only NosZ clade II activity.

In contrast, N_2O reduction into N_2 was suppressed compared to N_2O production in higher N_2O emitting rice cultivars indicated in red (Fig:3.4.4), even though the total denitrification process was limited. So, these rice cultivars may lower the ratio of NirS: NirK and, subsequently, NosZ clade I: NosZ clade II. Further studies are required to confirm the findings. I planned to analyse the community dynamics of the functional groups through a combination of quantitative PCR and metabarcoding using the soil samples collected from the rhizosphere and bulk compartments. However, I was unable to manage the experiments due to time constraints. The collected soil samples from the rice screening experiment are stored as snap-frozen samples in the laboratory.

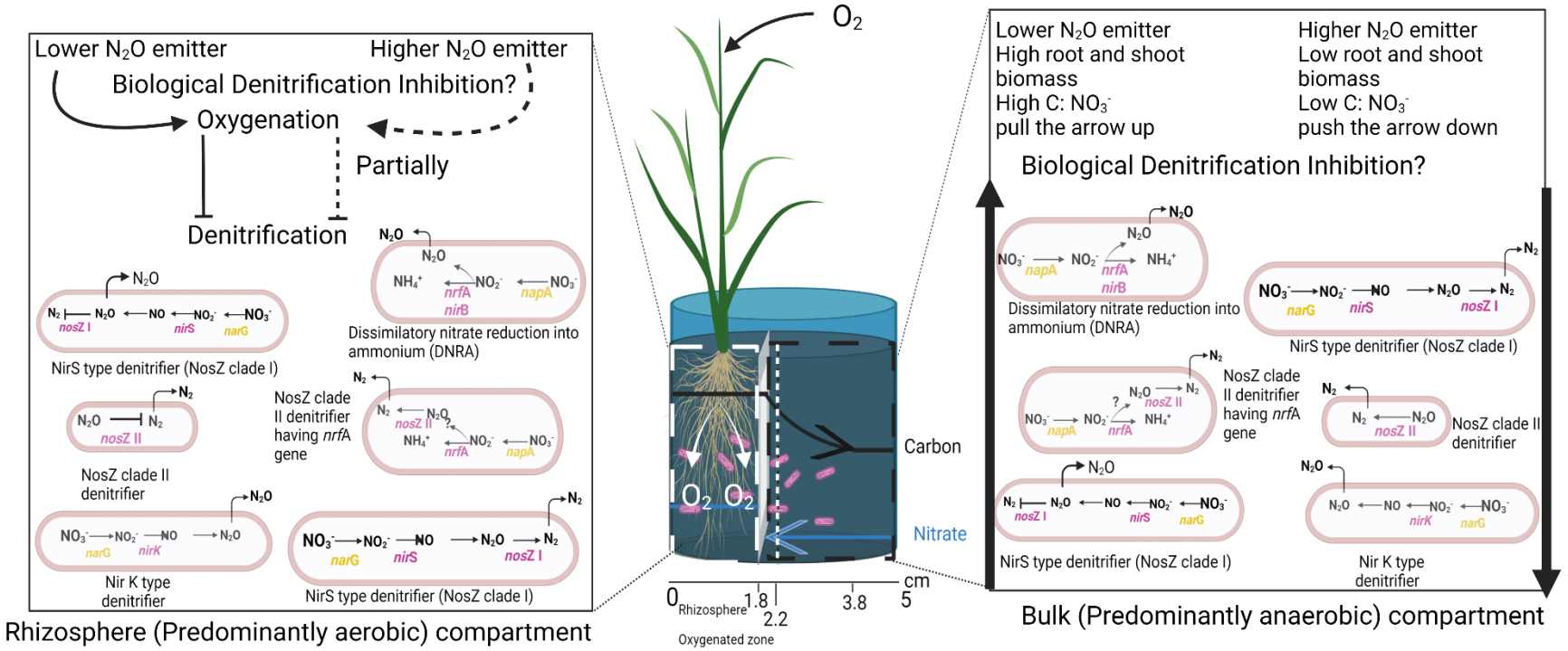

Fig 4.5.1: Hypothetical interaction of denitrifier and DNRA bacterial community with high and low N_2O emitting rice cultivars in the rhizosphere and bulk compartment of rice microcosm pot. Carbon from root exudates moves towards the bulk compartment with a gradient up to 2 cm from the barrier, and nitrate moves towards the rhizosphere due to the percolation of water and rice plant nutrient foraging. The positioning of bacteria in the cartoons is random. The thick black arrow at the two sides of the bulk compartment indicated denitrifiers and DNRA bacterial activity.

4.5.3 QTLs of rice genome involved in modulating denitrification

It was likely that different rice genotypes used different mechanisms to modulate the denitrifier community activity, and the GWAS analysis suggests that these mechanisms are directly linked to rice plant genetics. The same rice genome website that was used for nitrification variations was visited to explore the genetic relatedness associated with the denitrification modulation among the tested rice cultivars (Discussed in Chapter 3, Section 3.3.6). A similar methodology was followed to identify the loci within ±10 kbp of the top-ranked SNPs from the three GWAS outputs (Complete denitrification, Partial denitrification and ratio of partial and total denitrification) and summarised in the tables (Table: 4.4.4) (Table: 4.4.5) (Table: 4.4.6), respectively.

4.5.3.1 Probable potential candidate genes associated with complete denitrification variations

OsJ_09870, OsJ_09871 and Os03g0210200 genes associated with 1st top-ranked SNPs annotated three types of Oryzacystatin, this phytohormone provides immunity to rice plants by inhibiting extraneous cysteine proteinase (Premachandran & Srinivasan, 2023). Cytochrome P450 superfamily protein annotated with LOC_Os03g12660.1 based on GWAS analysis. This protein has a 94.47% similarity with Steroid (22S)-hydroxylase encoded from the CYP90B2 gene in **rice,** catalyses the C22-alpha-hydroxylation step in brassinosteroid biosynthesis, which is the rate-limiting step in this biosynthetic pathway (Sakamoto et al., 2006). Brassinosteroid can reduce rice root growth by reducing root meristem activity (Jantapo et al., 2021). ORF OsI_32887 and OsWRKY62, annotated with LOC_Os10g09820.1 and LOC_Os09g25070.1 loci, are involved in rice root meristem activity. ORF OsI_32887 encodes a NAC domain-containing protein (No apical meristem protein) (Kikuchi et al., 2000). OsWRKY62 is a salicylic acid inducible repressor that represses redox and ROS scavenging-related genes maintaining root mitotic activity by preventing ROS accumulation (Xu et al., 2017). Calcium/calmodulin-dependent protein kinases are involved in signal transduction in plants. In rice, calcineurin B-like protein-interacting protein kinases (CIPKs) involve in transcriptional responses to various abiotic stresses (e.g. drought, salinity, cold). CIPK16 annotated with LOC_Os09g25090.1 locus upregulation reported in salinity stress and induced by ABA and polyethene glycol (PEG) (Xiang et al., 2007).

4.5.3.2 Probable candidate genes associated with N_2O emission variations

OsJ_13920, ARD4, and MTN26L3 genes were found as QTLs for N_2O emission variations among the tested rice cultivars. OsJ_13920, annotated with a 95.14 % similarity, was found to be an OsFBX120- F-box domain-containing protein. F-box proteins play a crucial role in the controlled degradation of cellular protein through the ubiquitination process and might be involved in lysigenous rice aerenchyma formation. Higher levels of aerenchyma formation in the rice roots may oxygenate the rhizosphere more, potentially limiting denitrification near the root (Jain et al., 2007; Kawai et al., 1998). Indeed any fluctuation would affect the balance in N_2O production and consumption as it would affect the balance between C and O levels in the rhizosphere as changing aerenchyma levels could drive high flux and partial or complete denitrification. Rice cultivars with less aerenchyma in the root cortex might limit the denitrification partially, which could facilitate temporal N_2O emission from the rhizosphere (Fig: 3.3.1). *OsARD4* gene annotated with LOC_Os10g28360.1 associated with lone SNPs (8^{th} SNP rank) resided in chromosome 10 (Fig: 4.4.6). Lower N_2O emitting rice cultivar might increase LMW-C in their root exudates by increasing root biomass with the upregulation the *OsARD4* gene because this gene is involved in promoting secondary root architecture associated with root architecture development (Ramanathan et al., 2018). OSJNBb0006L01.5 gene from LOC_Os04g10400.1 annotated an electron transfer flavoprotein subunit beta, with 96.05 % similarity, used as an alternate electron source of carbohydrate substrates for respiration in plants under environmentally stressed conditions or in its developmental stage (Araújo et al., 2011; Yang et al., 2022). So, it could be speculated that lower N_2O-emitting rice cultivars might counterbalance C and O shortage by upregulating the gene to maintain respiration. MTN26L3 gene encodes MtN26 family protein precursor with antimicrobial activity, which might be a potential biological denitrification inhibitor secreted from the rice roots. So, the upregulation or downregulation of any of these three genes might be associated with the N_2O emission variations.

4.5.3.3 Probable candidate genes associated with the ratio of partial and total denitrification variations

The ratio of partial and total denitrification determines the emission of N_2O from the soil. OSJNBb0006L01.5 gene was also associated with SNPs of ratio GWAS result output. CYP99A2 gene annotated from LOC_Os04g10160.1 and the PHT1-4 gene annotated from LOC_Os04g10750.1 might be potential candidate genes that were associated with the ratio variations among the tested rice cultivars. CYP99A2 annotated Cytochrome P450 99A2 protein with 92.86 % similarity, and PHT1-4 annotated (OsPT4) that is probable inorganic phosphate transporter 1-4 with 94.98 % similarity. Cytochrome P450 99A2 is involved in the biosynthesis pathway of momilactone, a diterpenoid phytoalexin with antimicrobial activity (Shimura et al., 2007). Procyanidins, a flavonoid molecule, was found in the *Fallopia* spp plant (Bardon et al., 2014) that limits denitrification by inhibiting the membrane-bound NO_3 reductase denitrifier community. A field experiment using lettuce plants in upland agricultural soil reported that procyanidins limited potential denitrification activity by reducing the NirS and NirK denitrifier communities (Galland et al., 2019). The R83, the lowest N_2O-emitting rice cultivar, might limit denitrification by upregulating the CYP99A2 expression. The rice cultivars R3, R6 and R9 might scavenge more P for their growth by upregulating the expression of OsPT4 (inorganic phosphate transporter). Plants likely increase carboxylate exudation containing phosphatases, nucleases and various organic acids while uptaking inorganic P from the soil (Aziz et al., 2011; Huffman & Halloran, 2001; Pearse et al., 2006). So, root exudates of these three rice cultivars might be enriched with LMW-C that enhanced N_2O reduction by nitrous oxide reductase activity.

4.6 Concluding remarks

Evidence showed that rice plants reduce N_2O emissions from fertilised paddy soil by decreasing N_2O production by limiting NirS and NirK denitrifier activity or increasing N_2O reduction by enhancing NosZ clade I and NosZ clade II activity. The modulation of the denitrifier community varied among the tested rice cultivars due to genetic variation. So, manipulating rice plant genetics or selecting rice breeding are potential strategies to control N_2O emissions from rice cultivation. However, the linkages and potential mechanisms are highly speculative and further work are

required to confirm those probable candidate genes associated with N_2O emission variation among the tested rice cultivars. A Metabolomics study using significantly varied N_2O-emitting rice lines might give better insight into the findings. A whole genome sequence or segment of chromosomes based on the GWAS results of high and low N_2O-emitting rice cultivars might help identify the genes that triggered the N_2O emission variations. Further confirmation is also needed by transcriptomics analysis to understand the expression of those genes, either upregulation or downregulation, associated with the N_2O emission variation. Collected soil samples from the study were stored as snap-frozen, and community analysis from the collected soil samples might also help to understand the findings.

Chapter 5: Does the rice plant have the genetic ability to regulate anammox in the paddy soil?

5.1 Introduction

5.1.1 Anammox is a hidden gaseous N_2 lost process in paddy soil

Rice is an important agricultural crop, feeding over 50% of the world's population (Fukagawa & Ziska, 2019). According to FAO, ~800 million tons of rice were produced in 2021 using 165 million hectares of land, which was ~12 % of total agricultural land. 1994 (Chapter 1, Fig: 1.1). If fertilised by the IRRI recommended rate (130 kg N/hectare) this would result in the addition of approximately 21.45 million tons of N-fertilisers. (Yu et al., 2022) mentioned in their review that nitrogen uptake efficiency (NUE) in rice is low, only 42%. So, it could be assumed that less than half of the applied N was accumulated in rice biomass that was used for rice cultivation in 2021. Unutilised N by rice plants from paddy soil is lost through ammonia volatilisation, leaching, runoff, and gaseous loss as N_2O (potent greenhouse gas) and N_2. Rice is typically grown in lowland paddy soil, maintaining flooded conditions till harvesting, making the rice fields unique agroecosystems and anthropogenic wetlands and exacerbating gaseous loss through microbial anaerobic respiration process (Discussed in Chapter 2, Section: 2.1.1) (Li *et al.,* 2009)(Kögel-Knabner et al., 2010). Gaseous loss as N_2 contributes 38% to applied N-fertiliser in paddy soil (Nie et al., 2019). Until anammox was discovered (Mulder et al., 1995; Strous et al., 1999; Van De Graaf et al., 1996), denitrification was thought to be the only microbial process resulting in gaseous N loss to the atmosphere (Vitousek & Howarth, 1991). Anaerobic ammonium oxidation, anammox, is predominant in marine ecosystems, freshwater ecosystems and interfaces between land freshwater, contributing 20-80 % in total N_2 emission (Nie et al., 2019). In paddy soil, 4–37% N_2 is lost through anammox, depending on the depth of the soil (Zhu et al., 2011).

5.1.2 Anammox bacteria

Anaerobic ammonium oxidising (anammox) bacteria are obligate anaerobes, and as chemoautolithotrope can fix CO_2 for their growth by the oxidation of ammonium coupled to nitrite reduction (Burford & Bremner, 1975; C., 1982; Kartal et al., 2013; Strous et al., 1999). Anammox bacteria carry a cytochrome cd1nitrite reductase homologous to *nir*S to reduce nitrite into nitric oxide (Fülöp et al., 1995). Ammonium is then anaerobically oxidised by hydrazine synthetase (the key enzyme for the pathway) with nitric oxide and converted into N_2 via an intermediate, hydrazine

(N_2H_4), through anammox (Discussed in Chapter 1, Section 1.3.4). All five identified genera in the phylum *Planctomycetes*: *Candidatus* Brocadia, *Candidatus* Kuenenia, *Candidatus* Anammoxoglobus, *Candidatus* Jettenia and *Candidatus* Scalindua that are known to be capable of Anammox have been found in paddy soil (Jetten et al., 2009; J. Wang & Gu, 2013; G. Zhu et al., 2011). Anammox bacteria solely depend on other N-cycling processes for NO_2^-, transiently available in the paddy soil, to oxidise NH_4^+ because they lack nitrate reductase genes except one anammox bacteria, either *nap* or *nar* (Zhu et al., 2011). *Kuenenia stuttgartiensis*, an anammox bacteria reported in the paddy soil, does not need to rely on either NH_4^+ or NO_2^- as it has the DNRA capability, suggesting it can reduce NO_3^- into NH_4^+ via NO_2^- as the intermediate followed by the anaerobic oxidation of produced NH_4^+ and NO_2^- (Kartal et al., 2007; Sato et al., 2012).

5.1.3 Rice rhizosphere modulates anammox by regulating soil abiotic factors in paddy soil

The coexistence of oxidized (NH_4^+) and reduced (NO_2^-) N compounds is a prerequisite for anammox; as a result, aerobic/anaerobic interfaces provide suitable habitats for anammox. So, the rice rhizosphere and its adjacent oxic/anoxic interface with the bulk soil in flooded paddy is a recognised hotspot for anammox bacteria where N compounds are exchanged easily due to other simultaneous N-cycling processes (e.g., nitrification, denitrification and DNRA) (Zhu et al., 2010). Anammox bacteria depend on other N-cycling processes for NO_2^-, transiently available in the paddy soil, to oxidise NH_4^+. Anammox organisms typically lack the nitrate reductase gene, except for *nap* or *nar* (Zhu et al., 2011). *Kuenenia stuttgartiensis*, an anammox bacteria reported in the paddy soil, does not need to rely on either NH_4^+ or NO_2^- as it has the DNRA capability, suggesting it can reduce NO_3^- into NH_4^+ via NO_2^- as the intermediate followed by the anaerobic oxidation of produced NH_4^+ and NO_2^- (Kartal et al., 2007; Sato et al., 2012).

The abundance of anammox bacteria varied in paddy soil at different phenological stages of rice due to root exudation variations (Hu Li et al., 2016). Increased anammox activity was measured in the bulk soil than in the rice rhizosphere soil due to oxygenation (Xu et al., 2021). In contrast, opposite results were observed when the potential rate of anammox was measured due to root exudations (Nie et al., 2015). So, it is essential to separate anammox from denitrification in the fertilised paddy soil to fully understand gaseous N-loss because both processes contribute to N_2

emission. Anammox activity was higher in the high nitrification and denitrification-associated rice cultivar (Chapter 2, Fig: 2.3.4A). Indeed, significant nitrification and denitrification variation was observed among the tested rice cultivars, and anammox depends on both processes. So, I hypothesised that there would also be anammox rate variation among the tested rice cultivars.

5.2 Aim and Objectives

To test the hypothesis, I aimed to dissect the source partitioning of emitted total N-N_2 between denitrification and anammox by applying the equation I derived earlier while analysing the N-cycle dynamics. There were two main objectives of this study:

1. Assessing variation in anammox rate within the rice germplasm selection by comparing the ^{15}N signature of emitted N_2O and N_2 from rice microcosms.
2. Determining the quantitative trait loci (QTLs) to detect probable candidate genes in the rice genome associated with the anammox rate variations applying a Genome-Wide Association Study (GWAS) if variations are anticipated among the tested rice cultivars.

5.3 Methodology

5.3.1 Plant growth and sampling

A common microcosm experiment was used for plant screens as described in Chapter 3 (Section: 3.3) (Fig: 3.3.3). Briefly, a microcosm was established with bulk soil and rhizosphere compartments (33%:66%) using a divider with 30um mesh. The microcosm was packed with paddy soil and rice lines grown under standard agronomic fertilisation rates with an unplanted control. Samples were taken after the second fertilisation in which the nitrate was supplemented (4.67%) with ^{15}N nitrate. During sampling, gas samples were taken, and enrichment of N_2 emissions was assessed by isotope ratio modelling to partition gas between complete denitrification and anammox; the method is discussed in detail in Chapter 2 (Section: 2.3.12.4 and 2.3.12.4.1). Briefly, N_2 derived from complete denitrification is equivalent to the $^{44}N_2O$:$^{45}N_2O$:$^{46}N_2O$. Meanwhile, anammox-derived N2 will dilute this pool, and the N derived from ammonium will be unlabeled. Chapter 3 (Section 3.3.7) described statistical analysis using

R Studio version 4.0.2 (R Core Team, 2022). GWAS analysis was performed as described in Chapter 3 (Section: 3.3.5). A similar methodology was followed to identify the loci within ±10 kbp of the top-ranked SNPs from the GWAS output (Chapter 3, Section: 3.3.6).

5.4 Results

5.4.1 Anammox and complete denitrification rate in planted and unplanted microcosms

Total N-N_2 emission significantly varied between the planted and unplanted microcosms and between the N-N_2 emitting processes, anammox and complete denitrification, with no interaction between plant and N-N_2 emitting processes (Table:5.4.1). The unplanted microcosms maintained significantly higher rates of both processes with anammox higher than denitrification (346±9.51 ng N-N2/g dry weight soil/hour, and complete denitrification rate, 257±7.17 ng N-N_2/g dry weight soil/hour) overall and particularly in the unplanted pots (Fig 5.4.1).

Table 5.4.1: Two-way (Type II) Anova results for the rice plant effects on N-N_2 emission in ng N/g dry weight soil/hour through denitrification and anammox from planted soil (n=332) and unplanted soil (n=4) at the significance levels' ***' 0.001 '**' 0.01 '*' 0.05 '.' 0.1.

Source of variation: Total N-N_2 emissio	**Sum Square**	**Df**	**F-value**	**Pr(>F)**	**Significance code**
Presence of rice plant (R)	1245330	1	45.7112	2.727e-11	***
N-N_2 emitting processes (N)	1569016	1	57.5924	9.424e-14	***
R x N	30164	1	1.1072	0.293	

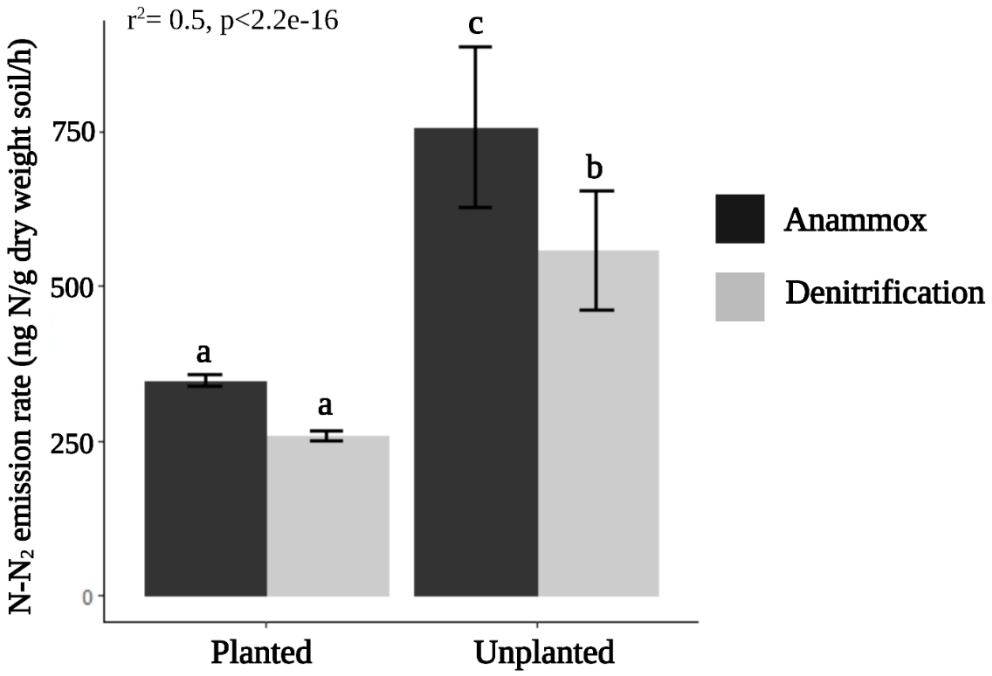

Fig 5.4.1: Mean±SE from two-way (Type II) ANOVA of N-N_2 emission rate in ng N/g dry weight soil/hour by denitrification and anammox of unplanted soil (n=4) and planted soil (n=332). The letters indicated a significantly different group (r^2= adjusted residual error, P<0.001, ANOVA, Tukey HSD).

5.4.2 Relationship between anammox and soil biotic and abiotic factors in planted microcosms

Spearman correlation matrix analysis was performed to understand the inter-correlation between measured N-cycle processes and other measured soil biotic and abiotic factors in planted rice microcosms. Anammox was positively correlated with partial denitrification (r^2=0.327, P<0.001), complete denitrification (r^2=0.99, P<0.001), total denitrification (r^2=0.844, P<0.001) and ^{15}N atom % in N_2O (r^2=0.239, P<0.001). No statistical correlations were observed with other measured biotic and abiotic factors (Fig: 5.4.3).

5.4.3 Anammox variations among the tested rice cultivars

Anammox rate significantly varied (r^2=0.56, *p*=3.047e-15) among the tested rice cultivars ranging from 47.27 to 867.12 ng N-N_2/g dry weight of soil/hour. Rice genotypes associated with high complete denitrification (R4, R3, R5, R10, R6, R7, R11 and R135) supported high anammox (Fig: 5.4.2). In addition, rice genotypes (R128, R136 and R137) high partial denitrification associated rice cultivars supported high anammox. Though rice genotypes (R133, R119 and R25) with low partial and complete denitrification supported high anammox. In contrast, rice genotypes (R83, R108, R72 and R86) with low partial denitrification supported low anammox. The rice genotype R83 also supported low complete denitrification. Another low complete denitrification-associated rice genotype, R74, supported low anammox (Fig: 5.4.2).

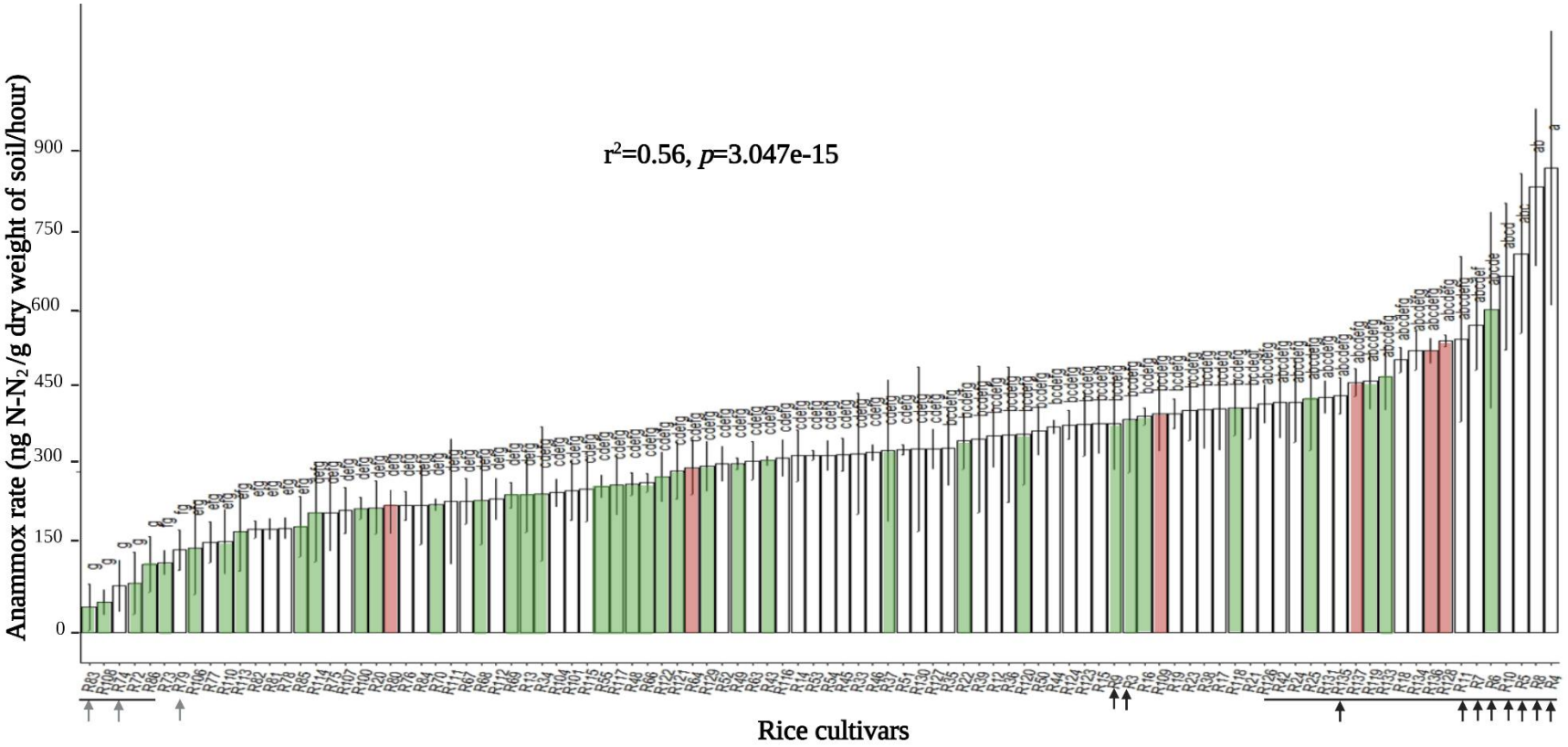

Fig 5.4.2: Mean±SE (n=4) from one-way (Type II) ANOVA of anammox rate in ng N/g dry-weight soil/hour of tested rice cultivars (n=98). Underlined rice lines indicated low and high anammox rice cultivars group. Rice cultivars associated with low partial denitrification were indicated by green-coloured bars, and rice cultivars associated with high partial denitrification were indicated by red-coloured bars. The letters indicated a significantly different group (r^2= adjusted residual error, P<0.001, ANOVA, Tukey HSD).

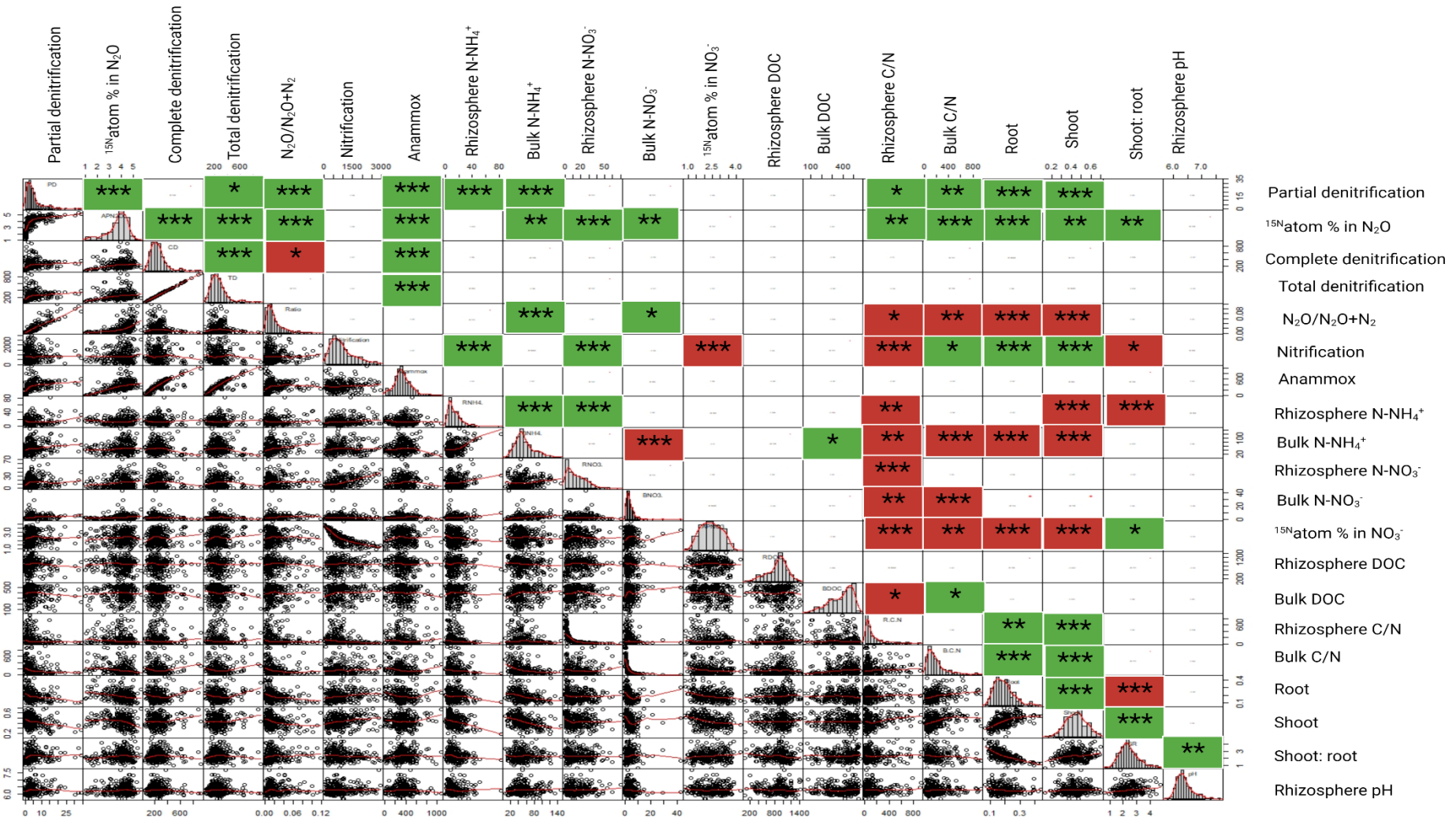

*Fig 5.4.3: Spearman correlation matrix analysis between all tested parameters from this study. The white box indicated no correlation, the green box indicated positive, and the red box indicated negative correlation at the significance level of ' ***' 0.001 '**' 0.01 '*' 0.05 '.' 0.1*

5.4.4 GWAS results for anammox variations as the phenotypic trait of tested rice cultivars

The GWAS analysis yielded a summary output file containing the most significant SNPs with the calculated major and minor allele effects. Manhattan plots were produced displaying significant single nucleotide polymorphisms (SNPs) associated with variation in anammox rate from the genome-wide analysis (Fig: 5.4.4). Genome order per chromosome was plotted on the X-axis against the −log10 of the p-values of SNPs on the Y-axis (Norton et al., 2018). The significant threshold limit indicated by the grey line for the SNPs associated with partial denitrification was measured at –log10 (6.5) for a false discovery rate (FDR) limit of 0.05 after generating a quantile-quantile (QQ) plot by plotting –log10 (expected p-value) and –log10 (observed p-value) on the X-axis and Y-axis respectively (Fig: 5.4.5) (Kaler & Purcell, 2019). SNPs associated with the complete denitrification rate significantly deviated from the null hypothesis (Grey straight line) outstandingly, suggesting less chance of being falsely positive (Fig: 5.4.5). The genomic inflation factor (known as λgc) value was 1.028 in the QQ plot, indicating that the model was well fitted with the complete denitrification rate phenotyping trait and –log10 of the p-values of most SNPs were uniformly distributed among the chromosomes means any bias occurred while modelling. Ten significant SNPs were observed above the FDR limit of 0.05 (Fig: 5.4.5), and details of the significant SNPs with identified loci as quantitative trait loci (QTLs) and annotated genes and protein and function from the Uniport Blast website (www.uniprot.org) summarised in the table (Table: 5.4.2).

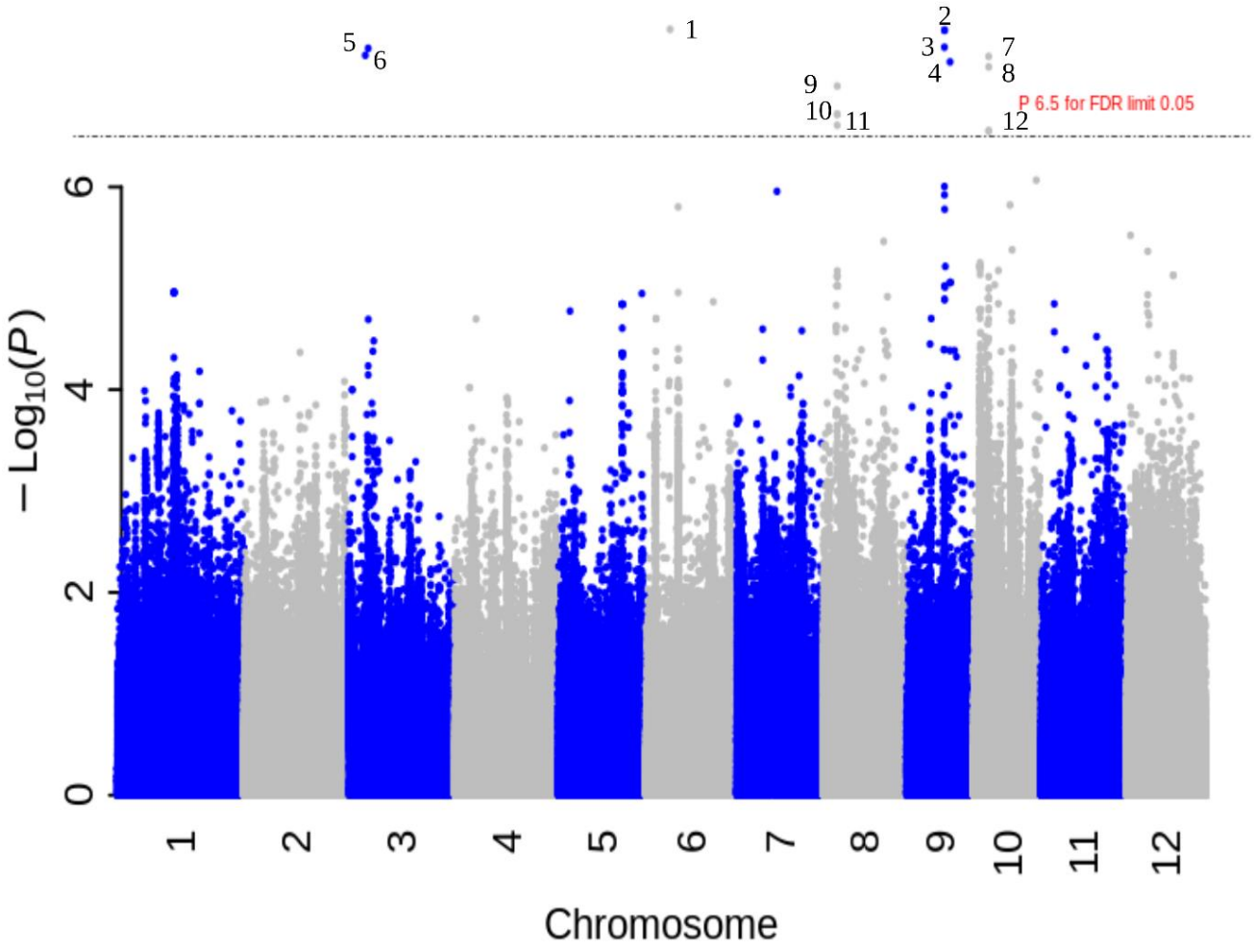

Fig 5.4.4: Manhattan plot from the GWAS analysis of SNPs in the chromosomes associated with anammox (N-N_2 emission) rate variations. Significant SNPs were above the grey dotted line, having $-Log_{10}(P) > 6.5$ for the FDR limit ($P<0.05$) marked with their rank number.

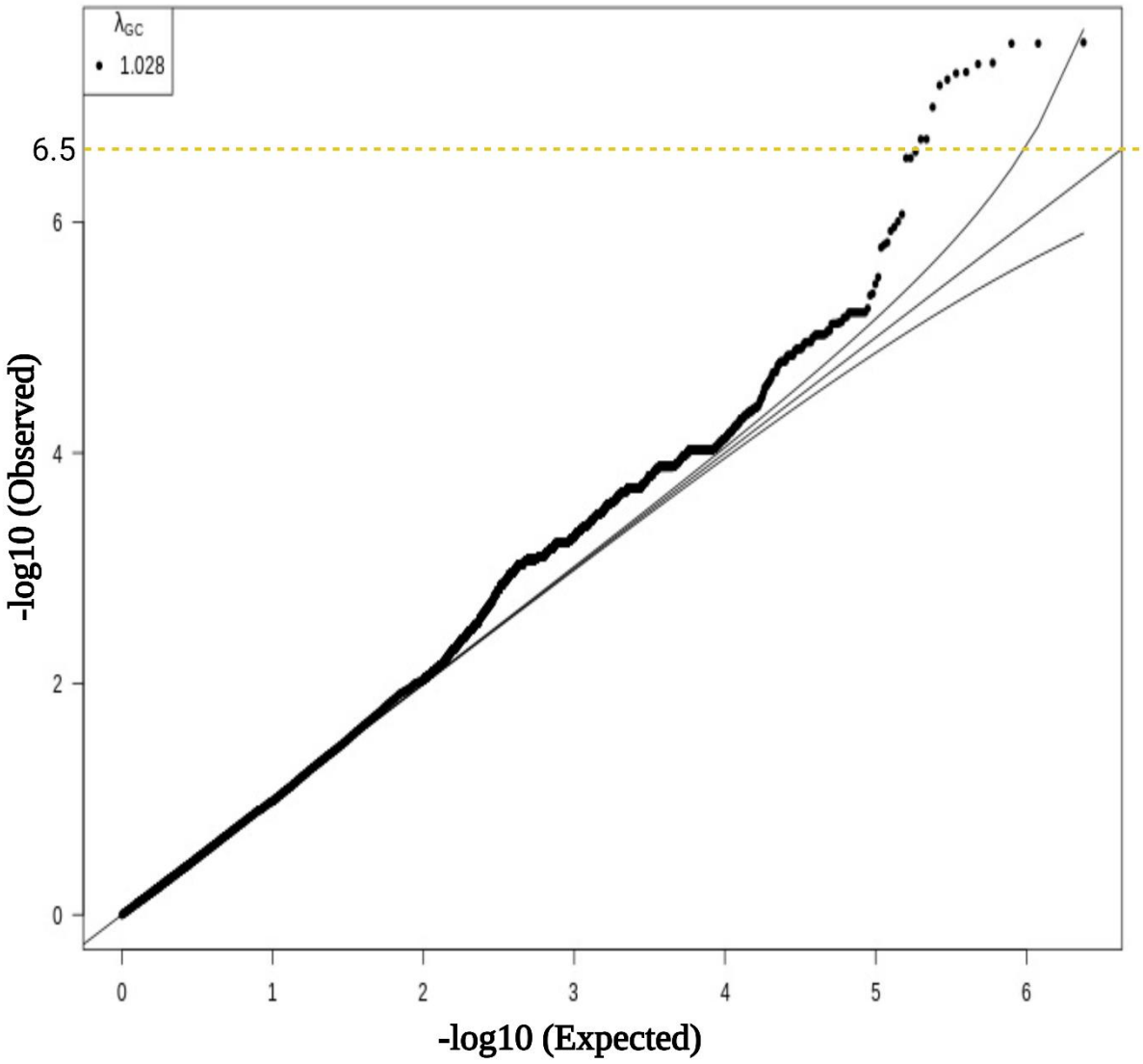

Fig 5.4.5: QQ-plot showing the distribution of the observed against the expected –log10 (*P*) for the SNPs of the rice genome associated with anammox (N-N_2 emission) rate variations, where the expected –log10 (*P*) under the null hypothesis were indicated by the straight grey line and observed values were indicated as the cluster of dots in black. The λ_{GC} at the left top corner, bounded by a box, indicated the genomic inflation of the model. The yellow dotted line indicated the SNPs threshold limit -log10(p)= 6.5 where observed and expected values were separated.

Table 5.4.2: Significant SNPs above the FDR limit (P<0.05) identified by the GWAS associated with the anammox rate variations among the tested rice cultivars, their location and position in the chromosome, -log10(P-value), and loci found within 10 kb upstream and downstream from the particular significant SNP in the rice genome, annotated gene and annotated protein and their function with similarity % from the http://rice.uga.edu website are mentioned in the table.

SNP rank	SNP name	Chr No.	Position	-log10 (P)	Locus name	Annotated gene	Annotated protein	Similarity %	Function
1	mlid0041514612	6	8387927	7.55	LOC_Os06g14790.1	OSJNBa0092H22.7	Ulp1 protease-like protein	100	peptidase activity
					LOC_Os06g14800.1		Expressed protein	NA	
2 & 3	mlid0064155385	9	13115747	7.55	LOC_Os09g21640.1	CIPK16	CBL-interacting protein kinase 16	93.42	calcium/calmodulin dependent protein kinases
	mlid0064155386		13115748		LOC_Os09g21650.1		Retrotransposon protein	NA	retrotransposon activity
					LOC_Os09g21660.1		Retrotransposon protein	NA	retrotransposon activity
4	mlid0064148632	9	13089525	7.38	LOC_Os09g21600.1	OSJNBb0015G09.8	OSJNBb0015G09.8 protein	93.15	retrotransposon activity
					LOC_Os09g21610.1	OSJNBb0086I08.6	Gag-pol	93.9	retrotransposon activity
5	mlid0018211001	3	6730958	7.37	LOC_Os03g12650.1		Retrotransposon protein	NA	retrotransposon activity
					LOC_Os03g12660.1	CYP90B2	Steroid (22S)-hydroxylase	94.47	brassinosteroid biosynthesis
6	mlid0018049836	3	5750805	7.30	LOC_Os03g11140.1	OSNPB_030209800	pleckstrin homology domain-containing protein-related taxo	91.2	nucleobase, nucleoside, nucleotide and nucleic acid metabolic process
					LOC_Os03g11170.1		Expressed protein	NA	uncharacterised
					LOC_Os03g11150.1	OsJ_09870	Oryzacystatin-9	100	cysteine proteinase inhibitor precursor

					LOC_Os03g11190.1	OsJ_09871	Oryzacystatin-7	84.62	cysteine proteinase inhibitor precursor
					LOC_Os03g11160.1	Os03g0210200	Oryzacystatin-6	89.38	cysteine proteinase inhibitor 6 precursor
					LOC_Os03g11180.1		Expressed protein	NA	uncharacterised
7	mlid00676759 27	10	5313635	7.25	LOC_Os10g09810.1	OSIGBa0157N01.6	RNA-directed DNA polymerase	93.55	retrotransposon activity
					LOC_Os10g09820.1	OsI_37448	NAC domain-containing protein	84.67	root meristem activity
					LOC_Os10g09830.1		Expressed protein	NA	uncharacterised
8	mlid00676732 69	10	5304063	7.18	LOC_Os10g09790.1		Retrotransposon protein	NA	retrotransposon activity
					LOC_Os10g09800.1		Retrotransposon protein	NA	retrotransposon activity
					LOC_Os10g09810.1		Retrotransposon protein	NA	retrotransposon activity
	mlid00548105 74	8	4731791	7.00	LOC_Os08g08260.1		Expressed protein	NA	uncharachtersied
	mlid00548108 18		4732469	7.00					
	mlid00548108 29		4732519	6.72					
12	mlid00676749 27	10	5311389	6.55	LOC_Os10g09800.1		Retrotransposon protein	NA	retrotransposon activity
					LOC_Os10g09810.1		Retrotransposon protein	NA	retrotransposon activity
					LOC_Os10g09820.1	OsI_37448	NAC domain-containing protein	85.48	root meristem activity
					LOC_Os10g09830.1		Expressed protein	NA	uncharacterised

5.5 Discussion

5.5.1 Rice rhizospheric effects on total N-N_2 emissions

In this study, total gaseous N_2 loss was significantly higher in unplanted microcosms than the planted ones, with a more than 2-fold increase. This is likely due to a combination of oxygenation of the rhizosphere and surrounding bulk soil due to radial oxygen loss (ROL) from roots limiting anaerobic respiration processes in the rhizosphere and adjacent bulk compartments in planted microcosms and higher inorganic N contents in these microcosms (Chapter 3, Fig: 3.4.1A). In unplanted microcosm pots, anammox contributed higher than that of denitrification to total N_2 emissions, even though anammox typically depends on denitrifiers for nitrite in anaerobic soil microsites. It seemed that due to CO_2 fixation capability as chemolithoautotrophs, anammox dominated over denitrification in unplanted soil; perhaps anammox bacteria used CO_2 released from denitrification respiration while performing anammox (Kartal et al., 2013). Furthermore, Due to the absence of plant inputs, the DOC: NO_3^- ratio was very low in unplanted pots (Fig: 4.4.1B) at 8:1, likely to encourage incomplete denitrification (Lycus et al., 2017). As stated in Chapter 4 (Fig: 4.4.1E), the ratio of partial and total denitrification (N-N_2O/N-N_2O+N_2), a truncation indicator, was significantly higher in unplanted soil from planted microcosms. Nitrite leakage from the denitrification pathway is likely to be used by anammox bacteria to oxidise NH_4^+. Additionally, there was no competition between nitrifiers and anammox bacteria for NH_4^+ due to nitrification inhibition in the unplanted soil (Chapter 3, Fig: 3.4.1B). Thus it seems likely that anammox bacteria are associated with denitrifiers rather than nitrifiers in the flooded paddy soil without plant presence.

Nevertheless, anammox and denitrification contributed equally to gaseous N_2-loss in the planted microcosms. Complete denitrifiers likely complete the pathway rather than truncate in the presence of low molecular organic carbons and also in a high C/N ratio (Described in Chapter 4, Section: 4.5.1). So, the quantity and types of organic carbon in the rice root exudates may affect the anammox process indirectly through nitrite supply as suggested by Shan *et al.*, (2018). Another possible reason might be the balance between their metabolism and respiration in the presence of LMW-C derived through root exudations in the bulk compartments. In the presence of LMW-C, anammox bacteria likely increase their biomass by incorporating that LMW-C rather than doing CO_2 fixation and respiration associated with less N_2 emission from the planted soil (Lawson et al., 2021; Shan et al., 2018).

5.5.2 Rice genotypes effects on anammox

Anammox bacteria likely depend on nitrification and denitrification for transiently available nitrite to oxidise ammonium. Anammox was observed higher in the high nitrification and denitrification associated rice cultivar (Discussed in Chapter 2, Section 2.5.4). Anammox was positively correlated with partial and complete denitrification in this rice screening experiment (Fig: 5.4.3). Anammox in the rice microcosms might be subordinated by denitrification due to nitrite dependency concerted with other results (G. Zhu et al., 2018). At the same time, in the oxic/anoxic interface in fertilised paddy soil, nitrification by ammonia oxidisers feed anammox by providing NO_2^- (L. J. Ding et al., 2019). Our study showed no relationship between anammox and rice rhizosphere nitrification (Fig: 5.4.3). So, it could be speculated that nitrite from nitrification might be oxidised before reaching the anaerobic soil microsites by nitrite oxidising bacteria (NOB) because NOB shares same niche with ammonia oxidisers. Rice cultivars, R83, might limit the anammox process by limiting/inhibiting denitrification. Rice cultivars associated with high partial (R128, R136 and R137) and complete denitrification (R4, R3, R5, R10, R6, R7, R11 and R135) might support anammox indirectly by encouraging denitrification. There was no association with denitrification and anammox in the rice cultivars R133, R119 and R25. The rice cultivar, R119, supported the second highest nitrification, and R133 supported similar nitrification in this microcosm experiment (Chapter 3, Fig: 3.4.2). So, nitrification might fuel the anammox in these two rice cultivars. However, no relationship was found between anammox with either nitrification and denitrification in the rice cultivar R25. Suggesting nitrite independency of anammox process. *Kuenenia stuttgartiensis*, an anammox bacteria reported in the paddy soil, does not need to rely on either NH_4^+ or NO_2^- as it has the DNRA capability, suggesting it can reduce NO_3^- into NH_4^+ via NO_2^- as the intermediate followed by the anaerobic oxidation of produced NH_4^+ and NO_2^- (Kartal et al., 2007; Sato et al., 2012). So, it could be speculated that rice cultivar R25 might support that type of unconventional anammox bacteria through root exudation. A soil slurry experiment found that in the presence of glucose and acetate, anammox bacteria outnumbered by denitrifiers (Shan et al., 2018).

5.5.3 Rice genetics involved in anammox rate variations among the tested rice cultivars

In this microcosm experiment, it was assumed that the key substrate (nitrite) for anammox bacteria was fed by denitrification and nitrification processes. So, GWAS output for anammox phenotypic traits among the rice cultivars might have resembled the GWAS output of these processes. Significant SNPs associated with GWAS output for the anammox phenotypic trait (Fig: 5.4.4) among the tested rice lines were found to be similar (but in a different order based on SNPs rank) to the complete denitrification phenotypic GWAS output (Chapter 4, Fig: 4.4.8). A similar methodology was followed to identify the loci within ±10 kbp of the top-ranked SNPs from the GWAS outputs summarised in the table (Table: 5.4.2). Significant SNPs associated loci found within the ±10 kbp genetic span and annotated gene and protein functions discussed in the previous chapter (Chapter 4, Section 4.5.3.1).

5.6 Concluding remarks

Rice plants can modulate anammox activity indirectly by regulating denitrification and/or nitrification in fertilised paddy soil. Anammox was found to dominate the N_2 loss process over denitrification in unplanted soil. Broadcasting application of N-fertiliser in the flooded paddy field may exacerbate gaseous N_2 loss by anammox because they can fix CO_2 or formate (Abundantly present in flooded paddy as microbial fermentative product) utilising the applied N. The anammox process was measured for the first time by using the isotope ratio between N_2O and N_2. Further studies are required to validate the model.

Chapter 6: General discussion

6.1 Microbial nitrogen loss and retention after the addition of fertilisation

In this study, four key aerobic and anaerobic nitrogen transformation processes of microbial N-cycle processes in paddy soil were measured simultaneously for the first time by applying the $^{15}N\text{-}NO_3^-$ stable isotope by the single rice microcosm experiment (Fig: 2.3.3). The Rice rhizosphere provides aerobic and anaerobic interfaces where these processes can coexist and are associated with nitrogen loss and retention after the addition of nitrogen fertilisers in rice paddies (Fig: 3.3.1). N_2-fixing cyanobacterial aggregates also provide similar aerobic and anaerobic interphases where reactive nitrogens are simultaneously transformed through these microbial processes. (Klawonn et al., 2015) measured these microbial nitrogen transformation processes by applying ^{15}N isotope pairing technique (Dalsgaard & Thamdrup, 2002; Nielsen, 1992) while different combinations of $^{15}N\text{-}NO_3^-$, $^{15}N\text{-}NH_4^+$, $^{14}N\text{-}NO_3^-$, and $^{14}N\text{-}NO_2^-$ as labelled and non-labelled N-compounds were used. Nevertheless, the applied combinations between labelled and non-labelled N-compounds were varied among incubated cyanobacterial aggregates to distinguish the microbial nitrogen pathways. In contrast, in this simultaneous microbial nitrogen transformation measurements, %5 ^{15}N atom % in NO_3^- as stable isotable, along with $^{14}N\text{-}NH_4^+$, was applied in the single rice microcosm. Nitrification and DNRA were measured by analysing the degree of ^{15}N atom % dilution and enrichment in NO_3^- and NH_4^+ pools, respectively, from the soil extracts of rice microcosms. Denitrification and anammox were measured by measuring the accumulation of N_2O and N_2 from the collected gas samples, incubating the same microcosms in the Kilner jar before distracting the microcosms. However, dissecting the processes was inevitable because both processes contribute to N_2 emission. ^{15}N stable isotope of both inorganic N with combinations are applied to dissect the processes by multiple incubations (Pandey et al., 2018a). During incubation, $^{15}N\text{-}NO_3^-$ with $^{14}N\text{-}NH_4^+$ was used to dissect complete denitrification and anammox (Thamdrup & Dalsgaard, 2002). However, $^{15}N\text{-}NO_3^-$ (~100 atom %) was applied and is currently followed while dissecting the complete denitrification and anammox (Long et al., 2013)(Bai et al., 2015)(Cheung et al., 2024)(Han et al., 2021)(Abbas et al., 2020). Nonenethesles, in this study, $^{45}N_2O/^{46}N_2O$:$^{29}N_2/^{30}N_2$ ratios were used to dissect the source partition of complete denitrification and anammox after applying only %5 ^{15}N atom % in NO_3^-. The sources of emitted $^{29}N_2$ and $^{30}N_2$ through complete denitrification are $^{45}N_2O$ and $^{46}N_2O$ derived from NO_3^- pool (as only $^{44}N_2O$ was produced from unlabelled NH_4^+ pool through nitrification). However, there was one possibility to derive $^{45}N_2O$ and $^{46}N_2O$ through nitrification if ammonified ^{15}N-

NH_4^+ nitrified, but that $^{15}N\text{-}NH_4^+$ needs to be diffused from anaerobic soil microsites to aerobic ones. In rice paddies, water might not be able to dislodge ammonified NH_4^+ from firmly attached clay particles in the soil. I have checked $N\text{-}NH_4^+$ recovery through water extraction after spiking a known amount of $N\text{-}NH_4^+$ in the paddy soil. A negligible amount of $N\text{-}NH_4^+$ was recovered through water extraction, whereas over 80% $N\text{-}NH_4^+$ was recovered through 2M KCl extraction (Supplementary 3). So, the ratio between $^{45}N_2O/^{46}N_2O$:$^{29}N_2/^{30}N_2$ is in equilibrium, and the ratio is 1. But the ratio is decreased by $^{29}N_2/^{30}N_2$ derived through anammox because $^{14}N\text{-}NH_4^+$ (applied inorganic N) and ammonified $^{14}N\text{-}NH_4^+$ and $^{15}N\text{-}NH_4^+$ might be oxidised anaerobically either by $^{14}N\text{-}NO_2^-$ or $^{15}N\text{-}NO_2^-$ by anammox process.

The DNRA rate was measured earlier by considering the negligible microbial immobilisation process rate after applying both inorganic forms of N (Pandey et al., 2018b). A congruent result was found, and nitrogen retention through DNRA was found insignificant in this study. Denitrification dominated the nitrogen loss process and was 100 times more prevalent than DNRA (Fig: 2.4.5A and 2.4.6A). Nitrate reduction into ammonium through the DNRA process dominates long-term low-nitrogen fertilised rice paddies (Pandey et al., 2019). In rice paddies, nitrogen addition decreases BNF and DNRA processes by altering the C/NO_3^- ratios (Pandey et al., 2018a). No rice genotypic effects on nitrogen retention were observed due to the limitation of the DNRA process in fertilised paddy soil (Fig: 2.4.6A), but significant compartment effects were observed (Fig: 2.4.6B). DNRA rate was found to be significantly higher in the rhizosphere than in the bulk compartment. However, the key microbial nitrogen loss processes (nitrification, denitrification, and anammox) significantly varied among the tested rice cultivars with interactions. The rice cultivar associated with high denitrification had been found to have high anammox.

6.2 Rice genotype effects on interactions between microbial N-cycle processes

The single rice screening experiment demonstrated that the fertilised paddy soil's microbial nitrogen cycle processes (e.g., nitrification, denitrification and anammox) varied significantly among the tested 98 rice cultivars (discussed in Chapters 3, 4 and 5). However, no interaction between nitrification and denitrification was found in the rice screening study (Fig: 3.4.3). In an ideal rice cultivation system, urea-based nitrogen fertilisers are used after hydrolysis of urea into NH_4^+, and nitrification converts NH_4^+ into NO_3^- that is used by denitrifiers. So, nitrification influences denitrification by providing a substrate. Applying urease inhibitors with urea

fertilisers in alkaline paddy soil prevented denitrification by reducing NH_4^+ availability, thus limiting activity (Meng et al., 2020). (Yang et al., 2017) found a significant positive relationship between nitrification and denitrification after applying only NH_4^+ as the nitrogen source while doing the rice microcosm experiment. Nevertheless, I used NH_4NO_3 as a nitrogen source, so both processes were independent in the rice microcosms. However, the earlier N-cycle dynamics experiment using two cultivars observed a significant positive relationship between nitrification and denitrification (Chapter 2).

The same method was followed for N-cycle dynamics and rice screening experiments except for the microcosm pot design (Fig: 3.3.1). In the N-cycle dynamics experiment, microcosm pots were largely aerobic, and nitrification happened even in the bulk compartments due to diffused oxygen from rice roots (Fig: 2.4.A). As a result, similar residual [NO_3^-] was found in the rhizosphere and bulk compartments of microcosm pots used for the N-cycle dynamics experiment, whereas residual [NO_3^-] was significantly varied between the compartments of designed pots used for the rice screening experiment. The residual [NO_3^-] in the bulk compartment was found to be significantly lower than in the rhizosphere compartment (Fig: 3.4.1A). The NO_3^- from nitrification potentially fueled denitrification when NO_3^- derived from nitrification diffused into the narrow hypothetical anaerobic zone in the bulk compartment, eliciting higher denitrification in the high nitrification rice cultivar. (Zhang et al., 2022) using a limited number of rice lines found that increased rates of nitrogen fertlisation minimised rice genotypic effects on the interaction between nitrfication and denitrfication. However, partial denitrification was reciprocally correlated with DOC: N-NO_3^- ratios of both compartments and nitrification showed a similar relationship with the ratios in the rhizosphere of the rice screening experiment, indicating indirect effects of nitrification on denitrification (Table: 4.4.4 and Table: 3.4.3). Rice plants might alter the ratios either through changing carbon flux in root exudations, taking up NO_3^- and/or nitrification. The nitrified NO_3^- might lower the ratios and thus could facilitate partial denitrification in the rice microcosms. Indeed, there was no significant interaction between nitrification and anammox processes, but a significant positive correlation between anammox and denitrification was observed among the tested rice cultivars (Fig: 5.4.3). Anammox bacteria depend on nitrification and denitrification due to NO_2^- dependency as they lack nitrate reductase. Denitrification fed anammox process in the rice microcosms of rice screening experiment by providing NO_2^-. Nitrite oxidising bacteria might consume NO_2^- produced by ammonia oxidisers in the rhizosphere before diffusion into bulk compartments. The interaction between nitrite oxidising bacteria and anammox bacteria in the

oxic/anoxic interface of rice rhizosphere is yet to be explored. So, no interaction between nitrification and anammox was observed. The applied NH_4^+ was abundantly present in the bulk compartments due to a lack of plant uptake and inhibition of nitrification since the bulk compartment was largely anaerobic (Fig: 3.4.1). As a result, Anammox rate was found to approximately double in the unplanted microcosm compared to planted microcosm and significantly higher than the denitrification (Fig: 5.4.1). Whereas, anammox and complete denitrification contributed equally in N_2 emission in the rice microcosms and higher denitrification associated rice cultivars had high anammox. Rice genotypic effects on the interactions between measured microbial nitrogen transformations were analysed using PCA analysis, which is discussed below.

The selected 98 rice cultivars originated from South-East Asia, including 3KG, Rice Diversity Panel 1 (RDP1), Rice Diversity Panel 2 (RDP2), and Bengal and Assam Aus Panel (BAAP) comprising seven subpopulation indica 1, indica2, indica3, admixed indica, tropical japonica, admixed japonica and aus. A PCA analysis was done by randomly taking 50K SNPs from the available genomic data set (Fig: 6.1).

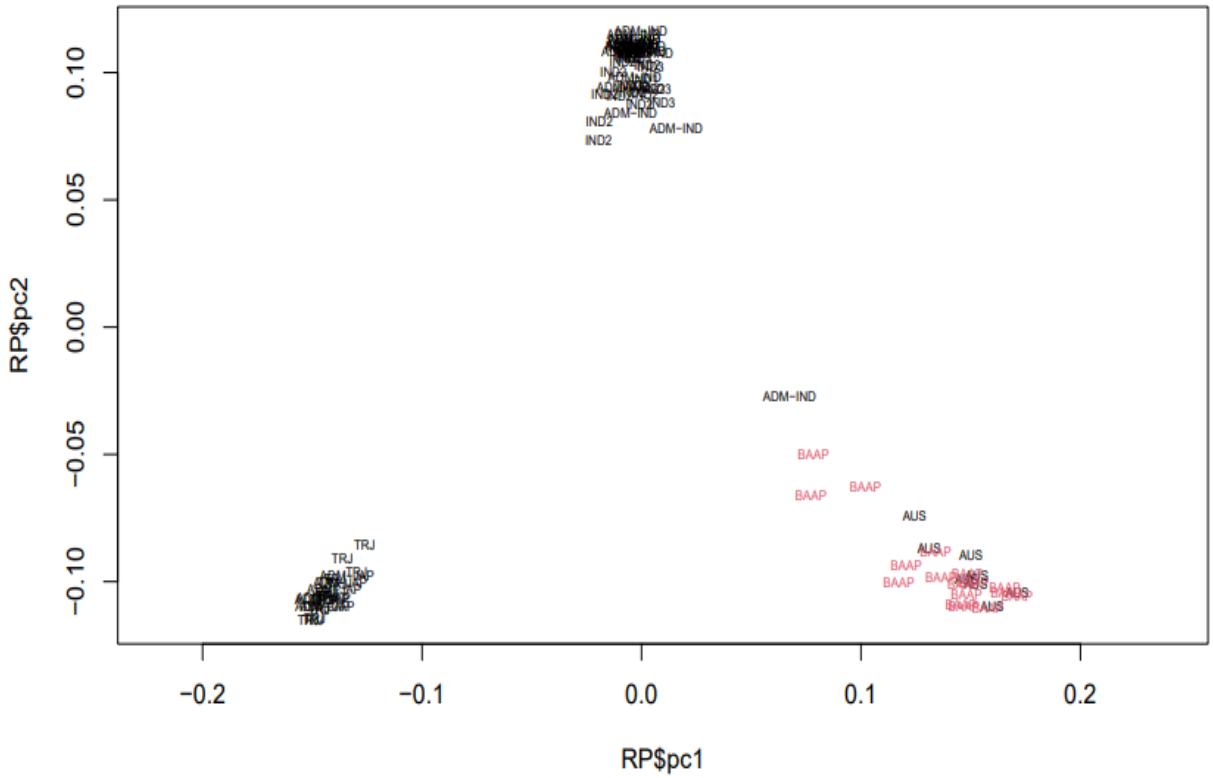

Fig 6.1: PCA analysis of 98 selected rice cultivars from merged RICE-RP and BAAP SNPs dataset. Tested rice cultivars included tropical japonica (TRJ), indica (IND1, IND2 and IND3), aus (AUS), admixed indica (ADM-IND), admixed japonica (ADM-JAP) and Bengal and Assam Aus Panel (BAAP) subpopulation.

Tested rice cultivar genotypes were clustered within three groups according to their genetic relatedness. The rice genotypes in the aus subpopulation selected from 3KG and RDP grouped distinctly with the BAAP panel. BAAP panel only includes AUS subpopulation that originated from Bangladesh, Bengal and Asam in India (Norton et al., 2018)

However, the tested rice genotypes, including indica, japonica, and aus subpopulations, were clustered based on measured N-cycling processes (Fig: 6.2, Supplementary 2). Suggested that modulating the N-cycling associated microbial community was not found variety specific; rather, it depends on individual rice genetics. A natural variation between indica and japonica in NRT1.1B gene involves NO_3^- uptaking and sensing NO_3^- in the soil. These two varieties were reported to recruit distinct N-cycle-associated microbiota in the rhizosphere due to the variations (Jingying Zhang et al., 2019). This study observed no variations after measuring nitrification, denitrification and anammox. Molecular analysis of collected rhizosphere soil samples among the indica and japonica will further confirm the findings.

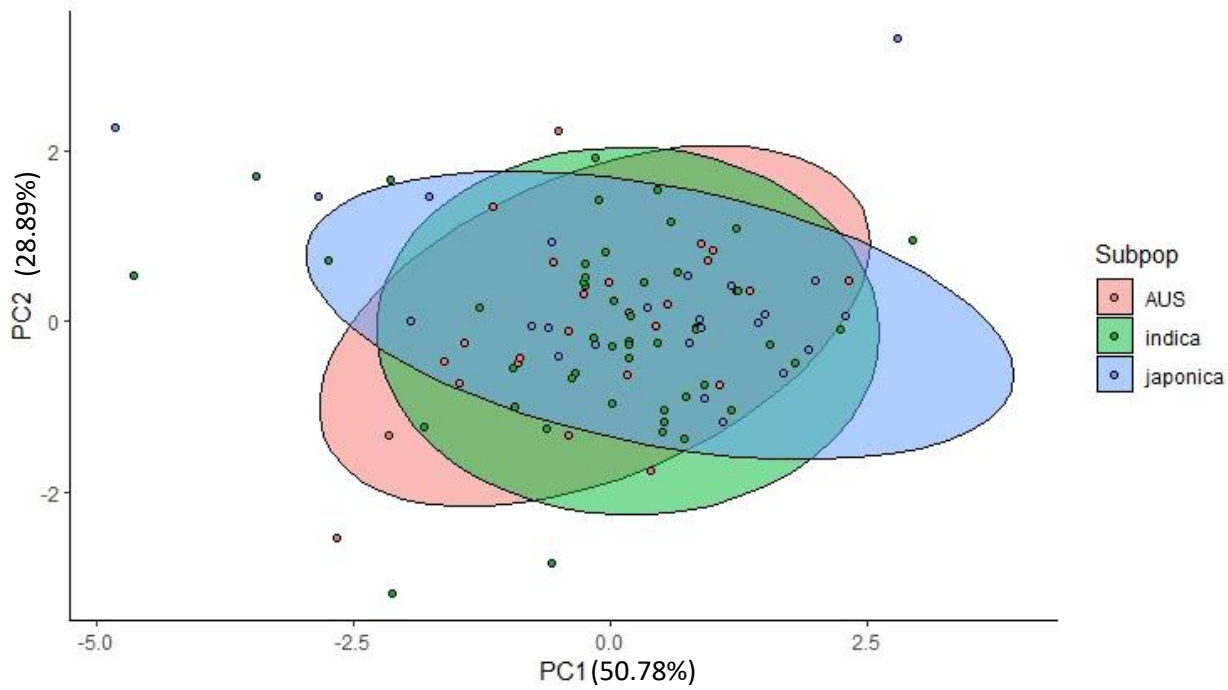

Fig 6.2: PCA analysis of 98 tested rice cultivars, including indica, japonica and aus, based on measured N-cycle processes.

6.3 Ideal rice genotypes

An ideal rice genotype in this study context would perform better in different agricultural systems (e.g., continuous flooding, (AWD) alternate wetting and drying) with minimum applied nitrogen loss and N_2O emission. It can also withstand limiting conditions such as nitrogen-limited and drought conditions without compromising yield. An ideal genotype selection based on multiple traits is pivotal for selection plant breeding. So, an ideal rice genotype and also outstanding rice genotypes with particular traits are screened from the tested 98 rice genotypes by yield*trait (GYT) biplot where N-N_2O emission as greenhouse gas (GHG) index, gaseous nitrogen loss as N-N_2 emission through complete denitrification and anammox, solid nitrogen loss as N-NO_3^- through nitrification, pH in the rice rhizosphere, average residual applied nitrogen ([NH_4^+] and [NO_3^-]) of rhizosphere and bulk soil and the ratio of dissolved organic carbon (DOC) and N-NO_3^- are considered as traits (Yan & Frégeau-Reid, 2018). In this study, total dry weight biomass was used as a proxy for yield as the experiment was harvested on the second fertilisation point and, therefore not grown to maturity. The GYT biplot ranked rice genotypes graphically based on their levels in combining yield with measured traits (Fig:

6.3). It also showed their trait profiles, i.e., their strengths and weaknesses. As target traits, N_2O emission and gaseous and solid nitrogen loss should be reciprocally correlated with yield in an ideal rice genotype. So, inverse results of N-N_2O emission rate, N-N_2 emission rate through complete denitrification and anammox, and nitrification rate against the rice genotypes were considered target traits. The genotype ranking biplot compares the tested 98 rice genotypes with the "ideal" rice genotype (Fig: 6.3). The nearest rice genotype from the small circle in the biplot was the "ideal" rice genotype because the small circle represents the placement of the "average yield-trait combination". It was mesured by the coordinates of all yield-trait combinations included in the biplot. The line with a single arrow passes through the biplot origin and the average yield-trait combination and is called the average tester axis (ATA). The ideal rice genotype R7, represented by the small circle with an arrow pointing to it, is defined as having the highest yield in all environments (here, the environment is yield-trait combination). R7 has the highest mean yield with stability. The remaining tested rice genotypes are ranked based on distance from the R7 rice genotype (Yan et al., 2007). The average tester axis (ATA) also ranks the genotypes based on their superiority. The line with a single arrow is the ATA that passes through the biplot origin and the average yield-trait combination (Fig: 6.3). The ATA ranks the genotypes based on their overall superiority or usefulness. Rice Genotypes (R7, R3, R12, R38, R101, R75 and R19) placed close to ATA (short distance) tended to have balanced trait profiles, whereas those (R83, R116 and R68) placed away from the ATA in either direction tended to have apparent strengths and/or weaknesses. However, rice genotypes (R49, R58, R79, R15, R107, R23 and R64) were not determined as balanced traits genotypes despite having the closest position to ATA as these rice genotypes resided at the other side of the blue line (Pointing outwards passed through the origin and is perpendicular to the ATA). This line separated rice genotypes that were better than average (placed on its left, on the same side as the ATA arrow) from those poorer than average (placed on the right side). The top three ranked rice cultivars in this study based on the yield-trait combinations included R7> R3> R37. The rice cultivar, R7, is the ideal genotype originating in the Philippines and is categorised into the tropical japonica subpopulation. The rhizospheric pH was determined as the best-ranked trait that strongly affects the yield since the yield-pH combination positioned in the innermost concentric circles confines the small circle representing the "average yield-trait combination". The following traits were ranked accordingly: lower N_2O emission > residual [NH_4^+] > DOC: N-NO_3^- > residual [NO_3-] > lower gaseous N loss > lower solid N loss based on distance from the best-ranked trait (pH) (Khan et al., 2021). The maximum yield of the ideal rice genotype, R7, was strongly associated with high pH in the rhizosphere. So, the ideal rice genotype might

not perform well in acidic soils as acidic pH might impair rice growth by restricting nutrient uptake (Fageria & Zimmermann, 1998). However, submerged conditions of the acidic paddy soil ameliorate acidic pH by increasing H^+ consumption (Yu, 1991). As a result, the yield of the ideal genotype might decrease if it is grown in upland soil or even in AWD conditions.

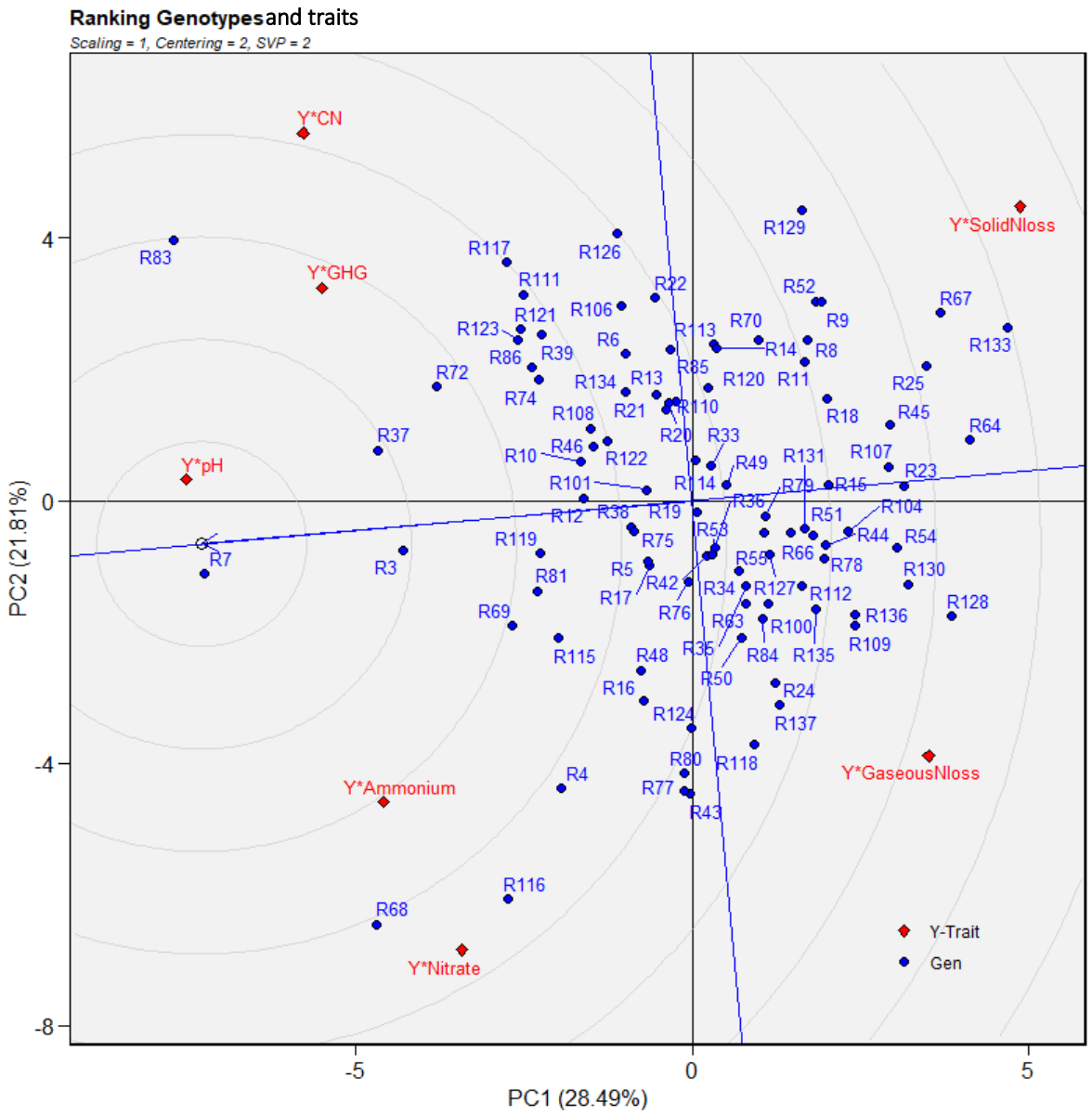

Fig 6.3: The GGE biplot 'ranking genotypes and traits' pattern for genotype comparison with ideal genotype showing G + G × E interaction effect of tested 98 rice genotypes. The ideal genotype is signified by a circle within the innermost concentric circles on the average yield-trait combination. The average texter axis (ATA) is a line with a single arrow passed through the biplot origin and the small circle (average yield-trait combination).The biplot was based on the singular value decomposition of the standardised GYT table ("Scaling = 1, Centering = 2"). The trait-focused singular value partition ("SVP = 2") was used. The trait codes are: GHG: 1/N-N_2O emission rate, GaseousNloss: 1/(Complete denitrification rate + Anammox rate), SolidNloss: 1/Nitrification rate, Ammonium: average residual [NH_4^+] of rhizosphere and bulk compartments, Nitrate: average residual [NO3-] of rhizosphere and bulk compartments, CN: average DOC to N-NO_3^- ratios of rhizosphere and bulk compartments, pH: pH in the rhizosphere compartment.

6.4 Rice genotypes with outstanding traits

Outstanding rice genotypes with specific target traits were determined by "which-won-where" graphical presentation through yield*trait GYT biplot (Fig: 6.4). In this biplot a polygon was drawn joining the rice genotypes (R7, R83, R129, R133, R128, R43, R116, and R68) that are located farthest from the biplot origin containing other rice genotypes in the polygon. The highlighted vertex rice genotypes had the most extended vectors compared to other rice genotypes confined inside the polygon in their respective directions, a measure of responsiveness to yield-trait combinations. The biplot was divided into sectors by the drawn perpendicular lines to the sides of the polygon, and each sector had vertex rice genotypes and yield-trait combinations. The vertex rice genotypes were the highest-yielding, with traits that shared the sector (Yan et al., 2007). For instance, R83 was the highest-yielding rice genotype with outstanding low N_2O emission. This type of rice genotype would be a better choice for selection breeders to improve the sustainability of rice cultivation. The rice genotype also shared a high DOC: $N\text{-}NO_3^-$ ratio, indicating better root traits (Fig: 6.4), a condition favourable for N_2O reduction into N_2 (Lycus et al., 2017; Rummel et al., 2021). A semi-dwarf hybrid rice genotype of the indica subpopulation was found to have the potential for high resource use efficiency and yield under alternate wetting and drying (AWD) irrigation due to superior root traits (Jing et al., 2022). The tentative mechanism behind the low N_2O emission of R83 was the ability to inhibit the total denitrification process rather than encouraging the N_2O reduction (Fig: 4.4.2 and 4.4.3). So, the R83 rice genotype would be an ideal option for the alternate wetting drying (AWD) irrigation system to mitigate the sharp increase of N_2O emissions during drying. In the AWD irrigation system, temporal N_2O emissions were anticipated during the drying period due to the inhibition of nitrous oxide reductase enzyme activity since the enzyme is more sensitive to oxygen exposure than other denitrifying enzymes (Cai et al., 1997; Smith & Patrick, 1983). The leftover $[N\text{-}NH_4^+]$ and $[N\text{-}NO_3^-]$ of the applied nitrogen fertiliser in the soil were outstandingly higher in the vertex rice genotypes R68, R116 and R43. So, these rice genotypes might withstand nitrogen-limited conditions in the soil without compromising yield. The vertex rice genotypes R129 and R133 had the highest yield with minimum solid nitrogen loss, whereas rice genotype R128 was observed as the highest yielding with minimum gaseous nitrogen loss. This study's identified outstanding rice genotypes might not be ideal if a particular target trait is considered (Oladosu et al., 2017). For instance, even though these three

rice genotypes are associated with the highest yield and lowest nitrogen loss trait combination, they were not performing well in the N_2O emission trait.

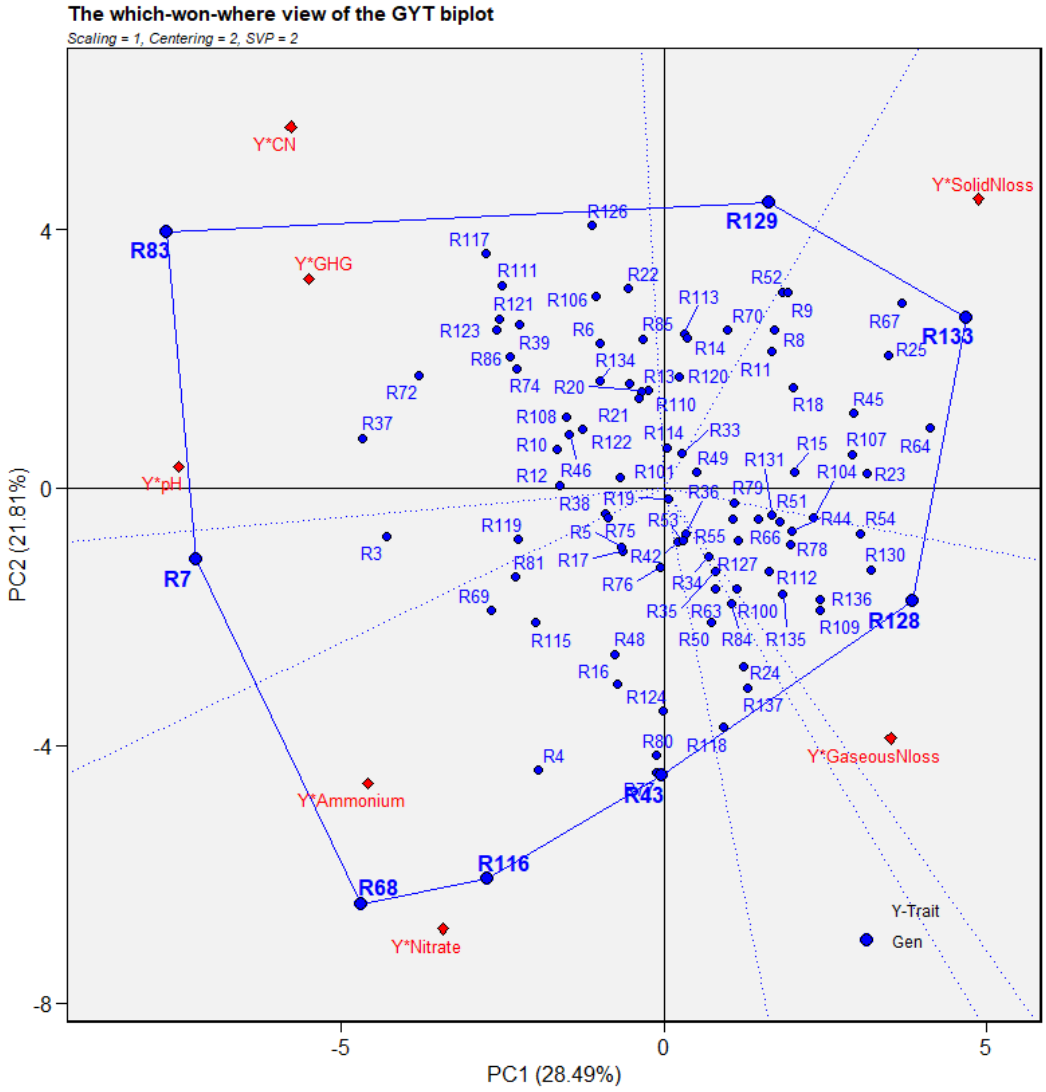

Fig 6.4: The which-won-where view of the genotype by yield*trait (GYT) biplot to highlight genotypes with outstanding profiles. The biplot was based on singular value decomposition of the standardised GYT table ("Scaling = 1, Centering = 2"). The trait-focused singular value partition ("SVP = 2") was used. The trait codes are: GHG: 1/N-N_2O emission rate, GaseousNloss: 1/(Complete denitrification rate + Anammox rate), SolidNloss: 1/Nitrification rate, Ammonium: average residual [NH_4^+] of rhizosphere and bulk compartments, Nitrate: average residual [NO3-] of rhizosphere and bulk compartments, CN: average DOC to N-NO_3^- ratios of rhizosphere and bulk compartments, pH: pH in the rhizosphere compartment.

The ideal rice genotype for sustainable agriculture would be one that can adapt to different environments (e.g., different soil types, pH) and management systems (e.g., irrigation regime, fertilisation) without compromising yield and GHG emissions. When considering rice selection breeding of target traits, the yield performance of the genotypes with stability in different environments and management systems is essential for improving genotypes. The best way to evaluate yield performances without compromising the interest of traits of rice genotypes in different environments and management systems is by genotype X environment X management (G X E X M) interaction analysis. G X E X M interaction analysis would be an appropriate tool for rice selection breeding in mitigating N_2O emission and nitrogen fertiliser loss from different rice cultivation systems, but it is yet to be explored (Hawkesford & Riche, 2020). A meta-analysis determined the significant effects of irrigation and nitrogen fertiliser management on rice yield and nitrogen loss (Qiu et al., 2022). Nonetheless, selection breeders are keen to know the responses of genotypes to different environments and management systems. Significant rice genotypic variation in yield was observed between rice cultivars while measuring genotype-by-environment interaction in high-yielding environments where irrigation and fertiliser were applied (Hanviriyapant & Fukai, 1997). In contrast, the genotypic variation was insignificant in environments without irrigation and fertiliser application. Significant rice genotypic effects on yield in different paddy soils with a pH range were recently reported under controlled irrigation management systems (Nikiema et al., 2023). Indeed, (Xie et al., 2022) demonstrated a significant interaction between rice genotype, fertiliser types and irrigation (G X E X M) on rhizosphere bacterial communities affecting soil inorganic nitrogen contents. (Oyserman et al., 2021) used the (G X E X M) model where genotype (G) X environment (E) X microbiome (M) to understand plant, soil and microbial interaction on plant phenotypes. In this model, microbiome (M) was added as an explanatory factor that a plant phenotype (Y) was determined by the relationship of genotype (G) x environment (E). So, the model (Y ~ G x E x M) explained plant yield as a function of the genotype, environment and microbiome interactions.

6.5 Limitations of the study

The availability of oxygen determines the fate of microbial nitrogen transformations in the soil. I planned to measure the partial oxygen pressure in the rhizosphere and bulk compartments using a microsensor without disrupting the plant growth. Unfortunately, due to time constraints and COVID-19, I could not measure the partial oxygen pressure in the rice microcosms. The experiment had few artefacts (e.g., cutting shoot and mineralisation) while measuring microbial N-cycle processes discussed below.

6.5.1 Artificial defoliation effects

Gas samples were collected to measure denitrification and anammox after cutting the rice shoot to accommodate the pots into the Kilner jar during incubation. Carbon flux might be altered in root exudations after artificial defoliation (cutting the shoot), influencing denitrification and the fate of end products during denitrification. Root growth stops immediately after defoliation, and fine roots may die (Luo *et al.*, 1995; Jarvis & MacDuff, 1989). Indeed, nutrient uptake and root respiration also decline after artificial defoliation. Rice root respiration might be inhibited quickly because the oxygen supply shuts down while cutting the shoot. Nitrification processes might be interrupted in the rhizosphere due to the shutdown of the oxygen supply. Indeed, unloaded sugars from phloem in the rice roots might be released into the rice rhizosphere instead of incorporated into root structural biomass and/or root respiration (Hartmann et al., 2018; Mannerheim et al., 2020). Immediate defoliation increased the total amount of sugars in the exudates, but sugar exudation reduced and induced changes in the exudation patterns of individual sugars over eight hours time period after defoliation in *Lolium perenne* L (Clayton et al., 2008). Defoliation enhanced the exudation of erythritol, threitol, and xylitol and reduced the exudation of glucose and arabitol over 24 hours period of defoliation (Clayton et al., 2008). This study observed N-N_2O and N-N_2 flux up to five hours after artificial defoliation. N_2O reduction into N_2 might be enhanced later in incubation due to artificial defoliation-induced carbon quality and quantity fluctuation in the root exudates. The types of carbon dictate the fate of denitrification end products depending on the O_2 concentration (Morley & Baggs, 2010). NO_3^- could be entirely reduced to N_2 under any carbon sources; however, the accumulation of N_2O is 27 times more in the presence of glucose groups than that of ethanol groups (Wei et al., 2022). There was not significant artificial defoliation effects on quantity of DOC among the

tested rice genotypes since no significant variations was found on measured DOC. Nevertheless, quality of carbons was not measured from the soil extracts in this study.

6.3.2 Mineralisation effects

DNRA, nitrogen retention process, was measured by analysing the degree of enrichment of ^{15}N in the NH_4^+ pool. Biological nitrogen fixation (BNF) and immobilisation are other microbial nitrogen retention processes in the soil that were not considered significant nitrogen retention processes after N fertilisation in this study. A global meta-analysis by (Zheng et al., 2019) found that adding nitrogen fertilisation inhibits BNF. Nitrogen fertilisation addition decreases the rice root-associated nitrogen-fixing bacteria (Liu et al., 2021). The conversion of applied $^{15}N\text{-}NO_3^-$ immobilisation into $^{15}N\text{-}NH_4^+$ through immobilisation was negligible as dual inorganic forms were provided as NH_4NO_3 (Pandey et al., 2018b; Puri & Ashman, 1999; Rice & Tiedje, 1989; Romero et al., 2015; Templer et al., 2008). NH_4^+ is preferentially immobilised in the microbial biomass over NO_3^- where both the inorganic N is provided simultaneously. The DNRA rate was also measured by considering the negligible microbial immobilisation process rate after applying both inorganic forms of N (Pandey et al., 2018b). However, nitrogen mineralisation might affect the DNRA rate by diluting the $^{15}N\text{-}NH_4^+$ pool after the decomposition of the organic substrate as the decomposition of the organic substrate under waterlogged conditions is increased (Wang et al., 2001). The potential mineralisation rate in the flooded paddy soil was reported to be a range of 21-84 ng N/g soil/h higher than the measured DNRA rate in this study (Huilin Li et al., 2003). This study did not measure the nitrogen mineralisation process, which might be why the insignificant DNRA rate was measured. DNRA rate was found to be significantly higher in the rhizosphere than in the bulk compartment. Prevailing anaerobic conditions in the bulk compartment might enhance mineralisation that dilutes the ammonified $^{15}N\text{-}NH_4^+$.

6.6 Final summary and concluding remarks

Despite having few artefacts, the four microbial nitrogen transformations were measured simultaneously for the first time by a single rice microcosm experiment. Simultaneous measurements of these microbial nitrogen transformations were evident in understanding the rice genotypic effects on the solid and gaseous N loss, including N_2O emission after nitrogen fertilisation, since the processes are interconnected and coincide in the oxic/anoxic interfaces of the rice rhizosphere. Due to varied rice rhizospheric effects, I hypothesised that these

microbial nitrogen transformation processes vary among rice cultivars. This study demonstrated that the measured microbial (nitrification, denitrification and anammox) nitrogen transformations, except DNRA, significantly varied among the tested rice cultivars, indicating rice genetics involvement in modulating N-cycle associated microbes in the rhizosphere and surrounding bulk soil. The genetic determinants are currently being emphasised to allow breeding for beneficial plant–microbiome interactions in sustainable agriculture (Hohmann et al., 2020). The QTLs as rice genetic determinants responsible for the microbial modulations were tentatively identified by GWAS analysis. Thus, it leaves an option to improve nitrogen productivity in the soil by modulating N-cycle-associated microbial communities in the rice rhizosphere through rice genotype selection. Indeed, the study identified an ideal rice genotype and the rice genotypes with outstanding traits for rice selection breeding to combat current and future climate challenges.

Zero hunger and climate action are two pivotal sustainable development goals (SDGs). However, growing more foods without compromising the climate further is a big challenge. According to the recent Emissions Gap Report 2022 of the UN Environment Programme, the food system was responsible for one-third of GHG emissions, and agriculture contributed 40% of its emissions, including fertiliser production (United Nations Environment Programme, 2020). This emission includes CO_2, CH_4, and N2O, but agriculture contributed half of the non-CO_2 emissions to the total non-CO_2 emission. Various strategies are extensively studied to mitigate GHG emissions, specifically N_2O, from agricultural land. For instance, controlled released fertiliser, synthetic nitrification inhibitors, arbuscular mycorrhizal fungi (Storer et al., 2018), supplementing manure in combination with synthetic N fertiliser (Q. Tang et al., 2022), liming (Wang et al., 2021), biochar application (Jindo et al., 2020). The basis for all strategies is to increase nitrous oxide reductase activity because it is the only known biological process that reduces N_2O to N_2 in the soil (Richardson et al., 2009). Flooded paddy is a unique agrosystem different from other arable agricultural lands due to its anaerobic condition with highly soil organic matter. Strategies suitable for mitigating N_2O emission from arable agriculture might not be attributed the same way in the flooded paddy. Application of manure and liming might increase ammonia volatilisation in flooded paddy soil and, in addition, increase methane emissions by enhancing methanogen diversity (Kim et al., 2014; Lee et al., 2021).

Rice selection breeding without further jeopardising the environment could be suitable to mitigate N_2O emissions from rice cultivation. This rice screening empirical data suggested that

rice genetics is involved in the altered emission of N_2O. The nitrification process dictates the fate of applied N in rice cultivation, and nitrification is reciprocally correlated with nitrogen uptake efficiency (NUE) in rice (Li et al., 2008). In addition, GWAS results suggested that low N_2O emitting rice genotypes might be resilient varieties that confer better immunity against bacterial and fungal infection. The results from this experiment are just the beginning and need further confirmation. The future works that are the logical next steps are discussed in the following section.

6.7 Future works

The immediate future works are extracting DNA and RNA from collected snap-frozen soil of rhizosphere and bulk compartments to understand the microbial networking related to nitrogen transformations. A more highly controlled rhizobox experiment performed on key cultivars would also provide a logical next step to work to confirm findings avoiding artificial defoliation while collecting the gas samples.

6.7.1 Community structure and networking analysis

Snap-frozen soil samples from the rhizosphere and bulk compartments from this experiment were stored at the lab. Microbial community abundance relating to nitrification, denitrification and anammox needs to be analysed further to corroborate this experiment's findings. Indeed, a community networking analysis also helps to understand the inter-community interaction with specific rice genotypes (Fig: 6.5). Sequencing data from the collected soil samples might also help to understand the ecophysiology of NosZ clade II (Hallin et al., 2018). The role of NosZ clade II having DNRA capability could be a potential bacteria in paddy soil that consumes N_2O and at the same time retains the N in the soil (Sanford et al., 2012). The interaction between nitrite oxidising bacteria and anammox bacteria in rice cultivars R25, R119 and R133 might reveal the anammox bacterial physiological mystery in the paddy soil.

6.7.2 Rhizobox experiment

A rhizobox experiment could be done by using the contrasting N_2O-emitting rice genotypes by compartmentalising the carbon gradient bulk compartment further to understand the interaction between rice plants and denitrifiers in that narrow space. Pore water collection strategy by keeping the rice plant intact will also help to source partition of emitted N_2O between nitrification and denitrification without any biases (Fig: 6.5).

6.7.3 Transcriptomics and metabolomics analysis

Contrasting rice genotypes similarly could be grown hydroponically, and downstream metabolomics analysis from root exudates and transcriptomics analysis from shoot and/or roots need to be done to validate the GWAS results (Fig: 6.5).

6.7.4 Field trial

The last logical step is to replicate the lab result in the field to test the feasibility of either rice breeding selection strategy to combat N_2O emission from fertilised paddy soil.

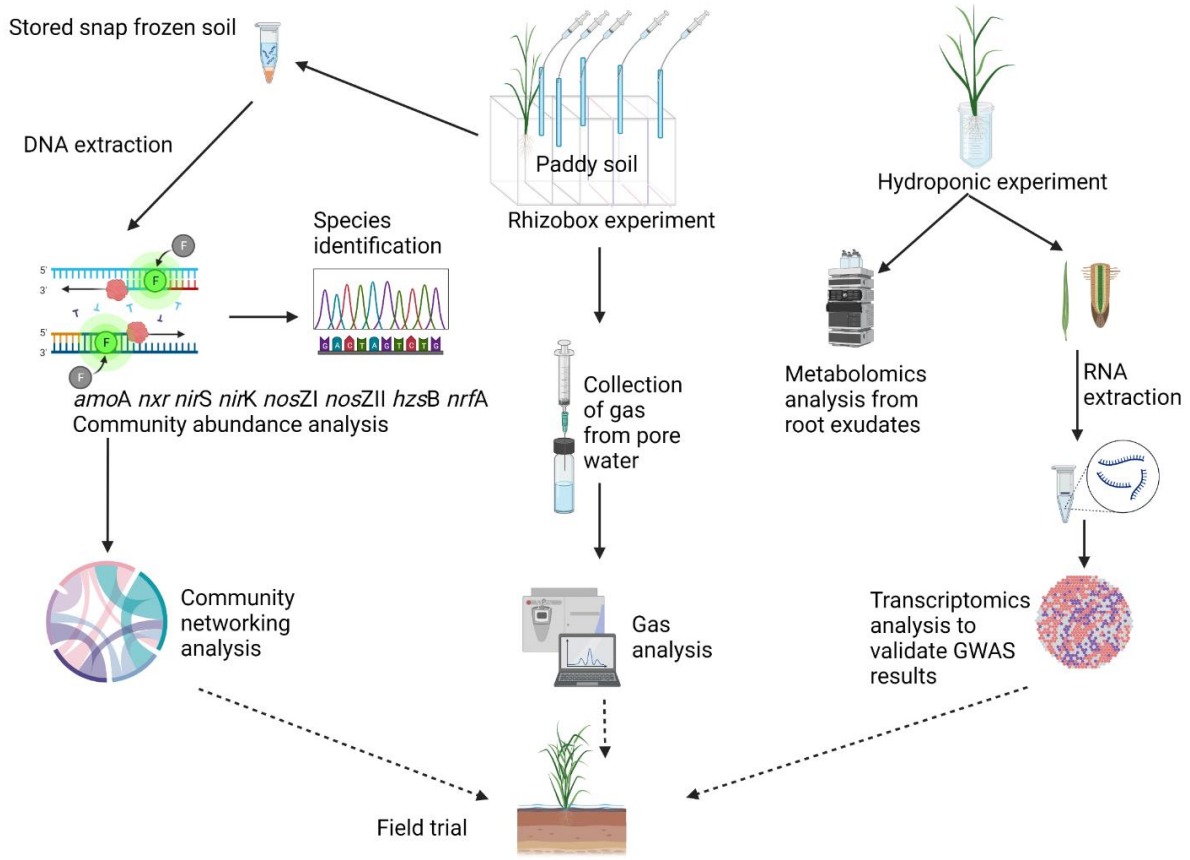

2 Fig 6.5: Schematic diagram of the future works that could be done further to validate rice selection breeding method in curbing N_2O emission from rice cultivation.

References

Abbas, T., Zhang, Q., Zou, X., Tahir, M., Wu, D., Jin, S. & Di, H. (2020). Soil anammox and denitrification processes connected with N cycling genes co-supporting or contrasting

under different water conditions. *Environment International*, *140*(March), 105757. https://doi.org/10.1016/j.envint.2020.105757

Abbasi, M. R. & Sepaskhah, A. R. (2023). Nitrogen leaching and groundwater N contamination risk in saffron/wheat intercropping under different irrigation and soil fertilizers regimes. *Scientific Reports*, *13*(1), 1–17. https://doi.org/10.1038/s41598-023-33817-5

Araújo, W. L., Tohge, T., Ishizaki, K., Leaver, C. J. & Fernie, A. R. (2011). Protein degradation - an alternative respiratory substrate for stressed plants. *Trends in Plant Science*, *16*(9), 489–498. https://doi.org/10.1016/j.tplants.2011.05.008

Arch, È., Wang, Z., Seto, H., Fujioka, S., Yoshida, S. & Chory, J. (2001). *BRI1 is a critical component of a plasma-membrane receptor for plant steroids*. *410*(December 2000), 380–383.

ARMSTRONG, W. (1971). Radial Oxygen Losses from Intact Rice Roots as Affected by Distance from the Apex, Respiration and Waterlogging. *Physiologia Plantarum*. https://doi.org/10.1111/j.1399-3054.1971.tb01427.x

Arth, I., Frenzel, P. & Conrad, R. (1998). Denitrification coupled to nitrification in the rhizosphere of rice. *Soil Biology and Biochemistry*, *30*(4), 509–515. https://doi.org/10.1016/S0038-0717(97)00143-0

Azadi, H., Ho, P. & Hasfiati, L. (2011). Agricultural land conversion drivers: A comparison between less developed, developing and developed countries. *Land Degradation and Development*, *22*(6), 596–604. https://doi.org/10.1002/ldr.1037

Aziz, T., Ahmed, I., Farooq, M., Maqsood, M. A. & Sabir, M. (2011). Variation in phosphorus efficiency among Brassica cultivars I: Internal utilization and phosphorus remobilization. *Journal of Plant Nutrition*, *34*(13), 2006–2017. https://doi.org/10.1080/01904167.2011.610487

Baggs, E. M. (2011). Soil microbial sources of nitrous oxide: Recent advances in knowledge, emerging challenges and future direction. *Current Opinion in Environmental Sustainability*, *3*(5), 321–327. https://doi.org/10.1016/j.cosust.2011.08.011

Bai, R., Xi, D., He, J. Z., Hu, H. W., Fang, Y. T. & Zhang, L. M. (2015). Activity, abundance

and community structure of anammox bacteria along depth profiles in three different paddy soils. *Soil Biology and Biochemistry*, *91*, 212–221. https://doi.org/10.1016/j.soilbio.2015.08.040

Bardon, C., Piola, F., Bellvert, F., Haichar, F. el Z., Comte, G., Meiffren, G., Pommier, T., Puijalon, S., Tsafack, N. & Poly, F. (2014). Evidence for biological denitrification inhibition (BDI) by plant secondary metabolites. *New Phytologist*, *204*(3), 620–630. https://doi.org/10.1111/nph.12944

Bateman, E. J. & Baggs, E. M. (2005a). Contributions of nitrification and denitrification to N2O emissions from soils at different water-filled pore space. *Biology and Fertility of Soils*, *41*(6), 379–388. https://doi.org/10.1007/s00374-005-0858-3

Bateman, E. J. & Baggs, E. M. (2005b). Contributions of nitrification and denitrification to N2O emissions from soils at different water-filled pore space. *Biology and Fertility of Soils*. https://doi.org/10.1007/s00374-005-0858-3

Bauer, N., Škiljaica, A., Malenica, N., Razdorov, G., Klasić, M., Juranić, M., Močibob, M., Sprunck, S., Dresselhaus, T. & Leljak Levanić, D. (2019). The MATH-BTB Protein TaMAB2 Accumulates in Ubiquitin-Containing Foci and Interacts With the Translation Initiation Machinery in Arabidopsis. *Frontiers in Plant Science*, *10*(November), 1–16. https://doi.org/10.3389/fpls.2019.01469

Baumann, B., Van Der Meer, J. R., Snozzi, M. & Zehnder, A. J. B. (1997). Inhibition of denitrification activity but not of mRNA induction in Paracoccus dentrificans by nitrite at a suboptimal pH. *Antonie van Leeuwenhoek, International Journal of General and Molecular Microbiology*. https://doi.org/10.1023/A:1000342125891

Beaudoin, N., Saad, J. K., Van Laethem, C., Machet, J. M., Maucorps, J. & Mary, B. (2005). Nitrate leaching in intensive agriculture in Northern France: Effect of farming practices, soils and crop rotations. *Agriculture, Ecosystems and Environment*, *111*(1–4), 292–310. https://doi.org/10.1016/j.agee.2005.06.006

Bergsma, T. T., Ostrom, N. E., Emmons, M. & Robertson, G. P. (2001). Measuring simultaneous fluxes from soil of N2O and N2 in the field using the 15N-gas "nonequilibrium" technique. *Environmental Science and Technology*.

https://doi.org/10.1021/es010885u

Berks, B. C., Ferguson, S. J., Moir, J. W. B. & Richardson, D. J. (1995). Enzymes and associated electron transport systems that catalyse the respiratory reduction of nitrogen oxides and oxyanions. In *BBA - Bioenergetics*. https://doi.org/10.1016/0005-2728(95)00092-5

Bhattacharyya, P., Dash, P. K., Swain, C. K., Padhy, S. R., Roy, K. S., Neogi, S., Berliner, J., Adak, T., Pokhare, S. S., Baig, M. J. & Mohapatra, T. (2019). Mechanism of plant mediated methane emission in tropical lowland rice. *Science of the Total Environment*, *651*, 84–92. https://doi.org/10.1016/j.scitotenv.2018.09.141

Blackmer, A. M. & Bremner, J. M. (1978). Inhibitory effect of nitrate on reduction of N2O to N2 by soil microorganisms. *Soil Biology and Biochemistry*, *10*(3), 187–191. https://doi.org/10.1016/0038-0717(78)90095-0

Boddey, R. M., Peoples, M. B., Palmer, B. & Dart, P. J. (2000). Use of the 15N natural abundance technique to quantify biological nitrogen fixation by woody perennials. *Nutrient Cycling in Agroecosystems*, *57*(3), 235–270. https://doi.org/10.1023/A:1009890514844

Boivin, P., Favre, F., Hammecker, C., Maeght, J. L., Delarivière, J., Poussin, J. C. & Wopereis, M. C. S. (2002). Processes driving soil solution chemistry in a flooded rice-cropped vertisol: Analysis of long-time monitoring data. *Geoderma*, *110*(1–2), 87–107. https://doi.org/10.1016/S0016-7061(02)00226-4

Bothe, H., Schmitz, O., Yates, M. G. & Newton, W. E. (2010). Nitrogen Fixation and Hydrogen Metabolism in Cyanobacteria. *Microbiology and Molecular Biology Reviews*, *74*(4), 529–551. https://doi.org/10.1128/mmbr.00033-10

Bowman, W. D., Cleveland, C. C., Halada, Ĺ., Hreško, J. & Baron, J. S. (2008). Negative impact of nitrogen deposition on soil buffering capacity. *Nature Geoscience*, *1*(11). https://doi.org/10.1038/ngeo339

Bracmort, K. (2010). *CRS Report for Congress Nitrous Oxide from Agricultural Sources: Potential Role in Greenhouse Gas Emission Reduction and Ozone Recovery N2O: Potential Role in Greenhouse Gas Emission Reduction and Ozone Recovery*

Congressional Research Service N2O: Potenti. www.crs.gov

Brundrett, M. (2004). Diversity and classification of mycorrhizal associations. *Biological Reviews*, *79*(3), 473–495. https://doi.org/https://doi.org/10.1017/S1464793103006316

Bruulsema, T., Lemunyon, J. & Herz, B. (2009). Know your fertilizer rights. *Crops & Soils*, *42*(2), 13–18. https://dl.sciencesocieties.org/publications/crops-and-soils/4202

Buchwald, C., Grabb, K., Hansel, C. M. & Wankel, S. D. (2016). Constraining the role of iron in environmental nitrogen transformations: Dual stable isotope systematics of abiotic NO2- reduction by Fe(II) and its production of N2O. *Geochimica et Cosmochimica Acta*, *186*, 1–12. https://doi.org/10.1016/j.gca.2016.04.041

Burford, J. R. & Bremner, J. M. (1975). Relationships between the denitrification capacities of soils and total, water-soluble and readily decomposable soil organic matter. *Soil Biology and Biochemistry*. https://doi.org/10.1016/0038-0717(75)90055-3

C., D. (1982). Denitrification, Nitrification, and Atmospheric Nitrous Oxide. *The Quarterly Review of Biology*, *57*(1), 81–82. https://doi.org/10.1086/412632

Cai, Z., Xing, G., Yan, X., Xu, H., Tsuruta, H., Yagi, K. & Minami, K. (1997). Methane and nitrous oxide emissions from rice paddy fields as affected by nitrogen fertilisers and water management. *Plant and Soil*, *196*(1), 7–14. https://doi.org/10.1023/A:1004263405020

Carlisle, E., Yarnes, C., Toney, M. D. & Bloom, A. J. (2014). Nitrate reductase 15N discrimination in Arabidopsis thaliana, Zea mays, Aspergillus niger, Pichea angusta, and Escherichia coli. *Frontiers in Plant Science*, *5*(JUL), 1–8. https://doi.org/10.3389/fpls.2014.00317

Carpentier, M. C., Manfroi, E., Wei, F. J., Wu, H. P., Lasserre, E., Llauro, C., Debladis, E., Akakpo, R., Hsing, Y. I. & Panaud, O. (2019). Retrotranspositional landscape of Asian rice revealed by 3000 genomes. *Nature Communications*, *10*(1). https://doi.org/10.1038/s41467-018-07974-5

Casali, L., Mazzei, L., Sun, R., Chierotti, M. R., Gobetto, R., Braga, D., Grepioni, F. & Ciurli, S. (2022). Thiocarbamoyl Disulfides as Inhibitors of Urease and Ammonia Monooxygenase: Crystal Engineering for Novel Materials. *Crystal Growth and Design*,

22(7), 4528–4537. https://doi.org/10.1021/acs.cgd.2c00439

Chen, P., Xu, J., Zhang, Z. & Nie, T. (2022). “Preferential” ammonium uptake by rice does not always turn into higher N recovery of fertilizer sources under water-saving irrigation. *Agricultural Water Management*, *272*(April), 107867. https://doi.org/10.1016/j.agwat.2022.107867

Chen, S., He, M., Zhao, C., Wang, W., Zhu, Q., Dan, X., He, X., Meng, L., Zhang, S., Cai, Z., Zhang, J. & Müller, C. (2022). Rice genotype affects nitrification inhibition in the rhizosphere. *Plant and Soil*, *481*(1–2), 35–48. https://doi.org/10.1007/s11104-022-05609-9

Chen, Y. & Wang, F. (2015). Insights on nitrate respiration by Shewanella. *Frontiers in Marine Science*, *1*(JAN), 1–9. https://doi.org/10.3389/fmars.2014.00080

Cheung, H. L. S., Hillman, J. R., Pilditch, C. A., Savage, C., Santos, I. R., Glud, R. N., Nascimento, F. J. A., Thrush, S. F. & Bonaglia, S. (2024). Denitrification, anammox, and DNRA in oligotrophic continental shelf sediments. *Limnology and Oceanography*, *69*(3), 621–637. https://doi.org/10.1002/lno.12512

Childs, N. & Skorbiansky, S. R. (2019). *Rice Outlook Rice Outlook U . S . 2018 /19 Rice Export Forecast Lowered to 94.0 Million Cwt*. 1–27.

Clayton, S. J., Read, D. B., Murray, P. J. & Gregory, P. J. (2008). Exudation of alcohol and aldehyde sugars from roots of defoliated Lolium perenne L. grown under sterile conditions. *Journal of Chemical Ecology*, *34*(11), 1411–1421. https://doi.org/10.1007/s10886-008-9536-x

Cole, J. (1996). Nitrate reduction to ammonia by enteric bacteria: Redundancy, or a strategy for survival during oxygen starvation? *FEMS Microbiology Letters*, *136*(1), 1–11. https://doi.org/10.1016/0378-1097(95)00480-7

Colmer, T D & Voesenek, L. A. C. J. (2009). *Flooding tolerance : suites of plant traits in variable environments*. *Grist 1986*, 665–681.

Colmer, Timothy David, Takahashi, H., Malik, A. I., Konnerup, D., Nakazono, M. & Pedersen, O. (2019). *Rice acclimation to soil flooding : Low concentrations of organic acids can*

trigger a barrier to radial oxygen loss in roots. *November 2018*, 2183–2197. https://doi.org/10.1111/pce.13562

Colombi, Tino, Arjun Chakrawal and Anke Herrmann, M. (2021). *Carbon consumption balance in plant roots : effects of carbon use efficiency and root anatomical plasticity*. https://doi.org/10.1111/nph.17598

Conrad, R. (2007). Microbial Ecology of Methanogens and Methanotrophs. *Advances in Agronomy*, *96*, 1–63. https://doi.org/10.1016/S0065-2113(07)96005-8

Coskun, D., Britto, D. T., Shi, W. & Kronzucker, H. J. (2017). How Plant Root Exudates Shape the Nitrogen Cycle. *Trends in Plant Science*, *22*(8), 661–673. https://doi.org/10.1016/j.tplants.2017.05.004

Costa, E., Pérez, J. & Kreft, J. U. (2006). Why is metabolic labour divided in nitrification? *Trends in Microbiology*, *14*(5), 213–219. https://doi.org/10.1016/j.tim.2006.03.006

Courty, P. E., Smith, P., Koegel, S., Redecker, D. & Wipf, D. (2015). Inorganic Nitrogen Uptake and Transport in Beneficial Plant Root-Microbe Interactions. *Critical Reviews in Plant Sciences*, *34*, 4–16. https://doi.org/10.1080/07352689.2014.897897

Craswell, E. T. & Vlek, P. L. G. (1983). Fate of fertilizer nitrogen applied to wetland rice. In J. R. Freney & J. R. Simpson (Eds.), *Gaseous Loss of Nitrogen from Plant-Soil Systems* (pp. 237–264). Springer Netherlands. https://doi.org/10.1007/978-94-017-1662-8_10

Dahab, M. F. & Woon Lee, Y. (1988). Nitrate removal from water supplied using biological denitrification. *Journal of the Water Pollution Control Federation*, *60*(9), 1670–1674.

Daims, H., Lebedeva, E. V., Pjevac, P., Han, P., Herbold, C., Albertsen, M., Jehmlich, N., Palatinszky, M., Vierheilig, J., Bulaev, A., Kirkegaard, R. H., Von Bergen, M., Rattei, T., Bendinger, B., Nielsen, P. H. & Wagner, M. (2015). Complete nitrification by Nitrospira bacteria. *Nature*, *528*(7583), 504–509. https://doi.org/10.1038/nature16461

Daims, H., Lücker, S. & Wagner, M. (2019). *A New Perspective on Microbes Formerly Known as Nitrite- Oxidizing Bacteria*. *24*(9), 699–712. https://doi.org/10.1016/j.tim.2016.05.004.A

Dalsgaard, T. & Thamdrup, B. (2002). Production of N2 through anaerobic ammonium

oxidation coupled to nitrate reduction in marine sediments. *Applied and Environmental Microbiology*, *68*(3), 1312–1318. https://doi.org/10.1128/AEM.68.3.1312

Davidson, E. A. (2009). The contribution of manure and fertilizer nitrogen to atmospheric nitrous oxide since 1860. *Nature Geoscience*, *2*(9), 659–662. https://doi.org/10.1038/ngeo608

Davidson, E. A. & Kanter, D. (2014). Inventories and scenarios of nitrous oxide emissions. *Environmental Research Letters*, *9*(10). https://doi.org/10.1088/1748-9326/9/10/105012

DiFonzo, N. & Bordia, P. (1998). Environmental factors influencing the nitrogen fixation activity of free-living terrestrial cyanobacteria from a high arctic area, Spitsbergen. *Journal of Allergy and Clinical Immunology*, *130*(2), 556. http://dx.doi.org/10.1016/j.jaci.2012.05.050

Ding, H., Hu, Q., Cai, M., Cao, C. & Jiang, Y. (2022). Effect of dissolved organic matter (DOM) on greenhouse gas emissions in rice varieties. *Agriculture, Ecosystems and Environment*, *330*(February), 107870. https://doi.org/10.1016/j.agee.2022.107870

Ding, L. J., Cui, H. L., Nie, S. A., Long, X. E., Duan, G. L. & Zhu, Y. G. (2019). Microbiomes inhabiting rice roots and rhizosphere. *FEMS Microbiology Ecology*, *95*(5), 1–13. https://doi.org/10.1093/femsec/fiz040

Domeignoz-Horta, L. A., Philippot, L., Peyrard, C., Bru, D., Breuil, M. C., Bizouard, F., Justes, E., Mary, B., Léonard, J. & Spor, A. (2018). Peaks of in situ N2O emissions are influenced by N2O-producing and reducing microbial communities across arable soils. *Global Change Biology*. https://doi.org/10.1111/gcb.13853

Drew, M. C., He, C. & Morgan, P. W. (2000). *Programmed cell death and aerenchyma formation in roots*. *5*(3), 123–127.

Eady, R. R. (1996). Structure−Function Relationships of Alternative Nitrogenases. *Chemical Reviews*, *96*(7), 3013–3030. https://doi.org/10.1021/cr950057h

Einsle, O., Messerschmidt, A., Huber, R., Kroneck, P. M. H. & Neese, F. (2002). Mechanism of the six-electron reduction of nitrite to ammonia by cytochrome c nitrite reductase. *Journal of the American Chemical Society*, *124*(39), 11737–11745.

https://doi.org/10.1021/ja0206487

Erisman, J. W., Sutton, M. A., Galloway, J., Klimont, Z. & Winiwarter, W. (2008). How a century of ammonia synthesis changed the world. *Nature Geoscience*, *1*(10), 636–639. https://doi.org/10.1038/ngeo325

Eryong, C. & Bo, S. (2022). OsABT, a Rice WD40 Domain-Containing Protein, Is Involved in Abiotic Stress Tolerance. *Rice Science*, *29*(3), 247–256. https://doi.org/10.1016/j.rsci.2021.07.012

Evans, R. D. (2001). Physiological mechanisms influencing plant nitrogen isotope composition. *Trends in Plant Science*, *6*(3), 121–126. https://doi.org/10.1016/S1360-1385(01)01889-1

Fageria, N. K. & Zimmermann, F. J. P. (1998). Influence of pH on growth and nutrient uptake by crop species in an Oxisol. *Communications in Soil Science and Plant Analysis*, *29*(17–18), 2675–2682. https://doi.org/10.1080/00103629809370142

FAO. (2022). *FAOSTAT "Nutrient nitrogen N (total) Agricultural Use in World + (Total)."* 2023. https://www.fao.org/faostat/en/#data/RFN/visualize

FAO. (2023). *Share in IPCC Agriculture total , World + (Total)*. 2023.

FAOSTAT. (2017). Agriculture: Emissions by sector (CO2 equivalent), World + (Total). *Report of Food and Agriculture of the Organization of United Nations*, 2020. http://www.fao.org/faostat/en/#data/GT/visualize

Firestone, M.K. & Davidson, E. A. (1989). Microbiological Basis of NO and N2O Production and Consumption in Soil. *Exchange of Trace Gases between Terresitrial Ecosystems and the Atmosphere*, *May*, 7–21. https://doi.org/citeulike-article-id:6223743

Firestone, Mary K., Firestone, R. B. & Tiedje, J. M. (1980). Nitrous oxide from soil denitrification: Factors controlling its biological production. *Science*. https://doi.org/10.1126/science.208.4445.749

Forster, P. & Ramaswamy, V. (2007). Changes in Atmospheric Constituents and in Radiative Forcing. *Change*, *30*(22), 129–234. https://doi.org/10.1103/PhysRevB.77.220407

Fowler, D., Steadman, C. E., Stevenson, D., Coyle, M., Rees, R. M., Skiba, U. M., Sutton, M. A., Cape, J. N., Dore, A. J., Vieno, M., Simpson, D., Zaehle, S., Stocker, B. D., Rinaldi, M., Facchini, M. C., Flechard, C. R., Nemitz, E., Twigg, M., Erisman, J. W., … Galloway, J. N. (2015). Effects of global change during the 21st century onthe nitrogen cycle. *Atmospheric Chemistry and Physics*, *15*(24), 13849–13893. https://doi.org/10.5194/acp-15-13849-2015

Fowler, David, Coyle, M., Skiba, U., Sutton, M. A., Cape, J. N., Reis, S., Sheppard, L. J., Jenkins, A., Grizzetti, B., Galloway, J. N., Vitousek, P., Leach, A., Bouwman, A. F., Butterbach-Bahl, K., Dentener, F., Stevenson, D., Amann, M. & Voss, M. (2013). The global nitrogen cycle in the Twentyfirst century. *Philosophical Transactions of the Royal Society B: Biological Sciences*, *368*(1621). https://doi.org/10.1098/rstb.2013.0164

Fukagawa, N. K. & Ziska, L. H. (2019). Rice: importance for global nutrition. *Journal of Nutritional Science and Vitaminology*, *65*, S2–S3. https://doi.org/10.3177/jnsv.65.S2

Fülöp, V., Moir, J. W. B., Ferguson, S. J. & Hajdu, J. (1995). The anatomy of a bifunctional enzyme: Structural basis for reduction of oxygen to water and synthesis of nitric oxide by cytochrome cd1. *Cell*, *81*(3), 369–377. https://doi.org/10.1016/0092-8674(95)90390-9

Galland, W., Piola, F., Burlet, A., Mathieu, C., Nardy, M., Poussineau, S., Blazère, L., Gervaix, J., Puijalon, S., Simon, L. & Haichar, F. el Z. (2019). Biological denitrification inhibition (BDI) in the field: A strategy to improve plant nutrition and growth. *Soil Biology and Biochemistry*, *136*(June). https://doi.org/10.1016/j.soilbio.2019.06.009

Galloway, J. N., Townsend, A. R., Erisman, J. W., Bekunda, M., Cai, Z., Freney, J. R., Martinelli, L. A., Seitzinger, S. P. & Sutton, M. A. (2008). Transformation of the Nitrogen Cycle: Recent Trends, Questions, and Potential Solutions. *Science*, *320*(5878), 889–892. https://doi.org/10.1126/science.1136674

Gaskell, J. F., Blackmer, A. M. & Bremner, J. M. (1981). Comparison of Effects of Nitrate, Nitrite, and Nitric Oxide on Reduction of Nitrous Oxide to Dinitrogen by Soil Microorganisms. *Soil Science Society of America Journal*. https://doi.org/10.2136/sssaj1981.03615995004500060022x

Ge, T., Liu, C., Yuan, H., Zhao, Z., Wu, X., Zhu, Z., Brookes, P. & Wu, J. (2015). Tracking the

photosynthesized carbon input into soil organic carbon pools in a rice soil fertilized with nitrogen. *Plant and Soil*, *392*(1–2), 17–25. https://doi.org/10.1007/s11104-014-2265-8

Giles, M. E., Daniell, T. J. & Baggs, E. M. (2017a). Compound driven differences in N2 and N2O emission from soil; the role of substrate use efficiency and the microbial community. *Soil Biology and Biochemistry*, *106*, 90–98. https://doi.org/10.1016/j.soilbio.2016.11.028

Giles, M. E., Daniell, T. J. & Baggs, E. M. (2017b). Compound driven differences in N2 and N2O emission from soil; the role of substrate use efficiency and the microbial community. *Soil Biology and Biochemistry*, *106*, 90–98. https://doi.org/10.1016/j.soilbio.2016.11.028

Giles, M., Morley, N., Baggs, E. M. & Daniell, T. J. (2012). Soil nitrate reducing processes - Drivers, mechanisms for spatial variation, and significance for nitrous oxide production. *Frontiers in Microbiology*, *3*(DEC), 1–16. https://doi.org/10.3389/fmicb.2012.00407

Gingerich, D. J., Hanada, K., Shiu, S. H. & Vierstra, R. D. (2007). Large-scale, lineage-specific expansion of a bric-a-brac/tramtrack/broad complex ubiquitin-ligase gene family in rice. *Plant Cell*, *19*(8), 2329–2348. https://doi.org/10.1105/tpc.107.051300

Godfray, H. C. J., Beddington, J. R., Crute, I. R., Haddad, L., Lawrence, D., Muir, J. F., Pretty, J., Robinson, S., Thomas, S. M. & Toulmin, C. (2010). Food Security: The Challenge of Feeding 9 Billion People. *Science*, *327*(5967), 812–818. https://doi.org/10.1126/science.1185383

Gogoi, B. & Baruah, K. K. (2012). Nitrous Oxide Emissions from Fields with Different Wheat and Rice Varieties. *Pedosphere*, *22*(1), 112–121. https://doi.org/10.1016/S1002-0160(11)60197-5

Grabb, K. C., Buchwald, C., Hansel, C. M. & Wankel, S. D. (2017). A dual nitrite isotopic investigation of chemodenitrification by mineral-associated Fe(II) and its production of nitrous oxide. *Geochimica et Cosmochimica Acta*, *196*, 388–402. https://doi.org/10.1016/j.gca.2016.10.026

Graf, D. R. H., Jones, C. M. & Hallin, S. (2014). Intergenomic comparisons highlight modularity of the denitrification pathway and underpin the importance of community structure for N 2 O emissions. *PLoS ONE*. https://doi.org/10.1371/journal.pone.0114118

Graf, D. R. H., Zhao, M., Jones, C. M. & Hallin, S. (2016). Soil type overrides plant effect on genetic and enzymatic N2O production potential in arable soils. *Soil Biology and Biochemistry*, *100*, 125–128. https://doi.org/10.1016/j.soilbio.2016.06.006

Granger, J., Sigman, D. M., Needoba, J. A. & Harrison, P. J. (2004). Coupled nitrogen and oxygen isotope fractionation of nitrate during assimilation by cultures of marine phytoplankton. *Limnology and Oceanography*, *49*(5), 1763–1773. https://doi.org/10.4319/lo.2004.49.5.1763

Guigard, L., Jobert, L., Busset, N., Moulin, L. & Czernic, P. (2023). Symbiotic compatibility between rice cultivars and arbuscular mycorrhizal fungi genotypes affects rice growth and mycorrhiza-induced resistance. *Frontiers in Plant Science*, *14*(October), 1–17. https://doi.org/10.3389/fpls.2023.1278990

Hallin, S., Philippot, L., Löffler, F. E., Sanford, R. A. & Jones, C. M. (2018). Genomics and Ecology of Novel N 2 O-Reducing Microorganisms. *Trends in Microbiology*, *26*(1), 43–55. https://doi.org/10.1016/j.tim.2017.07.003

Han, B., Mo, L. Y., Fang, Y. T., Di, H. J., Wang, J. T., Shen, J. P. & Zhang, L. M. (2021). Rates and microbial communities of denitrification and anammox across coastal tidal flat lands and inland paddy soils in East China. *Applied Soil Ecology*, *157*(September 2020), 103768. https://doi.org/10.1016/j.apsoil.2020.103768

Hanviriyapant, P. & Fukai, S. (1997). Effects of fertiliser application and irrigation on grain yield of rice cultivars grown under lowland conditions. *ACIAR PROCEEDINGS SERIES*, *77*, 231–238.

Hartmann, H., Adams, H. D., Hammond, W. M., Hoch, G., Landhäusser, S. M., Wiley, E. & Zaehle, S. (2018). Identifying differences in carbohydrate dynamics of seedlings and mature trees to improve carbon allocation in models for trees and forests. *Environmental and Experimental Botany*, *152*(September 2017), 7–18. https://doi.org/10.1016/j.envexpbot.2018.03.011

Hawkesford, M. J. & Riche, A. B. (2020). Impacts of G x E x M on Nitrogen Use Efficiency in Wheat and Future Prospects. *FRONTIERS IN PLANT SCIENCE*, *11*. https://doi.org/10.3389/fpls.2020.01157

He, T., Zhang, X., Du, J., Gilliam, F. S., Yang, S., Tian, M., Zhang, C. & Zhou, Y. (2023). Arbuscular Mycorrhizal Fungi Shift Soil Bacterial Community Composition and Reduce Soil Ammonia Volatilization and Nitrous Oxide Emissions. *Microbial Ecology*, *85*(3), 951–964. https://doi.org/10.1007/s00248-023-02172-3

He, X., Xu, M., Qiu, G. Y. & Zhou, J. (2009). Use of 15N stable isotope to quantify nitrogen transfer between mycorrhizal plants. *Journal of Plant Ecology*, *2*(3), 107–118. https://doi.org/10.1093/jpe/rtp015

Hernandez, D. & Rowe, J. J. (1987). Oxygen regulation of nitrate uptake in denitrifying Pseudomonas aeruginosa. *Applied and Environmental Microbiology*. https://doi.org/10.1128/aem.53.4.745-750.1987

Herold, M. B., Giles, M. E., Alexander, C. J., Baggs, E. M. & Daniell, T. J. (2018). Variable response of nirK and nirS containing denitrifier communities to long-term pH manipulation and cultivation. *FEMS Microbiology Letters*, *365*(7), 1–6. https://doi.org/10.1093/femsle/fny035

Hofman G., O. V. C. (2004). Soil and Plant Nitrogen. *IFA, Paris, France*, *January 2004*, 31.

Hohmann, P., Schlaeppi, K. & Sessitsch, A. (2020). MiCROPe 2019 - Emerging research priorities towards microbe-assisted crop production. *FEMS Microbiology Ecology*, *96*(10), 1–7. https://doi.org/10.1093/femsec/fiaa177

Holliday, V. T. (1990). Methods of soil analysis, part 1, physical and mineralogical methods (2nd edition), A. Klute, Ed., 1986, American Society of Agronomy, Agronomy Monographs 9(1), Madison, Wisconsin, 1188 pp., \$60.00. *Geoarchaeology*, *5*(1), 87–89. https://doi.org/https://doi.org/10.1002/gea.3340050110

Hollocher, T. C., Tate, M. E. & Nicholas, D. J. (1981). Oxidation of ammonia by Nitrosomonas europaea. Definite 18O-tracer evidence that hydroxylamine formation involves a monooxygenase. *Journal of Biological Chemistry*, *256*(21), 10834–10836.

Hou, P., Xue, L., Wang, J., Petropoulos, E., Deng, X., Qiao, J., Xue, L. & Yang, L. (2022). Continuous milk vetch amendment in rice-fallow rotation improves soil fertility and maintains rice yield without increasing CH4 emissions: Evidence from a long-term experiment. *Agriculture, Ecosystems and Environment*, *325*(November 2021), 107774.

https://doi.org/10.1016/j.agee.2021.107774

Hou, S., Ai, C., Zhou, W., Liang, G. & He, P. (2018). Structure and assembly cues for rhizospheric nirK- and nirS-type denitrifier communities in long-term fertilized soils. *Soil Biology and Biochemistry*, *119*(12), 32–40. https://doi.org/10.1016/j.soilbio.2018.01.007

Hu, Xiaojin, Xie, J., Xie, H., Huo, J., Wu, H., Hu, Z., Xue, K., Song, M., Liang, S. & Zhang, J. (2023). Towards a better and more complete understanding of microbial nitrogen transformation processes in the rhizosphere of subsurface flow constructed wetlands: Effect of plant root activities. *Chemical Engineering Journal*, *463*(March), 142455. https://doi.org/10.1016/j.cej.2023.142455

Hu, Xingming, Qian, Q., Xu, T., Zhang, Y., Dong, G., Gao, T., Xie, Q. & Xue, Y. (2013). The U-Box E3 Ubiquitin Ligase TUD1 Functions with a Heterotrimeric G α Subunit to Regulate Brassinosteroid-Mediated Growth in Rice. *PLoS Genetics*, *9*(3). https://doi.org/10.1371/journal.pgen.1003391

Huang, R., Wang, Y., Liu, J., Li, J., Xu, G., Luo, M., Xu, C., Ci, E. & Gao, M. (2019). Variation in N 2 O emission and N 2 O related microbial functional genes in straw- and biochar-amended and non-amended soils. *Applied Soil Ecology*, *137*(2), 57–68. https://doi.org/10.1016/j.apsoil.2019.01.010

Huffman, D. L. & Halloran, T. V. O. (2001). *Function and mechanism of organic anion exudation from plant roots*. 677–701.

Jahangir, M. M. R., Minet, E. P., Johnston, P., Premrov, A., Coxon, C. E., Hackett, R. & Richards, K. G. (2014). Mustard catch crop enhances denitrification in shallow groundwater beneath a spring barley field. *Chemosphere*, *103*, 234–239. https://doi.org/10.1016/j.chemosphere.2013.11.072

Jain, M., Nijhawan, A., Arora, R., Agarwal, P., Ray, S., Sharma, P., Kapoor, S., Tyagi, A. K. & Khurana, J. P. (2007). F-Box proteins in rice. Genome-wide analysis, classification, temporal and spatial gene expression during panicle and seed development, and regulation by light and abiotic stress. *Plant Physiology*, *143*(4), 1467–1483. https://doi.org/10.1104/pp.106.091900

Janssens-Maenhout, G., Crippa, M., Guizzardi, D., Muntean, M., Schaaf, E., Dentener, F.,

Bergamaschi, P., Pagliari, V., Olivier, J. G. J., Peters, J. A. H. W., Van Aardenne, J. A., Monni, S., Doering, U., Roxana Petrescu, A. M., Solazzo, E. & Oreggioni, G. D. (2019). EDGAR v4.3.2 Global Atlas of the three major greenhouse gas emissions for the period 1970-2012. *Earth System Science Data*, *11*(3), 959–1002. https://doi.org/10.5194/essd-11-959-2019

Jantapo, K., Wimonchaijit, W., Wang, W. & Chaiwanon, J. (2021). Supraoptimal brassinosteroid levels inhibit root growth by reducing root meristem and cell elongation in rice. *Plants*, *10*(9), 1–14. https://doi.org/10.3390/plants10091962

Jayaweera, G. R. & Mikkelsen, D. S. (1991). *Assessment Of Ammonia Volatilization From Flooded Soil Systems* (N. C. Brady (ed.); Vol. 45, pp. 303–356). Academic Press. https://doi.org/https://doi.org/10.1016/S0065-2113(08)60044-9

Jetten, M. S. M., Niftrik, L. Van, Strous, M., Kartal, B., Keltjens, J. T. & Op Den Camp, H. J. M. (2009). Biochemistry and molecular biology of anammox bacteria biochemistry and molecular biology of anammox bacteria. *Critical Reviews in Biochemistry and Molecular Biology*, *44*(2–3), 65–84. https://doi.org/10.1080/10409230902722783

Jiang, Y., Carrijo, D., Huang, S., Chen, J., Balaine, N., Zhang, W., van Groenigen, K. J. & Linquist, B. (2019). Water management to mitigate the global warming potential of rice systems: A global meta-analysis. *Field Crops Research*, *234*(February), 47–54. https://doi.org/10.1016/j.fcr.2019.02.010

Jiang, Y., Huang, X., Zhang, X., Zhang, X., Zhang, Y., Zheng, C., Deng, A., Zhang, J., Wu, L., Hu, S. & Zhang, W. (2016). Optimizing rice plant photosynthate allocation reduces N 2 O emissions from paddy fields. *Scientific Reports*, *6*(July), 1–9. https://doi.org/10.1038/srep29333

Jindo, K., Audette, Y., Higashikawa, F. S., Silva, C. A., Akashi, K., Mastrolonardo, G., Sánchez-Monedero, M. A. & Mondini, C. (2020). Role of biochar in promoting circular economy in the agriculture sector. Part 1: A review of the biochar roles in soil N, P and K cycles. *Chemical and Biological Technologies in Agriculture*, *7*(1), 1–12. https://doi.org/10.1186/s40538-020-00182-8

Jing, W., Wu, H., Gu, H., Xiao, Z., Wang, W., Zhang, W., Gu, J., Liu, L., Wang, Z., Zhang, J.,

Yang, J. & Zhang, H. (2022). Response of Grain Yield and Water Use Efficiency to Irrigation Regimes during Mid-Season indica Rice Genotype Improvement. *Agriculture (Switzerland)*, *12*(10). https://doi.org/10.3390/agriculture12101647

Jinping Deng, Lingyao Kong, Yinhua Zhu, Dan Pei, Xuexue Chen, Yu Wang1, Junsheng Qi, Chunpeng Song, S. Y. and Z. G. (n.d.). *BAK1 plays contrasting roles in regulating abscisic acid-induced stomatal closure and abscisic acid- inhibited primary root growth in Arabidopsis*.

Joachim Arend, Heribert Warzecha, Tobias Hefner, J. S. (n.d.). *Utilizing genetically engineered bacteria to produce plant-specific glucosides*.

Jones, C. M., Graf, D. R. H., Bru, D., Philippot, L. & Hallin, S. (2013). The unaccounted yet abundant nitrous oxide-reducing microbial community: A potential nitrous oxide sink. *ISME Journal*, *7*(2), 417–426. https://doi.org/10.1038/ismej.2012.125

Jones, C. M., Stres, B., Rosenquist, M. & Hallin, S. (2008). Phylogenetic analysis of nitrite, nitric oxide, and nitrous oxide respiratory enzymes reveal a complex evolutionary history for denitrification. *Molecular Biology and Evolution*, *25*(9), 1955–1966. https://doi.org/10.1093/molbev/msn146

Jones, L. C., Peters, B., Lezama Pacheco, J. S., Casciotti, K. L. & Fendorf, S. (2015). Stable isotopes and iron oxide mineral products as markers of chemodenitrification. *Environmental Science and Technology*, *49*(6), 3444–3452. https://doi.org/10.1021/es504862x

Kakuda, K. I., Ando, H. & Konno, T. (2000). Contribution of nitrogen absorption by rice plants and nitrogen immobilization enhanced by plant growth to the reduction of nitrogen loss through denitrification in rhizosphere soil. *Soil Science and Plant Nutrition*, *46*(3), 601–610. https://doi.org/10.1080/00380768.2000.10409125

Kaler, A. S. & Purcell, L. C. (2019). Estimation of a significance threshold for genome-wide association studies. *BMC Genomics*, *20*(1), 1–8. https://doi.org/10.1186/s12864-019-5992-7

Kanter, D., Mauzerall, D. L., Ravishankara, A. R., Daniel, J. S., Portmann, R. W., Grabiel, P. M., Moomaw, W. R. & Galloway, J. N. (2013). A post-Kyoto partner: Considering the

stratospheric ozone regime as a tool to manage nitrous oxide. *Proceedings of the National Academy of Sciences*, *110*(12), 4451–4457. https://doi.org/10.1073/pnas.1222231110

Kartal, B., De Almeida, N. M., Maalcke, W. J., Op den Camp, H. J. M., Jetten, M. S. M. & Keltjens, J. T. (2013). How to make a living from anaerobic ammonium oxidation. *FEMS Microbiology Reviews*, *37*(3), 428–461. https://doi.org/10.1111/1574-6976.12014

Kartal, B., Kuypers, M. M. M., Lavik, G., Schalk, J., Op Den Camp, H. J. M., Jetten, M. S. M. & Strous, M. (2007). Anammox bacteria disguised as denitrifiers: Nitrate reduction to dinitrogen gas via nitrite and ammonium. *Environmental Microbiology*, *9*(3), 635–642. https://doi.org/10.1111/j.1462-2920.2006.01183.x

Kartal, B., Maalcke, W. J., De Almeida, N. M., Cirpus, I., Gloerich, J., Geerts, W., Op Den Camp, H. J. M., Harhangi, H. R., Janssen-Megens, E. M., Francoijs, K. J., Stunnenberg, H. G., Keltjens, J. T., Jetten, M. S. M. & Strous, M. (2011). Molecular mechanism of anaerobic ammonium oxidation. *Nature*, *479*(7371), 127–130. https://doi.org/10.1038/nature10453

Kawai, M., Samarajeewa, P. K., Barrero, R. A., Nishiguchi, M. & Uchimiya, H. (1998). Cellular dissection of the degradation pattern of cortical cell death during aerenchyma formation of rice roots. *Planta*, *204*(3), 277–287. https://doi.org/10.1007/s004250050257

Kern, M. & Simon, J. (2009). Electron transport chains and bioenergetics of respiratory nitrogen metabolism in Wolinella succinogenes and other Epsilonproteobacteria. *Biochimica et Biophysica Acta - Bioenergetics*, *1787*(6), 646–656. https://doi.org/10.1016/j.bbabio.2008.12.010

Khan, M. M. H., Rafii, M. Y., Ramlee, S. I., Jusoh, M. & Al Mamun, M. (2021). AMMI and GGE biplot analysis for yield performance and stability assessment of selected Bambara groundnut (Vigna subterranea L. Verdc.) genotypes under the multi-environmental trails (METs). *Scientific Reports*, *11*(1), 1–17. https://doi.org/10.1038/s41598-021-01411-2

Kikuchi, K., Ueguchi-Tanaka, M., Yoshida, K. T., Nagato, Y., Matsusoka, M. & Hirano, H. Y. (2000). Molecular analysis of the NAC gene family in rice. *Molecular and General Genetics*, *262*(6), 1047–1051. https://doi.org/10.1007/PL00008647

Kim, J. H., Lim, S. D., Jung, K. H. & Jang, C. S. (2023). Overexpression of a C3HC4-type

RING E3 ligase gene, OsRFPHC-13, improves salinity resistance in rice, Oryza sativa, by altering the expression of Na+/K+ transporter genes. *Environmental and Experimental Botany*, *207*(August 2022), 105224. https://doi.org/10.1016/j.envexpbot.2023.105224

Kim, S. Y., Pramanik, P., Bodelier, P. L. E. & Kim, P. J. (2014). Cattle manure enhances methanogens diversity and methane emissions compared to swine manure under rice paddy. *PLoS ONE*, *9*(12), 1–18. https://doi.org/10.1371/journal.pone.0113593

Klawonn, I., Bonaglia, S., Brüchert, V. & Ploug, H. (2015). Aerobic and anaerobic nitrogen transformation processes in N2-fixing cyanobacterial aggregates. *ISME Journal*, *9*(6), 1456–1466. https://doi.org/10.1038/ismej.2014.232

Klemedtsson, L., Simkins, S., Svensson, B. H., Johnsson, H. & Rosswall, T. (1991). Soil denitrification in three cropping systems characterized by differences in nitrogen and carbon supply. *Plant and Soil*. https://doi.org/10.1007/bf00012254

Klemedtsson, L., Svensson, B. H. & Rosswall, T. (1987). Dinitrogen and nitrous oxide produced by denitrification and nitrification in soil with and without barley plants. *Plant and Soil*. https://doi.org/10.1007/BF02370877

Klinnawee, L., Noirungsee, N., Nopphakat, K., Runsaeng, P. & Chantarachot, T. (2021). Flooding overshadows phosphorus availability in controlling the intensity of arbuscular mycorrhizal colonization in Sangyod Muang Phatthalung lowland indica rice. *ScienceAsia*, *47*(2), 202–210. https://doi.org/10.2306/SCIENCEASIA1513-1874.2021.025

Knowles, R. (1982). Denitrification. In *Microbiological Reviews*. https://doi.org/10.1128/mmbr.46.1.43-70.1982

Kögel-Knabner, I., Amelung, W., Cao, Z., Fiedler, S., Frenzel, P., Jahn, R., Kalbitz, K., Kölbl, A. & Schloter, M. (2010). Biogeochemistry of paddy soils. *Geoderma*, *157*(1–2), 1–14. https://doi.org/10.1016/j.geoderma.2010.03.009

Kool, D. M., Dolfing, J., Wrage, N. & Van Groenigen, J. W. (2011). Nitrifier denitrification as a distinct and significant source of nitrous oxide from soil. *Soil Biology and Biochemistry*, *43*(1), 174–178. https://doi.org/10.1016/j.soilbio.2010.09.030

Kotula, L., Ranathunge, K., Schreiber, L. & Steudle, E. (2009). *Functional and chemical comparison of apoplastic barriers to radial oxygen loss in roots of rice (Oryza sativa L .) grown in aerated or deoxygenated solution*. *60*(7), 2155–2167. https://doi.org/10.1093/jxb/erp089

Kowalchuk, G. A. & Stephen, J. R. (2001). Ammonia-oxidizing bacteria: A model for molecular microbial ecology. *Annual Review of Microbiology*, *55*, 485–529. https://doi.org/10.1146/annurev.micro.55.1.485

Kulichikhin, K., Yamauchi, T., Watanabe, K. & Nakazono, M. (2014). Biochemical and molecular characterization of rice (Oryza sativaL.) roots forming a barrier to radial oxygen loss. *Plant Cell and Environment*, *37*(10), 2406–2420. https://doi.org/10.1111/pce.12294

Kuypers, M. M. M., Marchant, H. K. & Kartal, B. (2018). The microbial nitrogen-cycling network. *Nature Reviews Microbiology*, *16*(5), 263–276. https://doi.org/10.1038/nrmicro.2018.9

Lai, W., Zhang, Y. & Chen, Z. (2012). Radial oxygen loss , photosynthesis , and nutrient removal of 35 wetland plants. *Ecological Engineering*, *39*, 24–30. https://doi.org/10.1016/j.ecoleng.2011.11.010

Langarica-Fuentes, A., Manrubia, M., Giles, M. E., Mitchell, S. & Daniell, T. J. (2018a). Effect of model root exudate on denitrifier community dynamics and activity at different water-filled pore space levels in a fertilised soil. *Soil Biology and Biochemistry*, *120*(3), 70–79. https://doi.org/10.1016/j.soilbio.2018.01.034

Langarica-Fuentes, A., Manrubia, M., Giles, M. E., Mitchell, S. & Daniell, T. J. (2018b). Effect of model root exudate on denitrifier community dynamics and activity at different water-filled pore space levels in a fertilised soil. *Soil Biology and Biochemistry*, *120*(August 2017), 70–79. https://doi.org/10.1016/j.soilbio.2018.01.034

Lawson, C. E., Nuijten, G. H. L., de Graaf, R. M., Jacobson, T. B., Pabst, M., Stevenson, D. M., Jetten, M. S. M., Noguera, D. R., McMahon, K. D., Amador-Noguez, D. & Lücker, S. (2021). Autotrophic and mixotrophic metabolism of an anammox bacterium revealed by in vivo 13C and 2H metabolic network mapping. *ISME Journal*, *15*(3), 673–687. https://doi.org/10.1038/s41396-020-00805-w

Lee, J., Choi, S., Lee, Y. & Kim, S. Y. (2021). Impact of manure compost amendments on NH3 volatilization in rice paddy ecosystems during cultivation. *Environmental Pollution*, *288*(July), 117726. https://doi.org/10.1016/j.envpol.2021.117726

Levy-Booth, D. J., Prescott, C. E. & Grayston, S. J. (2014). Microbial functional genes involved in nitrogen fixation, nitrification and denitrification in forest ecosystems. *Soil Biology and Biochemistry*, *75*(September 2017), 11–25. https://doi.org/10.1016/j.soilbio.2014.03.021

Li, Hu, Yang, X., Weng, B., Su, J., Nie, S., Gilbert, J. A. & Zhu, Y. G. (2016). The phenological stage of rice growth determines anaerobic ammonium oxidation activity in rhizosphere soil. *Soil Biology and Biochemistry*, *100*, 59–65. https://doi.org/10.1016/j.soilbio.2016.05.015

Li, Huilin, Han, Y. & Cai, Z. (2003). Nitrogen mineralization in paddy soils of the Taihu Region of China under anaerobic conditions: Dynamics and model fitting. *Geoderma*, *115*(3–4), 161–175. https://doi.org/10.1016/S0016-7061(02)00358-0

Li, Y. L., Fan, X. R. & Shen, Q. R. (2008). The relationship between rhizosphere nitrification and nitrogen-use efficiency in rice plants. *Plant, Cell and Environment*. https://doi.org/10.1111/j.1365-3040.2007.01737.x

Li, Y. & Wang, X. (2013). Root-induced changes in radial oxygen loss, rhizosphere oxygen profile, and nitrification of two rice cultivars in Chinese red soil regions. *Plant and Soil*, *365*(1–2), 115–126. https://doi.org/10.1007/s11104-012-1378-1

Liang, H., Xu, J., Hou, H., Qi, Z., Yang, S., Li, Y. & Hu, K. (2022). Modeling CH4 and N2O emissions for continuous and noncontinuous flooding rice systems. *Agricultural Systems*, *203*(July), 103528. https://doi.org/10.1016/j.agsy.2022.103528

Liao, P., Sun, Y., Zhu, X., Wang, H., Wang, Y., Chen, J., Zhang, J., Zeng, Y., Zeng, Y. & Huang, S. (2021). Identifying agronomic practices with higher yield and lower global warming potential in rice paddies: a global meta-analysis. *Agriculture, Ecosystems and Environment*, *322*(June), 107663. https://doi.org/10.1016/j.agee.2021.107663

Lim, N. Y. N., Frostegård, Å. & Bakken, L. R. (2018). Nitrite kinetics during anoxia: The role of abiotic reactions versus microbial reduction. *Soil Biology and Biochemistry*,

119(November 2017), 203–209. https://doi.org/10.1016/j.soilbio.2018.01.006

Lin, C., Zhu, T., Ogorek, L. L. P., Wang, Y., Sauter, M. & Pedersen, O. (2022). The Pyramiding of Three Key Root Traits Aid Breeding of Flood-Tolerant Rice. *Plants*, *11*(15), 1–10. https://doi.org/10.3390/plants11152033

Linquist, B., Van Groenigen, K. J., Adviento-Borbe, M. A., Pittelkow, C. & Van Kessel, C. (2012). An agronomic assessment of greenhouse gas emissions from major cereal crops. *Global Change Biology*, *18*(1), 194–209. https://doi.org/10.1111/j.1365-2486.2011.02502.x

Liu, D., Zhang, X., Li, Q., Xiao, Y., Zhang, G., Yin, W., Niu, M., Meng, W., Dong, N., Liu, J., Yang, Y., Xie, Q., Chu, C. & Tong, H. (2022). The U-box ubiquitin ligase TUD1 promotes brassinosteroid-induced GSK2 degradation in rice. *Plant Communications*, *4*(2), 100450. https://doi.org/10.1016/j.xplc.2022.100450

Liu, H., Ding, Y., Zhang, Q., Liu, X., Xu, J., Li, Y. & Di, H. (2019). Heterotrophic nitrification and denitrification are the main sources of nitrous oxide in two paddy soils. *Plant and Soil*, *445*(1–2), 39–53. https://doi.org/10.1007/s11104-018-3860-x

Liu, J., Han, J., Zhu, C., Cao, W., Luo, Y., Zhang, M., Zhang, S., Jia, Z., Yu, R., Zhao, J. & Bao, Z. (2021). Elevated Atmospheric CO2 and Nitrogen Fertilization Affect the Abundance and Community Structure of Rice Root-Associated Nitrogen-Fixing Bacteria. *Frontiers in Microbiology*, *12*(April). https://doi.org/10.3389/fmicb.2021.628108

Liu, L., Zhang, X., Xu, W., Liu, X., Li, Y., Wei, J., Wang, Z. & Lu, X. (2020). Ammonia volatilization as the major nitrogen loss pathway in dryland agro-ecosystems. *Environmental Pollution*, *265*. https://doi.org/10.1016/j.envpol.2020.114862

Liu, X., Zhang, Y., Han, W., Tang, A., Shen, J., Cui, Z., Vitousek, P., Erisman, J. W., Goulding, K., Christie, P., Fangmeier, A. & Zhang, F. (2013). Enhanced nitrogen deposition over China. *Nature*, *494*(7438), 459–462. https://doi.org/10.1038/nature11917

Liu, Y., Ge, T., van Groenigen, K. J., Yang, Y., Wang, P., Cheng, K., Zhu, Z., Wang, J., Li, Y., Guggenberger, G., Sardans, J., Penuelas, J., Wu, J. & Kuzyakov, Y. (2021). Rice paddy soils are a quantitatively important carbon store according to a global synthesis. *Communications Earth and Environment*, *2*(1). https://doi.org/10.1038/s43247-021-

00229-0

Long, A., Heitman, J., Tobias, C., Philips, R. & Song, B. (2013). Co-occurring anammox, denitrification, and codenitrification in agricultural soils. *Applied and Environmental Microbiology*, *79*(1), 168–176. https://doi.org/10.1128/AEM.02520-12

Lu, Yahai, Watanabe, A. & Kimura, M. (2002). Contribution of plant-derived carbon to soil microbial biomass dynamics in a paddy rice microcosm. *Biology and Fertility of Soils*, *36*(2), 136–142. https://doi.org/10.1007/s00374-002-0504-2

Lu, Yufang, Zhang, X., Jiang, J., Kronzucker, H. J., Shen, W. & Shi, W. (2019). Effects of the biological nitrification inhibitor 1,9-decanediol on nitrification and ammonia oxidizers in three agricultural soils. *Soil Biology and Biochemistry*. https://doi.org/10.1016/j.soilbio.2018.11.008

Lu, Yufang, Zhang, X., Ma, M., Zu, W., Kronzucker, H. J. & Shi, W. (2022). Syringic acid from rice as a biological nitrification and urease inhibitor and its synergism with 1,9-decanediol. *Biology and Fertility of Soils*, *58*(3), 277–289. https://doi.org/10.1007/s00374-021-01584-y

Lycus, P., Bøthun, K. L., Bergaust, L., Shapleigh, J. P., Bakken, L. R. & Frostegård, Å. (2017). Phenotypic and genotypic richness of denitrifiers revealed by a novel isolation strategy. *ISME Journal*, *11*(10), 2219–2232. https://doi.org/10.1038/ismej.2017.82

Ma, K., Xiao, J., Li, X., Zhang, Q. & Lian, X. (2009). Sequence and expression analysis of the C3HC4-type RING finger gene family in rice. *Gene*, *444*(1–2), 33–45. https://doi.org/10.1016/j.gene.2009.05.018

Majumdar, D. (2003). Methane and nitrous oxide emission from irrigated rice fields: Proposed mitigation strategies. *Current Science*, *84*(10), 1317–1326.

Mannerheim, N., Blessing, C. H., Oren, I., Grünzweig, J. M., Bachofen, C. & Buchmann, N. (2020). Carbon allocation to the root system of tropical tree Ceiba pentandra using 13C pulse labelling in an aeroponic facility. *Tree Physiology*, *40*(3), 350–366. https://doi.org/10.1093/treephys/tpz142

Mansueto, L., Fuentes, R. R., Borja, F. N., Detras, J., Abrio-Santos, J. M., Chebotarov, D.,

Sanciangco, M., Palis, K., Copetti, D., Poliakov, A., Dubchak, I., Solovyev, V., Wing, R. A., Hamilton, R. S., Mauleon, R., McNally, K. L. & Alexandrov, N. (2017). Rice SNP-seek database update: New SNPs, indels, and queries. *Nucleic Acids Research*, *45*(D1), D1075–D1081. https://doi.org/10.1093/nar/gkw1135

Manzoni, S. & Porporato, A. (2009). Soil carbon and nitrogen mineralization: Theory and models across scales. *Soil Biology and Biochemistry*, *41*(7), 1355–1379. https://doi.org/https://doi.org/10.1016/j.soilbio.2009.02.031

Mazzei, L., Cianci, M. & Ciurli, S. (2022). Inhibition of Urease by Hydroquinones: A Structural and Kinetic Study. *Chemistry - A European Journal*, *28*(64). https://doi.org/10.1002/chem.202201770

McCarthy, M. C. & Enquist, B. J. (2007). Consistency between an allometric approach and optimal partitioning theory in global patterns of plant biomass allocation. *Functional Ecology*, *21*(4), 713–720. https://doi.org/10.1111/j.1365-2435.2007.01276.x

Meijide, A., Gruening, C., Goded, I., Seufert, G. & Cescatti, A. (2017). Water management reduces greenhouse gas emissions in a Mediterranean rice paddy field. *Agriculture, Ecosystems and Environment*, *238*, 168–178. https://doi.org/10.1016/j.agee.2016.08.017

Meng, X., Li, Y., Yao, H., Wang, J., Dai, F., Wu, Y. & Chapman, S. (2020). Nitrification and urease inhibitors improve rice nitrogen uptake and prevent denitrification in alkaline paddy soil. *Applied Soil Ecology*, *154*(June 2019), 103665. https://doi.org/10.1016/j.apsoil.2020.103665

Miao Yuan Wang, M. Yaeesh Siddiqi, Thomas J. Ruth, A. D. M. G. (1993). Ammonium Uptake by Rice Roots: II. Kinetics of 13NH+4 Influx across the Plasmalemma. *Plant Physiology*, *103*(4), 1259–1267. https://doi.org/10.1093/ITNOW/BWAA110

Milkha S. Aulukh, Reiner Wassmann, C. B. and H. R. (2001). Impact of root exudates of different cultivars and plant development stages of rice (Oryza sativa L.) on methane production in a paddy soil. *Plant and Soil*, *230*, 77–86.

Miranda, K. M. (2001). The chemistry of nitroxyl (HNO) and implications in biology. *Coordination Chemistry Reviews*, *249*(3-4 SPEC. ISS.), 433–455. https://doi.org/10.1016/j.ccr.2004.08.010

Moreau, D., Bardgett, R. D., Finlay, R. D., Jones, D. L. & Philippot, L. (2019a). A plant perspective on nitrogen cycling in the rhizosphere. *Functional Ecology*, *33*(4), 540–552. https://doi.org/10.1111/1365-2435.13303

Moreau, D., Bardgett, R. D., Finlay, R. D., Jones, D. L. & Philippot, L. (2019b). A plant perspective on nitrogen cycling in the rhizosphere. *Functional Ecology*, *33*(4), 540–552. https://doi.org/10.1111/1365-2435.13303

Moreno, F., Cayuela, J. A., Fernández, J. E., Fernández-Boy, E., Murillo, J. M. & Cabrera, F. (1996). Water balance and nitrate leaching in an irrigated maize crop in SW Spain. *Agricultural Water Management*, *32*(1), 71–83. https://doi.org/10.1016/S0378-3774(96)01256-5

Morley, N. & Baggs, E. M. (2010). Carbon and oxygen controls on N2O and N2 production during nitrate reduction. *Soil Biology and Biochemistry*, *42*(10), 1864–1871. https://doi.org/10.1016/j.soilbio.2010.07.008

Morley, N. J., Richardson, D. J. & Baggs, E. M. (2014). Substrate induced denitrification over or under estimates shifts in soil N2/N2O ratios. *PLoS ONE*, *9*(9), 1–6. https://doi.org/10.1371/journal.pone.0108144

Mulder, A., van de Graaf, A. A., Robertson, L. A. & Kuenen, J. G. (1995). Anaerobic ammonium oxidation discovered in a denitrifying fluidized bed reactor. *FEMS Microbiology Ecology*, *16*(3), 177–183. https://doi.org/10.1016/0168-6496(94)00081-7

Nie, San'An, Li, H., Yang, X., Zhang, Z., Weng, B., Huang, F., Zhu, G. B. & Zhu, Y. G. (2015). Nitrogen loss by anaerobic oxidation of ammonium in rice rhizosphere. *ISME Journal*, *9*(9), 2059–2067. https://doi.org/10.1038/ismej.2015.25

Nie, San'an, Zhu, G. B., Singh, B. & Zhu, Y. G. (2019). Anaerobic ammonium oxidation in agricultural soils-synthesis and prospective. In *Environmental Pollution*. https://doi.org/10.1016/j.envpol.2018.10.050

Nielsen, L. P. (1992). Denitrification in sediment determined from nitrogen isotope pairing. *FEMS Microbiology Letters*, *86*(4), 357–362. https://doi.org/10.1111/j.1574-6968.1992.tb04828.x

Nikiema, D., Sawadogo, N. & Sie, M. (2023). Genotype and irrigation regime interaction on agronomic traits of irrigated rice varieties cultivated in Burkina Faso. *Tropical Agriculture.*, *100*(3), 163–181.

Nini Ma , Nian Li , Zhongmao Yu , Chunli Chen , Dao-Xiu Zhou, and Y. Z. (n.d.). *The F-box protein SHORT PRIMARY ROOT modulates primary root meristem activity by targeting SEUSS-LIKE.pdf*.

Nojiri, Y., Kaneko, Y., Azegami, Y., Shiratori, Y., Ohte, N., Senoo, K., Otsuka, S. & Isobe, K. (2020). Dissimilatory nitrate reduction to ammonium and responsible microbes in japanese rice paddy soil. *Microbes and Environments*, *35*(4), 1–7. https://doi.org/10.1264/jsme2.ME20069

Norton, G. J., Travis, A. J., Douglas, A., Fairley, S., Alves, E. D. P., Ruang-areerate, P., Naredo, M. E. B., McNally, K. L., Hossain, M., Islam, M. R. & Price, A. H. (2018). Genome wide association mapping of grain and straw biomass traits in the rice bengal and assam aus panel (baap) grown under alternate wetting and drying and permanently flooded irrigation. *Frontiers in Plant Science*, *9*(September), 1–18. https://doi.org/10.3389/fpls.2018.01223

Oladosu, Y., Rafii, M. Y., Abdullah, N., Magaji, U., Miah, G., Hussin, G. & Ramli, A. (2017). Genotype × Environment interaction and stability analyses of yield and yield components of established and mutant rice genotypes tested in multiple locations in Malaysia*. *Acta Agriculturae Scandinavica Section B: Soil and Plant Science*, *67*(7), 590–606. https://doi.org/10.1080/09064710.2017.1321138

Otte, J. M., Blackwell, N., Ruser, R., Kappler, A., Kleindienst, S. & Schmidt, C. (2019). N2O formation by nitrite-induced (chemo)denitrification in coastal marine sediment. *Scientific Reports*, *9*(1), 10691. https://doi.org/10.1038/s41598-019-47172-x

Oyserman, B. O., Cordovez, V., Flores, S. S., Leite, M. F. A., Nijveen, H., Medema, M. H. & Raaijmakers, J. M. (2021). Extracting the GEMs: Genotype, Environment, and Microbiome Interactions Shaping Host Phenotypes. *Frontiers in Microbiology*, *11*(January), 1–8. https://doi.org/10.3389/fmicb.2020.574053

Pan, B., Lam, S. K., Mosier, A., Luo, Y. & Chen, D. (2016). Ammonia volatilization from synthetic fertilizers and its mitigation strategies: A global synthesis. *Agriculture,*

Ecosystems and Environment, *232*, 283–289. https://doi.org/10.1016/j.agee.2016.08.019

Pandey, A., Suter, H., He, J. Z., Hu, H. W. & Chen, D. (2018a). Nitrogen addition decreases dissimilatory nitrate reduction to ammonium in rice paddies. *Applied and Environmental Microbiology*, *84*(17), 1–14. https://doi.org/10.1128/AEM.00870-18

Pandey, A., Suter, H., He, J. Z., Hu, H. W. & Chen, D. (2018b). Nitrogen addition decreases dissimilatory nitrate reduction to ammonium in rice paddies. *Applied and Environmental Microbiology*, *84*(17), 1–14. https://doi.org/10.1128/AEM.00870-18

Pandey, A., Suter, H., He, J. Z., Hu, H. W. & Chen, D. (2019). Dissimilatory nitrate reduction to ammonium dominates nitrate reduction in long-term low nitrogen fertilized rice paddies. *Soil Biology and Biochemistry*. https://doi.org/10.1016/j.soilbio.2019.01.007

Pandey, C. B., Kumar, U., Kaviraj, M., Minick, K. J., Mishra, A. K. & Singh, J. S. (2020). DNRA: A short-circuit in biological N-cycling to conserve nitrogen in terrestrial ecosystems. *Science of the Total Environment*, *738*, 139710. https://doi.org/10.1016/j.scitotenv.2020.139710

Pearse, S. J., Veneklaas, E. J., Cawthray, G. R., Bolland, M. D. A. & Lambers, H. (2006). Carboxylate release of wheat, canola and 11 grain legume species as affected by phosphorus status. *Plant and Soil*, *288*(1–2), 127–139. https://doi.org/10.1007/s11104-006-9099-y

Peralta Ogorek, L. L., Takahashi, H., Nakazono, M. & Pedersen, O. (2023). The barrier to radial oxygen loss protects roots against hydrogen sulphide intrusion and its toxic effect. *New Phytologist*, 1825–1837. https://doi.org/10.1111/nph.18883

Pett-Ridge, J., Silver, W. L. & Firestone, M. K. (2006). Redox fluctuations frame microbial community impacts on N-cycling rates in a humid tropical forest soil. *Biogeochemistry*, *81*(1), 95–110. https://doi.org/10.1007/s10533-006-9032-8

Philippot, L. (2006). Use of functional genes to quantify denitrifiers in the environment: Figure 1. *Biochemical Society Transactions*. https://doi.org/10.1042/bst0340101

Philippot, Laurent. (2002). Philippot 2002 Denitrifying genes in bacterial and Archaeal genomes. *Biochim. Biophys. Acta*, *1577*, 355–376.

Philippot, Laurent, Čuhel, J., Saby, N. P. A., Chèneby, D., Chroňáková, A., Bru, D., Arrouays, D., Martin-Laurent, F. & Šimek, M. (2009). Mapping field-scale spatial patterns of size and activity of the denitrifier community. *Environmental Microbiology*. https://doi.org/10.1111/j.1462-2920.2009.01879.x

Piegu, B., Guyot, R., Picault, N., Roulin, A., Sanyal, A., Kim, H., Collura, K., Brar, D. S., Jackson, S., Wing, R. A. & Panaud, O. (2011). Doubling genome size without polyploidization: Dynamics of retrotransposition-driven genomic expansions in Oryza australiensis, a wild relative of rice (Genome Research (2006). *Genome Research*, *21*(7), 1201. https://doi.org/10.1101/gr.5290206.of

Premachandran, K. & Srinivasan, T. S. (2023). A brief review on oryzacystatin: a potent phytocystatin for crop management. *Molecular Biology Reports*, *50*(2), 1799–1807. https://doi.org/10.1007/s11033-022-08161-y

Prokopiou, M., Sapart, C. J., Rosen, J., Sperlich, P., Blunier, T., Brook, E., van de Wal, R. S. W. & Röckmann, T. (2018). Changes in the Isotopic Signature of Atmospheric Nitrous Oxide and Its Global Average Source During the Last Three Millennia. *Journal of Geophysical Research: Atmospheres*, *123*(18), 10,757-10,773. https://doi.org/10.1029/2018JD029008

Puri, G. & Ashman, M. R. (1999). Microbial immobilization of 15N-labelled ammonium and nitrate in a temperate woodland soil. *Soil Biology and Biochemistry*, *31*(6), 929–931. https://doi.org/10.1016/S0038-0717(98)00172-2

Putz, M., Schleusner, P., Rütting, T. & Hallin, S. (2018). Relative abundance of denitrifying and DNRA bacteria and their activity determine nitrogen retention or loss in agricultural soil. *Soil Biology and Biochemistry*, *123*. https://doi.org/10.1016/j.soilbio.2018.05.006

Qian, X., Shen, Q., Xu, G., Wang, J. & Zhou, M. (2004). Nitrogen form effects on yield and nitrogen uptake of rice crop grown in aerobic soil. *Journal of Plant Nutrition*, *27*(6), 1061–1076. https://doi.org/10.1081/PLN-120037536

Qiao, X., Zhang, L., Qiu, Z., Wang, L., Wu, Y., Deng, C., Su, J., Zhang, X., Wang, Y., Li, B., Zhou, L., Ma, A. Y. W., Zhuang, W. Q. & Yu, K. (2022). Specific Denitrifying and Dissimilatory Nitrate Reduction to Ammonium Bacteria Assisted the Recovery of

Anammox Community From Nitrite Inhibition. *Frontiers in Microbiology*, *12*(January), 1–13. https://doi.org/10.3389/fmicb.2021.781156

Qin, S., Hu, C., Clough, T. J., Luo, J., Oenema, O. & Zhou, S. (2017). Irrigation of DOC-rich liquid promotes potential denitrification rate and decreases N2O/(N2O+N2) product ratio in a 0–2 m soil profile. *Soil Biology and Biochemistry*, *106*, 1–8. https://doi.org/10.1016/j.soilbio.2016.12.001

Qin, Z., Huang, Y. & Zhuang, Q. (2013). Soil organic carbon sequestration potential of cropland in China. *Global Biogeochemical Cycles*, *27*(3), 711–722. https://doi.org/10.1002/gbc.20068

Qiu, H., Yang, S., Jiang, Z., Xu, Y. & Jiao, X. (2022). Effect of Irrigation and Fertilizer Management on Rice Yield and Nitrogen Loss: A Meta-Analysis. *Plants*, *11*(13). https://doi.org/10.3390/plants11131690

Ramanathan, V., Rahman, H., Subramanian, S., Nallathambi, J., Kaliyaperumal, A., Manickam, S., Ranganathan, C. & Raveendran, M. (2018). OsARD4 encoding an acireductone dioxygenase improves root architecture in rice by promoting development of secondary roots. *Scientific Reports*, *8*(1), 1–15. https://doi.org/10.1038/s41598-018-34053-y

Ramos, C., Varela, M. & Calvet, R. P. (1990). *Nitrate leaching in two irrigated fields in the region of Valencia (Spain).* https://api.semanticscholar.org/CorpusID:127619279

Raun, W. R. & Johnson, G. V. (1999). Improving nitrogen use efficiency for cereal production. *Agronomy Journal*, *91*(3), 357–363. https://doi.org/10.2134/agronj1999.00021962009100030001x

Rice, C. W. & Tiedje, J. M. (1989). Regulation of nitrate assimilation by ammonium in soils and in isolated soil microorganisms. *Soil Biology and Biochemistry*, *21*(4), 597–602. https://doi.org/10.1016/0038-0717(89)90135-1

Richardson, D., Felgate, H., Watmough, N., Thomson, A. & Baggs, E. (2009). Mitigating release of the potent greenhouse gas N2O from the nitrogen cycle - could enzymic regulation hold the key? *Trends in Biotechnology*, *27*(7), 388–397. https://doi.org/10.1016/j.tibtech.2009.03.009

Richardson, D. J. (2000). Bacterial respiration: a flexible process for a changing environment. *Microbiology (Reading, England)*, *146 (Pt 3*, 551–571. https://doi.org/10.1099/00221287-146-3-551

Robertson, G. P. & Groffman, P. M. (2006). Nitrogen transformations in soil. In *Soil Microbiology, Ecology and Biochemistry: Third Edition* (4th ed.). Elsevier Inc. https://doi.org/10.1016/b978-0-12-415955-6.00014-1

Robinson, D. (2001). δ15N as an integrator of the nitrogen cycle. *Trends in Ecology and Evolution*, *16*(3), 153–162. https://doi.org/10.1016/S0169-5347(00)02098-X

Romero, C. M., Engel, R., Chen, C. & Wallander, R. (2015). Microbial Immobilization of Nitrogen-15 Labelled Ammonium and Nitrate in an Agricultural Soil. *Soil Science Society of America Journal*, *79*(2), 595–602. https://doi.org/10.2136/sssaj2014.08.0332

Rummel, P. S., Well, R., Pfeiffer, B., Dittert, K., Floßmann, S. & Pausch, J. (2021). Nitrate uptake and carbon exudation – do plant roots stimulate or inhibit denitrification? *Plant and Soil*, *459*(1–2), 217–233. https://doi.org/10.1007/s11104-020-04750-7

Ryden, J. C., Lund, L. J. & Focht, D. D. (1979). Direct Measurement of Denitrification Loss from Soils: I. Laboratory Evaluation of Acetylene Inhibition of Nitrous Oxide Reduction. *Soil Science Society of America Journal*, *43*(1), 104–110. https://doi.org/https://doi.org/10.2136/sssaj1979.03615995004300010019x

S. Gao, K. K. Tanji, S. C. Scardaci, and A. T. C. (n.d.). *Comparison of Redox Indicators in a Paddy Soil during Rice-Growing Season*.

Sakamoto, T., Morinaka, Y., Ohnishi, T., Sunohara, H., Fujioka, S., Ueguchi-Tanaka, M., Mizutani, M., Sakata, K., Takatsuto, S., Yoshida, S., Tanaka, H., Kitano, H. & Matsuoka, M. (2006). Erect leaves caused by brassinosteroid deficiency increase biomass production and grain yield in rice. *Nature Biotechnology*, *24*(1), 105–109. https://doi.org/10.1038/nbt1173

Sanford, R. A., Wagner, D. D., Wu, Q., Chee-Sanford, J. C., Thomas, S. H., Cruz-García, C., Rodríguez, G., Massol-Deyá, A., Krishnani, K. K., Ritalahti, K. M., Nissen, S., Konstantinidis, K. T. & Löffler, F. E. (2012). Unexpected nondenitrifier nitrous oxide reductase gene diversity and abundance in soils. *Proceedings of the National Academy of*

Sciences of the United States of America. https://doi.org/10.1073/pnas.1211238109

Sato, Y., Ohta, H., Yamagishi, T., Guo, Y., Nishizawa, T., Habibur Rahman, M., Kuroda, H., Kato, T., Saito, M., Yoshinaga, I., Inubushi, K. & Suwa, Y. (2012). Detection of anammox activity and 16S rRNA genes in ravine paddy field soil. *Microbes and Environments*, *27*(3), 316–319. https://doi.org/10.1264/jsme2.ME11330

Schmidt-Rohr, K., Mao, J. D. & Olk, D. C. (2004). Nitrogen-bonded aromatics in soil organic matter and their implications for a yield decline in intensive rice cropping. *Proceedings of the National Academy of Sciences of the United States of America*, *101*(17), 6351–6354. https://doi.org/10.1073/pnas.0401349101

Schmidt, H.-L. & Medina, R. (1991). Possibilities and Scope of the Double Isotope Effect Method in the Elucidation of Mechanisms of Enzyme Catalyzed Reactions. *Isotopenpraxis Isotopes in Environmental and Health Studies*, *27*(1), 1–4. https://doi.org/10.1080/10256019108622450

Sebilo, M., Mayer, B., Nicolardot, B., Pinay, G. & Mariotti, A. (2013). Long-term fate of nitrate fertilizer in agricultural soils. *Proceedings of the National Academy of Sciences of the United States of America*, *110*(45), 18185–18189. https://doi.org/10.1073/pnas.1305372110

Senbayram, M, Chen, R., Budai, A., Bakken, L. & Dittert, K. (2012). N2O emission and the N2O/(N2O+N2) product ratio of denitrification as controlled by available carbon substrates and nitrate concentrations. *Agriculture, Ecosystems & Environment*, *147*, 4–12. https://doi.org/https://doi.org/10.1016/j.agee.2011.06.022

Senbayram, Mehmet, Budai, A., Bol, R., Chadwick, D., Marton, L., Gündogan, R. & Wu, D. (2019). Soil NO 3− level and O 2 availability are key factors in controlling N 2 O reduction to N 2 following long-term liming of an acidic sandy soil. *Soil Biology and Biochemistry*, *132*(3), 165–173. https://doi.org/10.1016/j.soilbio.2019.02.009

Shan, J., Yang, P., Shang, X., Rahman, M. M. & Yan, X. (2018). Anaerobic ammonium oxidation and denitrification in a paddy soil as affected by temperature, pH, organic carbon, and substrates. *Biology and Fertility of Soils*, *54*(3), 341–348. https://doi.org/10.1007/s00374-018-1263-z

Shearer, G. B. & Kohl, D. H. (1986). N2-Fixation in Field Settings: Estimations Based on Natural 15N Abundance. *Australian Journal of Plant Physiology*, *13*, 699–756. https://api.semanticscholar.org/CorpusID:84146700

Shimura, K., Okada, A., Okada, K., Jikumaru, Y., Ko, K. W., Toyomasu, T., Sassa, T., Hasegawa, M., Kodama, O., Shibuya, N., Koga, J., Nojiri, H. & Yamane, H. (2007). Identification of a biosynthetic gene cluster in rice for momilactones. *Journal of Biological Chemistry*, *282*(47), 34013–34018. https://doi.org/10.1074/jbc.M703344200

Shiono, K., Yamauchi, T., Yamazaki, S., Mohanty, B., Imran Malik, A., Nagamura, Y., Nishizawa, N. K., Tsutsumi, N., Colmer, T. D. & Nakazono, M. (2014). Microarray analysis of laser-microdissected tissues indicates the biosynthesis of suberin in the outer part of roots during formation of a barrier to radial oxygen loss in rice (Oryza sativa). *Journal of Experimental Botany*, *65*(17), 4795–4806. https://doi.org/10.1093/jxb/eru235

Shiono, K., Yoshikawa, M., Kreszies, T., Yamada, S., Hojo, Y., Matsuura, T., Mori, I. C., Schreiber, L. & Yoshioka, T. (2022). Abscisic acid is required for exodermal suberization to form a barrier to radial oxygen loss in the adventitious roots of rice (Oryza sativa). *New Phytologist*, *233*(2), 655–669. https://doi.org/10.1111/nph.17751

Šimek, M. & Cooper, J. E. (2002). The influence of soil pH on denitrification: Progress towards the understanding of this interaction over the last 50 years. *European Journal of Soil Science*. https://doi.org/10.1046/j.1365-2389.2002.00461.x

Simon, J. & Klotz, M. G. (2013). Diversity and evolution of bioenergetic systems involved in microbial nitrogen compound transformations. *Biochimica et Biophysica Acta - Bioenergetics*, *1827*(2), 114–135. https://doi.org/10.1016/j.bbabio.2012.07.005

Skiba, M. W., George, T. S., Baggs, E. M. & Daniell, T. J. (2011). Plant influence on nitrification. *Biochemical Society Transactions*, *39*(1), 275–278. https://doi.org/10.1042/BST0390275

Smith, C. J. & Patrick, W. H. (1983). Nitrous oxide emission as affected by alternate anaerobic and aerobic conditions from soil suspensions enriched with ammonium sulfate. *Soil Biology and Biochemistry*, *15*(6), 693–697. https://doi.org/10.1016/0038-0717(83)90034-2

Smith, M. S. & Tiedje, J. M. (1979). The Effect of Roots on Soil Denitrification. *Soil Science Society of America Journal*. https://doi.org/10.2136/sssaj1979.03615995004300050027x

Song, B., Lisa, J. A. & Tobias, C. R. (2014). Linking DNRA community structure and activity in a shallow lagoonal estuarine system. *Frontiers in Microbiology*, *5*(SEP), 1–10. https://doi.org/10.3389/fmicb.2014.00460

Stewart, V., Lu, Y. & Darwin, A. J. (2002). Periplasmic nitrate reductase (NapABC enzyme) supports anaerobic respiration by Escherichia coli K-12. *Journal of Bacteriology*, *184*(5), 1314–1323. https://doi.org/10.1128/JB.184.5.1314-1323.2002

Storer, K., Coggan, A., Ineson, P. & Hodge, A. (2018). Arbuscular mycorrhizal fungi reduce nitrous oxide emissions from N2O hotspots. *New Phytologist*, *220*(4), 1285–1295. https://doi.org/10.1111/nph.14931

Strous, M., Planet, E., Mechanics, T., America, M., Appl, P., Island, A., Islands, A., Init, O. D. P., Rica, C., Fuerst, J. A., Kramer, E. H. M., Logemann, S., Muyzer, G., van de Pas-Schoonen, K. T., Webb, R., Kuenen, J. G. & Jetten, M. S. M. (1999). Missing lithotroph identified as new planctomycete. *Nature*, *400*(July), 446. https://doi.org/10.1038/22749%0Ahttp://10.0.4.14/22749

Subbarao, G., Ito, O., Sahrawat, K., Berry, W., Nakahara, K., Ishikawa, T., Watanabe, T., Suenaga, K., Rondon, M. & Rao, I. (2006). Scope and strategies for regulation of nitrification in agricultural systems - Challenges and opportunities. *Critical Reviews in Plant Sciences*, *25*(4), 303–335. https://doi.org/10.1080/07352680600794232

Subbarao, G. V., Yoshihashi, T., Worthington, M., Nakahara, K., Ando, Y., Sahrawat, K. L., Rao, I. M., Lata, J.-C., Kishii, M. & Braun, H.-J. (2015). Suppression of soil nitrification by plants. *Plant Science*, *233*, 155–164. https://doi.org/https://doi.org/10.1016/j.plantsci.2015.01.012

Subbarao, G. V., Nakahara, K., Hurtado, M. P., Ono, H., Moreta, D. E., Salcedo, A. F., Yoshihashi, A. T., Ishikawa, T., Ishitani, M., Ohnishi-Kameyama, M., Yoshida, M., Rondon, M., Rao, I. M., Lascano, C. E., Berry, W. L. & Ito, O. (2009). Evidence for biological nitrification inhibition in Brachiaria pastures. *Proceedings of the National Academy of Sciences of the United States of America*, *106*(41), 17302–17307.

https://doi.org/10.1073/pnas.0903694106

Subbarao, G. V, Arango, J., Masahiro, K., Hooper, A. M., Yoshihashi, T., Ando, Y., Nakahara, K., Deshpande, S., Ortiz-Monasterio, I., Ishitani, M., Peters, M., Chirinda, N., Wollenberg, L., Lata, J. C., Gerard, B., Tobita, S., Rao, I. M., Braun, H. J., Kommerell, V., … Iwanaga, M. (2017). Genetic mitigation strategies to tackle agricultural GHG emissions: The case for biological nitrification inhibition technology. *Plant Science*, *262*, 165–168. https://doi.org/https://doi.org/10.1016/j.plantsci.2017.05.004

Subbarao, G. V, Sahrawat, K. L., Nakahara, K., Ishikawa, T., Kishii, M., Rao, I. M., Hash, C. T., George, T. S., Srinivasa Rao, P., Nardi, P., Bonnett, D., Berry, W., Suenaga, K. & Lata, J. C. (2012). Nitrification Inhibition—A Novel Strategy to Regulate Nitrification in Agricultural Systems. In D. L. Sparks (Ed.), *Advances in Agronomy* (Vol. 114, pp. 249–302). Academic Press. https://doi.org/https://doi.org/10.1016/B978-0-12-394275-3.00001-8

Sun, D., Kotianová, M., Rozmoš, M., Hršelová, H., Bukovská, P. & Jansa, J. (2023). Arbuscular mycorrhizal hyphae selectively suppress soil ammonia oxidizers – but probably not by production of biological nitrification inhibitors. *Plant and Soil*, *491*(1–2), 627–643. https://doi.org/10.1007/s11104-023-06144-x

Sun, L., Lu, Y., Yu, F., Kronzucker, H. J. & Shi, W. (2016). Biological nitrification inhibition by rice root exudates and its relationship with nitrogen-use efficiency. *New Phytologist*, *212*(3), 646–656. https://doi.org/10.1111/nph.14057

Sun, R., Ding, J., Li, H., Wang, X., Li, W., Li, K., Ye, X. & Sun, S. (2023). Mitigating nitrate leaching in cropland by enhancing microbial nitrate transformation through the addition of liquid biogas slurry. *Agriculture, Ecosystems and Environment*, *345*(July 2022), 108324. https://doi.org/10.1016/j.agee.2022.108324

Takahashi, H., Yamauchi, T. & Colmer, T. D. (2014). *Aerenchyma Formation in Plants Aerenchyma Formation in Plants*. *December*. https://doi.org/10.1007/978-3-7091-1254-0

Tang, L., Zhang, F., Liu, A., Sun, J., Mei, S., Wang, X., Liu, Z., Liu, W., Lu, Q. & Chen, S. (2019). Genome-Wide Association Analysis Dissects the Genetic Basis of the Grain Carbon and Nitrogen Contents in Milled Rice. *Rice*, *12*(1).

https://doi.org/10.1186/s12284-019-0362-2

Tang, Q., Cotton, A., Wei, Z., Xia, Y., Daniell, T. & Yan, X. (2022). How does partial substitution of chemical fertiliser with organic forms increase sustainability of agricultural production? *Science of the Total Environment*, *803*, 149933. https://doi.org/10.1016/j.scitotenv.2021.149933

Tanji, K. K., Gao, S., Scardaci, S. C. & Chow, A. T. (2003). Characterizing redox status of paddy soils with incorporated rice straw. *Geoderma*, *114*(3–4), 333–353. https://doi.org/10.1016/S0016-7061(03)00048-X

Templer, P. H., Silver, W. L., Pett-Ridge, J., DeAngelis, K. M. & Firestone, M. K. (2008). Plant and microbial controls on nitrogen retention and loss in a humid tropical forest. *Ecology*, *89*(11), 3030–3040. https://doi.org/10.1890/07-1631.1

Thamdrup, B. & Dalsgaard, T. (2002). Production of N2 through anaerobic ammonium oxidation coupled to nitrate reduction in marine sediments. *Applied and Environmental Microbiology*, *68*(3), 1312–1318. https://doi.org/10.1128/AEM.68.3.1312-1318.2002

Tiedje, J. M. (1988). Ecology of denitrification and dissimilatory nitrate reduction to ammonium. *Environmental Microbiology of Anaerobes*, *April*, 179–244.

Tiedje, J. M., Sexstone, A. J., Myrold, D. D. & Robinson, J. A. (1983). Denitrification: ecological niches, competition and survival. *Antonie van Leeuwenhoek*, *48*(6), 569–583. https://doi.org/10.1007/BF00399542

Tilman, D., Fargione, J., Wolff, B., D'Antonio, C., Dobson, A., Howarth, R., Schindler, D., Schlesinger, W. H., Simberloff, D. & Swackhamer, D. (2001). Forecasting agriculturally driven global environmental change. *Science*, *292*(5515), 281–284. https://doi.org/10.1126/science.1057544

Tyson, K. L., Bell, A. I., Cole, J. A. & Busby, S. J. W. (1993). Definition of nitrite and nitrate response elements at the anaerobically inducible Escherichia coli nirB promoter: interactions between FNR and NarL. *Molecular Microbiology*, *7*(1), 151–157. https://doi.org/10.1111/j.1365-2958.1993.tb01106.x

United Nations Environment Programme. (2020). *Emissions Gap Emissions Gap Report 2020*.

https://www.unenvironment.org/interactive/emissions-gap-report/2019/

Valiente, N., Jirsa, F., Hein, T., Wanek, W., Prommer, J., Bonin, P. & Gómez-Alday, J. J. (2022). The role of coupled DNRA-Anammox during nitrate removal in a highly saline lake. *Science of the Total Environment*, *806*. https://doi.org/10.1016/j.scitotenv.2021.150726

Van De Graaf, A. A., De Bruijn, P., Robertson, L. A., Jetten, M. S. M. & Kuenen, J. G. (1996). Autotrophic growth of anaerobic ammonium-oxidizing micro-organisms in a fluidized bed reactor. *Microbiology*, *142*(8), 2187–2196. https://doi.org/10.1099/13500872-142-8-2187

van den Berg, S., Vandenplas, J., van Eeuwijk, F. A., Lopes, M. S. & Veerkamp, R. F. (2019). Significance testing and genomic inflation factor using high-density genotypes or whole-genome sequence data. *Journal of Animal Breeding and Genetics*, *136*(6), 418–429. https://doi.org/10.1111/jbg.12419

Van Duyen, D., Kwon, Y., Kabange, N. R., Lee, J. Y., Lee, S. M., Kang, J. W., Park, H., Cha, J. K., Cho, J. H., Shin, D. & Lee, J. H. (2022). Novel QTL Associated with Aerenchyma-Mediated Radial Oxygen Loss (ROL) in Rice (Oryza sativa L.) under Iron (II) Sulfide. *Plants*, *11*(6), 1–21. https://doi.org/10.3390/plants11060788

Van Kessel, M. A. H. J., Speth, D. R., Albertsen, M., Nielsen, P. H., Op Den Camp, H. J. M., Kartal, B., Jetten, M. S. M. & Lücker, S. (2015). Complete nitrification by a single microorganism. *Nature*, *528*(7583). https://doi.org/10.1038/nature16459

Verhoeven, E., Decock, C., Barthel, M., Bertora, C., Sacco, D., Romani, M., Sleutel, S. & Six, J. (2018a). Nitrification and coupled nitrification-denitrification at shallow depths are responsible for early season N2O emissions under alternate wetting and drying management in an Italian rice paddy system. *Soil Biology and Biochemistry*, *120*, 58–69. https://doi.org/10.1016/j.soilbio.2018.01.032

Verhoeven, E., Decock, C., Barthel, M., Bertora, C., Sacco, D., Romani, M., Sleutel, S. & Six, J. (2018b). Nitrification and coupled nitrification-denitrification at shallow depths are responsible for early season N2O emissions under alternate wetting and drying management in an Italian rice paddy system. *Soil Biology and Biochemistry*. https://doi.org/10.1016/j.soilbio.2018.01.032

Vitousek, P. M. & Howarth, R. W. (1991). Nitrogen limitation on land and in the sea: How can it occur? *Biogeochemistry*, *13*(2), 87–115. https://doi.org/10.1007/BF00002772

Wallenstein, M. D., Myrold, D. D., Firestone, M. & Voytek, M. (2006). Environmental controls on denitrifying communities and denitrification rates: Insights from molecular methods. *Ecological Applications*, *16*(6), 2143–2152. https://doi.org/10.1890/1051-0761(2006)016[2143:ECODCA]2.0.CO;2

Wang, Henian, Tseng, C. P. & Gunsalus, R. P. (1999). The napF and narG nitrate reductase operons in Escherichia coli are differentially expressed in response to submicromolar concentrations of nitrate but not nitrite. *Journal of Bacteriology*, *181*(17), 5303–5308. https://doi.org/10.1128/jb.181.17.5303-5308.1999

Wang, Hui, Yan, Z., Ju, X., Song, X., Zhang, J., Li, S. & Zhu-Barker, X. (2023). Quantifying nitrous oxide production rates from nitrification and denitrification under various moisture conditions in agricultural soils: Laboratory study and literature synthesis. *Frontiers in Microbiology*, *13*(January), 1–10. https://doi.org/10.3389/fmicb.2022.1110151

Wang, J. & Gu, J. D. (2013). Dominance of Candidatus Scalindua species in anammox community revealed in soils with different duration of rice paddy cultivation in Northeast China. *Applied Microbiology and Biotechnology*, *97*(4), 1785–1798. https://doi.org/10.1007/s00253-012-4036-x

Wang, W. J., Chalk, P. M., Chen, D. & Smith, C. J. (2001). Nitrogen mineralisation, immobilisation and loss, and their role in determining differences in net nitrogen production during waterlogged and aerobic incubation of soils. *Soil Biology and Biochemistry*, *33*(10), 1305–1315. https://doi.org/10.1016/S0038-0717(01)00034-7

Wang, Xiaoguang, Tamiev, D., Alagurajan, J., DiSpirito, A. A., Phillips, G. J. & Hargrove, M. S. (2019). The role of the NADH-dependent nitrite reductase, Nir, from Escherichia coli in fermentative ammonification. *Archives of Microbiology*, *201*(4), 519–530. https://doi.org/10.1007/s00203-018-1590-3

Wang, Xiaoting, Chen, R., Jing, Z., Yao, T., Feng, Y. & Lin, X. (2018). Root derived carbon transport extends the rhizosphere of rice compared to wheat. *Soil Biology and Biochemistry*, *122*(March), 211–219. https://doi.org/10.1016/j.soilbio.2018.03.024

Wang, Yan, Yao, Z., Zhan, Y., Zheng, X., Zhou, M., Yan, G., Wang, L., Werner, C. & Butterbach-Bahl, K. (2021). Potential benefits of liming to acid soils on climate change mitigation and food security. *Global Change Biology*, *27*(12), 2807–2821. https://doi.org/10.1111/gcb.15607

Wang, Yingcheng, Ying, H., Yin, Y., Zheng, H. & Cui, Z. (2019). Estimating soil nitrate leaching of nitrogen fertilizer from global meta-analysis. *Science of the Total Environment*, *657*, 96–102. https://doi.org/10.1016/j.scitotenv.2018.12.029

Wankel, S. D., Ziebis, W., Buchwald, C., Charoenpong, C., De Beer, Di., Dentinger, J., Xu, Z. & Zengler, K. (2017). Evidence for fungal and chemodenitrification based N2O flux from nitrogen impacted coastal sediments. *Nature Communications*, *8*, 1–11. https://doi.org/10.1038/ncomms15595

Warington, R. (1878). IV.—On nitrification. *J. Chem. Soc.{,} Trans.*, *33*(0), 44–51. https://doi.org/10.1039/CT8783300044

Wei, L., Ge, T., Zhu, Z., Ye, R., Peñuelas, J., Li, Y., Lynn, T. M., Jones, D. L., Wu, J. & Kuzyakov, Y. (2022). Paddy soils have a much higher microbial biomass content than upland soils: A review of the origin, mechanisms, and drivers. *Agriculture, Ecosystems and Environment*, *326*. https://doi.org/10.1016/j.agee.2021.107798

Wei, Q., Zhang, J., Luo, F., Shi, D., Liu, Y., Liu, S., Zhang, Q., Sun, W., Yuan, J., Fan, H., Wang, H., Qi, L. & Liu, G. (2022). Molecular mechanisms through which different carbon sources affect denitrification by Thauera linaloolentis: Electron generation, transfer, and competition. *Environment International*, *170*(September). https://doi.org/10.1016/j.envint.2022.107598

Wei, Z., Jin, K., Li, C., Wu, M., Shan, J. & Yan, X. (2022). Environmental Factors Controlling Dissimilatory Nitrate Reduction to Ammonium in Paddy Soil. *Journal of Soil Science and Plant Nutrition*, 4241–4248. https://doi.org/10.1007/s42729-022-01022-4

Wei, Z., Senbayram, M., Zhao, X., Li, C., Jin, K., Wu, M., Rahman, M. M., Shan, J. & Yan, X. (2022). Biochar amendment alters the partitioning of nitrate reduction by significantly enhancing DNRA in a paddy field. *Biochar*, *4*(1). https://doi.org/10.1007/s42773-022-00166-x

Weier, K. L., Doran, J. W., Power, J. F. & Walters, D. T. (2010). Denitrification and the Dinitrogen/Nitrous Oxide Ratio as Affected by Soil Water, Available Carbon, and Nitrate. *Soil Science Society of America Journal*, *57*(1), 66. https://doi.org/10.2136/sssaj1993.03615995005700010013x

Wells, K. C., Millet, D. B., Bousserez, N., Henze, D. K., Griffis, T. J., Chaliyakunnel, S., Dlugokencky, E. J., Saikawa, E., Xiang, G., Prinn, R. G., O'Doherty, S., Young, D., Weiss, R. F., Dutton, G. S., Elkins, J. W., Krummel, P. B., Langenfelds, R. & Paul Steele, L. (2018). Top-down constraints on global N2O emissions at optimal resolution: Application of a new dimension reduction technique. *Atmospheric Chemistry and Physics*, *18*(2), 735–756. https://doi.org/10.5194/acp-18-735-2018

Xiang, Y., Huang, Y. & Xiong, L. (2007). Characterization of stress-responsive CIPK genes in rice for stress tolerance improvement. *Plant Physiology*, *144*(3), 1416–1428. https://doi.org/10.1104/pp.107.101295

Xiao, X., Delgado-Baquerizo, M., Shen, H., Ma, Z., Zhou, J., Sun, B. & Liang, Y. (n.d.). Microbial Interactions Related to N_2O Emissions and Temperature Sensitivity from Rice Paddy Fields. *MBio*, *0*(0), e03262-22. https://doi.org/10.1128/mbio.03262-22

Xie, Y., Wang, Z., Cheng, X., Qiu, R., Hamoud, Y. A., Hong, C., Zong, X., Wang, Y., Agathokleous, E. & Guo, X. (2022). Dissecting the combined effects of cultivar, fertilization, and irrigation on rhizosphere bacterial communities and nitrogen productivity in rice. *Science of the Total Environment*, *835*(March), 155534. https://doi.org/10.1016/j.scitotenv.2022.155534

Xu, J., Han, C., Jiang, Y. & Zhong, W. (2021). Spatial distribution and co-occurrence of aerobic ammonia oxidation and anaerobic ammonium oxidation activities in the water-soil interface, bulk, and rhizosphere regions of paddy soil. *Plant and Soil*, *466*(1–2), 557–568. https://doi.org/10.1007/s11104-021-04987-w

Xu, L., Zhao, H., Ruan, W., Deng, M., Wang, F., Peng, J., Luo, J., Chen, Z. & Yi, K. (2017). ABNORMAL INFLORESCENCE MERISTEM1 functions in salicylic acid biosynthesis to maintain proper reactive oxygen species levels for root meristem activity in rice. *Plant Cell*, *29*(3), 560–574. https://doi.org/10.1105/tpc.16.00665

Yamauchi, T., Shimamura, S., Nakazono, M. & Mochizuki, T. (2013). Aerenchyma formation in crop species: A review. *Field Crops Research*, *152*, 8–16. https://doi.org/https://doi.org/10.1016/j.fcr.2012.12.008

Yamauchi, T., Tanaka, A., Inahashi, H., Nishizawa, N. K., Tsutsumi, N. & Inukai, Y. (2019). *Fine control of aerenchyma and lateral root development through AUX / IAA- and ARF-dependent auxin signaling*. https://doi.org/10.1073/pnas.1907181116

Yamauchi, T., Yoshioka, M., Fukazawa, A., Mori, H., Nishizawa, N. K. & Tsutsumi, N. (2017). *An NADPH Oxidase RBOH Functions in Rice Roots during Lysigenous Aerenchyma Formation under Oxygen-De fi cient Conditions*. *29*(April), 775–790. https://doi.org/10.1105/tpc.16.00976

Yan, W. & Frégeau-Reid, J. (2018). Genotype by Yield*Trait (GYT) Biplot: A Novel Approach for Genotype Selection based on Multiple Traits. *Scientific Reports*, *8*(1), 1–10. https://doi.org/10.1038/s41598-018-26688-8

Yan, W., Kang, M. S., Ma, B., Woods, S. & Cornelius, P. L. (2007). GGE Biplot vs. AMMI Analysis of Genotype-by-Environment Data. *Crop Science*, *47*(2), 643–653. https://doi.org/https://doi.org/10.2135/cropsci2006.06.0374

Yang, H., Li, Y., Cao, Y., Shi, W., Xie, E., Mu, N., Du, G., Shen, Y., Tang, D. & Cheng, Z. (2022). Nitrogen nutrition contributes to plant fertility by affecting meiosis initiation. *Nature Communications*, *13*(1), 1–15. https://doi.org/10.1038/s41467-022-28173-3

Yang, Y., Meng, T., Qian, X., Zhang, J. & Cai, Z. (2017). Evidence for nitrification ability controlling nitrogen use efficiency and N losses via denitrification in paddy soils. *Biology and Fertility of Soils*, *53*(3), 349–356. https://doi.org/10.1007/s00374-017-1185-1

Yoo, Y., Choi, H. & Jung, K. (2015). *Genome-wide Identification and Analysis of Genes Associated with Lysigenous Aerenchyma Formation in Rice Roots*. 117–127. https://doi.org/10.1007/s12374-014-0486-2

Yoon, S., Cruz-García, C., Sanford, R., Ritalahti, K. M. & Löffler, F. E. (2015). Denitrification versus respiratory ammonification: Environmental controls of two competing dissimilatory NO 3-/NO 2-reduction pathways in Shewanella loihica strain PV-4. *ISME Journal*, *9*(5), 1093–1104. https://doi.org/10.1038/ismej.2014.201

You, M. K., Lee, Y. J., Yu, J. S. & Ha, S. H. (2020). The predicted functional compartmentation of rice terpenoid metabolism by trans-prenyltransferase structural analysis, expression and localization. *International Journal of Molecular Sciences*, *21*(23), 1–19. https://doi.org/10.3390/ijms21238927

Yu, F., Kronzucker, H. J., Lu, Y., Shi, W. & Sun, L. (2016). Biological nitrification inhibition by rice root exudates and its relationship with nitrogen-use efficiency. *New Phytologist*, *212*(3), 646–656. https://doi.org/10.1111/nph.14057

Yu, T. R. (1991). *Characteristics of soil acidity of paddy soils in relation to rice growth*. *0*(4), 107–108.

Yu, X., Keitel, C., Zhang, Y., Wangeci, A. N. & Dijkstra, F. A. (2022). Global meta-analysis of nitrogen fertilizer use efficiency in rice, wheat and maize. *Agriculture, Ecosystems and Environment*, *338*(January), 108089. https://doi.org/10.1016/j.agee.2022.108089

Yuan, X., Nico, P. S., Huang, X., Liu, T., Ulrich, C., Williams, K. H. & Davis, J. A. (2017). Production of Hydrogen Peroxide in Groundwater at Rifle, Colorado. *Environmental Science and Technology*, *51*(14), 7881–7891. https://doi.org/10.1021/acs.est.6b04803

Zehr, J. P., Jenkins, B. D., Short, S. M. & Steward, G. F. (2003). Nitrogenase gene diversity and microbial community structure: A cross-system comparison. *Environmental Microbiology*, *5*(7), 539–554. https://doi.org/10.1046/j.1462-2920.2003.00451.x

Zhang, Jinbo, Lan, T., Müller, C. & Cai, Z. (2015). Dissimilatory nitrate reduction to ammonium (DNRA) plays an important role in soil nitrogen conservation in neutral and alkaline but not acidic rice soil. *Journal of Soils and Sediments*, *15*(3), 523–531. https://doi.org/10.1007/s11368-014-1037-7

Zhang, Jingying, Liu, Y. X., Zhang, N., Hu, B., Jin, T., Xu, H., Qin, Y., Yan, P., Zhang, X., Guo, X., Hui, J., Cao, S., Wang, X., Wang, C., Wang, H., Qu, B., Fan, G., Yuan, L., Garrido-Oter, R., … Bai, Y. (2019). NRT1.1B is associated with root microbiota composition and nitrogen use in field-grown rice. *Nature Biotechnology*, *37*(6), 676–684. https://doi.org/10.1038/s41587-019-0104-4

Zhang, M., Zeng, H., Rahil, M., Xiang, A., Yixuan, G., Guntur, L. & Subbarao, V. (2022). BNI - release mechanisms in plant root systems : current status of understanding. *Biology and*

Fertility of Soils, 225–233. https://doi.org/10.1007/s00374-021-01568-y

Zhang, Q., Li, Y., Wang, M., Wang, K., Meng, F., Liu, L., Zhao, Y., Ma, L., Zhu, Q., Xu, W. & Zhang, F. (2021). Atmospheric nitrogen deposition: A review of quantification methods and its spatial pattern derived from the global monitoring networks. *Ecotoxicology and Environmental Safety*, *216*, 112180. https://doi.org/10.1016/j.ecoenv.2021.112180

Zhang, X., Lu, Y., Yang, T., Kronzucker, H. J. & Shi, W. (2019). Factors influencing the release of the biological nitrification inhibitor 1,9-decanediol from rice (Oryza sativa L.) roots. *Plant and Soil*, *436*(1–2), 253–265. https://doi.org/10.1007/s11104-019-03933-1

Zhang, Y., Liu, L., Li, Q., Dai, Q. & Hu, J. (2022). Responses of nitrification and denitrification in the rhizosphere of mudflat paddy to rice genotype and nitrogen fertilization. *European Journal of Soil Biology*, *113*(August), 103452. https://doi.org/10.1016/j.ejsobi.2022.103452

Zheng, M., Zhou, Z., Luo, Y., Zhao, P. & Mo, J. (2019). Global pattern and controls of biological nitrogen fixation under nutrient enrichment: A meta-analysis. *Global Change Biology*, *25*(9), 3018–3030. https://doi.org/10.1111/gcb.14705

Zhou, S. Q. (2001). Theoretical stoichiometry of biological denitrifications. *Environmental Technology (United Kingdom)*, *22*(8), 869–880. https://doi.org/10.1080/09593332208618223

Zhu, G., Jetten, M. S. M., Kuschk, P., Ettwig, K. F. & Yin, C. (2010). Potential roles of anaerobic ammonium and methane oxidation in the nitrogen cycle of wetland ecosystems. *Applied Microbiology and Biotechnology*, *86*(4), 1043–1055. https://doi.org/10.1007/s00253-010-2451-4

Zhu, G., Wang, S., Li, Y., Zhuang, L., Zhao, S., Wang, C., Kuypers, M. M. M., Jetten, M. S. M. & Zhu, Y. (2018). Microbial pathways for nitrogen loss in an upland soil. *Environmental Microbiology*, *20*(5), 1723–1738. https://doi.org/10.1111/1462-2920.14098

Zhu, G., Wang, S., Wang, Y., Wang, C., Risgaard-Petersen, N., Jetten, M. S. & Yin, C. (2011). Anaerobic ammonia oxidation in a fertilized paddy soil. *ISME Journal*, *5*(12), 1905–1912. https://doi.org/10.1038/ismej.2011.63

Zhu, X., Burger, M., Doane, T. A. & Horwath, W. R. (2013). Ammonia oxidation pathways and nitrifier denitrification are significant sources of N2O and NO under low oxygen availability. *Proceedings of the National Academy of Sciences of the United States of America*, *110*(16), 6328–6333. https://doi.org/10.1073/pnas.1219993110

Zumft, W. G. (1997). *Zumft 1997 Cell Biology and Molecular Basis of Denitrification*. *61*(4), 533–616.

Supplementary

Supplementary: 1

The python-coded pipeline

Phenotype data

Check if the phenotype file has the right line endings

file phenotypefile.txt

Windows format line endings are present if the output is: ASCII text, with CRLF line terminators

Change Windows style line endings to Linux line endings

sed -i 's/\r$//' pathtofile/file.name

Check with:

file phenotypefile.txt

Windows format line endings changed if output is: ASCII text

Build sample information file (originally lines_info_G6_4.tsv)

In Excel, build a lines_info file by copying into a separate space, the Wang germplasm information without column names for: Genotype_assay_ID, Subpop, SampleSet, and "O. sativa"

Drop headings and be careful to keep formatting (avoid text converting to numbers)

Copy into notepad and save as a .tsv file (lines_RPy.tsv)

Use WinSCP to move it to the working folder

Change Windows style line endings to Linux line endings as above

Genotype data

#The plink manual can be found at https://www.cog-genomics.org/plink/1.9/

#RICE_RP dataset, only this large dataset contained all the varieties used in your study.

#There are three files in binary PLINK format:

#RICE_RP_mLIDs.bim contains SNP info,

#RICE_RP_mLIDs.bed contains genotypes,

#RICE_RP_mLIDs.fam contains phenotypes (listed as -9 missing values here).

#Copy these files to the plink folder

cp filenames fullpathtofolder/plink/filenames

#Filter these files to only include your samples by copying the phenotype and genotype files to the plink folder using WinSCP and using the command

#Copy the phenotype file to the plink folder

cp filenames fullpathtofolder/plink/filenames

./plink --bfile RICE_RP_mLIDs --make-bed --keep NitrificationData2018short.txt --out RICE_short

#Output will be three RICE_short files with .bim, .bed, and .fam extensions

#Reorder the samples to the same order as the phenotype file with the instruction

./plink --bfile RICE_short --make-bed --indiv-sort file NitrificationData2018short.txt --out RICE_shortorder

#filter for minor allele frequencies and minimum counts so that covariate file matches final SNP file

./plink --bfile RICE_shortorder --make-bed --maf 0.1 --mac 1 --out RICE_shortorderMM

#Build SNP information file

#Use the final .bim file as the SNPsDATA file (originally HDRA-6-4-snp-map.tsv)

#Rebuild to snp-map format by reordering columns and adding "Chr" to chromosome numbers with the command:

awk '{print $2 "\t" "Chr" $1 "\t" $4 "\t" $5 "\t" $6 "\t6"}' RICE_shortorderMM.bim > RICE_shortorderMM-snp-map.tsv

#Check the new file with the instruction

head -10 ./RICE_shortorderMM-snp-map.tsv | cut -c 1-100

#Recode the alleles as A or B

#First make a SNP list of the form: SNPname firstallele secondallele A B, with the instruction

awk '{print $2 "\t" $5 "\t" $6 "\tA\tB"}' RICE_shortorderMM.bim > RICE_shortorderMMlist.txt

#Use the SNP list to update the alleles of the ped file

./plink --bfile RICE_shortorderMM --make-bed --update-alleles RICE_shortorderMMlist.txt --out RICE_shortorderMMAB

#Convert to .ped and .map format

./plink --bfile RICE_shortorderMMAB --recode tab --out RICE_shortorderMMAB

#Copy the final .ped and .map files to the working folder (Nitrification2020Data) and the SNP information file to the working folder (HDRA6.4_GWAS_pipeline) with WinSCP

cp RICE_shortorderMM-snp-map.tsv ../HDRA6.4_GWAS_pipeline/Nitrification2018

Tools

Go to websites of missing programs (PLINK, emmax) to download them and unpack them in the working directory

load recent version of R software from the available modules using the command

module add r/gcc/3.4.4

Make a directory called Rpackages

mkdir ./Rpackages

Download required R package GenABEL and its dependency GenABEL data

from (https://cran.r-project.org/src/contrib/Archive/GenABEL/)

and (https://cran.r-project.org/src/contrib/Archive/GenABEL.data/)

Add them to the Rpackages directory

#Allow R to access these packages by adding an instruction file called .Renviron to the working directory

#nano .Renviron

#R_LIBS=/Rpackages/

Install packages, dependency first, to the Rpackages folder with the command

R CMD INSTALL -l ./Rpackages nameofpackagefile.tar.gz

open support_gwa.R file in WinSCP

The R package multicore has been replaced with base package parallel

modify the load multicore package instruction as

library(parallel)

modify the load package instructions to include the Rpackages location

and add a line to load the GenABEL dependency GenABEL.data first

library(GenABEL.data, lib.loc = "/ddn/data/cznm22/Rpackages/")

library(GenABEL, lib.loc = "./Rpackages")

Configuration

#Copy the appconfig.ini file to appconfig_original.ini

cp appconfig.ini appconfig_original.ini

#Open and modify the appconfig.ini to change the locations and names of working files, either directly using WinSCP or with the command

#nano appconfig.ini

Covariates files

Covariate file function in gwas_lib.py not working so using this work around instead

Move the genotype ped and map files to the plink folder

#Make several 50,000 SNP subset files because full SNP file is too large to run in R

#Each subset file is a different random set of SNPs

./plink --file RICE_shortorderMMAB --recode tab --thin-count 50000 --out RICE_shortorderMMAB50k1

#Use plink to create raw file from these files using the command:

./plink --file RICE_shortorderMMAB --recode A --out RICE_shortorderMMAB

Move the ped, map, raw, and pheno files to a working folder on your own computer using WinSCP

Open R_GWAS1z.R file in R

Change the file names in the R script to match your data files.

Run the R script to perform a PCoA of the genetic data and generate principle components.

Plot the Eigen values to decide how many PCs to include as covariates in the analysis (larger values mean they are more important)

Save the first 50k results file as pc1, the second 50k results file as pc2, etc

Repeat the R_GWAS1z.R instructions for the next 50k file until all 50k files have been run

Run the final steps to get average pc values

Specify the pheno name in the nBase <- () instruction It will be something like phenotypefilename_RP_mLIDs_RDP12_ALL_maf0.1_v1.txt

#Run the command “write.table” to write the table of covariates to the working directory

#Move the covariate file to the working directory using WinSCP

#If you are using a Windows computer, check the file format with:

file file nameoffile.ending

#DOS format will show: ASCII text, with CRLF line terminators

#If so, convert file format to linux compatible with

sed -i 's/\r$//' nameoffilex.ending

#Check the file format again with

file file nameoffile.ending

#Linux format will show: ASCII text

Running GWAS

#Make sure R and python software is loaded. On my system the command is:

module load r/gcc/3.4.4

module load python/2.7.13

#note that more recent versions of R and Python register errors.

#run the following python program

python gwas_lib.py

A successful run will create and add output files to two folders called plots and results.

Use WinSCP to move the plots to your own computer to view them

Make a subset of the top 1000 SNPs

Head -n 1000 ./results/resultsname.csv > resultsnametop1000.csv

Use WinSCP to move the 1000 SNPS file to your own computer to view them

Supplementary: 2

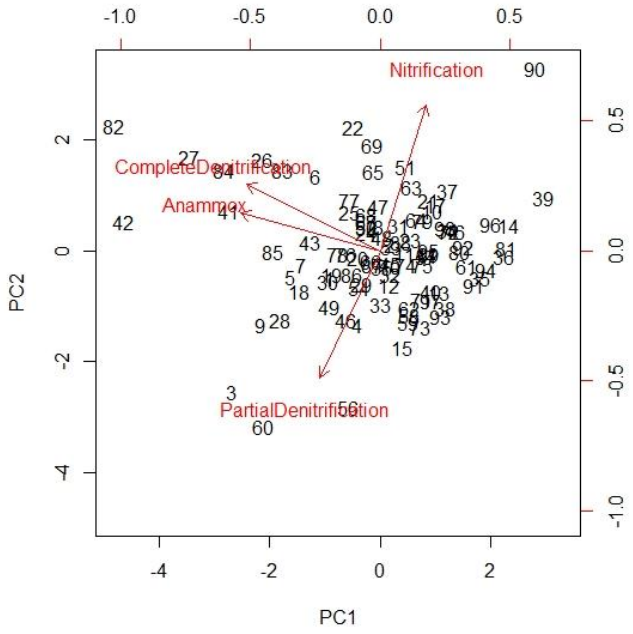

Supplementary 2: PCA analysis based on partial denitrification, anammox, complete denitrification and nitrification of the tested rice cultivars.

Supplementary 3

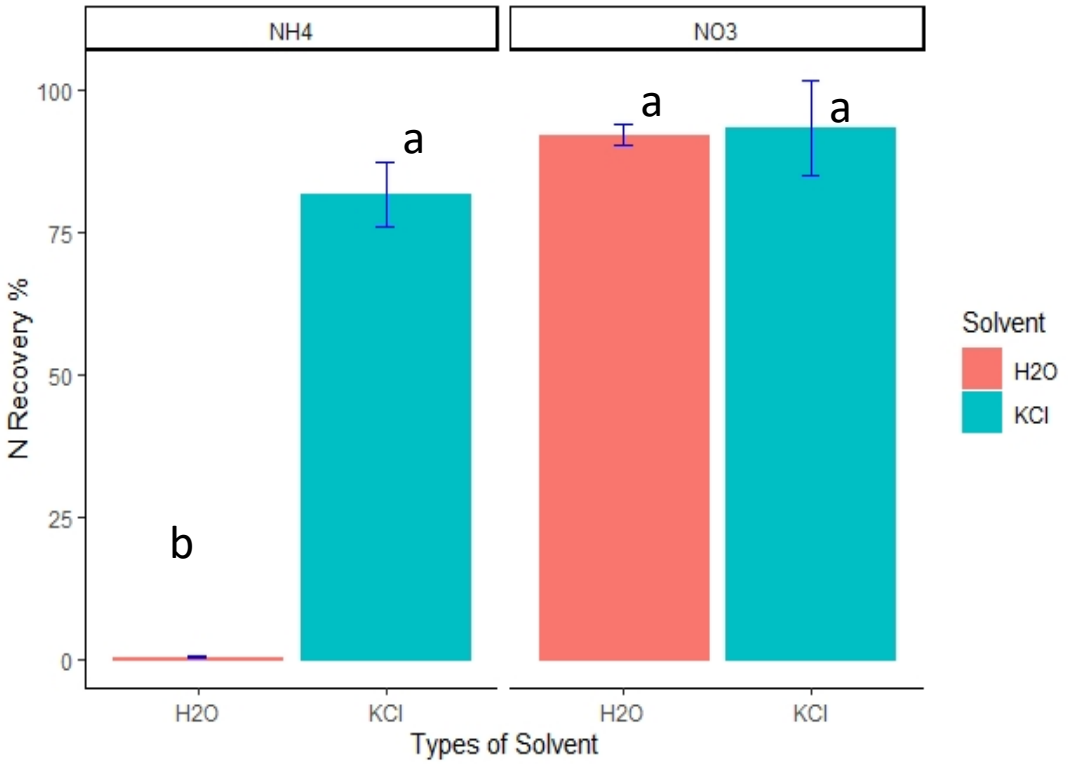

Supplementary 3: The bar plot indicates the nitrogen recovery (%) after spiking 100 N-NH_4NO_3/g dry-weight soil while extracting it using water and 2M KCl as solvents. The different letter indicates a significantly different group (P <0.05, ANOVA, Tukey HSD).